

University of Windsor

## Scholarship at UWindor

---

Electronic Theses and Dissertations

Theses, Dissertations, and Major Papers

---

2014

### Study of fuels and fuelling strategies for enabling clean combustion in compression ignition engines

Xiaoye Han  
*University of Windsor*

Follow this and additional works at: <https://scholar.uwindsor.ca/etd>

---

#### Recommended Citation

Han, Xiaoye, "Study of fuels and fuelling strategies for enabling clean combustion in compression ignition engines" (2014). *Electronic Theses and Dissertations*. 5103.  
<https://scholar.uwindsor.ca/etd/5103>

This online database contains the full-text of PhD dissertations and Masters' theses of University of Windsor students from 1954 forward. These documents are made available for personal study and research purposes only, in accordance with the Canadian Copyright Act and the Creative Commons license—CC BY-NC-ND (Attribution, Non-Commercial, No Derivative Works). Under this license, works must always be attributed to the copyright holder (original author), cannot be used for any commercial purposes, and may not be altered. Any other use would require the permission of the copyright holder. Students may inquire about withdrawing their dissertation and/or thesis from this database. For additional inquiries, please contact the repository administrator via email ([scholarship@uwindsor.ca](mailto:scholarship@uwindsor.ca)) or by telephone at 519-253-3000ext. 3208.

STUDY OF FUELS AND FUELLING STRATEGIES FOR ENABLING CLEAN  
COMBUSTION IN COMPRESSION IGNITION ENGINES

by

Xiaoye Han

A Dissertation  
Submitted to the Faculty of Graduate Studies  
through the Department of Mechanical, Automotive and Material Engineering  
in Partial Fulfillment of the Requirements for  
the Degree of Doctor of Philosophy at the  
University of Windsor

Windsor, Ontario, Canada

2014

© 2014 Xiaoye Han

STUDY OF FUELS AND FUELLING STRATEGIES FOR ENABLING CLEAN  
COMBUSTION IN COMPRESSION IGNITION ENGINES

by

Xiaoye Han

APPROVED BY:

---

C. R. Koch

Department of Mechanical Engineering, University of Alberta

---

X. Chen

Department of Electrical and Computer Engineering

---

D. Ting

Department of Mechanical, Automotive and Materials Engineering

---

J. Tjong

Department of Mechanical, Automotive and Materials Engineering

---

M. Zheng, Advisor

Department of Mechanical, Automotive and Materials Engineering

---

G. T. Reader, Co-advisor

Department of Mechanical, Automotive and Materials Engineering

26 May 2014

## **DECLARATION OF ORIGINALITY**

I hereby certify that I am the sole author of this dissertation and that no part of this dissertation has been published or submitted for publication.

I certify that, to the best of my knowledge, my dissertation does not infringe upon anyone's copyright nor violate any proprietary rights and that any ideas, techniques, quotations, or any other material from the work of other people included in my dissertation, published or otherwise, are fully acknowledged in accordance with the standard referencing practices. Furthermore, to the extent that I have included copyrighted material that surpasses the bounds of fair dealing within the meaning of the Canada Copyright Act, I certify that I have obtained a written permission from the copyright owner(s) to include such material(s) in my dissertation and have included copies of such copyright clearances to my appendix.

I declare that this is a true copy of my dissertation, including any final revisions, as approved by my dissertation committee and the Graduate Studies office, and that this dissertation has not been submitted for a higher degree to any other University or Institution.

**ABSTRACT**

The main objective of this dissertation is to improve the efficiency and emissions of compression ignition engines. Adaptive fuelling control strategies are applied for enabling the low temperature combustion on the research engines of high compression ratios using a selected set of fuels that are vastly different from the conventional diesel. These fuels include n-butanol, gasoline, ethanol, and nine diesel fuels with specifically formulated Cetane numbers, aromatic contents, and boiling temperatures. The effects of these fuels on the engine performance are compared with those of diesel in both the high temperature combustion and low temperature combustion modes in terms of the combustion characteristics, exhaust emissions, and combustion controllability.

Extensive engine experiments are conducted to demonstrate that the variations in the Cetane numbers, aromatic contents, and boiling temperatures of diesel fuels, within the investigated range, have nearly negligible effects on the conventional diesel high temperature combustion. However, as the engine operation approaches low temperature combustion where the prolonged ignition delay allows the cylinder charge to undergo extended durations for physical changes and chemical reactions (pre-reactions) prior to the start of main combustion events, the changes of fuel properties start to substantially impact the pre-reactions, the subsequent combustion processes, and exhaust emissions.

With the same engine hardware, the replacement of diesel with a less reactive and more volatile fuel (*e.g.* n-butanol in this dissertation) significantly facilitates the enabling of low temperature combustion. The fast evaporation of n-butanol coupled with a prolonged ignition delay substantially enhances the cylinder charge homogeneity, thereby offering ultra-low nitrogen oxides and smoke emissions simultaneously.

The dual-fuel combustion using a port injected fuel (gasoline or ethanol) along with a diesel pilot demonstrates desirable combustion controllability to avoid misfire or rough combustion incidences. A new combustion control algorithm correlating smoke emissions with the temporal overlap of the diesel injection and combustion events is proposed and validated with optimized engine efficiency and emissions. Ultra-low nitrogen oxides and smoke emissions are achieved simultaneously at the engine full load

with ethanol and diesel fuels, which is currently unachievable with the same engine hardware for diesel low temperature combustion.

*Keywords:* Clean combustion, low temperature combustion, active combustion control, diesel, n-butanol, gasoline, ethanol, dual-fuel, exhaust gas recirculation, near-zero NOx and smoke, emissions, engine efficiency.

**DEDICATION**

*Words can't say what love can do.*

*To my parents,*

*my wife,*

*and Connie.*

## ACKNOWLEDGEMENTS

With great pleasure, I would like to express the deepest appreciation to my advisor, Dr. Ming Zheng. His intuitive wisdom, stimulating inspiration, and constant supervision throughout the PhD program have been instrumental for me to complete the dissertation. I also express my gratitude towards my co-advisor, Dr. Graham T. Reader, for giving me such attention and time to my dissertation writing. My thanks and appreciations also go to the committee members Dr. Jimi Tjong, Dr. David Ting, and Dr. Xiang Chen for their valuable advices to improve the quality of my PhD work. With deep appreciation I acknowledge Professor C.R. Koch from University of Alberta for his helpful suggestions and corrections on my dissertation.

I have received tremendous contribution my colleagues in the Clean Diesel Engine Laboratory during the entire course of my PhD study. I am grateful for the valuable discussions and encouragement from Dr. Meiping Wang, Dr. Clarence Mulenga, Dr. Raj Kumar, Dr. Usman Asad, Dr. Shui Yu, Dr. Tadori Yanai, Marko Jetic, Kelvin Xie, Tongyang Gao, Prasad Divekar, Shouvik Dev, Qingyuan Tan, and Xiaoxi Zhang. Bruce Durfy is specially acknowledged for his technical support. I wish my colleagues all the best in their endeavours. Special thanks to Dr. Meiping Wang and Dr. Usman Asad for their efforts and time spent on my dissertation improvements.

I am also grateful for the support from the University of Windsor, AUTO21, Canada Research Chair Program, Canada Foundation of Innovation, Ontario Innovation Trust, Natural Sciences and Engineering Research Council of Canada, and Ford Motor Company Canada.

Xiaoye Han

Windsor, Ontario Canada

April, 2014.

---

**TABLE OF CONTENTS**

<b>DECLARATION OF ORIGINALITY</b> .....	iii
<b>ABSTRACT</b> .....	iv
<b>DEDICATION</b> .....	vi
<b>ACKNOWLEDGEMENTS</b> .....	vii
<b>LIST OF TABLES</b> .....	xiii
<b>LIST OF FIGURES</b> .....	xiv
<b>LIST OF APPENDICES</b> .....	xix
<b>NOMENCLATURE</b> .....	xx
<b>PREFACE</b> .....	1
A. Motivation and Objectives.....	1
B. Dissertation Significance .....	2
C. Dissertation Organization .....	3
<b>1. INTRODUCTION</b> .....	6
1.1 Diesel Engines.....	6
1.1.1 High Compression Ratio and Engine Efficiency .....	9
1.1.2 In-cylinder Air-fuel Mixing .....	14
1.2 Diesel Combustion .....	14
1.2.1 Combustion Analyses.....	17
1.3 Diesel Exhaust Emissions .....	19
1.3.1 Oxides of Nitrogen .....	20
1.3.2 Particulate Matter .....	22
1.3.3 Incomplete Combustion Products .....	22
1.3.4 Carbon Dioxide .....	23
1.4 Emission Regulations.....	24

---

1.5	Hydrocarbon Fuels and Other Energy Sources for Automotive Use .....	25
1.6	Engine Operating Limits .....	29
1.6.1	Peak Cylinder Pressure.....	29
1.6.2	Maximum Pressure Rise Rate .....	30
<b>2.</b>	<b>LITERATURE REVIEW .....</b>	<b>31</b>
2.1	Low Temperature Combustion.....	31
2.2	Fuel Property Effects on LTC Enabling.....	32
2.2.1	Impacts of Cetane and Octane Numbers .....	34
2.2.2	Impacts of Fuel Volatility .....	35
2.2.3	Impacts of Latent Heat of Evaporation .....	35
2.2.4	Impacts of Fuel Composition .....	36
2.2.5	Impacts of Fuel-borne Oxygen.....	37
2.3	LTC Enabling with Different Fuels .....	37
2.3.1	Low Temperature Combustion with Gasoline .....	37
2.3.2	Low Temperature Combustion with Diesel .....	38
2.3.3	Alternative Fuels .....	39
2.3.3.1	Natural Gas.....	39
2.3.3.2	Dimethyl Ether .....	39
2.3.3.3	Alcohol Fuels.....	41
2.4	Fuelling Strategies for LTC Enabling .....	41
<b>3.</b>	<b>METHODOLOGY .....</b>	<b>44</b>
3.1	Numerical Simulation .....	46
3.2	Empirical Investigation .....	46
3.2.1	Study of Fuels and Fuelling Strategies.....	48
3.2.1.1	Research Fuels.....	48

---

3.2.1.2 Fuelling Strategy Investigation.....	51
3.2.1.3 Advanced Fuelling Control Hardware.....	53
3.2.2 Flexible Air Management Control .....	54
3.2.2.1 Intake Boost Control.....	54
3.2.2.2 EGR Control.....	56
3.2.3 Advanced Research Platform .....	57
3.2.3.1 Advanced Research Engines .....	58
3.2.3.2 Evaluation of Engine Emissions.....	60
<b>4. BENCHMARKING OF FUEL PROPERTY IMPACTS .....</b>	<b>61</b>
4.1 Fuel Property Effects on NOx Emissions .....	62
4.2 Fuel Property Effects on Smoke Emissions .....	64
4.3 Cetane Number Effects on Ignition Delay and Smoke Emissions.....	66
4.4 Aromatic Effects on Ignition Delay and Smoke Emissions.....	70
4.5 Fuel Property Effects on HTC and LTC .....	73
4.6 Fuel Property Effects on Incomplete Combustion Products .....	78
4.7 Summary of Diesel Fuel Property Effects.....	81
<b>5. FUELS AND FUELLING STRATEGIES FOR CLEAN COMBUSTION.....</b>	<b>82</b>
5.1 LTC Enabling with Regular Diesel.....	82
5.2 n-Butanol LTC Enabling.....	91
5.2.1 n-Butanol Single-shot Direct-injection .....	92
5.2.2 n-Butanol Multiple-shot Direct-injection.....	102
5.2.3 n-Butanol HCCI via Port Injection.....	110
5.2.4 Dual-fuel Combustion of n-Butanol and Diesel.....	113
5.3 Gasoline LTC Enabling.....	116
5.3.1 Gasoline HCCI .....	116

---

5.3.2 Dual-fuel Combustion of Gasoline and Diesel .....	121
5.4 Ethanol LTC Enabling .....	126
5.5 Comparison of Different Fuels.....	136
<b>6. DYNAMIC COMBUSTION CONTROL .....</b>	<b>139</b>
6.1 Injection Pressure Control.....	139
6.2 Injection Timing and Duration Control.....	140
6.3 Real-time Feedback Control.....	142
6.4 Correlation of Injection, Combustion, and Smoke Emissions .....	145
6.5 Control Validation.....	150
<b>7. HIGH LOAD IMPROVEMENTS WITH CLEAN COMBUSTION .....</b>	<b>156</b>
7.1 Load Sweep with Gasoline Diesel DFC.....	156
7.2 High Load LTC Enabling.....	163
<b>8. CONCLUSIONS.....</b>	<b>168</b>
8.1 Impact of Diesel Fuel Properties .....	168
8.2 Fuel Types and Fuelling Strategies for Clean CI Combustion.....	170
8.3 Dynamic Combustion Control and High Load LTC.....	172
8.4 Additional Remarks and Future Work .....	173
<b>REFERENCES.....</b>	<b>174</b>
<b>APPENDICES.....</b>	<b>188</b>
A. Zero-dimensional Simulation.....	188
A.1 Indicated Thermal Efficiency .....	189
A.2 Maximum Pressure Rise Rate.....	191
A.3 Peak Cylinder Pressure .....	194
B. Evaluation of Engine Performance .....	197
B.1 Engine Power Performance Characteristics.....	197

B.2 Apparent Heat Release Analysis .....	198
B.3 Exhaust Emission Calculation .....	199
C. Modelling of Injector Delays .....	200
D. Equipment List .....	204
E. Specifications of Diesel Fuel.....	205
<b>LIST OF PUBLICATIONS</b> .....	<b>206</b>
<b>VITA AUCTORIS</b> .....	<b>213</b>

**LIST OF TABLES**

Table 1.1 Engine Compression Ratio and Power Density .....	10
Table 1.2 Selected Diesel Fuel Grading Criteria (as of 2013).....	27
Table 2.1 Fuel Properties of Commonly Used Fuels .....	33
Table 3.1 Major Fuel Properties of FACE <sup>1</sup> .....	49
Table 3.2 Major Fuel Properties of Examined Fuels <sup>1</sup> .....	50
Table 3.3 Engine Specifications .....	59
Table 3.4 Emission Analyzers .....	60
Table 4.1 Engine Operating Conditions for Diesel Property Study.....	62
Table 6.1 Specifications of Hardware for Injection Control.....	140
Table 7.1 Optimized Fuel & Air Management for Engine Load Sweeps.....	157
Table A.1 Simulation Conditions .....	189
Table D.1 List of Equipment for Engine Tests .....	204
Table E.1 Specifications of Studied Diesel Fuel .....	205

---

**LIST OF FIGURES**

Figure P.1 Dissertation Organization.....	4
Figure 1.1 Schematic of an Advanced Diesel Engine Configuration .....	7
Figure 1.2 Engine Cycle of Four-stroke Diesel and Gasoline Engines .....	8
Figure 1.3 Ideal Air Standard Dual Cycle .....	12
Figure 1.4 Ideal Dual Cycle Efficiency versus Compression Ratio .....	13
Figure 1.5 Combustion in Diesel Engines – High Speed Images.....	15
Figure 1.6 Pathways for HTC and LTC in Diesel Engines.....	16
Figure 1.7 Typical Heat Release Rate and Rate of Injection.....	18
Figure 1.8 Normalized Cumulative Heat Release and Fuel Injection .....	18
Figure 1.9 Relative Concentration of Diesel Exhaust Emissions .....	19
Figure 1.10 EPA Emission Regulations and Technology Development .....	24
Figure 1.11 Gravimetric Energy Densities of Selected Fuels and Battery Packs.....	26
Figure 1.12 Volumetric Energy Densities of Selected Fuels and Battery Packs .....	26
Figure 2.1 Injection Strategies for Diesel Combustion.....	42
Figure 3.1 Schematic of Research Methodology .....	45
Figure 3.2 Mixture Preparation for LTC with Conventional Diesel Fuels .....	47
Figure 3.3 Fuels for Advanced Combustion Engines (FACE) .....	48
Figure 3.4 Fuel Boiling Temperature Range, Auto-ignition Temperature .....	51
Figure 3.5 Investigated Injection Strategies.....	52
Figure 3.6 Injection Control – Hardware Connections.....	53
Figure 3.7 Research Engine Air System .....	55
Figure 3.8 Advanced Research Platform .....	57
Figure 4.1 FACE EGR Sweep 5.5 bar IMEP – NO <sub>x</sub> .....	62
Figure 4.2 FACE EGR Sweep 10.6 bar IMEP – NO <sub>x</sub> .....	63
Figure 4.3 FACE EGR Sweep 14.6 bar IMEP – NO <sub>x</sub> .....	63
Figure 4.4 FACE EGR Sweep 5.5 bar IMEP – Smoke NO <sub>x</sub> Trade-off .....	64
Figure 4.5 FACE EGR Sweep 10.6 bar IMEP – Smoke NO <sub>x</sub> Trade-off .....	65
Figure 4.6 FACE EGR Sweep 14.6 bar IMEP – Smoke NO <sub>x</sub> Trade-off .....	65
Figure 4.7 Cetane Effect 5.5 bar IMEP – Ignition Delay, Smoke .....	67
Figure 4.8 Cetane Effect 10.6 bar IMEP – Ignition Delay, Smoke .....	67

---

Figure 4.9 Cetane Effect 14.6 bar IMEP – Ignition Delay, Smoke .....	68
Figure 4.10 Cetane Number Effect 5.5 bar IMEP – Pressure, Heat Release .....	69
Figure 4.11 Cetane Effect 10.6 bar IMEP – Pressure, Heat Release .....	69
Figure 4.12 Cetane Effect 14.6 bar IMEP – Pressure, Heat Release .....	70
Figure 4.13 Aromatic Effects 5.5 bar IMEP – Ignition Delay, Smoke.....	71
Figure 4.14 Aromatic Effect 14.6 bar IMEP – Ignition Delay, Smoke .....	71
Figure 4.15 Aromatic Effect 10.6 bar IMEP – Low T90, ID, Smoke .....	72
Figure 4.16 FACE HTC Low Load – Heat Release .....	74
Figure 4.17 FACE LTC Low Load – Heat Release.....	74
Figure 4.18 FACE HTC Low Load – NO <sub>x</sub> , Smoke .....	75
Figure 4.19 FACE LTC Low Load – NO <sub>x</sub> , Smoke.....	75
Figure 4.20 FACE LTC High Load – Heat Release .....	77
Figure 4.21 FACE LTC High Load – NO <sub>x</sub> , Smoke .....	77
Figure 4.22 FACE EGR Sweep 5.5 bar IMEP – HC, CO .....	79
Figure 4.23 FACE EGR Sweep 10.6 bar IMEP – HC, CO .....	79
Figure 4.24 FACE EGR Sweep 14.6 bar IMEP – HC, CO .....	80
Figure 4.25 Cetane Number Effects 5.5 bar IMEP – Smoke, HC, CO.....	80
Figure 5.1 Diesel Baseline EGR Sweeps – NO <sub>x</sub> .....	84
Figure 5.2 Diesel Baseline EGR Sweeps – Smoke.....	84
Figure 5.3 Diesel Baseline EGR Sweeps – HC .....	85
Figure 5.4 Diesel Baseline EGR Sweeps – CO .....	85
Figure 5.5 Diesel Baseline EGR Sweeps – Exhaust O <sub>2</sub> .....	87
Figure 5.6 Diesel Baseline EGR Sweeps – HC, Exhaust O <sub>2</sub> .....	87
Figure 5.7 Diesel Baseline EGR Sweeps – CO, Exhaust O <sub>2</sub> .....	88
Figure 5.8 Diesel Baseline EGR Sweeps – Ignition Delay, DI SOI.....	89
Figure 5.9 Diesel Baseline EGR Sweeps – IMEP .....	90
Figure 5.10 Diesel Baseline EGR Sweeps – Indicated Efficiency .....	90
Figure 5.11 Schematic of n-Butanol Single-shot Injection Strategy .....	92
Figure 5.12 n-Butanol versus Diesel Single-shot SOI Sweep – CA50.....	93
Figure 5.13 n-Butanol versus Diesel Single-shot – IMEP, PRR <sub>max</sub> .....	93
Figure 5.14 n-Butanol versus Diesel Single-shot SOI Sweep – Ignition Delay .....	95

Figure 5.15 n-Butanol versus Diesel Single-shot SOI Sweep – CA5.....	95
Figure 5.16 n-Butanol versus Diesel Single-shot – Pressure.....	97
Figure 5.17 n-Butanol versus Diesel Single-shot – Heat Release .....	97
Figure 5.18 n-Butanol versus Diesel Single--shot – Smoke.....	99
Figure 5.19 n-Butanol versus Diesel Single-shot – NOx.....	99
Figure 5.20 n-Butanol versus Diesel Single-shot – HC.....	100
Figure 5.21 n-Butanol versus Diesel Single-shot – CO.....	100
Figure 5.22 n-Butanol Single-shot with EGR – Heat Release.....	101
Figure 5.23 n-Butanol DI Single-shot with EGR – Pressure .....	102
Figure 5.24 Schematic of Butanol Multiple-shot Injection Strategy .....	103
Figure 5.25 n-Butanol DI Pilot Plus Main – Pressure .....	104
Figure 5.26 n-Butanol DI Pilot Plus Main – Heat Release.....	104
Figure 5.27 n-Butanol DI Pilot Plus Main – NOx and Smoke .....	105
Figure 5.28 n-Butanol Pilot Plus Main – CA5, CA50, and Ignition Delay .....	106
Figure 5.29 n-Butanol DI Triple-shot, Two Pilots Plus Main – Heat Release .....	107
Figure 5.30 n-Butanol Triple-shot, Two Pilots Plus Main – Pressure .....	107
Figure 5.31 n-Butanol DI Double-shot, Two Early Pilots – Heat Release.....	109
Figure 5.32 n-Butanol DI Double-shot, Two Early Pilots – Pressure .....	109
Figure 5.33 n-Butanol HCCI without EGR – Heat Release .....	111
Figure 5.34 n-Butanol HCCI without EGR – Pressure, Temperature .....	111
Figure 5.35 n-Butanol HCCI without EGR – $dp_{max}$ , $p_{max}$ .....	112
Figure 5.36 n-Butanol HCCI with EGR – Pressure, Heat Release.....	112
Figure 5.37 DFC of n-Butanol and Diesel – Pressure, Heat Release .....	114
Figure 5.38 DFC of n-Butanol and Diesel – NOx, Smoke .....	115
Figure 5.39 Gasoline Compression Ignition – Heat Release, Load.....	117
Figure 5.40 Gasoline HCCI – Pressure, Heat Release.....	118
Figure 5.41 Gasoline HCCI – Emissions, $PRR_{max}$ , Efficiency .....	119
Figure 5.42 Gasoline HCCI with EGR – Pressure, Heat Release.....	120
Figure 5.43 Gasoline HCCI with EGR – Emissions, Intake Boost, EGR .....	120
Figure 5.44 DFC with Gasoline and Diesel – Heat Release.....	121
Figure 5.45 DFC with Gasoline and Diesel – $\chi_{gas}$ , NOx, Smoke.....	122

Figure 5.46 DFC with Gasoline and Diesel – $\chi_{gas}$ , HC, CO .....	123
Figure 5.47 DFC with Gasoline and Diesel – EGR, NOx, Smoke .....	124
Figure 5.48 DFC with Gasoline and Diesel – EGR, HC, CO.....	125
Figure 5.49 DFC with Gasoline and Diesel – EGR, $dp_{max}$ .....	125
Figure 5.50 Injection Strategy for DFC with Ethanol and Diesel.....	127
Figure 5.51 DFC with Ethanol and Diesel – Pressure, Heat Release .....	127
Figure 5.52 DFC with Ethanol and Diesel – $\chi_{eth}$ , NOx, Smoke.....	128
Figure 5.53 DFC with Ethanol and Diesel – $\chi_{eth}$ , HC, CO.....	129
Figure 5.54 DFC with Ethanol and Diesel – DI $p_{inj}$ , Smoke.....	130
Figure 5.55 DFC with Ethanol and Diesel – DI $p_{inj}$ , NOx .....	131
Figure 5.56 DFC with Ethanol and Diesel – DI $p_{inj}$ , NOx, Smoke.....	131
Figure 5.57 DFC with Ethanol and Diesel versus Diesel LTC.....	132
Figure 5.58 DFC with Ethanol and Diesel with EGR – $\chi_{eth}$ , NOx.....	133
Figure 5.59 DFC with Ethanol and Diesel with EGR – $\chi_{eth}$ , Smoke.....	133
Figure 5.60 DFC with Ethanol and Diesel with EGR – $\chi_{eth}$ , DI SOI.....	134
Figure 5.61 DFC with Ethanol and Diesel with EGR – $\chi_{eth}$ , Ignition Delay .....	135
Figure 5.62 DFC with Ethanol and Diesel with EGR – $\chi_{eth}$ , Efficiency .....	135
Figure 5.63 Comparison of Fuel Types and Fuelling Strategies .....	137
Figure 6.1 Feedback Injection Control – Flow Chart .....	143
Figure 6.2 DFC with Ethanol and Diesel – CA50, Diesel Ignition Delay .....	144
Figure 6.3 Schematic of Injection Command, ROI, and Heat Release.....	146
Figure 6.4 Correlation between Separation $\delta$ and Smoke .....	147
Figure 6.5 Effectiveness of $\chi_{eth}$ Control on Separation $\delta$ and Smoke .....	149
Figure 6.6 Dynamic Control Validation – Separation .....	151
Figure 6.7 Dynamic Control Validation – Ethanol Injection Duration .....	151
Figure 6.8 Dynamic Control Validation – Diesel Injection Duration.....	152
Figure 6.9 Dynamic Control Validation – IMEP.....	152
Figure 6.10 Dynamic Control Validation – Diesel SOI.....	153
Figure 6.11 Dynamic Control Validation – CA50.....	153
Figure 6.12 Dynamic Control Validation – Initial Heat Release.....	154
Figure 6.13 Dynamic Control Validation – Heat Release during Transient.....	155

---

Figure 6.14 Dynamic Control Validation – Final Heat Release .....	155
Figure 7.1 DFC versus Diesel Baseline – Load Sweep, Smoke .....	158
Figure 7.2 DFC versus Diesel Baseline – Load Sweep, NO <sub>x</sub> .....	158
Figure 7.3 DFC versus Diesel Baseline – Load Sweep, HC.....	159
Figure 7.4 DFC versus Diesel Baseline – Load Sweep, CO.....	159
Figure 7.5 DFC – Load Sweep, $\chi_{gas}$ .....	161
Figure 7.6 DFC versus Diesel Baseline – Load Sweep, EGR Rate .....	161
Figure 7.7 DFC versus Diesel Baseline – Load Sweep, $dp_{max}$ .....	162
Figure 7.8 DFC versus Diesel Baseline – Load Sweep, CA50.....	162
Figure 7.9 DFC versus Diesel Baseline – Load Sweep, Efficiency.....	163
Figure 7.10 DFC with Ethanol and Diesel – High Load, NO <sub>x</sub> .....	164
Figure 7.11 DFC with Ethanol and Diesel – High Load, Smoke .....	164
Figure 7.12 DFC with Ethanol and Diesel at 16.4 bar IMEP .....	165
Figure 7.13 DFC with Ethanol and Diesel at 18.1 bar IMEP .....	166
Figure 7.14 DFC with Ethanol and Diesel at 18.5 bar IMEP .....	166
Figure A.1 Simulation Inputs – Heat Release Phasing and Duration.....	188
Figure A.2 Simulated Low Load – Indicated Thermal Efficiency .....	190
Figure A.3 Simulated Medium Load – Indicated Thermal Efficiency .....	190
Figure A.4 Simulated High Load – Indicated Thermal Efficiency.....	191
Figure A.5 Simulated Low Load – Maximum Pressure Rise Rate.....	192
Figure A.6 Simulated Medium Load – Maximum Pressure Rise Rate.....	192
Figure A.7 Simulated High Load – Maximum Pressure Rise Rate .....	193
Figure A.8 Simulated Low Load – Peak Cylinder Pressure .....	194
Figure A.9 Simulated Medium Load – Peak Cylinder Pressure.....	195
Figure A.10 Simulated High Load – Peak Cylinder Pressure .....	195

**LIST OF APPENDICES**

Appendix A Zero-dimensional Simulation.....	188
Appendix B Evaluation of Engine Performance.....	197
Appendix C Modelling of Injector Delays.....	200
Appendix D Equipment List .....	204
Appendix E Specifications of Diesel Fuel.....	205

---

**NOMENCLATURE**

<b>AI</b>	Analogue Input	[-]
<b>AO</b>	Analogue Output	[-]
<b>aTDC</b>	After Top Dead Centre	[°CA]
<b>BDC</b>	Bottom Dead Centre	[-]
<b>bhp·hr</b>	Brake Horsepower Hour	[bhp·hr]
<b>BMEP</b>	Brake Mean Effective Pressure	[bar]
<b>BSFC</b>	Brake Specific Fuel Consumption	[g/kW-hr]
<b>bTDC</b>	Before Top Dead Centre	[°CA]
<b>CA</b>	Crank Angle	[°CA]
<b>CA10</b>	Crank Angle of 10% Heat Release	[°CA]
<b>CA5</b>	Crank Angle of 5% Heat Release	[°CA]
<b>CA50</b>	Crank Angle of 50% Heat Release	[°CA]
<b>CAN</b>	Controller Area Network	[-]
<b>CAI</b>	California Analytical Instruments	[-]
<b>CH<sub>4</sub></b>	Methane	[-]
<b>CI</b>	Compression Ignition	[-]
<b>CN</b>	Cetane Number	[-]
<b>CO</b>	Carbon Monoxide	[-]
<b>COV<sub>IMEP</sub></b>	Coefficient of Variation of IMEP	[%]

---

<b>cSt</b>	CentiStoke	[-]
<b>DAQ</b>	Data Acquisition	[-]
<b>DC</b>	Direct Current	[-]
<b>DFC</b>	Dual-fuel Combustion	[-]
<b>DI</b>	Direct-injection	[-]
<b>DIO</b>	Digital Input and Output	[-]
<b>DMA</b>	Direct Memory Access	[-]
<b>DOC</b>	Diesel Oxidation Catalyst	[-]
<b>DPF</b>	Diesel Particulate Filter	[-]
<b>ECU</b>	Engine Control Unit	[-]
<b>EGR</b>	Exhaust Gas Recirculation	[-]
<b>EOC</b>	End of Combustion	[°CA]
<b>EOI<sub>cmd</sub></b>	Commanded End of Injection	[°CA]
<b>EOI<sub>mdl</sub></b>	Modeled End of Injection	[°CA]
<b>EP</b>	End Point	[°F]
<b>EPA</b>	Environmental Protection Agency	[-]
<b>EVO</b>	Exhaust Valve Open	[°CA]
<b>FACE</b>	Fuels for Advanced Combustion Engines	[-]
<b>FPGA</b>	Field Programmable Gate Array	[-]
<b>FSN</b>	Filter Smoke Number	[FSN]
<b>H<sub>2</sub>O</b>	Water	[-]

---

<b>HC</b>	Hydrocarbon	[-]
<b>HCCI</b>	Homogeneous Charge Compression Ignition	[-]
<b>HFID</b>	Heated Flame Ionization Detector	[-]
<b>HP</b>	High Pressure	[-]
<b>HTC</b>	High Temperature Combustion	[-]
<b>HTR</b>	High Temperature Reactions	[-]
<b>IBP</b>	Initial Boiling Point	[°F]
<b>ICE</b>	Internal Combustion Engine	[-]
<b>ID</b>	Ignition Delay	[ms], [°CA]
<b>IDI</b>	Indirect-injection	[-]
<b>IMEP</b>	Indicated Mean Effective Pressure	[bar]
<b>Int.</b>	Intake	[-]
<b>Inj.</b>	Injection	[-]
<b>ISFC</b>	Indicated Specific Fuel Consumption	[g/kW-hr]
<b>IVC</b>	Intake Valve Close	[°CA]
<b>LHV</b>	Lower Heating Value	[MJ/kg]
<b>LNT</b>	Lean NO <sub>x</sub> Trap	[-]
<b>LTC</b>	Low Temperature Combustion	[-]
<b>LTR</b>	Low Temperature Reactions	[-]
<b>MAF</b>	Mass Air Flow	[g/s]
<b>max</b>	Maximum	[-]

---

<b>min</b>	Minimum	[-]
$\dot{m}_f$	Fuelling Rate	[g/s], [mg/cycle]
<b>MU</b>	Mechanical Unit	[-]
$n$	Engine Speed, Revolution per Minute	[rpm]
<b>N<sub>2</sub></b>	Nitrogen	[-]
<b>NDIR</b>	Non-Dispersive Infra-Red	[-]
<b>NO</b>	Nitric Oxide	[-]
<b>NO<sub>2</sub></b>	Nitrogen Dioxide	[-]
<b>NO<sub>x</sub></b>	Oxides of Nitrogen	[-]
<b>O<sub>2</sub></b>	Oxygen Gas	[-]
<b>OEMs</b>	Original Equipment Manufacturers	[-]
<b>OS</b>	Operating System	[-]
<b>PFI</b>	Port Fuel Injection	[-]
$p_{inj}$	Injection Pressure	[bar],[MPa]
$p_{int}$	Intake Pressure	[bar],[kPa],[MPa]
<b>PM</b>	Particulate Matter	[-]
<b>ppm</b>	Parts per Million	[ppm]
<b>PREDIC</b>	Premixed Lean Diesel Combustion	[-]
<b>PRF</b>	Primary Reference Fuels	[-]
<b>PRR<sub>max</sub></b>	Maximum Pressure Rise Rate	[bar/°CA]
<b>Q<sub>evaporation</sub></b>	Latent Heat of Evaporation	[kJ/kg]

---

<b>RCCI</b>	Reactivity Controlled Compression Ignition	[-]
<b>rpm</b>	Revolutions per Minute	[rpm]
<b>RT</b>	Real-time	[-]
<b>SCRE</b>	Single Cylinder Research Engine	[-]
<b>SI</b>	Spark Ignition	[-]
<b>SOC</b>	Start of Combustion	[°CA]
<b>SOI</b>	Start of Injection	[°CA]
<b>SOI<sub>cmd</sub></b>	Commanded Start of Injection	[°CA]
<b>SOI<sub>main</sub></b>	Start of Main Injection	[°CA]
<b>SOI<sub>mdl</sub></b>	Modelled Start of Injection	[°CA]
<b>T</b>	Temperature	[°C], [K]
<b>T90</b>	90% Distillation Temperature	[°C], [K]
<b>TDC</b>	Top Dead Centre	[-]
<b>TTL</b>	Transistor-transistor Logic	[-]
<b>TWC</b>	Three-Way Catalytic Converter	[-]
<b>ULSD</b>	Ultra-low Sulfur Diesel	[-]
<b>US</b>	United States	[-]
<b>V<sub>d</sub></b>	Engine Displacement	[m <sup>3</sup> ], [L]
<b>VGT</b>	Variable Geometry Turbocharger	[-]
<b>VVA</b>	Variable Valve Actuation	[-]
<b>VVT</b>	Variable Valve Timing	[-]

---

$\dot{W}_{brake}$	Brake Power	[kW]
$\dot{W}_{ind}$	Indicated Power	[kW]
$X_i$	Specific Emission	[g/kW-hr]
$Y_i$	Volumetric Concentration of Exhaust Emission	[ppm]
$\varepsilon$	Compression Ratio	[:1]
$\delta$	Separation of Injection and Combustion Events	[°CA]
$\tau_{CD}$	Injector Closing Delay	[ $\mu$ s]
$\tau_{CID}$	Commanded Injection Duration	[ $\mu$ s]
$\tau_{OD}$	Injector Opening Delay	[ $\mu$ s]
$\lambda$	Excess-air Ratio	[-]
$\theta$	Crank Angle	[°CA]
$\eta_{brake}$	Brake Thermal Efficiency	[%]
$\eta_{ind}$	Indicated Thermal Efficiency	[%]
$\chi$	Non-dimensional Constituent of Port Fuel in DFC	[%]
$\chi_{eth}$	Non-dimensional Constituent of Ethanol in DFC	[%]
$\chi_{gas}$	Non-dimensional Constituent of Gasoline in DFC	[%]
$\chi_{n-but}$	Non-dimensional Constituent of n-Butanol in DFC	[%]

## PREFACE

### A. Motivation and Objectives

The superior energy efficiency of diesel engines over other internal combustion engines (ICEs) is primarily attributed to the high compression and expansion ratios, lean-burn combustion, and the non-throttling operation. However, the raw exhaust of diesel engines normally contains particulate matter (PM), oxides of nitrogen (NO<sub>x</sub>), unburned hydrocarbon (HC), and carbon monoxide (CO) that are harmful pollutants stringently regulated by legislative authorities.

The enabling of low temperature combustion (LTC) has great potentials to improve the emissions and efficiency of diesel engines. However, the LTC operation is typically limited to the low and medium engine loads. As indicated by recent research, certain fuels are more suitable to implement the low temperature combustion than conventional diesel fuels.

This dissertation work therefore focuses on exploring the desirable fuels and fuel properties for the clean and efficient combustion in compression ignition engines. The objectives are summarized as follows:

1. Understand the effects of different fuel properties on engine performance under the conventional high temperature combustion (HTC) and the LTC, with a set of fuelling strategies on a selected group of fuels;
2. Identify the fuel types and major fuel properties that can substantially facilitate the enabling of LTC in diesel engines;

3. Improve the high load performance under LTC operation on a high compression ratio diesel engine;
4. Dynamically control the ignition and combustion processes in relation to the exhaust emissions;
5. Analyze the correlation between combustion characteristics and emissions, and provide solutions to the enabling of clean and efficient combustion.

## **B. Dissertation Significance**

The dissertation investigates the engine performance with different fuels under HTC and LTC operations. The results have substantially improved the understanding of fuel effects on the LTC enabling strategies. The contributions of the dissertation are summarized as follows:

1. Identified that the fuel properties have significantly greater impacts on the LTC operation than on the HTC;
2. Demonstrated that the replacement of diesel with more volatile and less reactive fuels (*e.g.* n-butanol) can substantially facilitate the LTC enabling on compression ignition engines;
3. Identified applicable LTC load ranges for different fuel types (*i.e.* diesel, n-butanol, gasoline, and ethanol) with advanced fuelling strategies and air handling;
4. Substantially extended the LTC load range up to an indicated mean effective pressure (IMEP) of 18.5 bar on a high compression ratio (18.2:1) diesel engine;
5. Realized a new control strategy to reduce the diffusion burning for smoke reduction by actively controlling the injection and ignition events;

6. Investigated the fuel property impacts on engine emissions and efficiency using nine diesel fuels with specifically formulated fuel properties. The research outcome contributes to the database of diesel fuel properties and helps the regulatory authorities and fuel producers for deciding the next generation fuels;
7. Demonstrated the use of alcohol fuels (n-butanol and ethanol) on a production engine to achieve ultra-low NO<sub>x</sub> and smoke emissions across a wide engine load range. The results support the efforts of engine manufacturers to explore clean and efficient engine designs that can utilize biofuels as a renewable energy source;
8. Accomplished the cycle-to-cycle feedback control to simultaneously manage the engine load and combustion phasing for improvements in the LTC stability.

### **C. Dissertation Organization**

The dissertation consists of eight chapters as illustrated in Figure P.1. In Chapter 1, the fundamental knowledge of diesel combustion and the primary exhaust emissions are introduced, and the challenges of enabling clean combustion are highlighted through discussions on the combustion process in diesel engines. The background study in Chapter 2 consists of a review over previously published research work including recent developments in emission reduction and combustion control for compression ignition engines. The research methodology is described in Chapter 3 focusing on the LTC enabling approaches including the use of different fuels and fuelling strategies, along with the precise control of the engine air system, such as the intake boost and exhaust gas recirculation.

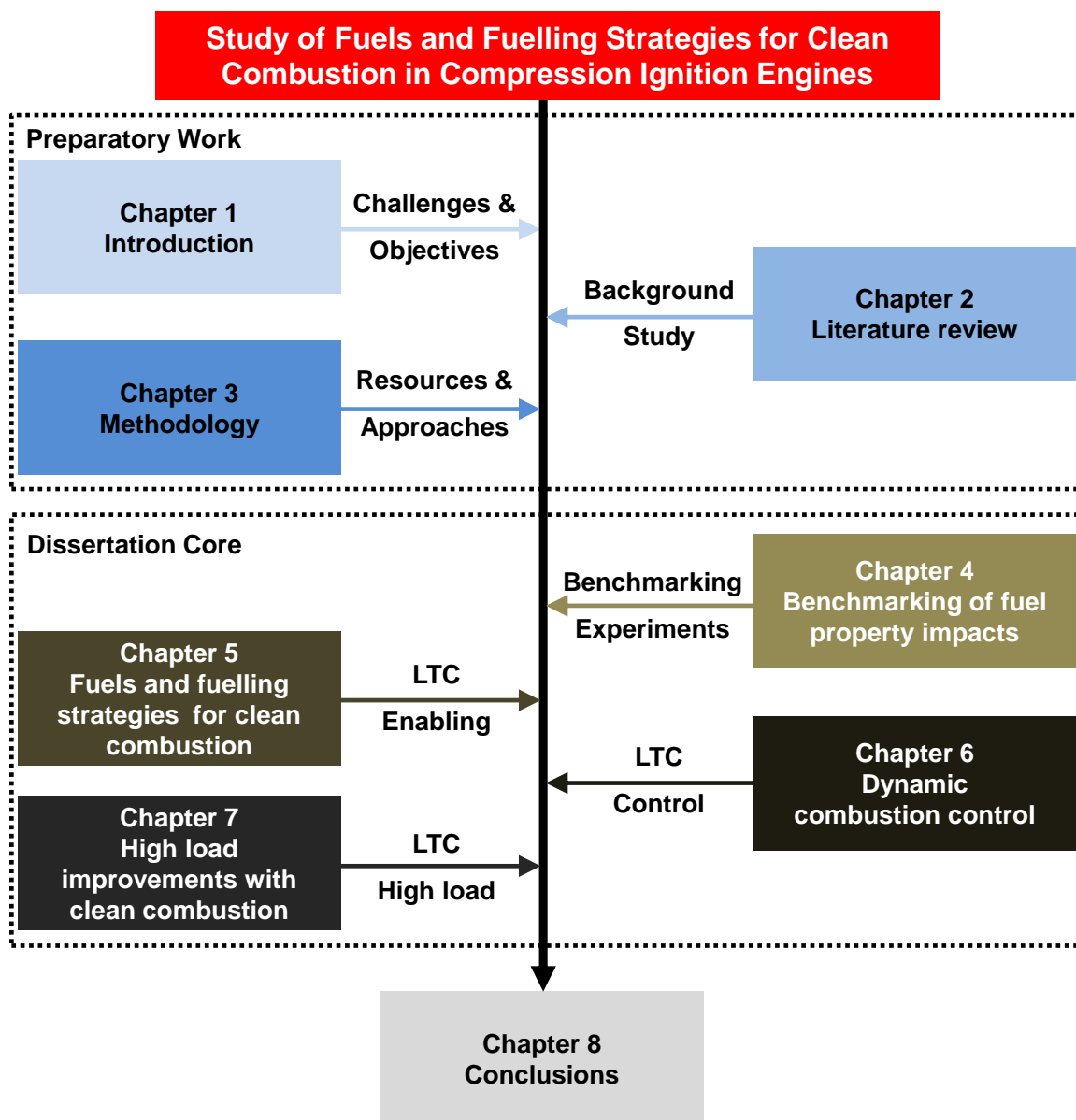


Figure P.1 Dissertation Organization

The main body of the dissertation work is presented in Chapters 4 to 7. In Chapter 4, the effects of three primary fuel properties (Cetane number, aromatic content, and boiling temperature) are investigated using nine specifically formulated diesel fuels. The experimental results reveal the significance of the fuel property changes on the engine performance under the conventional HTC and the targeted LTC modes.

In Chapter 5, investigations on different fuel types are carried out to examine their suitability for enabling the LTC operation. The fuels include the regular diesel, n-butanol, high Octane gasoline, and ethanol. The fuel delivery methods consist of port fuel injection and in-cylinder direct-injection. Accordingly, different LTC modes are enabled, including the homogeneous charge compression ignition (HCCI), partially-premixed compression ignition (PPCI), and stratified charge compression ignition (SCCI). Intensive engine experiments are conducted to investigate the combustion controllability and load applicability under LTC engine operations for different fuels and fuelling strategies.

Chapter 6 focuses on the ignition and combustion control via the active modulation of the injection events of ethanol and diesel in the dual-fuel combustion. The accomplishment of the real-time feedback injection control is described in this chapter. A new combustion control method is realized to actively modulate the diffusion burning of the diesel pilot for smoke reduction, by dynamically controlling the ethanol and diesel fuel ratio.

Chapter 7 presents LTC engine operations at high engine loads that are considered extremely challenging for diesel LTC to achieve. With the dual-fuel application of gasoline and diesel, the improved engine performance is compared with the diesel baseline at engine loads up to 16 bar IMEP. The LTC engine operations at the engine full load are achieved using ethanol and diesel fuels.

The conclusions are presented in Chapter 8, along with limitations and future directions of the present work.

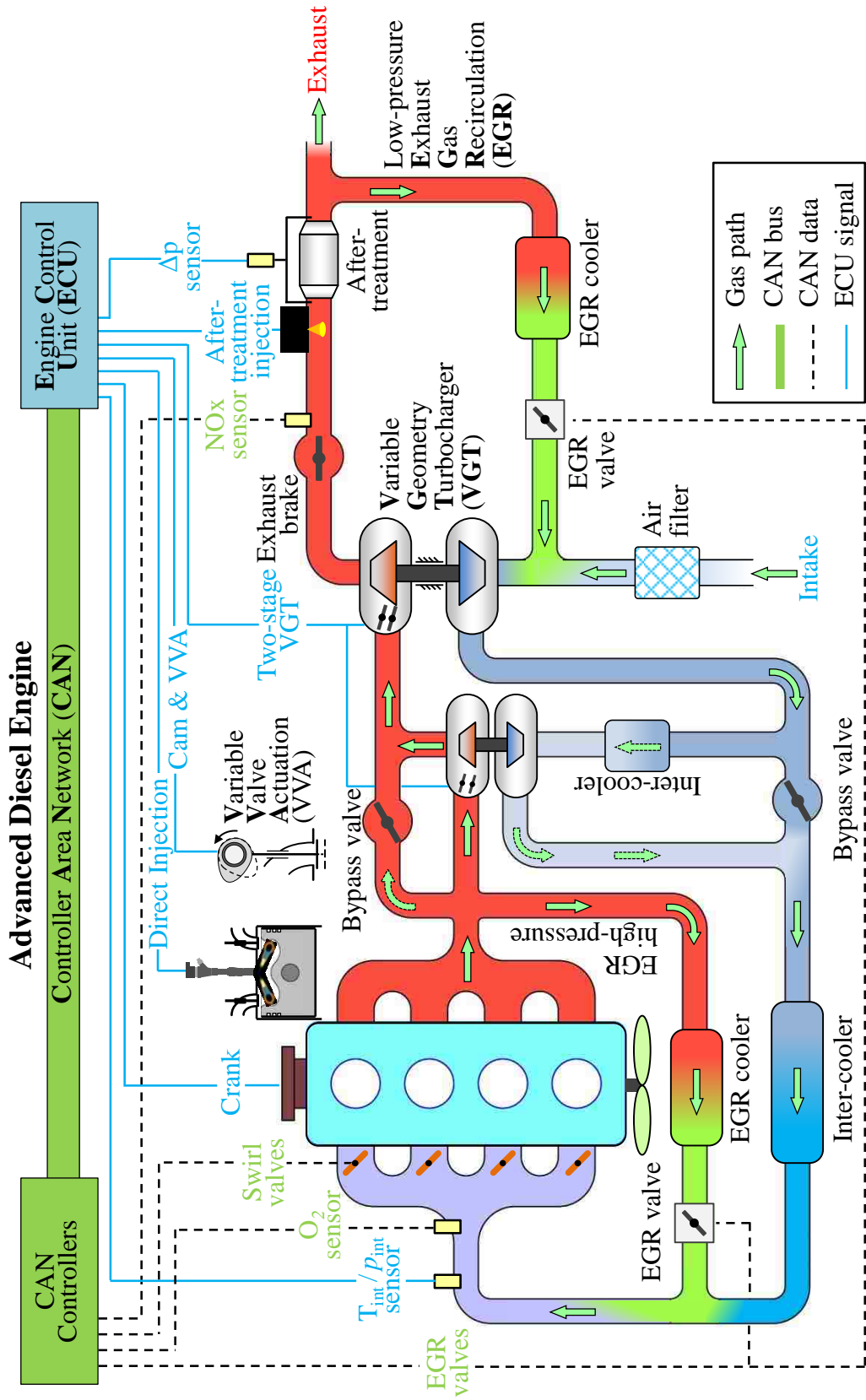
## CHAPTER I

### INTRODUCTION

#### 1.1 Diesel Engines

Modern diesel engines are generally equipped with advanced air and fuel systems to provide high engine efficiency and low exhaust emissions. An example of an advanced diesel engine configuration, currently sought after by the automotive industry, is illustrated in Figure 1.1. The engine air management employs a dual-loop exhaust gas recirculation (EGR) system and a two-stage turbocharger, along with the variable valve actuation (VVA). Such an advanced air system offers the ability to apply substantially elevated boost pressure and extended EGR range for the in-cylinder control of smoke and NO<sub>x</sub> emissions. The VVA system allows to dynamically change the effective compression stroke during engine operations, which provides additional measures of modulating the compression pressure and temperature to facilitate the clean combustion enabling under different engine operating conditions (*e.g.* during load/speed changes).

The fuel system in this engine configuration consists of a high-pressure common-rail application for the in-cylinder direct-injection and a supplementary low-pressure injection device for the exhaust after-treatment. The common-rail injection system and electronic injection control allow multiple injection events in a single engine cycle of each cylinder, for combustion noise reduction, exhaust emission minimization, and engine efficiency improvements. The supplementary injector in the exhaust line delivers additional fuel to the after-treatment devices as needed for their proper function, such as during the regeneration of a diesel particulate filter (DPF) [1].



An increasing number of advanced sensors and actuators are employed to coordinate the air and fuel handling for optimal engine performance. For instance, a recent development integrates the cylinder pressure sensor into a glow plug, which enables the real-time heat release analysis for active injection/combustion control on production engines [2]. The dual-loop EGR system and the two-stage turbocharger are being increasingly applied to modern diesel engines for the compliance with stringent emission regulations. These new technologies for clean combustion also complicate the engine air-path configuration and necessitate the active control of additional actuators such as the EGR bypass valves.

Despite the tremendous improvements in engine control systems, the fundamental working principle of the diesel engine remains nearly unchanged. For the prevailing four-stroke diesel engine, the operating strokes are compared with those of gasoline engines in Figure 1.2.

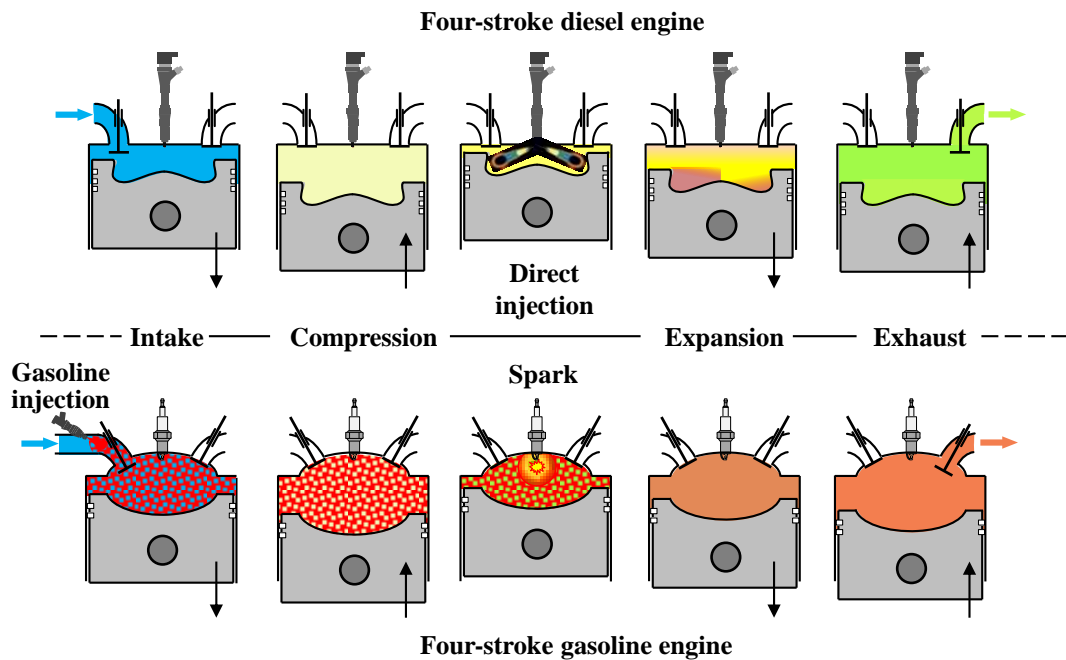


Figure 1.2 Engine Cycle of Four-stroke Diesel and Gasoline Engines

The onset of a combustion event requires three elements to be present, namely the fuel, oxygen (or air), and the ignition energy that usually appears in the form of a high temperature source or heat. Prevailing spark ignition (SI) engines, such as gasoline engines, introduce both the fuel and air from the intake ports to the cylinder and thereafter trigger the combustion events by supplying the required ignition energy through spark plug arcing.

In stark contrast, the compression ignition (CI) engines, such as diesel engines, draw in only air (including EGR for most modern diesel engines) during the intake stroke and compress the gas inside the combustion chamber to generate a sufficiently high temperature that serves as the ignition energy source. When the diesel fuel is subsequently injected into a hot, oxygen abundant environment, the combustion occurs through the auto-ignition of a locally mixed air-fuel charge.

### **1.1.1 High Compression Ratio and Engine Efficiency**

Both SI and CI engines conform to the working principle of reciprocating internal combustion engines, and a compression stroke always coexists with an expansion stroke in an operating cycle. Prevailing engine designs have the same geometric expansion and compression ratios, and the compression ratio is commonly listed in engine specifications. For explanation purposes, the prevalent compression ratios of the contemporary engines are listed in Table 1.1; and the compression ratios of diesel engines are typically in a higher range between 16:1 and 24:1, compared to their counterparts (7:1~11:1) of gasoline engines [3]. Moreover, diesel engines can achieve a much higher power density for heavy-duty application, represented by the high brake mean effective pressure (BMEP).

Table 1.1 Engine Compression Ratio and Power Density

<i>Diesel Engines</i>		
<i>Engine Type</i>	<i>Compression Ratio</i>	<i>BMEP<sup>1</sup> [bar]</i>
IDI <sup>2</sup> naturally aspirated car engines	20 ~ 24:1	7 ~ 9
IDI turbocharged car engines	20 ~ 24:1	9 ~ 12
DI <sup>3</sup> naturally aspirated car engines	19 ~ 21:1	7 ~ 9
DI turbocharged car engines with inter-cooler	16 ~ 20:1	8 ~ 22
Naturally aspirated commercial vehicle engines	16 ~ 18:1	7 ~ 10
Turbocharged commercial vehicle engines with inter-cooler	16 ~ 18:1	15 ~ 25
<i>Gasoline Engines</i>		
<i>Engine Type</i>	<i>Compression Ratio</i>	<i>BMEP [bar]</i>
Naturally aspirated car engines	10 ~ 11:1	12 ~ 15
Turbocharged car engines	7 ~ 9:1	11 ~ 15
Commercial vehicle engines	7 ~ 9:1	8 ~ 10

Note: the values of compression ratios are obtained from [3]

<sup>1</sup> Break Mean Effective Pressure

<sup>2</sup> Indirect-injection

<sup>3</sup> Direct-injection

The diesel engine operation allows the use of a substantially higher compression ratio than what SI engines can afford. For SI engines, an increase of the compression ratio generally requires the use of a higher Octane fuel; otherwise the engine may experience knocking incidences. The method of preparing the air-fuel mixture in SI engines fundamentally inhibits the use of high compression ratios, since the air-fuel mixture must undergo the compression stroke, during which this combustible cylinder charge is exposed to the increasing ambient pressure and temperature. With high compression ratios, the in-cylinder temperature can easily exceed the auto-ignition temperature of the gasoline-air mixture prior to the spark events and consequently, abnormal combustion may occur across the combustion chamber, resulting in rough operation and even engine failures.

However, a higher compression (expansion) ratio is desirable for the improvements of engine efficiency. The operation of internal combustion engines extracts the energy contained in fuels through the heat released during the combustion events and converts the energy into useful work during the expansion stroke. An increase of the expansion ratio allows converting additional energy that is otherwise discharged along with the engine exhaust into useful work at the engine crankshaft.

For theoretical analysis, the ideal air standard dual cycle is often used to represent the thermodynamic process of a closed cycle for diesel engines [4]. An illustrative diagram of the cylinder pressure versus volume is shown in Figure 1.3 for the ideal air standard dual cycle.

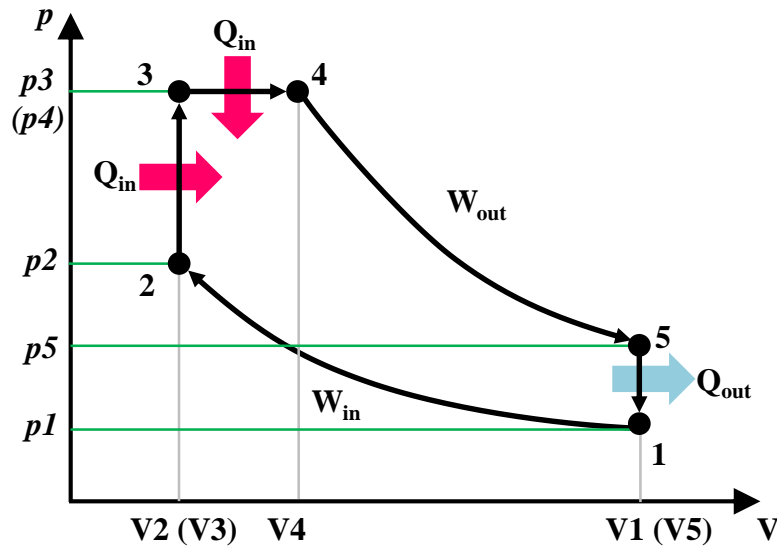


Figure 1.3 Ideal Air Standard Dual Cycle

The ideal air standard dual cycle consists of five thermodynamic processes:

1 to 2: Isentropic compression;

2 to 3: Constant volume heat addition with the pressure ratio  $r_p = p_3/p_2$ ;

3 to 4: Constant pressure heat addition with the cut-off ratio  $\psi = V_4/V_3$ ;

4 to 5: Isentropic expansion;

5 to 1: Constant volume heat rejection.

In relation to the diesel engine operation, the constant volume heat addition (Step 2-3) of the dual cycle corresponds to the premixed phase of combustion, while the constant pressure heat addition (Step 3-4) corresponds to the diffusion phase. The thermal

efficiency of the dual cycle depends on the gas specific heat ratio  $\kappa$ , engine compression ratio  $\varepsilon$ , pressure ratio  $r_p$ , and cut-off ratio  $\psi$ , as governed by Equation (1-1).

$$\eta = 1 - \frac{1}{\varepsilon^{\kappa-1}} \left[ \frac{r_p \psi^\gamma - 1}{(r_p - 1) + \kappa r_p (\psi - 1)} \right] \quad (1-1)$$

The energy efficiencies are plotted against the engine compression (expansion) ratio in Figure 1.4 for the ideal air standard dual cycle. The increase of the compression ratio improves the ideal cycle efficiency, which supports the fact that diesel engines offer superior fuel economy over gasoline engines. It is also noted that the reduction of the cut-off ratio  $\psi$  also increases the energy efficiency of the ideal air standard dual cycle.

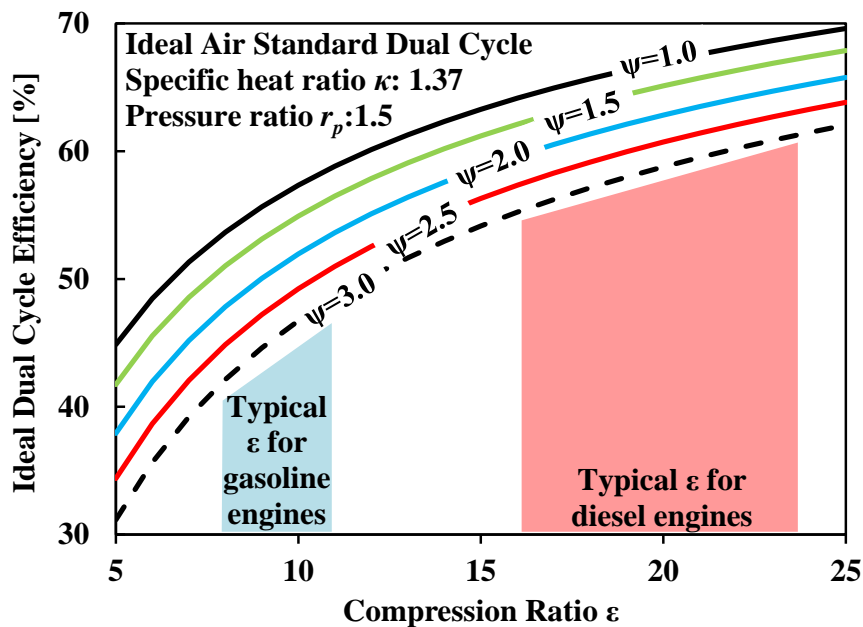


Figure 1.4 Ideal Dual Cycle Efficiency versus Compression Ratio

### **1.1.2 In-cylinder Air-fuel Mixing**

Another distinctive feature of the diesel engine is the in-cylinder air-fuel mixing. Unlike conventional gasoline engines, the diesel fuel mixes with air inside the cylinder. More precisely, a part of the air-fuel mixing happens during the combustion event, usually resulting in a diffusion burning process.

Prior to the diesel fuel injection, the piston compression raises the in-cylinder gas temperature higher than the diesel auto-ignition temperature, and thus the diesel fuel ignites almost spontaneously as it enters the combustion chamber. Consequently, the injected fuel has too little time to thoroughly mix with the surrounding air, and a heterogeneous air-fuel mixture is usually formed. In conventional diesel combustion, a significant portion of the diesel injection process overlaps with the combustion event in the time domain. The fuel injection therefore has critical impacts on the combustion characteristics including power output, combustion noise, and exhaust emissions.

## **1.2 Diesel Combustion**

The diesel combustion is complex and its detailed mechanisms are not yet fully understood. The high-speed photography used on optically accessible engines is helpful to develop deeper understandings on the diesel combustion process. In Figure 1.5, an example of the diesel combustion process is illustrated with three high-speed images captured on an optical engine [5]. The temporal overlap of the injection and combustion events is shown in Figure 1.5 (a), manifested by the coexistence of the flame in the front part of the spray and the liquid fuel near the injector nozzle.

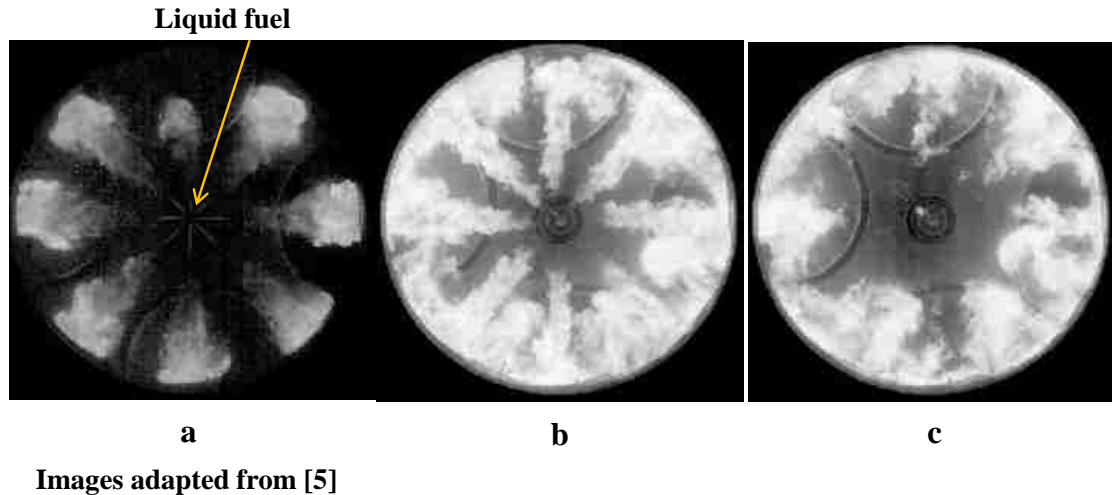


Figure 1.5 Combustion in Diesel Engines – High Speed Images

By convention, the time period between the start of the injection and the onset of the combustion is defined as the ignition delay. The classical diesel combustion generally has ignition delay periods as short as a fraction of one millisecond. Nonetheless, the air-fuel reactions during such a short period can significantly affect the subsequent combustion process. Immediately upon the injection start, the air-fuel mixing takes place as the fuel penetrates through the hot compressed air inside the combustion chamber wherein different hydrocarbon species of the fuel undergo a variety of physical changes and chemical reactions. A gradient of the air-fuel ratio is formed across each individual fuel spray and its surrounding air, resulting in a heterogenous mixture [4].

The auto-ignition tends to occur near the stoichiometric and slightly fuel-rich regions that, at large, localize around the interfaces of the fuel spray and air [4]. To a certain extent, the combustion shown in Figure 1.5 (a) can be attributed to the burning of the partially premixed air-fuel mixture that is formed during the ignition delay period. As the combustion develops, the flame primarily follows the pathway of the fuel diffusion as the fuel spray disperses inside the combustion chamber, as shown in Figure 1.5 (b).

In general, the diffusion burning produces more smoke than the premixed combustion. The locally fuel-rich conditions are difficult to avoid when the air-fuel mixing process takes place in the course of the diffusion burning. At the same time, the locally near-stoichiometric burning generates high flame temperatures and produces high NO<sub>x</sub> emissions. As illustrated in the  $\Phi$ -T diagram (Figure 1.6), the high temperature combustion of a heterogeneous fuel-air mixture typically leads to in-cylinder formation of both the smoke and NO<sub>x</sub> emissions. In order to circumvent these emission formation zones, the flame temperature should be kept low, regardless of the equivalence ratio. Therefore, the clean combustion enabling investigated in this dissertation primarily relies on the implementation of the low temperature combustion for simultaneous NO<sub>x</sub> and soot reduction, as indicated by the low NO<sub>x</sub> and soot pathway in Figure 1.6.

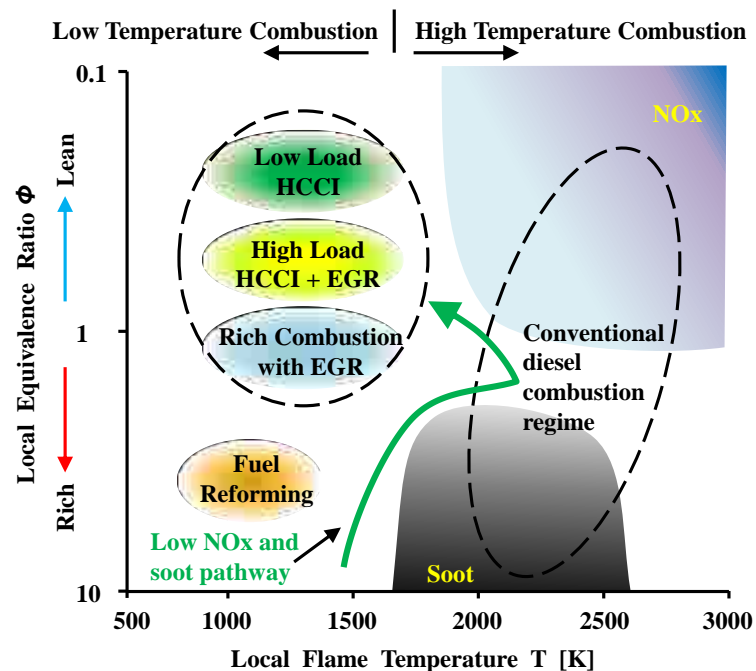


Figure 1.6 Pathways for HTC and LTC in Diesel Engines

### 1.2.1 Combustion Analyses

A common practice to analyze the combustion process is the heat release analysis based on the cylinder pressure measurements. The injection process can usually be characterized by the rate of injection profiles. In Figures 1.7 & 1.8, for example, the heat release traces and injection rate profiles are used to analyze the conventional diesel combustion.

The injection pressure and injection duration are different for the above cases, while the other engine operating conditions are kept the same. By examining the trace of the heat release rate, the diesel combustion apparently exhibits both the premixed and diffusion phases of combustion in the lower injection pressure case (*i.e.* 600 bar). On the other hand, a shorter injection duration is commanded to deliver approximately the same amount of fuel at an elevated injection pressure (*i.e.* 1100 bar), and a higher peak of the heat release rate is observed during the premixed phase of combustion.

Comparing the heat release rate traces with the rate of injection (ROI) profiles, a temporal overlap of the injection and combustion events can be identified. Such a temporary overlap indicates that a portion of the injected fuel enters the combustion chamber during the combustion event, and the diffusion burning takes place. As shown in Figure 1.8, the increase of injection pressure leads to a much larger portion (60% versus 20%) of the total fuel entering the combustion chamber prior to the onset of combustion and, as a result, the combustion exhibits a higher degree of premixed burning.

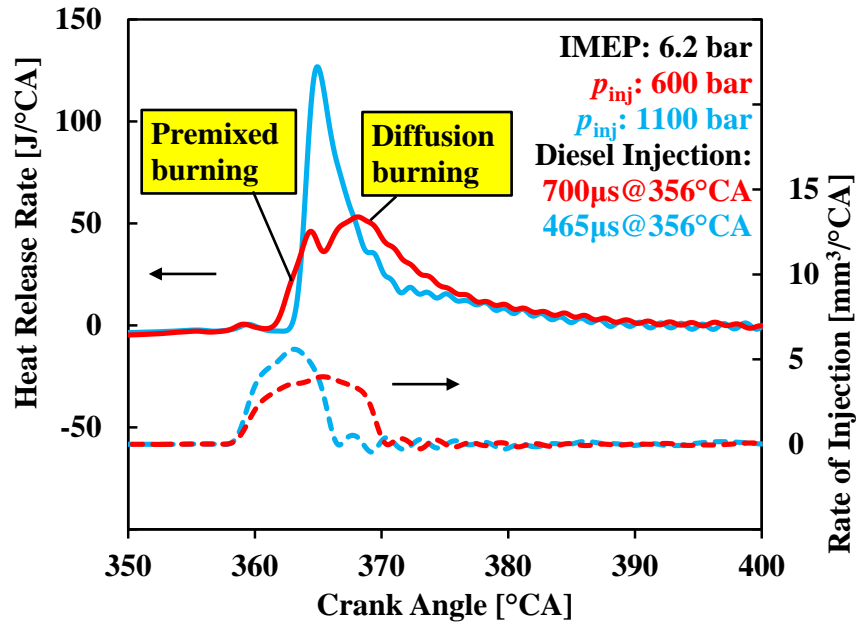


Figure 1.7 Typical Heat Release Rate and Rate of Injection

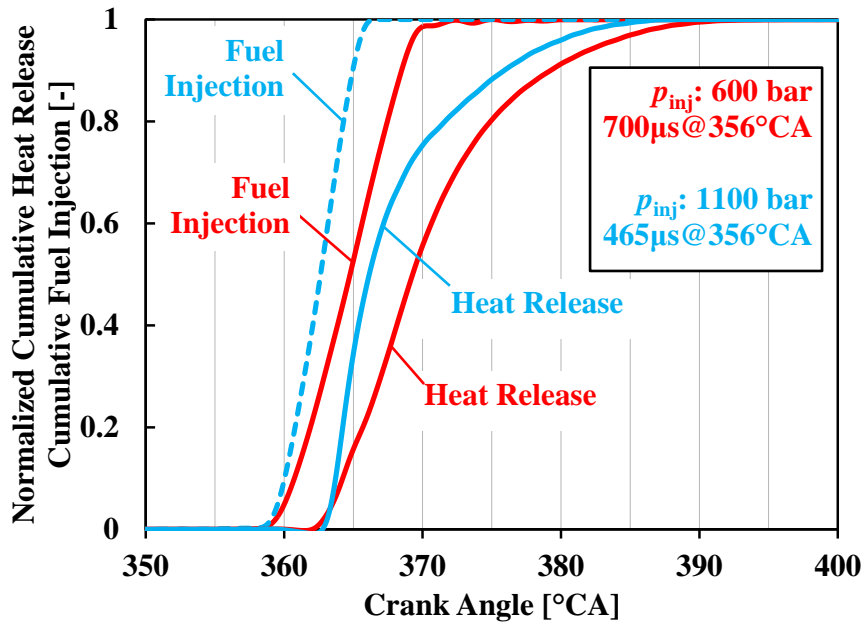


Figure 1.8 Normalized Cumulative Heat Release and Fuel Injection

### 1.3 Diesel Exhaust Emissions

The raw exhaust gas of a modern diesel engine primarily consists of the excess intake air (nitrogen and oxygen) and the combustion products (mainly carbon dioxide and water), as shown in Figure 1.9. Nitrogen from the engine intake air remains nearly unchanged throughout the combustion process and constitutes the majority of the exhaust gas. Due to the overall lean-burn operation, the raw diesel exhaust usually contains a certain amount of oxygen. The amounts of carbon dioxide and water vapor directly depend on the fuelling rate/engine load. More importantly, the raw exhaust gas also contains pollutants harmful to human and/or the environment, despite the relatively low concentrations. For diesel engines/vehicles, the commonly regulated emissions include oxides of nitrogen, particulate matter, unburned hydrocarbons, carbon monoxide, and carbon dioxide. Each of these emissions is briefly discussed in subsections 1.3.1 to 1.3.4.

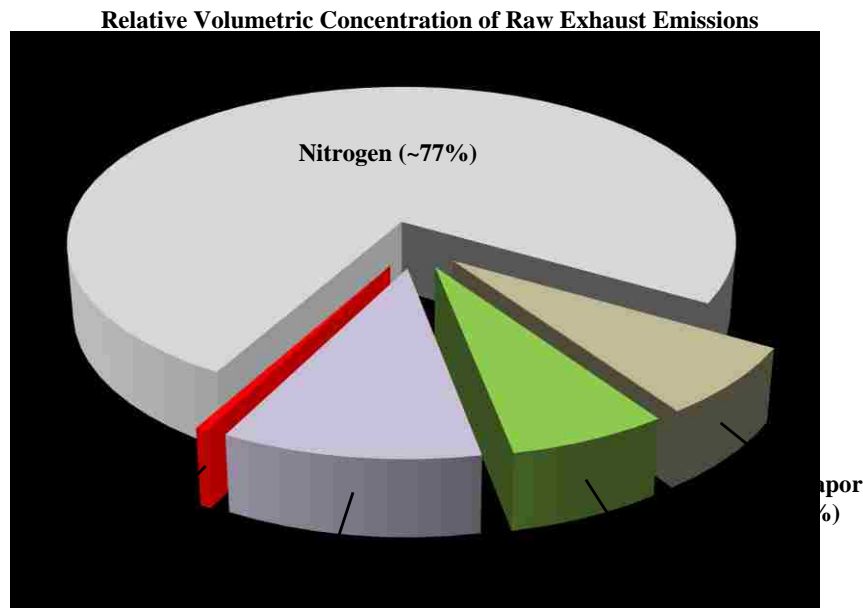


Figure 1.9 Relative Concentration of Diesel Exhaust Emissions

### 1.3.1 Oxides of Nitrogen

The oxides of nitrogen considered in this dissertation include nitrogen monoxide (NO) and nitrogen dioxide (NO<sub>2</sub>). The notation of “NO<sub>x</sub>” is generally used for the oxides of nitrogen (NO and NO<sub>2</sub>). In the raw exhaust of the conventional diesel HTC, NO typically constitutes approximately 90% of the total oxides of nitrogen by volume [4]. However, the regulatory authorities, such as the environmental protection agency (EPA) in the United States (US), treat oxides of nitrogen as NO<sub>2</sub>, since the NO eventually converts to NO<sub>2</sub> in the atmosphere. The chemical reactions below show the conversion between NO and NO<sub>2</sub> with the presence of oxygen and ozone [6].



For conventional diesel combustion, the *extended Zeldovich mechanism* explains the NO generation by the following chemical reactions:



The NO formation requires a high level of the activation energy. The flame temperature therefore has a major effect on the NO<sub>x</sub> formation. During the combustion process, when the flame temperature exceeds a threshold, for instance, around 1800 ~ 2000 K as suggested in [6], the NO generation can be primarily explained with these reactions. As the combustion event approaches to the end and the gas temperature drops, the formation of NO eventually ceases. Therefore the *extended Zeldovich mechanism* is often called the *thermal NO<sub>x</sub> mechanism*. Accordingly, techniques that can lower the flame temperature are deemed as the primary measures to reduce NO<sub>x</sub> emissions.

For LTC operations, the *dinitrogen monoxide (N<sub>2</sub>O) intermediate mechanism* is important, as it accounts for the NO generation from the low temperature combustion process of a lean premixed mixture at elevated pressures. This mechanism is governed by Equations (1-7), (1-8), and (1-9):



In Equation (1-7), a general third body (M) is required for this reaction to complete. The third body (M) represents any molecule that is needed as the “collision partner” to carry on the reaction. The generated N<sub>2</sub>O subsequently reacts with oxygen and hydrogen to form NO.

### **1.3.2 Particulate Matter**

Depending on the types of fuels and modes of combustion, the particulate matter of diesel exhaust comprises various amounts of elemental carbon with adsorbed compounds including unburned or partially oxidized hydrocarbons, organic compounds, sulfate, nitrate, and ashes. Due to the heterogeneity of the air-fuel mixture, the hydrocarbon species can have thermal decomposition before air is available for combustion. The high temperature cracking reactions cause the formation of carbonaceous soot particles, on which unburned and/or partially burned hydrocarbons can condense and deposit. Ultimately, the particles agglomerate into larger clusters, becoming smoke emissions. This type of smoke formation generally takes place in the locally fuel-rich combustion regions, and a part of such smoke production can be oxidized under high temperature once oxygen becomes available [7].

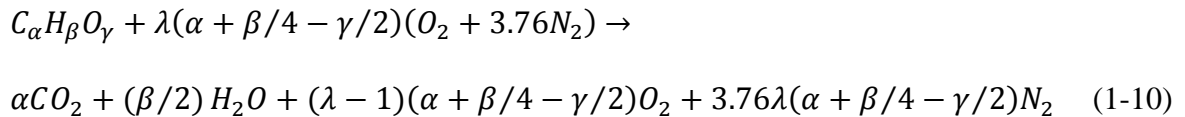
### **1.3.3 Incomplete Combustion Products**

Due to the overall lean-burn operation, diesel engines inherently produce very little incomplete combustion products, namely CO and unburned HC. The air deficiency in the locally fuel-rich pockets causes partial oxidation and leads to CO production. The notation of “HC” is a generic term that stands for the entire range of chemical compounds containing hydrogen and carbon in the exhaust. Although HC emissions are treated as unburned fuel, they usually contain hydrocarbon species that are not originally present in the fuel. Partially oxidized hydrocarbons can also include by-products containing oxygen, such as aldehydes and ketones. The HC emissions are greatly related to the fuel condensation and flame quenching on the surfaces of the combustion chamber and the cylinder walls [8].

Traditionally, diesel combustion can achieve a high degree of combustion completeness owing to the excess background  $O_2$  and high flame temperatures. The small amount of CO and HC emissions only contain a negligible percentage of the total fuel energy. However, the HC and CO emissions tend to increase considerably when the flame temperature is substantially lowered for  $NO_x$  reduction, for instance, in the diesel LTC operation, and these incomplete combustion products may drain a significant amount of the fuel energy and deteriorate the overall engine efficiency.

### 1.3.4 Carbon Dioxide

The complete combustion of a hydrocarbon fuel can be expressed by Equation (1-10). Conventional diesel fuels do not contain oxygen, and thus in the fuel formula the value of  $\gamma$  should be zero for diesel combustion. In this complete reaction, the hydrocarbon fuel converts into carbon dioxide ( $CO_2$ ) and water ( $H_2O$ ). According to the conservation law of mass, the amount of carbon dioxide in the exhaust directly relates to the fuel consumption. Therefore, for engines running standard fuels, the  $CO_2$  reduction essentially relies on improvements of the fuel consumption.



It is noted that  $CO_2$  is not classified as a toxic pollutant. However, the greenhouse effect of  $CO_2$  is considered to contribute to the global climate change, and thus  $CO_2$  regulations will phase in from Year 2014 for heavy-duty diesel engines in the US [9].

## 1.4 Emission Regulations

Regulatory authorities set statutory limits for a specific exhaust emission according to prescribed categories of vehicles and engines. Different countries and regions establish their own regulations or adopt from other developed countries. As of today, the emission standards are at different levels across the world, the US EPA's being the most stringent for the NO<sub>x</sub> and smoke emissions of heavy-duty diesel engines.

In recent decades, the control of exhaust emissions has been facing a moving target that became tougher once an existing standard was about to be met. Figure 1.10 shows the NO<sub>x</sub> and PM emission limits for heavy-duty diesel engines in the US. The US EPA has progressively enforced the statutes that mandate original equipment manufacturers (OEMs) to produce engines/vehicles with after-treatment devices to achieve near-zero NO<sub>x</sub> and PM emissions.

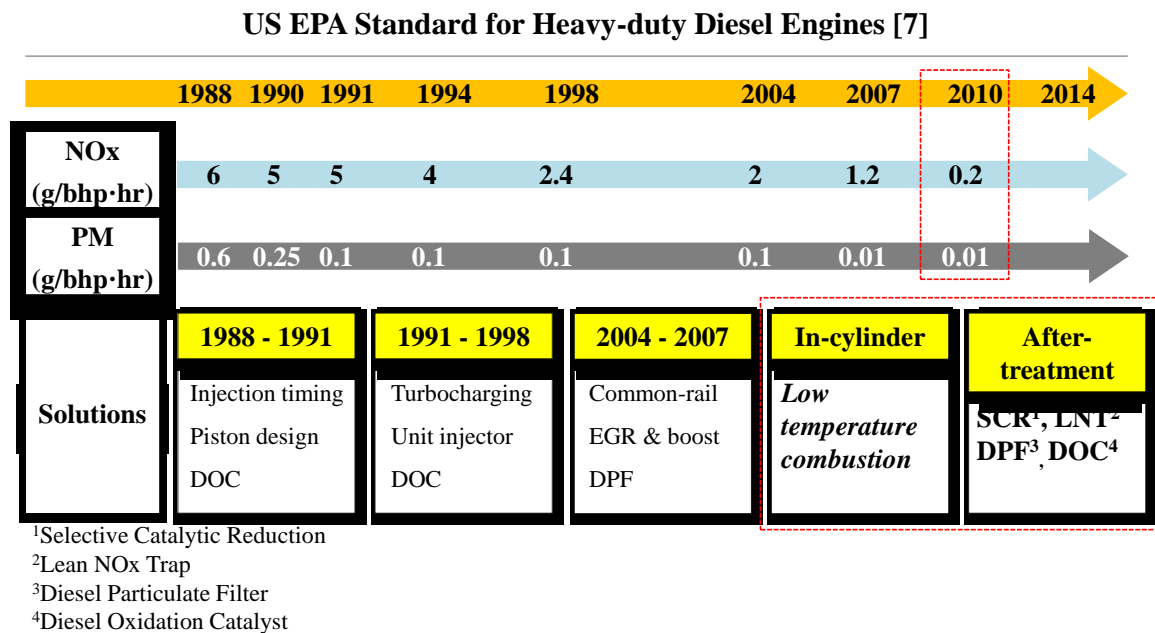


Figure 1.10 EPA Emission Regulations and Technology Development

## 1.5 Hydrocarbon Fuels and Other Energy Sources for Automotive Use

Hydrocarbon fuels such as diesel and gasoline have the advantage of offering greater energy densities among the world's primary energy sources. The high gravimetric as well as volumetric energy densities make hydrocarbon fuels suitable for use in vehicles and other non-stationary applications. In Figures 1.11 & 1.12, comparisons are made for the energy densities of different fuels and other energy sources including electrical battery packs. On the mass basis, the gaseous fuels have comparable (or even higher) energy densities than traditional liquid fuels (*e.g.* diesel and gasoline). However, the extremely low volumetric energy densities prevent the use in mobile applications. When compressed under high pressures, *e.g.* 700 bar, hydrogen has a volumetric energy density of ~5 MJ/L, a merely acceptable level compared to those of diesel and gasoline fuels.

Compared to petroleum fuels, the state-of-the-art electrical battery packs also have very low energy densities. It still requires technology breakthroughs to completely replace the internal combustion engines running on hydrocarbon fuels with electrical motors powered by batteries. On the other hand, the comparisons of energy densities suggest that the alcohol fuels can be a promising alternate energy source for automotive applications. These alcohol fuels (*i.e.* butanol, ethanol, and methanol) have similar energy densities as diesel and gasoline fuels. Moreover, the alcohol fuels produced from biomass feedstock are deemed as renewable energy sources.

It is important to note that the energy density is only one aspect to evaluate a fuel for the automotive use while other fuel properties can also be the predominant factors. For example, fuel standards with detailed grading criteria are established and enforced to regulate diesel fuels for automotive applications.

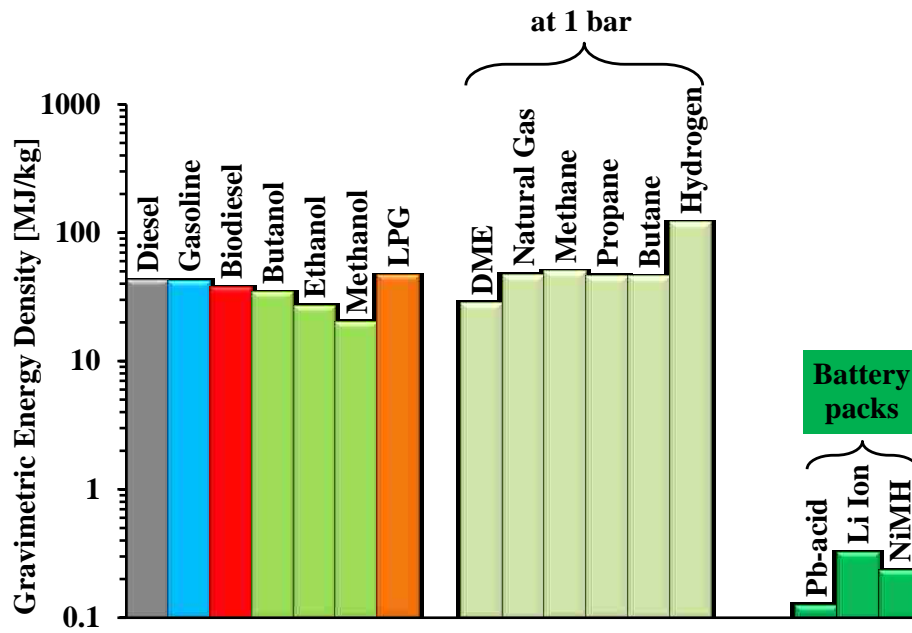


Figure 1.11 Gravimetric Energy Densities of Selected Fuels and Battery Packs

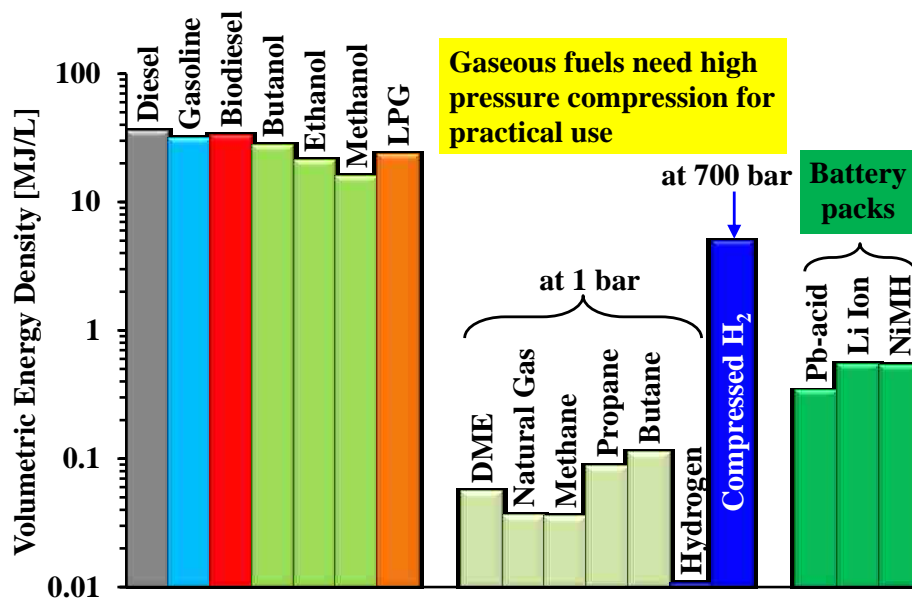


Figure 1.12 Volumetric Energy Densities of Selected Fuels and Battery Packs

In Table 1.2, the major regulated diesel properties are listed as in the fuel standards established by the regulatory authorities [10].

Table 1.2 Selected Diesel Fuel Grading Criteria (as of 2013)

Fuel Property	US	Europe	Japan	China	Brazil
Cetane Number [-], min	40	51	-	47	48
Cetane Index [-], min	40	46	50	-	-
Density [kg/m <sup>3</sup> ] @15°C	876,max	845,max	860,max	810-850	820-850
T90, vol. [°C]	282-338	-	350,max	355,max	370,max
T95, vol. [°C]	-	360,max	-	365,max	-
Aromatics [%], max	35 (vol.)	11 (wt.)	-	11 (wt.)	11 (wt.)
Sulfur [ppm, wt.], max	15	10	10	50	10
Viscosity [mm <sup>2</sup> /s] @40°C	1.9-4.1	2.0-4.5	2.5 min	1.8-8.0	2.0-4.5
Lubricity, HFRR <sup>1</sup> [μm] @60°C, max	520	460	-	460	520

<sup>1</sup> High Frequency Reciprocating Rig

These fuel standards from different regulatory authorities all require a minimum Cetane number or Cetane index for diesel fuels. The Cetane number or Cetane index is a measure of how readily the fuel starts to burn under diesel engine operating conditions; a higher Cetane number basically indicates a higher tendency to auto-ignite under the specified test conditions. It is however noted that a major reason for the requirement of a minimal Cetane number/index is to accommodate the engine operation at low ambient

temperatures. Leakage, wear, and heat losses during the engine operation all can reduce the compression pressure and temperature, and thus fuels become difficult to ignite in a cold engine. Therefore, engines can benefit from a high Cetane diesel for cold start to avoid misfire for smoother operation.

The public commonly perceives that a higher Cetane number symbolizes a better quality diesel; it would be true if the diesel quality only corresponded to propensity for the auto-ignition. However, when the engine runs in clean combustion modes such as the low temperature combustion, a fuel with a lower Cetane number/index is preferred to provide a prolonged ignition delay for enhanced air-fuel mixing. The high Cetane fuels, therefore, may not be deemed “better quality” for the emission reduction purposes.

On a modern diesel engine, the diesel fuel also serves as a lubricant and protects moving components from excessive wear in the injection systems, such as the high-pressure pump and injectors. The lubrication of the diesel injection system generally involves two mechanisms, namely the hydrodynamic lubrication and boundary lubrication. The hydrodynamic lubrication requires a layer of fuel between the sliding surfaces to prevent direct contacts. A higher viscosity typically provides better hydrodynamic lubrication. The boundary lubrication becomes necessary when direct contacts occur between the moving surfaces. Certain compounds in diesel fuels adhere to the moving surfaces and form an anti-wear protection layer. Additives can also be applied to enhance the fuel lubricity at an increased cost.

## **1.6 Engine Operating Limits**

Although diesel engines can suit a wide range of applications and endure a variety of running conditions, the engine operation must conform to certain operating limits such as the peak cylinder pressure and the maximum pressure rise rate.

### **1.6.1 Peak Cylinder Pressure**

In the combustion process, the partially premixed cylinder charge ignites and releases heat rapidly in a short duration. The combustion pressure can therefore rise sharply to a hazardous level. Especially for single cylinder engines, the cyclic combustion pressure causes periodic alternating stress on engine components, which places a challenging demand on the design of engine dimensions and the strength of materials.

In addition, the upper limit of the cylinder pressure ultimately restricts the application of ultra-high intake boost. The combination of the high compression ratios and the elevated intake pressure can result in a considerably high compression pressure prior to the combustion events. When combustion takes place, the cylinder pressure usually further increases to a higher level than the compression pressure, unless the combustion phasing is substantially postponed. However, the postponement of the combustion phasing may sacrifice the engine efficiency. If the combustion takes place prior to the completion of the compression stroke, which is prone to occur for certain clean combustion modes (*e.g.* HCCI), the combustion pressure is further increased by the compression. Since the prevailing engine designs cannot alter the compression ratio dynamically, the permissible peak cylinder pressure places an upper limit on the intake pressure, especially at high engine loads, unless the engine is equipped with technologies such as the variable valve timing (VVT).

### **1.6.2 Maximum Pressure Rise Rate**

A higher pressure rise rate normally leads to a more audible combustion noise. The modern diesel engine design for transportation applications generally limit the maximum pressure rise rates at levels below 4~6 bar/°CA to contain engine noise, although the engine mechanical strength can stand significantly higher levels. From the combustion study perspective, the pressure rise rate is an important characteristic that effectively indicates the combustion roughness. An excessively high pressure rise rate or high pressure oscillation is a representative sign of engine knocking that can potentially destroy the piston and damage the crankshaft in a few engine cycles. The combustion modes investigated in this dissertation generally use a highly premixed cylinder charge and such combustion tends to produce higher levels of the maximum pressure rise rate than the conventional diesel combustion.

## CHAPTER II

### LITERATURE REVIEW

This chapter provides a review of the previously published work on the improvements in the efficiency and emissions of compression ignition engines. The review focuses on the enabling techniques for the low temperature combustion and various mechanisms for NO<sub>x</sub> and smoke reduction. The review also includes the impacts of major fuel properties on the LTC enabling as reported in the literature. A summary is presented for the LTC operation achieved in the previous research using different fuels and fuelling strategies.

#### 2.1 Low Temperature Combustion

The enabling of LTC in diesel engines is recognized as an effective technique to achieve clean and efficient engine operations [11-12]. The lowered flame temperature is helpful to reduce NO<sub>x</sub> and soot emissions simultaneously [13-17].

Ideally, the LTC operation of a diesel engine prefers a homogeneous air-fuel mixture that auto-ignites under the compression heat within a proper timing window of an engine operating cycle. In reality, a majority of diesel fuels have relatively high viscosity and a wide range of boiling temperatures. As a result, a sufficiently long mixing period is usually required to attain the desired homogeneous cylinder charge. However, most diesel fuels have high tendency to auto-ignite, which only allows a short time for the mixing process prior to the ignition [18]. The conventional diesel combustion is essentially the combustion of a heterogeneous air-fuel mixture. Therefore, the LTC enabling strategies comprise the engine control technologies to assist the transition from the conventional heterogeneous cylinder charge to a more homogeneous cylinder charge.

When the engine runs on conventional diesel fuels, the advanced air management is typically employed as a primary LTC enabling technique that includes the intake boost and EGR applications [19-20]. The use of EGR dilutes the engine intake and reduces the in-cylinder oxygen. The ignition delay is prolonged for an enhanced mixing process. The increased heat capacity of the in-cylinder gas also helps to lower the flame temperature, often resulting in reduced NO<sub>x</sub> emissions.

The smoke emissions tend to increase with EGR. However, as a sufficiently long ignition delay is attained and the engine operation enters the LTC mode, the smoke emissions usually drop sharply while the HC and CO emissions start to rise [12-13, 15]. The LTC therefore exhibits a new emission trade-off in terms of the NO<sub>x</sub> and smoke emissions versus the HC and CO emissions.

In regard to the ignition and combustion, the EGR application has a strong impact on the timing and phasing, and thus it can also be used as a control measure to attain a preferred combustion phasing, especially when undesired early combustion tends to occur.

## **2.2 Fuel Property Effects on LTC Enabling**

For the LTC enabling, the major fuel properties that affect the ignition and combustion processes include the ignition quality, volatility, latent heat of evaporation, fuel composition (molecular structure), and the fuel-borne oxygen content [20-21]. A review is performed on the impacts of these fuel properties as reported in the literature. In order to highlight the contrast of fuel property differences, a fuel property table of commonly used fuels is shown in Table 2.1.

	Diesel	Gasoline	Biodiesel	Butanol	Ethanol	Methanol	DME	LPG	Methane	Propane
<b>Octane number</b>	25	87	30	87	110 - 115	99	13	105	120	104.5
<b>Cetane number</b>	43	10 - 17	52 - 62	17 - 25	8 - 11	3	55	~5	0	5
<b>LHV [MJ/kg]</b>	43	43	36.7 - 40.5	~36	27	20	28.4	46	50	46.4
<b>Oxygen mass [%]</b>	0	0	10 - 11	21.62	34.8	50	35	0	0	0
<b>Boiling T. @ 1 bar [°C]</b>	246 - 388	60 - 200	~350	117.5	78	65	-25	~ -43	-162	-42
<b>Q<sub>evaporation</sub> [kJ/kg]</b>	316.6	303	-	595	728.2	1100	465	426.2	510	426.2
<b>Density [kg/m<sup>3</sup>]</b>	840 - 880	720 - 780	860 - 900	810	780	790	1.97	2	0.72	1.91
<b>Auto-ignition T. [°C]</b>	180 - 240	220 - 260	~260	340	360 - 422	464	350	470	540	470
<b>Kinematic viscosity [cSt]</b>	>3	0.4 - 0.8	3.5 - 5	3.64	1.52	0.64	0.184	51	13.8	51

### 2.2.1 Impacts of Cetane and Octane Numbers

The Cetane or Octane number is used to evaluate the auto-ignition quality of a fuel. A high Cetane fuel typically has a short ignition delay with predominantly diffusion-controlled combustion that suppresses HC and CO emissions [21]. However, a low Cetane fuel is beneficial for enabling premixed LTC, because the prolonged ignition delay allows more time for the air-fuel mixing. Conventional diesel fuels with high Cetane numbers are prone to auto-ignition, and thus it is very difficult to prepare a satisfactory homogeneous air-fuel mixture prior to the combustion, unless the engine compression ratio is reduced substantially.

Ickes *et al* and Waley *et al* have demonstrated significant improvements of the NO<sub>x</sub> and smoke emissions by lowering the fuel Cetane numbers [22-23]. Bessonette *et al* indicated that a Cetane number between those of the conventional diesel and gasoline fuels was preferred for the enabling of low temperature combustion. In their tests, an engine load of 16 bar BMEP was achieved using a fuel with Cetane number 27, while the compression ratio was lowered to 12:1 [24-25].

In order to understand the correlation between the Octane number and the auto-ignition quality, a series of tests have been reported using a group of high Octane fuels with different Octane numbers under varied engine operating conditions [26-29]. The test results suggested that the increase of the compression pressure and temperature required an increase of the Octane number to maintain the same combustion phasing. In addition, the variation of the Octane number also had impacts on the pattern of the heat release. Shibata *et al* tested three fuel blends of Octane number 70, 82, and 92 [30]. The high Octane fuel showed a small amount of heat release during the pre-reactions and a slow

reaction rate during the main combustion event, which effectively reduced the pressure rise rate and the peak cylinder pressure. The use of high Octane fuels could therefore allow an increase of the engine load under LTC operations [31-34].

As suggested by the literatures, a fuel with a lower Cetane number than that of the regular diesel was desired for the enabling of the LTC operation. A lowered compression ratio was often used along with the low Cetane fuels to achieve LTC, especially at higher engine loads.

### **2.2.2 Impacts of Fuel Volatility**

The fuel volatility is another major factor affecting the mixing. Cheng *et al* [35] tested five fuel blends of similar Cetane number but different boiling temperatures. The increase of the fuel volatility reduced or eliminated the liquid fuel film on the cylinder wall and in the piston bowl. In their tests, the highly volatile fuels produced near-zero smoke in the LTC operation. Kalghatgi *et al* also suggested that in LTC operations the conventional gasoline outperformed diesel in terms of NO<sub>x</sub> and smoke emissions attributable to the higher volatility and lower Cetane number [36]. In general, a more volatile fuel facilitated the preparation of a homogeneous air-fuel mixture, thereby lowering the NO<sub>x</sub> and smoke emissions.

### **2.2.3 Impacts of Latent Heat of Evaporation**

The evaporation of the injected fuel absorbs energy from the cylinder charge. A large latent heat of evaporation therefore counteracts the temperature rise during the compression process. As a result, the lowered in-cylinder temperature (and pressure) leads to a prolonged ignition delay, a retarded ignition timing, and reduced flame

temperature. As indicated by experimental results, a fuel with a large latent heat had advantages for the LTC enabling at higher engine loads [37].

#### **2.2.4 Impacts of Fuel Composition**

Most petroleum fuels are complex blends containing over thousands of hydrocarbon species. A change of the fuel composition can result in a significant difference of the ignition and heat release processes [38-40]. Shibata *et al* demonstrated that n-paraffin tended to produce a large amount of heat release during the low temperature reactions while aromatics appeared insensitive to low temperature reactions [41-42]. Therefore, the modulation of the ignition and combustion processes could be accomplished by designing the fuel composition.

When different fuels are present simultaneously in a combustion chamber, they can interact with each other. For instance, the ethanol fuel could inhibit the OH formation [43] and thus reduced the heat release from the low temperature reactions, resulting in prolonged ignition delay [44]. The same effects were reported by Saisirirat *et al* using fuel blends of n-heptane with ethanol, n-butanol, and iso-octane respectively, among which the addition of ethanol showed the most significant effect [45]. Similarly, Lu *et al* investigated methanol, ethanol, and iso-propanol and their inhibiting effects on the n-heptane HCCI combustion [46-48], and the test results suggested the methanol had an even stronger effects than ethanol on retarding the ignition timing. The use of these fuels as reaction suppressors helped to expand the LTC operating range [49].

### **2.2.5 Impacts of Fuel-borne Oxygen**

In comparison to conventional gasoline and diesel fuels that do not contain oxygen, the oxygenated fuels (*e.g.* biodiesel) have shown advantages for the LTC enabling. Zheng *et al* demonstrated the engine operation with neat biodiesel running in the LTC mode [50]. The fuel-borne oxygen helped to lower the smoke emissions and thus alleviated the negative impact from the use of high EGR rates [51-52]. The biodiesel combustion also exhibited low cycle-to-cycle variations and robust combustion stability [53-54].

## **2.3 LTC Enabling with Different Fuels**

The fundamental studies normally employ fuel blends of primary reference fuels (*i.e.* iso-octane and n-heptane) for desired fuel properties to achieve LTC operations. The use of commercial fuels is also an active research field for enabling LTC. The literature review in the next sections focuses on the LTC research using commercially available fuels, which provides a guideline for the selection of the research fuels used in this dissertation.

### **2.3.1 Low Temperature Combustion with Gasoline**

The port fuel injection is usually applied in a majority of the gasoline LTC research, while the lean-burn HCCI is a primary LTC combustion mode using the gasoline fuel. In the conventional operation of a gasoline engine, the spark events determine the ignition of a precisely metered stoichiometric mixture. However, a successful ignition becomes challenging in the lean-burn HCCI combustion mode. In order to solve the ignition problem, researchers apply additional control techniques such as pre-heating the intake, increasing the compression ratio, and trapping residual gas [55-59]. It is noted that the gasoline HCCI suffers the major drawback of limited engine load range.

Recently, Dec *et al* substantially expanded the gasoline HCCI load range with well controlled intake boost and EGR applications [60-61]. Other researchers have also demonstrated improved engine performance using the combination of intake boost and internal and/or external EGR applications at extended engine loads [62-65]. In general, the advanced air handling (*e.g.* boost and EGR) is critical for the implementation of gasoline HCCI.

### **2.3.2 Low Temperature Combustion with Diesel**

The control of the intake boost and the EGR rate is also of great importance for diesel LTC enabling [66-70]. A gradient of the in-cylinder air-fuel ratio is created as the fuel enters the combustion chamber [71]. The dilution of the intake air with EGR assists to reduce the fuel-rich and stoichiometric regimes, and thus lowers the flame temperature [72]. A number of researchers have made substantial progresses on enabling and controlling the LTC engine operation through precisely modulated intake boost, EGR, and intake valve timing [73-77].

The fuel injection plays an increasingly important role in the diesel LTC enabling, as the common-rail high-pressure injection system and electronically controlled fuel injectors offer a higher degree of control flexibility over the fuel injection. These technologies allow the diesel fuel to enter the combustion system in a controllable manner. For instance, the electronic injection control permits multiple injection events to occur at desired crank angles. Therefore, innovative injection strategies have been developed to deliver the fuel at early and/or late timings to improve the air-fuel mixing [78-82]. The fuel injection strategies will be discussed in Section 2.4.

### **2.3.3 Alternative Fuels**

In addition to conventional gasoline and diesel fuels, the use of alternative fuels has shown substantial progress in clean combustion research. The literature review therefore covers the research with alternative fuels including natural gas, dimethyl ether (DME) and alcohol fuels.

#### **2.3.3.1 Natural Gas**

Natural gas or compressed natural gas comprises mainly methane ( $\text{CH}_4$ ) along with a series of other light hydrocarbons. The strong carbon-hydrogen bonds make methane almost inert to oxidation in the low and medium temperature ranges. Therefore, the natural gas compression ignition commonly requires additional intake heating or increased compression ratios [83-84]. Some researchers also apply the exhaust rebreathing to enhance the ignition quality of the natural gas [85-86].

In general, the natural gas application for LTC (*e.g.* HCCI) has major concerns stemming from the consistency of the fuel composition depending on the gas source, in addition to the higher levels of unburned HC emissions. Experimental results also demonstrated that an increase of the higher hydrocarbons in natural gas could lower the ignition temperature significantly [40]. The practical use of the natural gas in HCCI combustion hence requires advanced adaptive control strategies to compensate the potential change of fuel composition.

#### **2.3.3.2 Dimethyl Ether**

On diesel engines, the use of dimethyl ether (DME) can yield comparable energy efficiency with significantly improved smoke emissions [87-89]. The DME fuel has a

high Cetane number of 60. The fuel auto-ignites spontaneously when directly injected into the combustion chamber. Even under diffusion burning, due to the extremely high fuel volatility along with hefty fuel-borne oxygen (34.8% by mass), the DME combustion typically produces near-zero smoke.

Depending on the fuel injection strategies, the NO<sub>x</sub> emissions of the DME combustion are comparable to those of the conventional diesel HTC, which necessitates the use of EGR. Although the DME high-pressure direct-injection shows a great potential for engine applications, it requires significant modifications to the existing fuel injection system. For instance, additional cooling is necessary to avoid vaporization along the low-pressure fuel lines. Furthermore, certain DME properties inherently oppose the high-pressure injection. The inadequate lubricity can damage the high-pressure fuel pump in a short running time, while the use of lubricity additives may increase the cost. The low fuel viscosity incurs a substantial amount of internal leakage in the plunger chamber of the pump, which ultimately requires a larger pump size that normally consumes extra energy.

Researchers also applied the DME intake port injection to run HCCI type of combustion. DME usually presented strong low temperature reactions and therefore exhibited two-stage combustion [90]. The early low temperature reactions could cause engine knocking, and the early heat release in the compression stroke produced negative work, deteriorated the engine efficiency, and limited the feasible engine load. In order to overcome these challenges, researchers typically applied lower compression ratios with heavy EGR usage [91-93].

### **2.3.3.3 Alcohol Fuels**

Another actively studied fuel group is the alcohol fuels. At present, the alcohol fuels are primary alternatives to potentially replace fossil fuels. In Brazil, for instance, the ethanol fuel has become the main fuel for light-duty vehicles [94]. In the research community, the most investigated alcohol fuels include methanol, ethanol, and butanol. These alcohol fuels have similar physical properties to gasoline. The studies commonly focus on the HCCI type of combustion on gasoline engines. Due to the high Octane rating, alcohol fuels allow the use of higher compression ratios and researchers often apply additional intake heating to elevate the initial temperature of the cylinder charge for successful ignition [95]. Compared with gasoline, the experimental results indicate that the alcohol fuels are more suitable for LTC in the lean-burn operation [96].

In the studies with diesel engines, the alcohol fuels are normally blended with the diesel fuel. The low reactivity of the alcohol fuels reduces the overall Cetane number of the fuel blends and, as a result, the ignition delay is generally prolonged [97]. The combustion of such fuel blends usually exhibit a greater extent of premixed combustion. Accordingly, the addition of the alcohol fuels leads to a reduction in the smoke emissions [98]. However, the reduction of NO<sub>x</sub> emissions still requires EGR application [99]. In general, the use of the alcohol fuels incurs penalty of increased HC emissions.

## **2.4 Fuelling Strategies for LTC Enabling**

In addition to the use of different fuels, the fuel delivery also plays a vital role for the LTC enabling. In Figure 2.1, a comparison is made for the fuelling strategies of conventional and novel combustion modes in compression ignition engines [100]. In the

conventional direct-injection engines, the fuel delivery occurs near the compression top dead centre (TDC). In most cases, the combustion starts during the fuel injection process, and the combustion rate is primarily controlled by the mixing rate. On the contrary, novel combustion modes either advance or postpone the injection events away from the conventional injection timing window and, assisted by other control measures (*e.g.* EGR), create separations between the injection and combustion events to provide a prolonged mixing time. When the engine runs on conventional diesel fuels, the off-timing injection strategies typically result in off-phasing combustion.

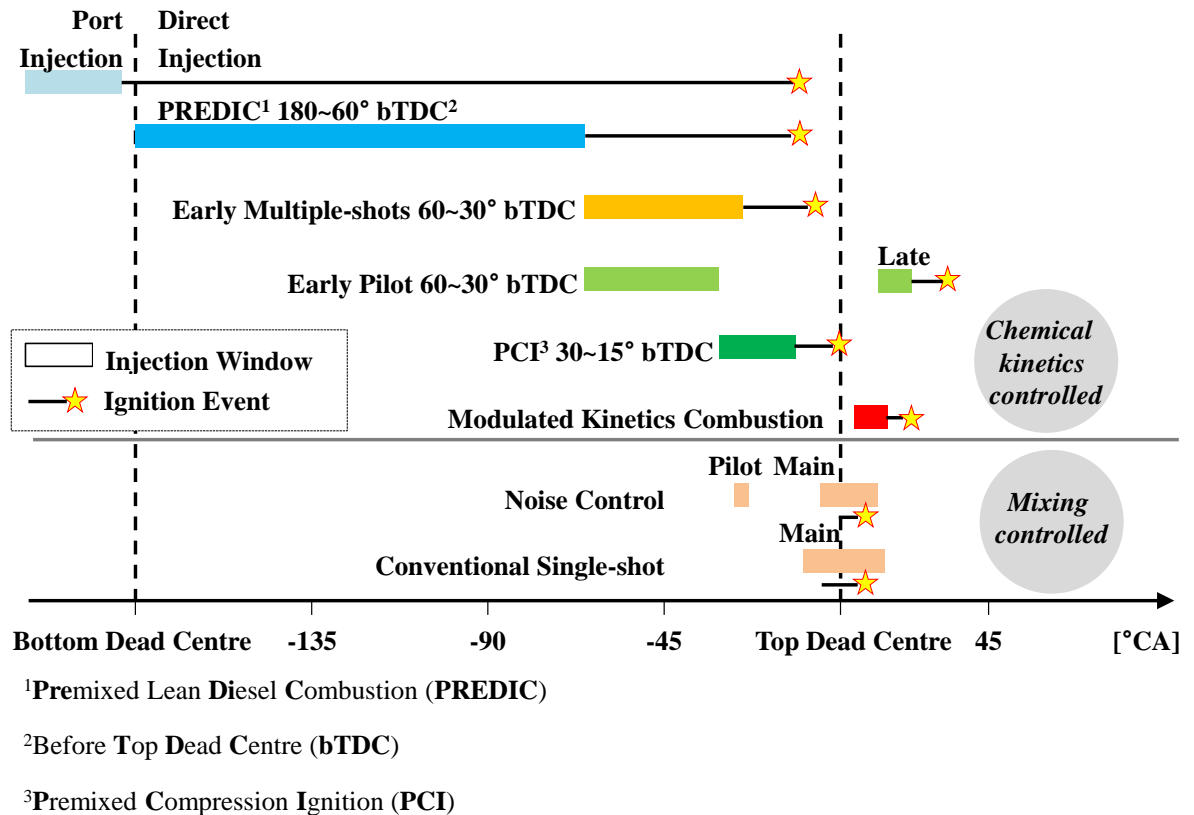


Figure 2.1 Injection Strategies for Diesel Combustion

It is important to understand that the unconventional fuelling strategies may not match properly with the fuel properties for a particular fuel. For instance, due to the low volatility, the use of the port-injection with regular diesel typically requires additional intake heating to avoid significant wall wetting and fuel condensation; however, the high Cetane number and the elevated intake temperature can lead to excessively early auto-ignition.

The fuelling strategies also need to accommodate different engine operating conditions, such as a transient load change. It is thus desirable to have the ability to modulate the fuel properties and adjust the fuelling strategies in real time. Recent studies have shown promising progress with the dual-fuel applications. In the dual-fuel application, a less reactive fuel (*e.g.* gasoline) is delivered at the intake port to form a highly homogeneous air-fuel mixture prior to the ignition, and diesel pilots are directly injected into the combustion chamber to initialize the combustion events. The injection control can therefore dynamically modulate the preparation process of the cylinder charge by adjusting the ratio between the two fuels [101-103].

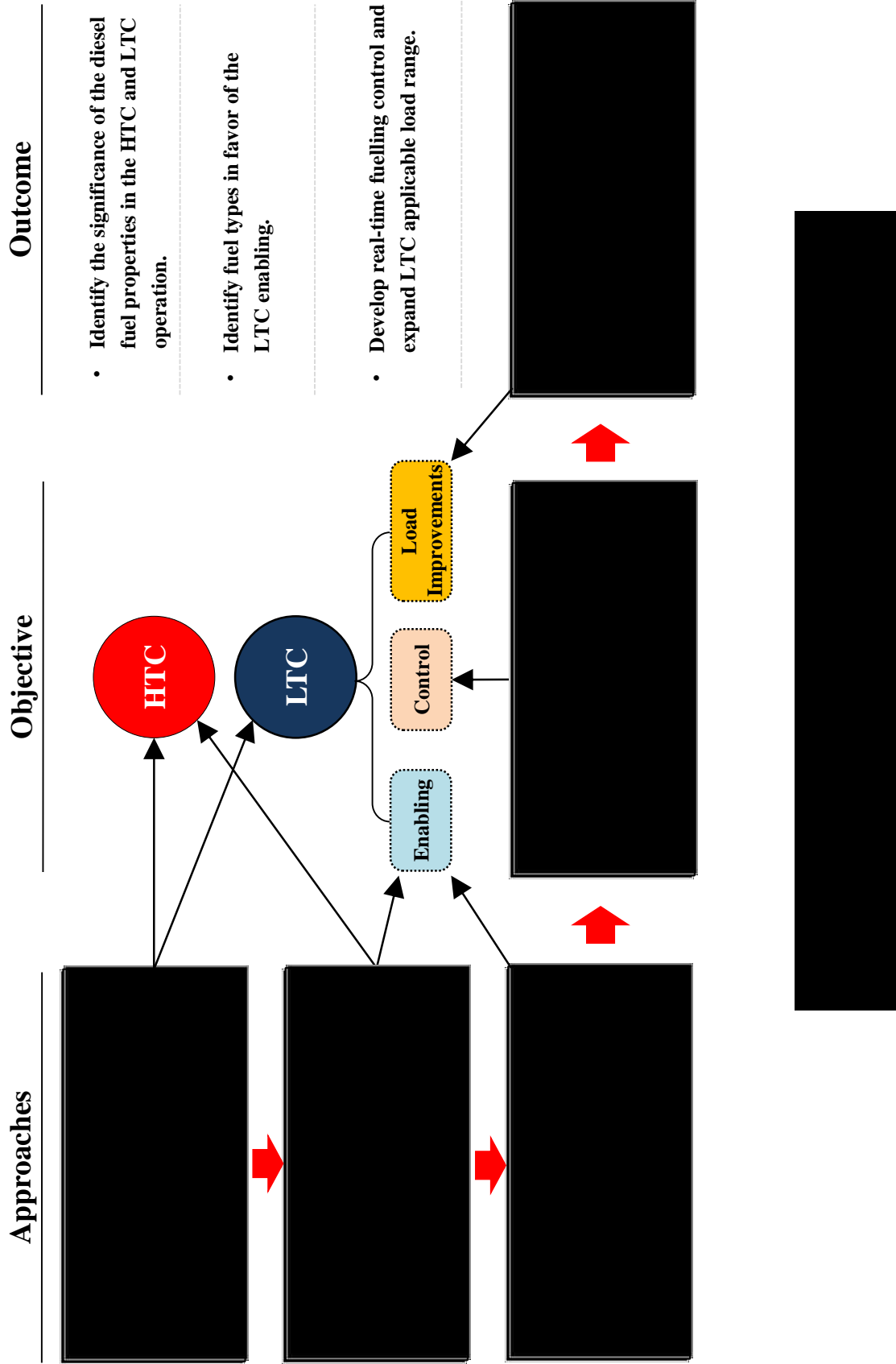
In summary, the literature review indicates that the LTC operation in compression ignition engines is typically applicable within limited load ranges and under tightly controlled engine operating conditions. The change of fuel types is one possibility to extend the achievable engine load, while the use of lowered compression ratios is another feasible option. However, it is extremely difficult to find research results of LTC studies with high compression ratios and under high load operations at the same time. This dissertation therefore aims to provide solutions to these challenges by investigating the fuels and fuelling strategies for LTC enabling on high compression ratio diesel engines.

## CHAPTER III

### METHODOLOGY

The literature review in Chapter II has shown the importance of the fuel types, fuel properties, and fuelling strategies to the enabling of low temperature combustion. In order to study their impacts on the combustion control and exhaust emissions, this dissertation primarily relies on the experimental approaches that, in part, are supported by numerical simulations, as shown in Figure 3.1. The conventional HTC and advanced LTC engine operations are compared through engine experiments. The LTC study mainly focuses on three aspects, namely the enabling, control, and high load improvements.

The numerical simulations are firstly performed to identify the boundary conditions for the subsequent empirical engine experiments, with emphases on the maximum pressure rise rate and the peak cylinder pressure. In order to develop in-depth understanding of the fuel property effects, the empirical investigation starts with nine different diesel fuels of specifically formulated Cetane numbers, aromatic contents, and boiling temperatures. These nine fuels are known as *fuels for advanced combustion engines* (FACE). The LTC enabling is further investigated using fuels that are drastically different from a conventional diesel, including n-butanol, gasoline, and ethanol. The fuelling strategies are developed to accommodate different fuel types and engine operating conditions. An active LTC control algorithm is implemented for LTC improvements by modulating the fuel injections in real time. The active LTC control ultimately assists to achieve LTC operations at high loads that are considered extremely challenging to realize on a high compression ratio engine with conventional diesel fuels.



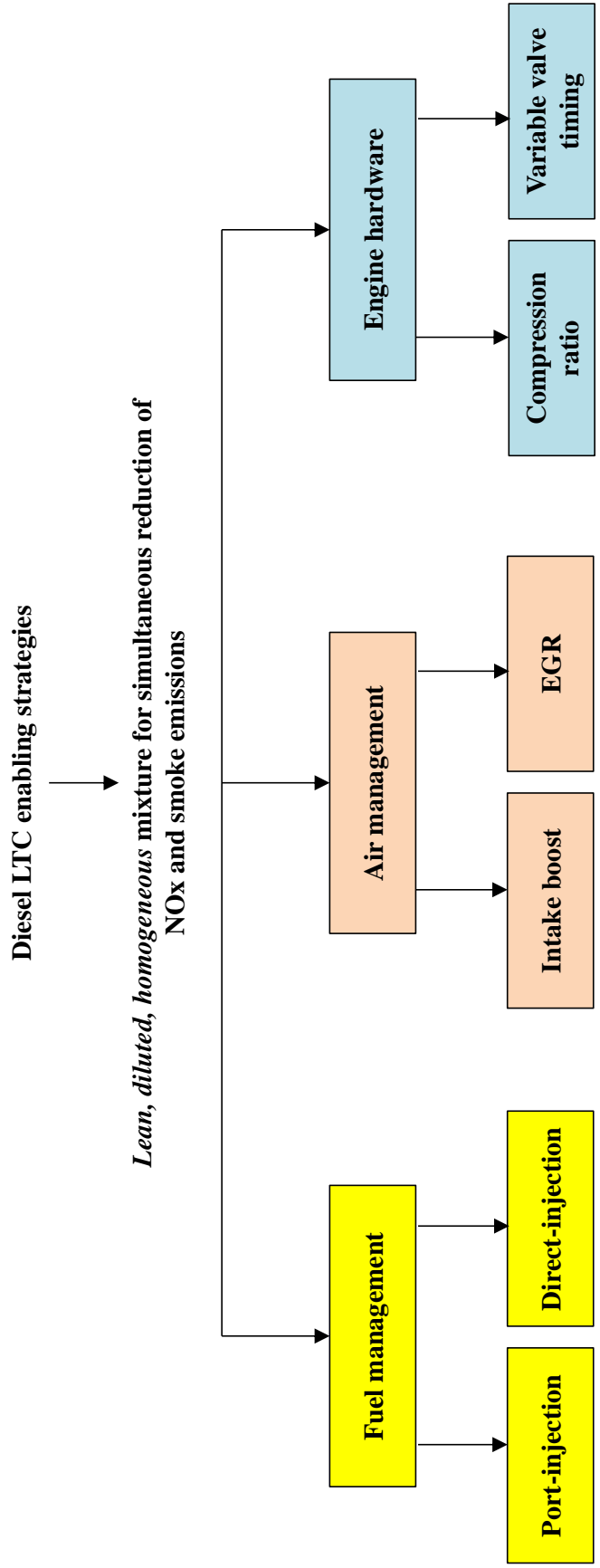
### **3.1 Numerical Simulation**

Due to the complexities of the diesel combustion process, especially in LTC, high-fidelity simulations of the exhaust emissions are considered as beyond the current combustion models' capability. Nevertheless, when tuned appropriately according to a particular engine setup, numerical simulations can calculate the cylinder pressure with an acceptable accuracy to represent the combustion process. In that sense, simulations can become a convenient research tool to analyze possible experimental extremes and effectively help to identify the permissible boundary conditions in the experiments.

In this dissertation, a zero-dimensional code, developed by the Clean Diesel Engine Group at University of Windsor, is used to help to identify the boundary conditions for the subsequent empirical studies. The simulation results indicate that the combustion phasing should be maintained in the window of 7~12 °CA after TDC for the efficient combustion. As the engine load increases, the postponement of the combustion becomes necessary to avoid excessively high pressure rise rate and peak cylinder pressure. The detailed simulation results are presented in Appendix A.

### **3.2 Empirical Investigation**

In general, researchers approach the enabling of diesel LTC from three aspects, namely the fuel management, air management, and engine hardware improvements, as shown in Figure 3.2. This dissertation primarily investigates the LTC improvements using a selected group of fuels with adaptive fuelling strategies, assisted by the advanced control over the engine air system.



### 3.2.1 Study of Fuels and Fuelling Strategies

The investigation of the fuel management focuses on three aspects: fuel types (properties), fuelling strategies, and fuelling/injection control.

#### 3.2.1.1 Research Fuels

The research fuels include ten types of diesel fuels and three other fuels, which provide a desirable range of the fuel reactivity and volatility for studying the fuel effects. The *fuels for advanced combustion engines*, also known as the FACE fuels, comprise nine diesel fuels with specifically formulated Cetane numbers, aromatic contents, and boiling temperatures (as shown in Figure 3.3). Fuel #9 at the centre of the fuel cube has almost the same properties as the regular ultra-low sulfur diesel (ULSD). The values of each fuel property are listed in Table 3.1.

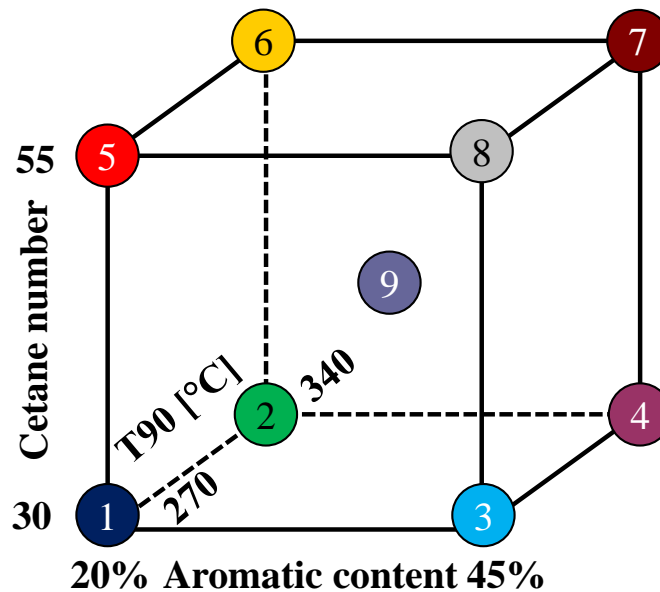


Figure 3.3 Fuels for Advanced Combustion Engines (FACE)

Table 3.1 Major Fuel Properties of FACE<sup>1</sup>

Fuel #	Cetane Number	Distillation T90 <sup>2</sup> [°C]	Aromatic, vol. %
1	29.93	269.4	22.2
2	28	336.1	19.4
3	32.02	270.0	45
4	28.44	337.2	46.6
5	54.2	275.6	19.5
6	53.3	341.1	21.3
7	44.3	267.2	42.3
8	50	342.2	43.3
9	44.95	321.1	32.5

<sup>1</sup> Note: these fuel properties are obtained from [21]

<sup>2</sup> T90: 90% distillation temperature

The additional fuels used in this work include n-butanol, gasoline, and ethanol. These fuels provide an extended range of the fuel reactivity and volatility. Their major fuel properties are compared with those of the regular diesel fuel in Table 3.2.

Table 3.2 Major Fuel Properties of Examined Fuels<sup>1</sup>

Fuel property	Diesel	n-Butanol	Gasoline	Ethanol
Density [kg/m <sup>3</sup> ]	846	813	740	788
Cetane number [-]	46.5	~25	~16	8-11
Octane number [-]	~25	~87	91	110-115
LHV [MJ/kg]	43.5	33.2	42.9	27
Oxygen content [%] (by mass)	0	21.62	0	34.78
Boiling T. [°C]	246-388	117.5	60-200	78.3
Air-fuel stoichiometry (by mass)	14.7	11.2	14.7	9
Q <sub>evaporation</sub> [kJ/kg]	316.6	595	303	728.2
Kinematic viscosity [cSt]	>3	3.64	0.4-0.8	1.52

<sup>1</sup> Note: Properties of n-butanol, gasoline, and ethanol are obtained from [104].

These additional fuels have lower Cetane numbers and lower boiling temperatures compared to the regular diesel fuel used in this research. In Figure 3.4, a comparison is made for the boiling temperatures and auto-ignition temperatures for n-butanol, gasoline, ethanol and diesel, against the in-cylinder mean temperature traces during the compression stroke at different compression ratios. It should be noted that the boiling temperatures and the auto-ignition temperatures are often obtained under ambient

pressure. As indicated by Figure 3.4, only diesel among the four fuels has an auto-ignition temperature lower than its distillation temperature range (T10~T90). The other three fuels tend to withhold the auto-ignition and evaporate fast, which allows extended mixing prior to the onset of combustion and assists the preparation of a highly homogeneous cylinder charge. Moreover, the fuel-borne oxygen contents in n-butanol and ethanol are deemed helpful for smoke reduction, particularly at the high engine load conditions [105].

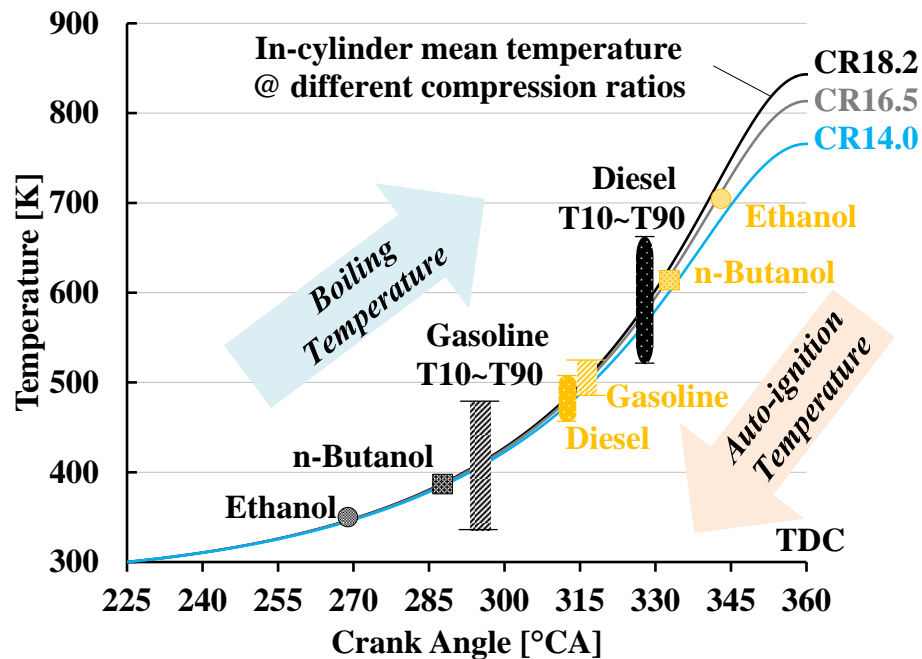


Figure 3.4 Fuel Boiling Temperature Range, Auto-ignition Temperature

### 3.2.1.2 Fuelling Strategy Investigation

The research employs a number of fuelling strategies for the LTC enabling (Figure 3.5). In general, the fuel delivery can be categorized into two methods, namely the intake port injection and the high-pressure direct-injection. Based on the compatibility, the port-injection is applied to n-butanol, gasoline, and ethanol fuels, while the high-pressure

direct-injection is applied to n-butanol and diesel fuels. With the intake port injection, the HCCI type of combustion is studied. On the other hand, the common-rail direct-injection offers the flexibility of modulating the number of injections and adjusting the injection timing for each injection event. Therefore, the investigated fuelling strategies include the single-shot near-TDC injection, the early multi-pulse injection, and the early pilots plus the main injection. In addition, the dual-fuel application, which simultaneously employs the intake port injection and the high-pressure direct-injection to improve the preparation and ignition of the cylinder charge, is another primary injection strategy investigated in this work.

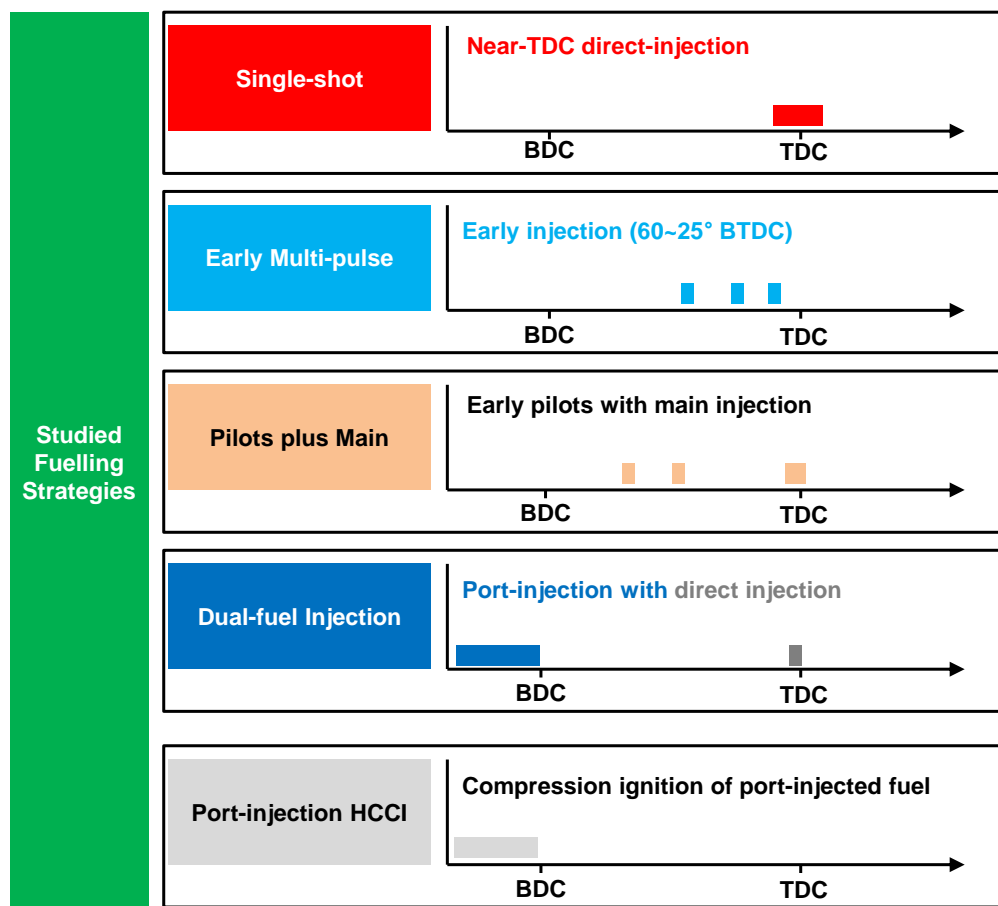


Figure 3.5 Investigated Injection Strategies

### 3.2.1.3 Advanced Fuelling Control Hardware

In order to implement the advanced fuelling strategies, the injection control requires hardware that can provide full control flexibility over the fuel pressure, injection timing, and the fuelling quantity. The injection process generally completes within extremely short durations (*e.g.* a fraction of one millisecond) and the execution runs in a fast recurring pattern (*e.g.* 20 times per second). This occurs too rapidly for human beings to timely respond to any malfunctions, but an injection malfunction may cause disastrous engine damage. Due to concerns on unexpected millisecond glitches, it is considered that the Windows™ operating system on personal computers cannot fulfill such challenging demands. The control platform hence utilizes the real-time (RT) operating systems on embedded controllers from National Instrument™ to ensure the control reliability. The overall hardware connections for the injection control are illustrated in Figure 3.6. The core computation is executed in a chassis comprising of embedded controllers and the field programmable gate array (FPGA) devices.

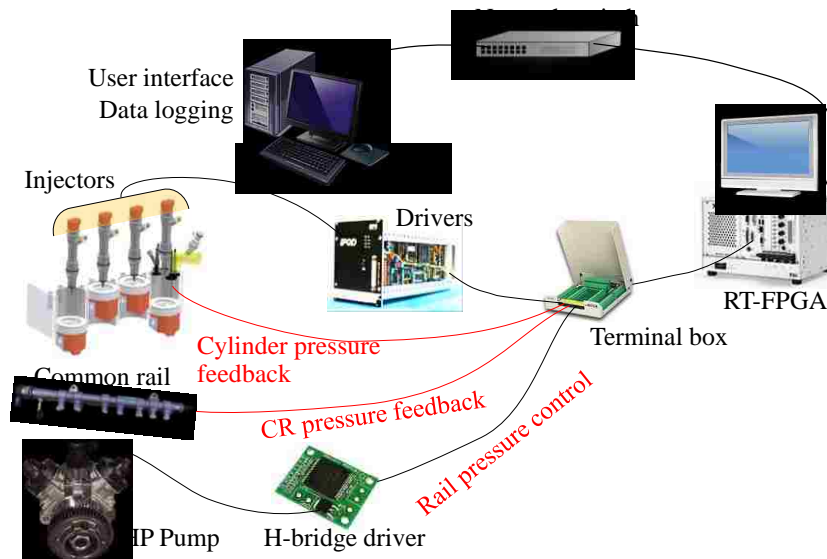


Figure 3.6 Injection Control – Hardware Connections

Through the high-speed network connection, the chassis is connected to a host computer that provides the control interface and stores data. The network traffic therefore contains commands and feedbacks for the users to intervene. The critical decisions are programmed in the RT controller and FPGA devices to respond promptly and timely. Each FPGA card is connected to a set of terminal boxes. These terminal boxes serve as the interface for the input and output signals transmitted from and to the sensors, drivers, and actuators. The injector drivers made by EFS<sup>TM</sup> are employed to receive the injection command signals from RT-FPGA controllers, and thus to energize the injector accordingly. Different models of the injector drivers are used for the piezo and solenoid injectors respectively. An H-bridge driver is used to regulate the valves on the high-pressure injection pump. The control feedback includes the common-rail pressure and the cylinder pressure signals.

### **3.2.2 Flexible Air Management Control**

The air management of this work primarily involves the modulation of the EGR and intake boost. The research platform used in this dissertation offers ideal controls over the intake boost and the EGR application.

#### **3.2.2.1 Intake Boost Control**

As shown in Figure 3.7, an air compressor with an auxiliary conditioning system is used to supply compressed air to simulate the intake boost of a turbocharged engine. The independent intake supply in lieu of a turbocharger essentially broadens the possible intake pressure range that otherwise is restricted by the turbocharger operating limits.

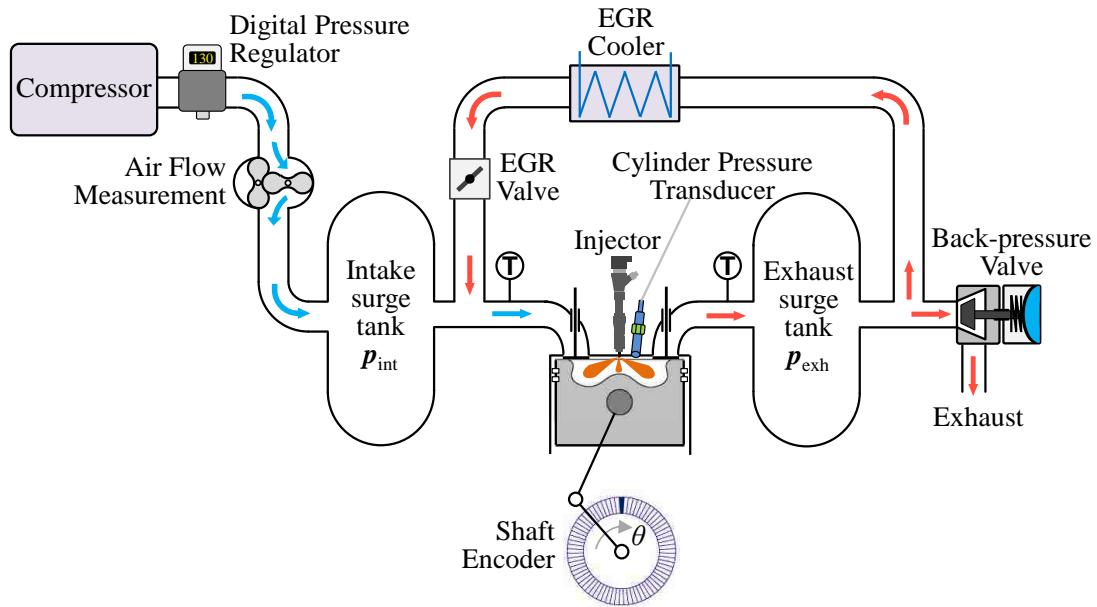


Figure 3.7 Research Engine Air System

The air is externally compressed up to 8.5 bar absolute, and a series of oil and dust filters are used to clean the air before it reaches the intake surge tank. The inclusion of a surge tank is to dampen the pressure fluctuations generated by the cyclic opening and closing events of the intake valves. It is of particular importance for the air flow rate measurement of a single cylinder engine. An electronically controlled pressure regulator is installed upstream of the intake surge tank to precisely control the intake pressure. Two pressure sensors are used to measure the intake pressure at the surge tank and the intake manifold. At the operating station, the control system comprises multiple personal computers equipped with DAQ devices. The in-house developed programs provide user-friendly interfaces to conveniently control and monitor the intake boost level. The intake boost setup also includes a safety relief valve on the surge tank. In case of the malfunction of the pressure regulators, the safety valve can release pressure to avoid combustion cycles with excessive high intake pressures.

### 3.2.2.2 EGR Control

The amount of the recirculated exhaust basically depends on the EGR valve opening and the pressure difference across the EGR valve. Typically, a digitally controlled EGR valve has discrete opening positions (*e.g.* 32 steps to fully open). As a result, the resolution of the opening steps is often insufficient to control the EGR rate precisely. In a research environment, however, the desire for a finer EGR control necessitates the differential pressure control across the EGR valve. This is achieved through the modulation of the exhaust backpressure at a given intake boost pressure.

A pneumatic valve (backpressure valve) is installed downstream of the exhaust surge tank, and the exhaust backpressure is controlled by changing the exhaust flow area (as shown in Figure 3.7). At a fixed EGR valve opening, as the engine continues pumping exhaust gas into the exhaust surge tank and the backpressure valve restricts the exhaust outflow, the pressure inside the exhaust surge tank increases, thereby creating a higher differential pressure across the EGR valve. In general, the exhaust backpressure control has finer resolution than the EGR valve opening.

In order to obtain the desired exhaust backpressure, the size of the backpressure valve needs to be matched with the engine exhaust flow rates. For a research setup, the engine exhaust flow is typically divided into three streams, namely the EGR flow, exhaust sampling, and exhaust outflow to the ambient. The exhaust sampling always requires a certain portion of the exhaust flow, and the amount may vary depending on the equipment used. In certain cases, the backpressure valve needs to have an extremely small opening (*e.g.* 5 mm<sup>2</sup>) to maintain a sufficient backpressure for achieving high EGR rates. In this scenario, small disturbances may result in substantial fluctuations in the

EGR flow. For example, the soot accumulated on the backpressure valve can fall off, which will suddenly increase the flow area and result in a backpressure drop.

The digital control over the sensors and actuators offers prompt response. However, it is also noted that the surge tanks and long piping along the engine air loops can substantially delay the overall system response.

### 3.2.3 Advanced Research Platform

In addition to the advanced fuel and air management, the research platform employs a set of additional equipment to enhance the research quality, as shown in Figure 3.8. A set of dedicated lubricant and coolant conditioning units are employed to control the engine oil and coolant temperatures (normally both set to 80°C) throughout the experiments. A dynamometer is coupled to the research engine for the speed and load management.

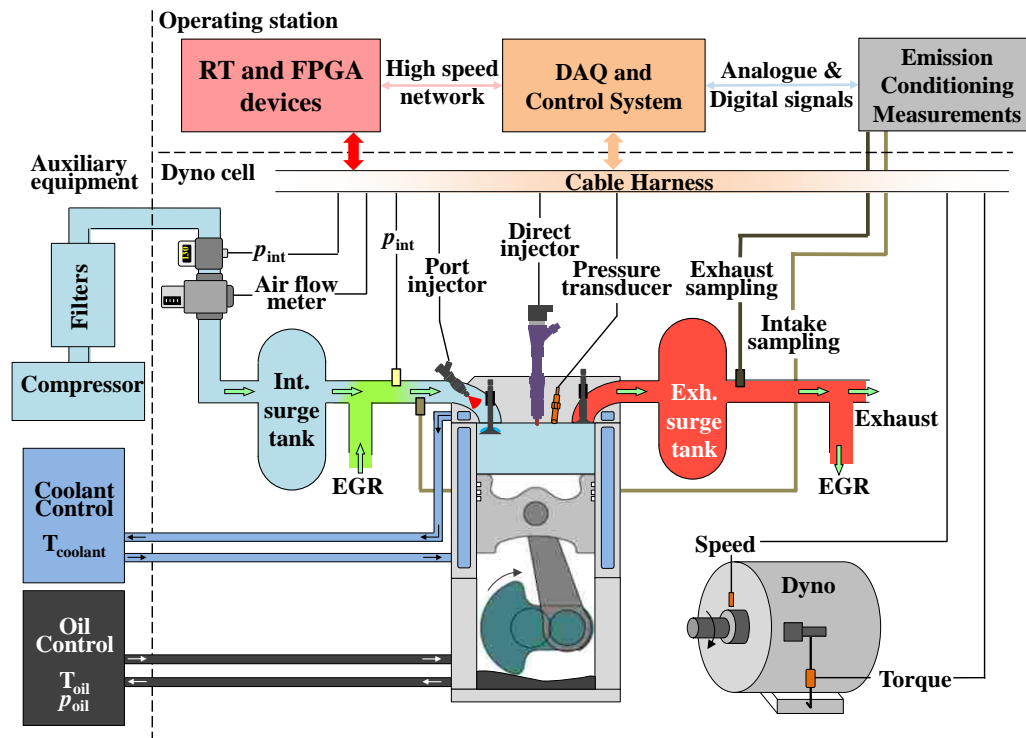


Figure 3.8 Advanced Research Platform

The research engine is comprehensively instrumented for combustion diagnosis. A pressure transducer is flush-mounted in the combustion chamber for the cylinder pressure sampling. The pressure recording for each data point is an average over 200 continuously engine cycles. An optical encoder with 0.1 degree crank angle resolution is installed on the engine crank shaft to accurately obtain the piston position. The engine operating conditions are controlled and recorded through high-speed DAQ systems.

### **3.2.3.1 Advanced Research Engines**

Two advanced research engines are used in this dissertation. The major engine specifications are tabulated in Table 3.3. The single cylinder research engine (SCRE) is designed to withstand a peak cylinder pressure of 200 bar. For the fuel injection, this engine is equipped with a Siemens common-rail injection system consisting of a piezo injector and a high-pressure pump driven by the engine. This injection system offers an injection pressure up to 2200 bar, representative of the latest technologies within this particular engine size class. As shown in Figure 3.8, the fuel system of the SCRE also includes a secondary fuel delivery at the engine intake ports. A low-pressure common rail serves as a pressurized volume reservoir for the secondary fuel delivery. One intake port injector is installed in each of the two intake runners.

The other research engine is a modified Ford production diesel engine. According to the manufacturer, this Ford engine can deliver a maximum torque of 280 Nm at 1900 rpm, which indicates a peak BMEP of 17.6 bar. The stock compression ratio (18.2:1) makes this engine significantly valuable for the intended research. Compared with prevalent compression ratios of today's diesel engines (~16:1), such a high compression (and expansion) ratio permits a greater achievable upper limit of the cycle efficiency. However,

it is also noted that the high compression ratio results in increased compression pressure and temperature, which challenges the LTC enabling. Similar to the SCRE, the Ford research engine also includes a secondary fuelling system at the intake ports. Stand-alone fuel carts are fabricated to deliver different secondary fuels.

Table 3.3 Engine Specifications

Research Engine	SCRE	Ford Duratorq
Engine Type	Single Cylinder 4-Stroke	4-Cylinder <sup>1</sup> 4-Stroke
Displacement [cm <sup>3</sup> ]	744	1998
Bore x Stroke [mm]	95 x 105	86 x 86
Compression Ratio [-]	16.2:1	18.2:1
Max. Cylinder Pressure [bar]	200	180
Piston Bowl	Stepped Omega	Deep Omega
Swirl Ratio [-]	~1.5	1.7
Direct-injection System	Common-rail (max. 2200 bar)	Common-rail (max. 1600 bar)
Direct Injector	Piezo, 7 hole Umbrella angle 156°	Solenoid, 6 hole
Port-injection System	Low-pressure rail (5 bar abs)	Low-pressure rail (up to 7 bar abs)
Port Injector	Gasoline type injector One per each port	Gasoline type injector One per each port

<sup>1</sup> The 4-cylinder production engine is reconfigured into a single cylinder research engine

### 3.2.3.2 Evaluation of Engine Emissions

The combustion products are quantified by emission analyzers. Besides the regulated emissions (*i.e.* NO<sub>x</sub>, unburned HC, CO, and smoke), additional gases (CO<sub>2</sub> and O<sub>2</sub>) at the engine intake and exhaust are required to be measured in a research setup for engine control and combustion analysis.

The gas sampling points are located at the intake and exhaust manifolds respectively. A heated sampling line is used to sample the exhaust gas at a temperature of 191°C according to the EPA requirements [108]. The sampled gas first passes an in-house built conditioning unit that removes particulates and water before it reaches the analyzer benches. The analyzers are listed in Table 3.4. The engine performance evaluation (*e.g.* IMEP calculation) and emission conversion (ppm to g/kW-hr) are shown in Appendix B.

Table 3.4 Emission Analyzers

Analyzer Type	Measured Emissions	Model
Paramagnetic	O <sub>2</sub> [%]	CAI 602P
Heated Flame ionization (HFID)	THC [ppm]	CAI 300M HFID
Non-dispersive infrared (NDIR)	CO [ppm] CO <sub>2</sub> [%]	CAI 200/300 NDIR
Chemiluminescence (CLD)	NO & NO <sub>2</sub> [ppm]	CAI 600 HCLD
Smoke meter	Smoke [FSN]	AVL Model 415S

## CHAPTER IV

### BENCHMARKING OF FUEL PROPERTY IMPACTS

A diesel fuel is constituted of a variety of hydrocarbons. As suggested in the literature, the fuel composition changes can lead to variations of the chemical and physical properties of the diesel fuel over a wide range. Moreover, the fuel properties significantly affect the combustion processes and hence the exhaust emissions. This chapter therefore explores a set of diesel fuels (known as the FACE fuels) with specifically formulated Cetane numbers, aromatic contents, and boiling temperatures. Compared with the effects on the conventional HTC, the difference of fuel properties has much greater impacts on the LTC process where a prolonged duration is available for the physical mixing and chemical reactions of the cylinder charge prior to the start of main combustion events.

In order to fairly compare the effects of the fuel property variation, the engine operating conditions are kept consistent in the experiments for all the fuels. The fuel swapping process follows a rigid procedure to prevent cross contamination. The major experiment conditions are summarized in Table 4.1. For the reported data, the engine runs at a constant speed of 1671 rpm. The results are obtained at three engine load levels, namely 5.5, 10.6, and 14.6 bar IMEP, which adequately cover the load range of typical light-duty operation of on-road vehicles. The pressure settings of the engine intake and the fuel injection are commensurate with the engine load, to match those of a modern production diesel engine. For each of the nine fuels, the engine runs EGR sweeps at the three engine loads, and the EGR addition gradually increases until the NO<sub>x</sub> emissions decrease to levels below 0.2 g/kW-hr. The following subsections present the findings derived from extensive experimental results.

Table 4.1 Engine Operating Conditions for Diesel Property Study

IMEP	$p_{int}$	$p_{inj}$	CA50	Sweep	NOx	Peak Smoke
[bar]	[bar abs]	[bar]	[°CA]	[-]	[g/kW-hr]	[FSN]
5.5	1.45	700	372.5	EGR	0.15~1	2.5
10.6	2.3	1300	372.5	EGR	0.15~1	5.5
14.6	2.8	1600	372.5	EGR	0.18~1	6

#### 4.1 Fuel Property Effects on NOx Emissions

The intake O<sub>2</sub> concentration is used to represent the EGR level. In Figures 4.1 to 4.3, the NOx emissions are shown for the nine fuels across the EGR sweeps at different engine load conditions.

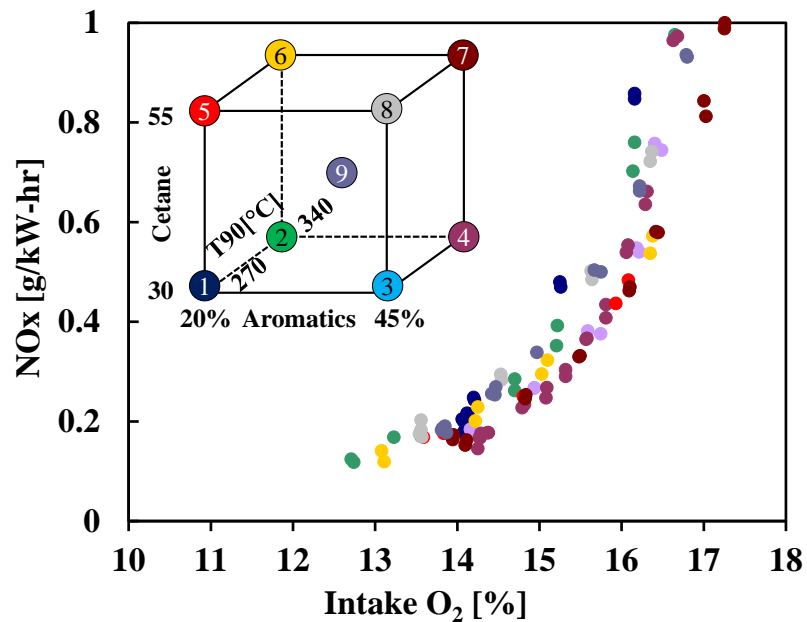
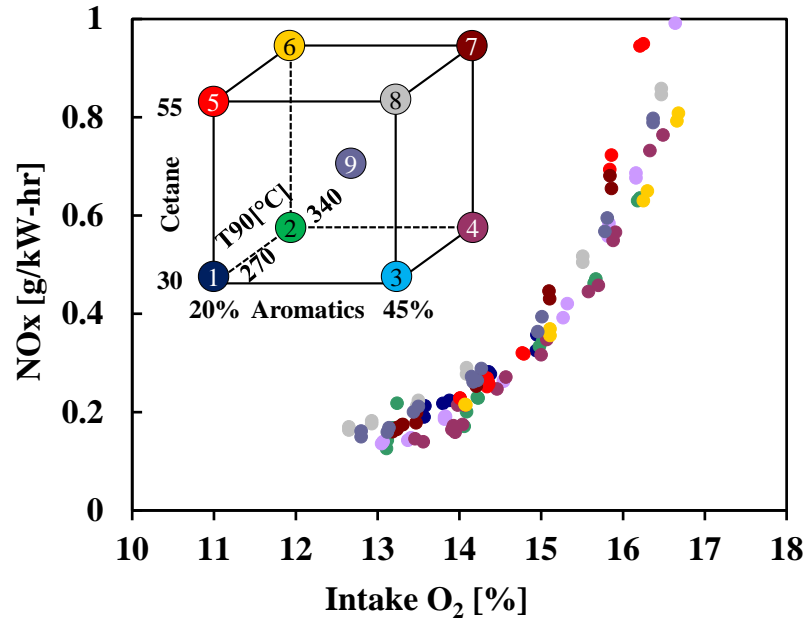
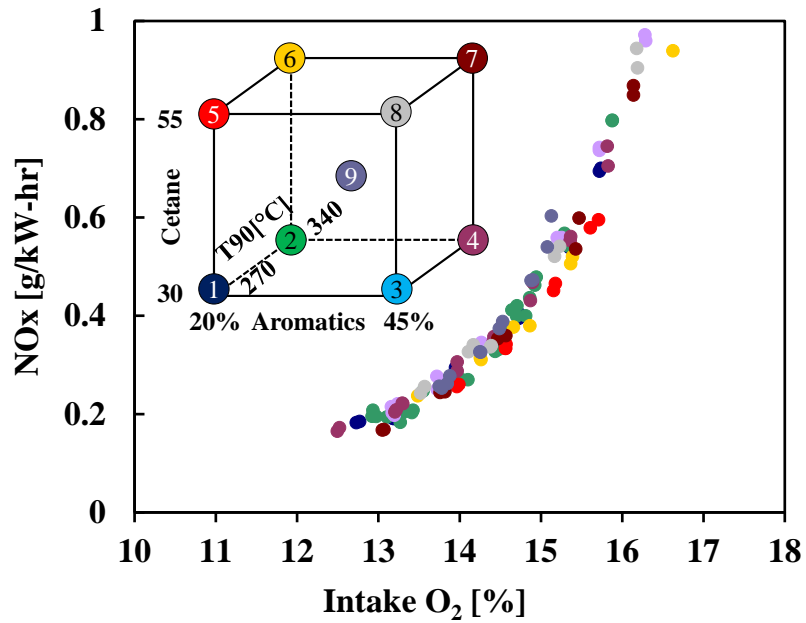


Figure 4.1 FACE EGR Sweep 5.5 bar IMEP – NOx

Figure 4.2 FACE EGR Sweep 10.6 bar IMEP – NO<sub>x</sub>Figure 4.3 FACE EGR Sweep 14.6 bar IMEP – NO<sub>x</sub>

Within the investigated range, the fuel property changes merely affect the NO<sub>x</sub> emissions, while the EGR application has a predominant effect. As the EGR addition decreases the intake O<sub>2</sub> concentration progressively, the NO<sub>x</sub> emissions reduce monotonically for all the fuels. The NO<sub>x</sub> emissions of different fuels largely overlap with one another, especially when approaching the desired low levels (*e.g.* below 0.5 g/kW-hr). As the engine load increases, the extent of the overlap becomes even greater.

#### 4.2 Fuel Property Effects on Smoke Emissions

The smoke emissions are often evaluated by the NO<sub>x</sub> versus smoke trade-off for diesel engines. While minor, albeit inconclusive, impacts are observed on the NO<sub>x</sub> emissions, the changes of fuel properties have noticeable effects on the smoke emissions. In Figures 4.4 to 4.6, the NO<sub>x</sub> and smoke emissions are shown for the nine fuels across the EGR sweeps.

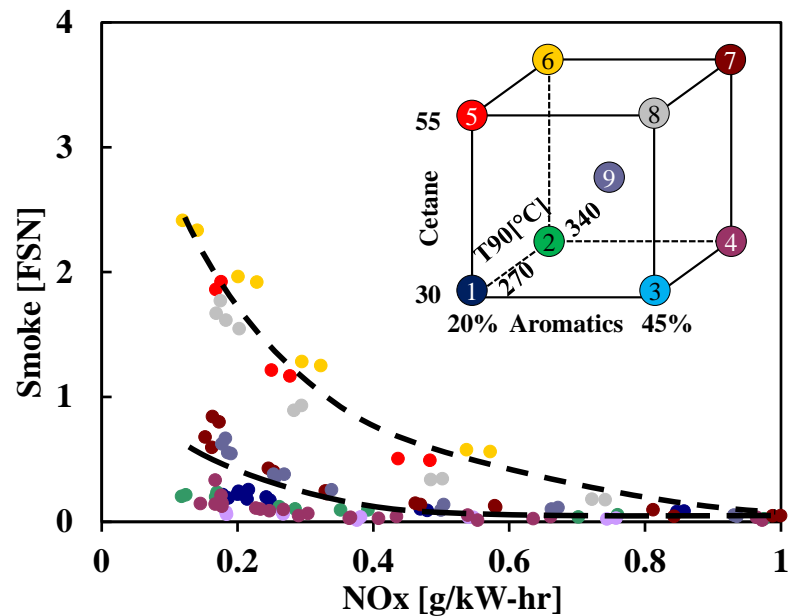


Figure 4.4 FACE EGR Sweep 5.5 bar IMEP – Smoke NO<sub>x</sub> Trade-off

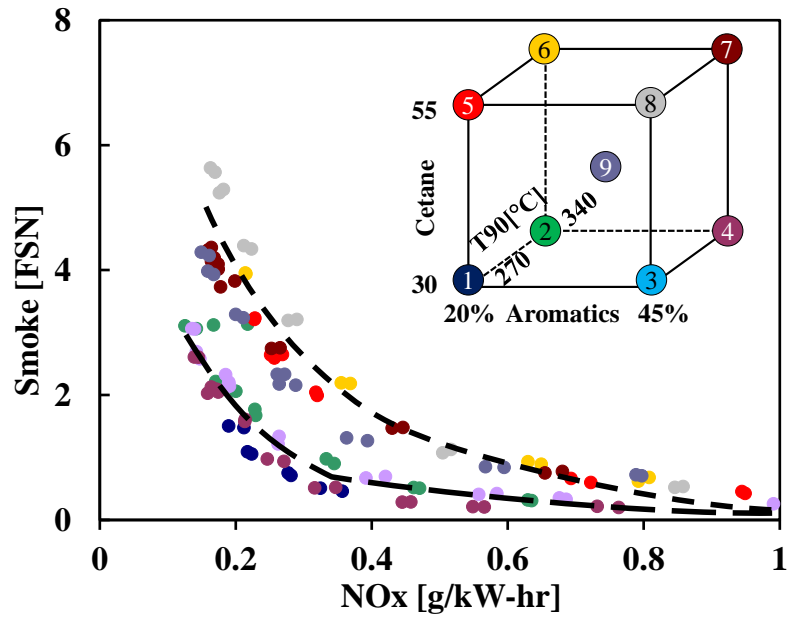


Figure 4.5 FACE EGR Sweep 10.6 bar IMEP – Smoke NOx Trade-off

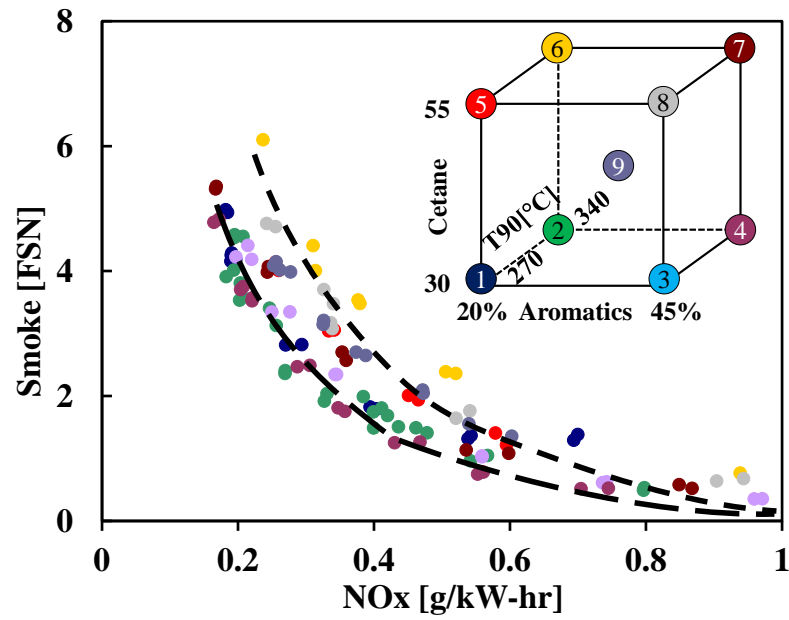


Figure 4.6 FACE EGR Sweep 14.6 bar IMEP – Smoke NOx Trade-off

These results indicate that the effects of the Cetane numbers outweigh those of the aromatic contents and the boiling temperature. By large, the low Cetane fuels offer improved smoke emissions when the NO<sub>x</sub> emissions decrease to desired low levels (*e.g.* below 0.5 g/kW-hr). However, the benefits from using low Cetane fuels become less significant as the engine load increases.

### **4.3 Cetane Number Effects on Ignition Delay and Smoke Emissions**

In order to better understand the influence of the Cetane number, the ignition delay is calculated and correlated to the smoke emissions. The ignition delay herein, for the convenience of reporting, is defined as the time period between the start of the injection command and the crank angle of 5% heat release (CA5). As shown in Figures 4.7 to 4.9, the fuel Cetane numbers are examined for the effects on the ignition delay and smoke emissions by comparing fuels #1, 2, 5, and 6. These fuels are intentionally selected to exclude the influence of the aromatic variation, as they have similar aromatic contents.

The results demonstrate that the progressively increased EGR prolongs the ignition delay for all selected fuels. Moreover, it is easy to distinguish two fuel groups based on the ignition delay durations, namely the low Cetane fuels with longer ignition delay and high Cetane fuels with shorter ignition delay. The smoke emissions also correlate well with these two groups. A longer ignition delay generally leads to reduced smoke emissions. The results also indicate that the fuel volatility (represented by T90) has minor effects on the ignition delay under the engine testing conditions.

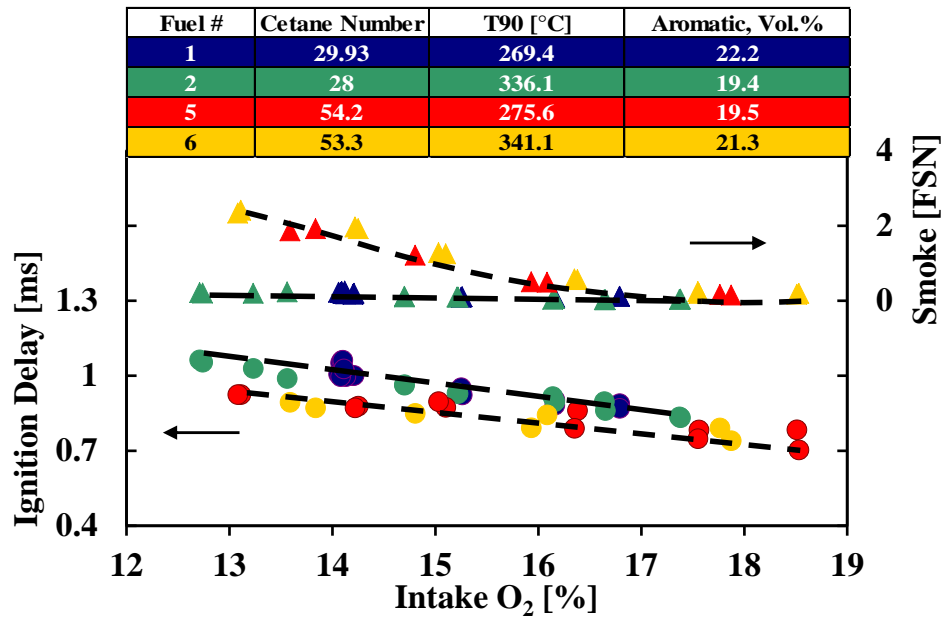


Figure 4.7 Cetane Effect 5.5 bar IMEP – Ignition Delay, Smoke

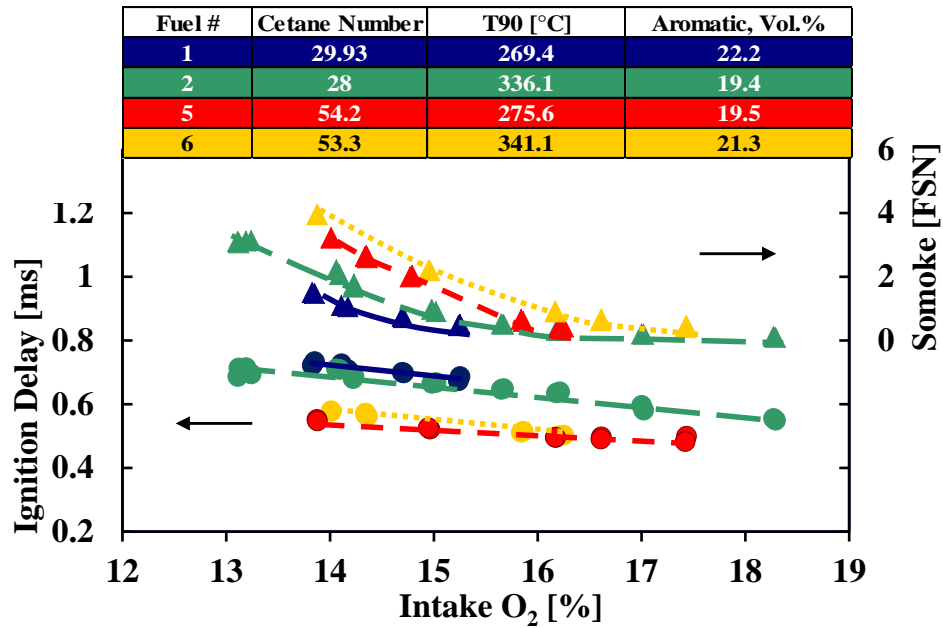


Figure 4.8 Cetane Effect 10.6 bar IMEP – Ignition Delay, Smoke

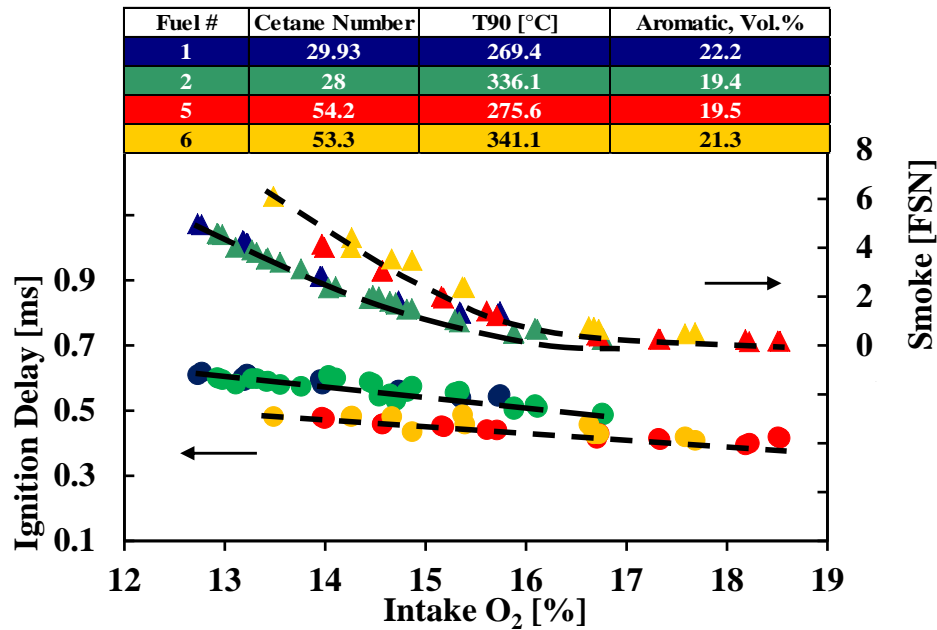


Figure 4.9 Cetane Effect 14.6 bar IMEP – Ignition Delay, Smoke

In Figure 4.10, a comparison is shown for the heat release rate and cylinder pressure traces of fuel #2 and fuel #6 at the low engine load. Comparing these two fuels, the low Cetane fuel (fuel #2, Cetane number 28) has a slower ignition process with apparent pre-reactions prior to the start of main combustion events; on the other hand, the high Cetane fuel (fuel #6, Cetane number 53.3) exhibits a much faster ignition process and a higher peak heat release rate. In order to keep the same combustion phasing (CA50), the injection timing for fuel #2 is advanced by 4.5°CA from that for fuel #6. The smoke emissions decrease from 1.92 FSN (fuel #6) to 0.24 FSN (fuel #2).

The same comparisons are made at the medium and high engine loads (as shown in Figures 4.11 & 4.12). As the engine load increases, the pre-reactions become less obvious for the low Cetane fuel (*i.e.*). Nonetheless, fuel #2 still exhibits a lesser degree of diffusion burning and offers reduced smoke emissions.

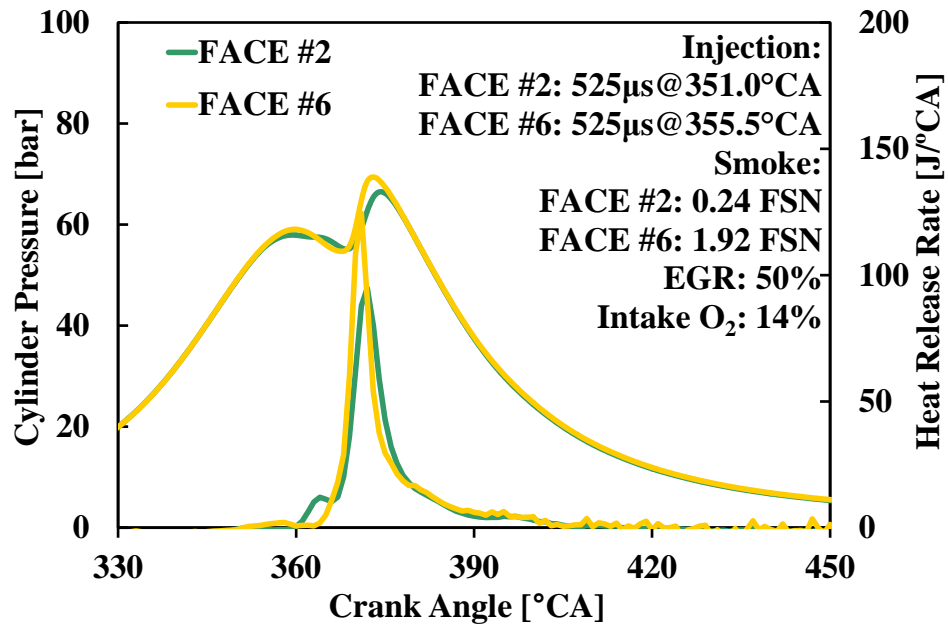


Figure 4.10 Cetane Number Effect 5.5 bar IMEP – Pressure, Heat Release

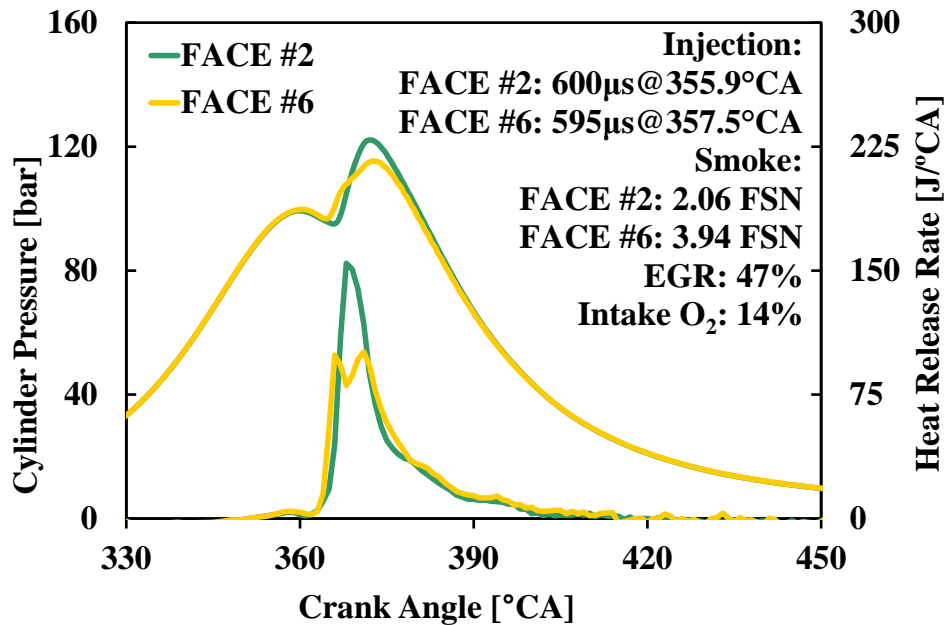


Figure 4.11 Cetane Effect 10.6 bar IMEP – Pressure, Heat Release

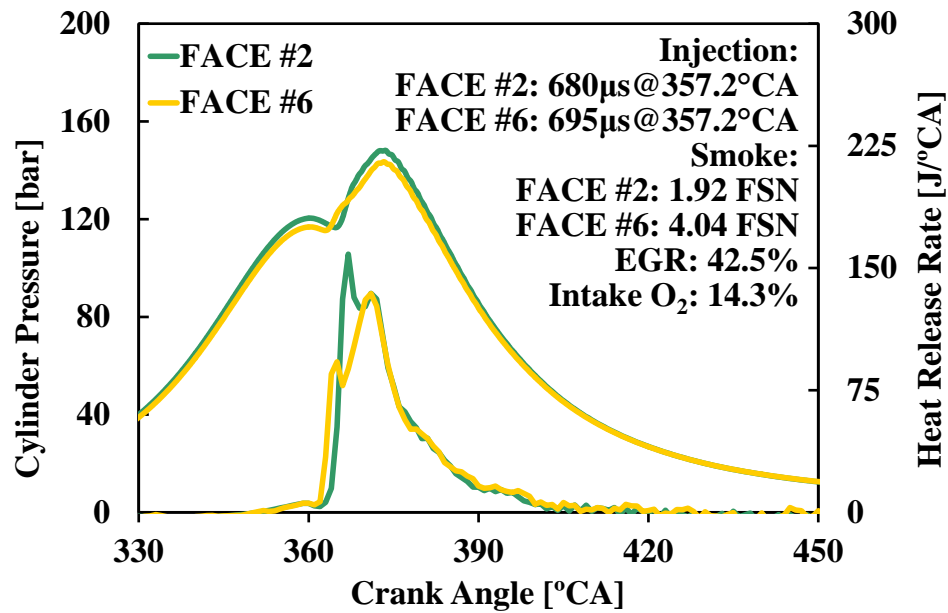


Figure 4.12 Cetane Effect 14.6 bar IMEP – Pressure, Heat Release

As the fuelling rate increases at high engine loads (Figure 4.12), the heat release profiles of both fuels present two humps, despite the large difference in their fuel Cetane numbers. The sharp rise of the heat release rate occurs earlier but lesser for the high Cetane fuel. In the presented case, the combustion of fuel #6 produces 4.04 FSN of smoke emissions, compared to 1.92 FSN for fuel #2. The heat release rate profiles indicate that the high Cetane fuel tends to produce a greater degree of diffusion combustion, which contributes to the high smoke emissions.

#### 4.4 Aromatic Effects on Ignition Delay and Smoke Emissions

The aromatic contents can affect the ignition delay of diesel fuels. In general, a higher aromatic content leads to a prolonged ignition delay. Fuels #1, 2, 3, and 4 have varied aromatic contents but similar Cetane numbers, and they are therefore selected to study the aromatic effects on the ignition delay and smoke emissions.

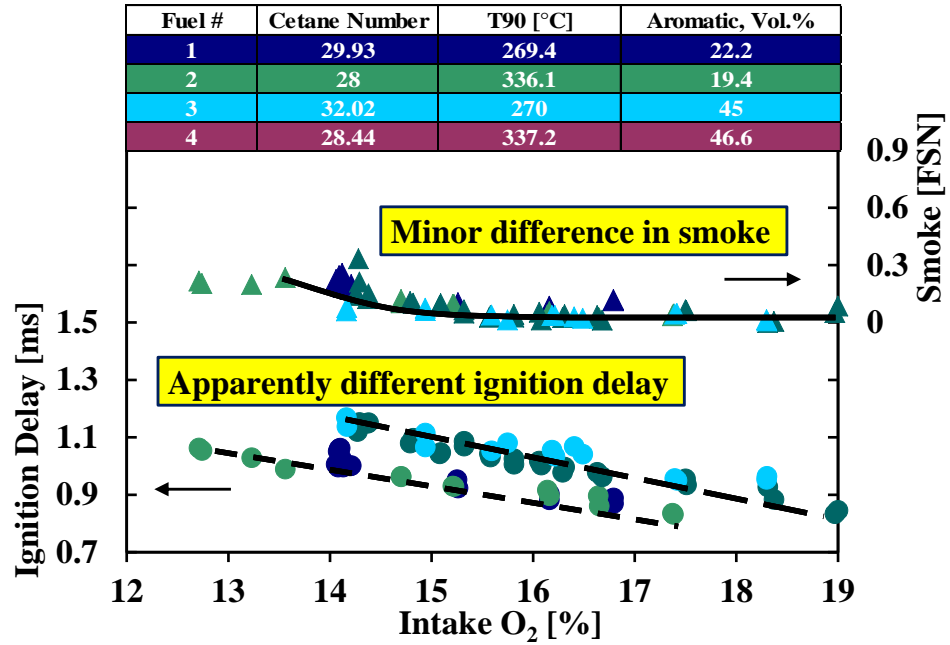


Figure 4.13 Aromatic Effects 5.5 bar IMEP – Ignition Delay, Smoke

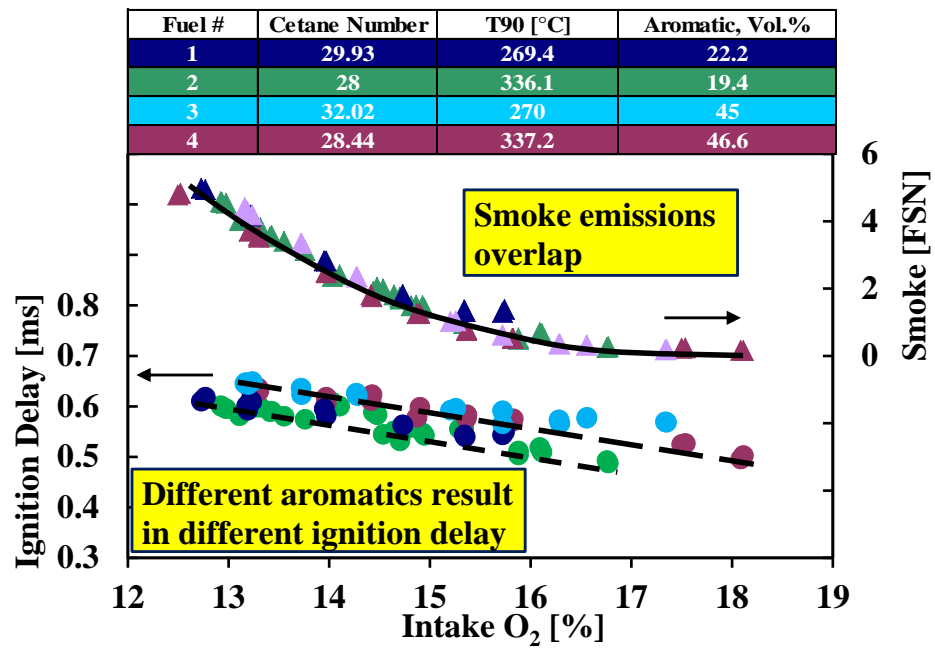


Figure 4.14 Aromatic Effect 14.6 bar IMEP – Ignition Delay, Smoke

As shown in Figures 4.13 & 4.14, the experimental results present two groups of the ignition delay durations in relation to aromatic contents. Compared with fuel #1 (aromatic 22.2%) and #2 (aromatic 19.4%), the ignition delay is noticeably prolonged for fuel #3 (aromatics 45%) and #4 (aromatics 46.6%). However, the prolonged ignition delay does not offer any appreciable smoke reduction. The known higher smoke propensity of the aromatic ingredients appears to compete with the effect of the prolonged ignition delay [7, 30, 41].

The smoke emissions and the ignition delay are compared for fuels #1 and #3 at the medium engine load in Figure 4.15. The higher aromatic content of fuel #3 results in a slightly longer ignition delay compared with that of fuel #1. However, fuel #3 produces more smoke emissions than fuel #1. The noticeably increased smoke emissions of fuel #3 can be attributed to the higher aromatic contents that are considered as the smoke precursors [7, 30, 41].

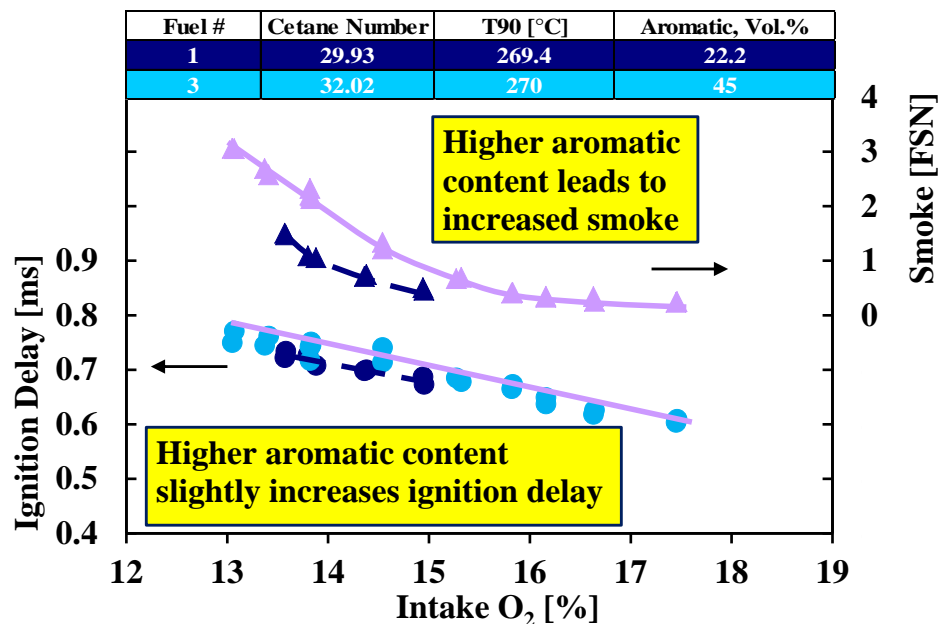


Figure 4.15 Aromatic Effect 10.6 bar IMEP – Low T90, ID, Smoke

#### 4.5 Fuel Property Effects on HTC and LTC

Due to the fact that the NO<sub>x</sub> formation is highly sensitive to the flame temperature, the level of the NO<sub>x</sub> emissions can be used to indirectly evaluate the flame temperature of the diesel combustion. Under the same engine operating conditions (*e.g.* the engine load), less NO<sub>x</sub> production, to a certain extent, indicates a lowered flame temperature. In fact, a direct measurement of the flame temperature is extremely challenging for the internal combustion in diesel engines, and thus the NO<sub>x</sub> emissions are used herein to estimate the relative flame temperatures.

The profiles of the heat release rate for all the FACE fuels are shown in Figures 4.16 & 4.17 for HTC and LTC respectively. At the low load of 5.6 bar IMEP, the engine produces approximately 200 ppm (~1.5 g/kW-hr) NO<sub>x</sub> emissions in the HTC mode (Figure 4.16), while the NO<sub>x</sub> level drops to around 30 ppm (~0.2 g/kW-hr) during LTC operation (Figure 4.17). In Figure 4.16, the traces of the main heat release largely overlap with each other for all the fuels. Minor differences are observed in the pre-reactions. In general, the low Cetane fuels tend to produce more noticeable heat release from the pre-reactions in HTC under the tested conditions.

On the contrary, when the engine operation enters the LTC regime (Figure 4.17), the heat release profiles present prolonged pre-reaction durations and large variations across different fuels. In LTC, the changes of the fuel physical and chemical properties start to remarkably impact the ignition and subsequent combustion processes.

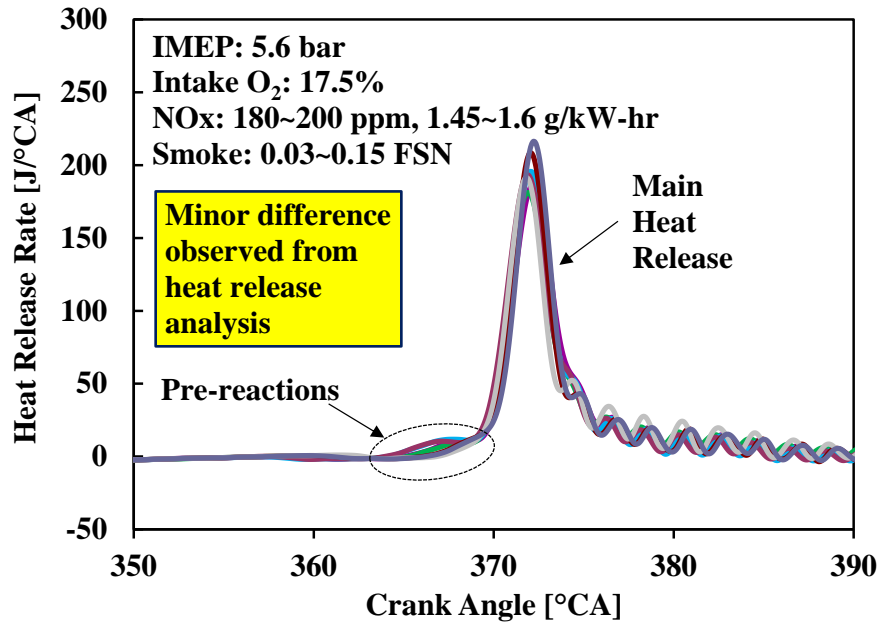


Figure 4.16 FACE HTC Low Load – Heat Release

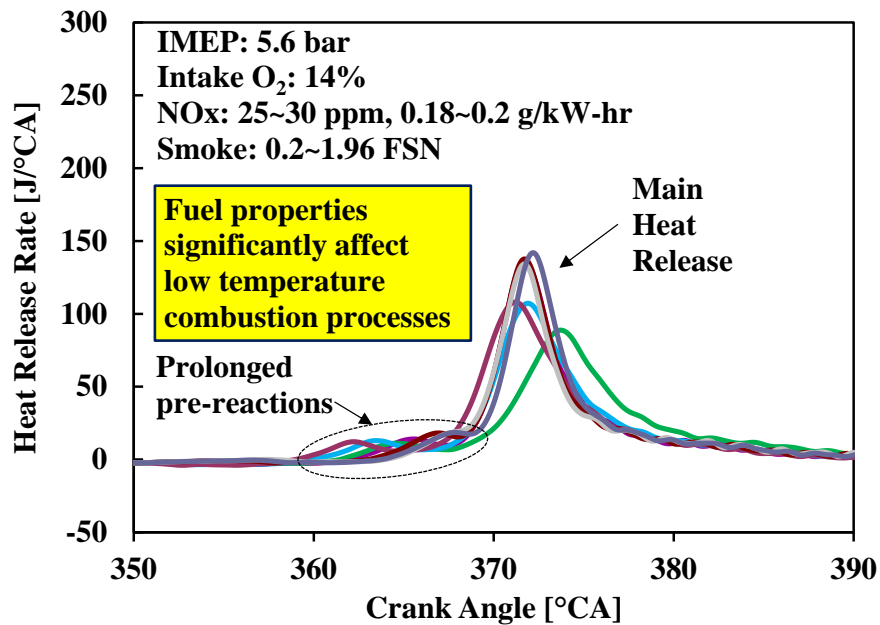


Figure 4.17 FACE LTC Low Load – Heat Release

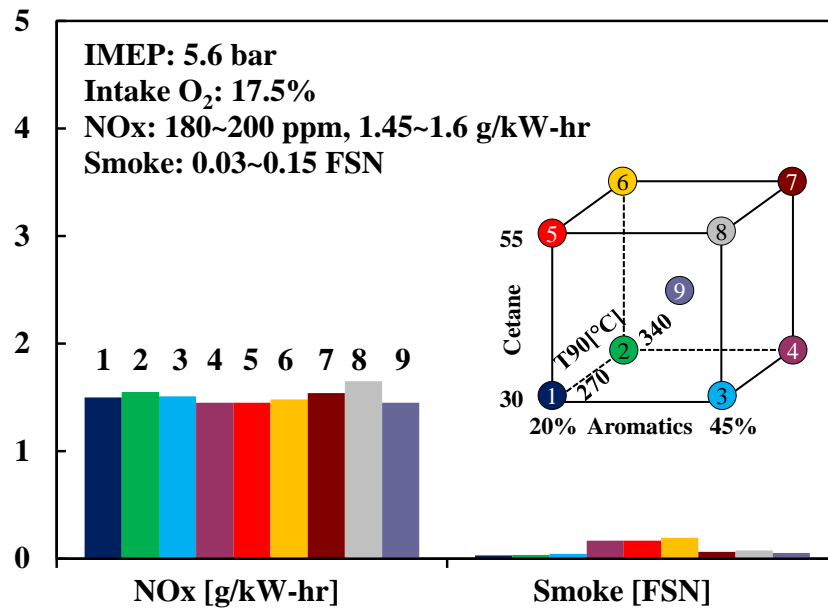


Figure 4.18 FACE HTC Low Load – NOx, Smoke

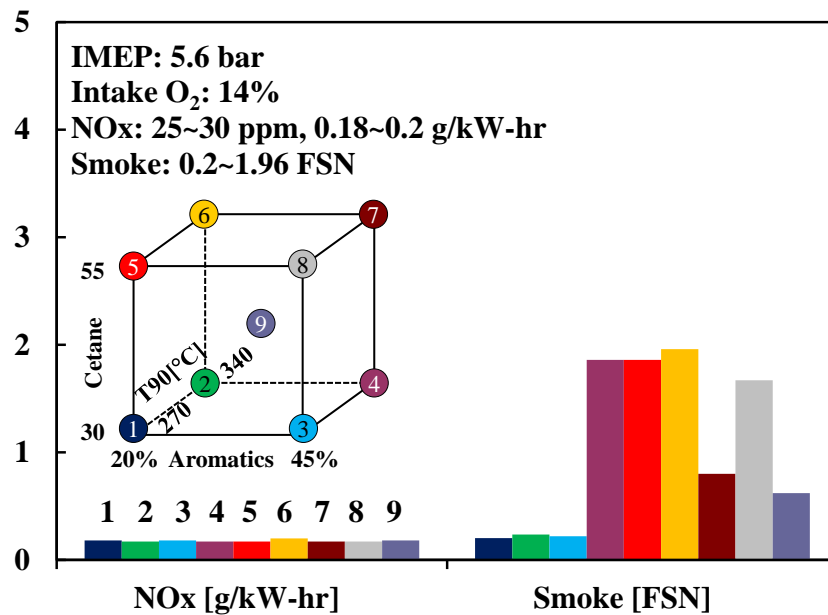


Figure 4.19 FACE LTC Low Load – NOx, Smoke

The NO<sub>x</sub> and smoke emissions are compared for the HTC and LTC modes in Figure 4.18 and Figure 4.19. The smoke emissions are at a near-zero level (0.03~0.15 FSN) for all the fuels in the HTC mode. The difference of the fuel properties does not make a major difference in the exhaust emissions. In the LTC mode (Figure 4.19), however, the smoke emissions exhibit large variations across the fuels. The low Cetane fuels can produce smoke emissions as low as 0.2 FSN, while the high Cetane fuels generate 1.96 FSN under the same engine operating conditions.

These experimental results indicate that the fuel property variations within the tested range make a significant difference to the LTC operation. In other words, when the engine is tuned to run under LTC mode, the fuel properties become an influencing factor and they should be considered in the combustion control strategies. This perspective may have been overlooked, because the conventional HTC, as demonstrated in this study, is insensitive to such fuel property variations.

The effectiveness of the fuel property variation reduces as the engine load increases. In Figures 4.20 & 4.21, the heat release rate traces and exhaust emissions are shown for all the fuels under LTC at the high engine load. Comparing the heat release profiles with the ones at low loads, the pre-reactions disappear at the high engine load as the reactions rapidly transit into the main heat release phase. However, the low Cetane fuels clearly present retarded ignition timings and higher degrees of the premixed combustion.

The smoke emissions exhibit apparent differences across the nine fuels. Comparing the lowest and highest smoke emissions of 2.4 FSN and 4.7 FSN, the low Cetane fuels still offer benefits of smoke reduction. However, if compared with the low load conditions, such a smoke advantage diminishes at the increased engine load.

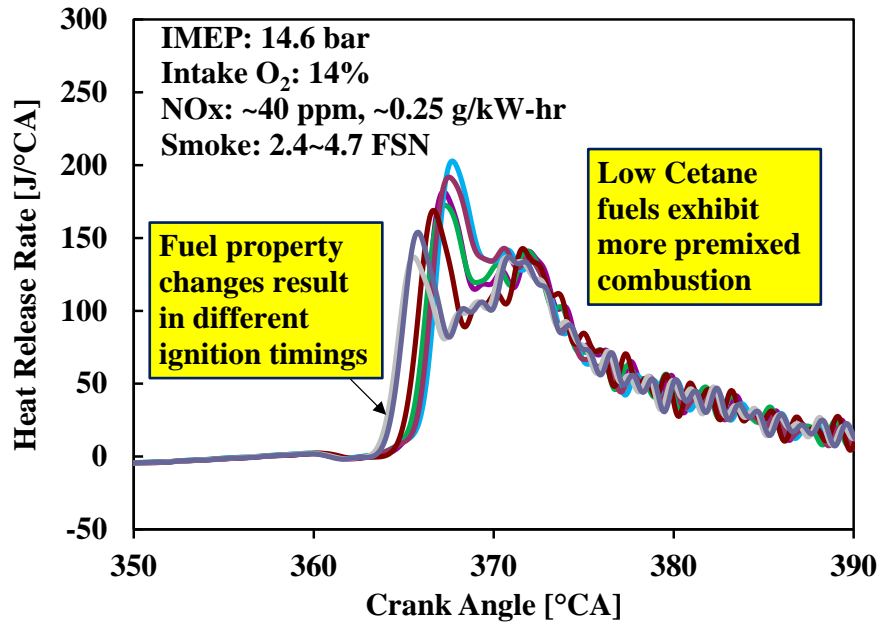


Figure 4.20 FACE LTC High Load – Heat Release

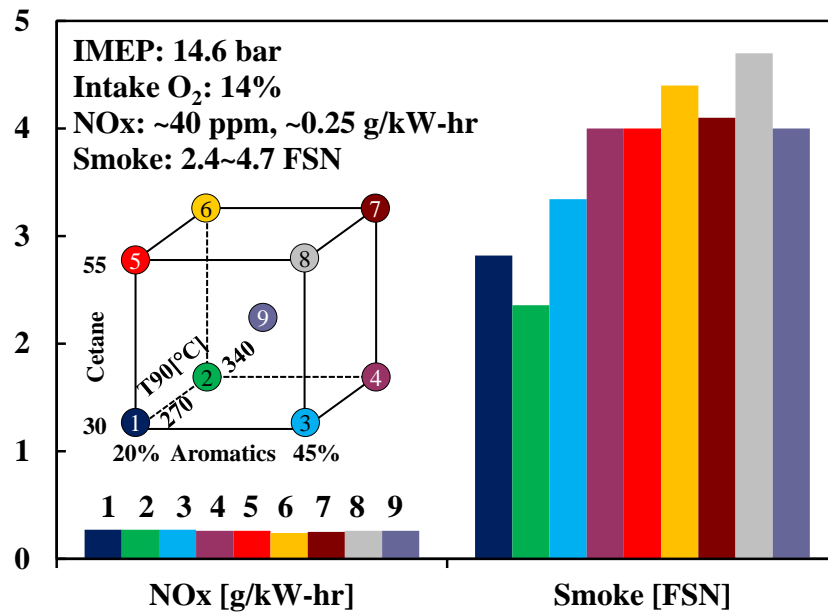


Figure 4.21 FACE LTC High Load – NO<sub>x</sub>, Smoke

#### **4.6 Fuel Property Effects on Incomplete Combustion Products**

The experimental results of incomplete combustion products for all the fuels are shown in Figures 4.22 to 4.24 across the EGR sweeps at different engine loads. Higher HC and CO emissions are generated from the combustion of low Cetane fuels. The greater resistance to the auto-ignition of low Cetane fuels, such as fuel #1, causes the increased HC and CO productions from incomplete reactions. In addition, the low Cetane fuels with higher aromatic contents (fuel #3 and #4) yield the highest HC and CO emissions, which is an indication that the aromatics also contribute to the products of the incomplete oxidization. The HC emissions reduce substantially as the engine load increases to higher levels. The difference in HC emissions from different fuels becomes insignificant at the high engine load.

When low NO<sub>x</sub> emissions are achieved through EGR at the low engine load, the changes of Cetane numbers lead to a trade-off between the smoke emissions and the incomplete combustion products. In Figure 4.25, the results of smoke, CO, and HC emissions are correlated for fuels with different Cetane numbers at a constant intake oxygen concentration of 14%, regardless of the change in boiling temperature or aromatic contents. As the Cetane number increases, the smoke emissions present a clear ascending trend whereas the incomplete combustion products decrease. These experimental results demonstrate that the lower Cetane helps to reduce smoke emissions but the greater resistance to ignition tends to cause incomplete oxidation.

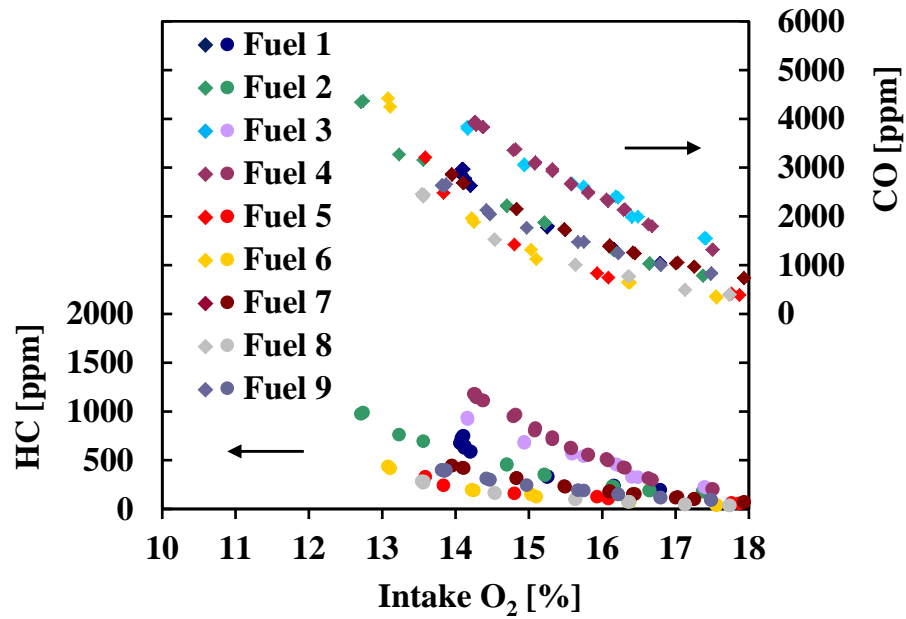


Figure 4.22 FACE EGR Sweep 5.5 bar IMEP – HC, CO

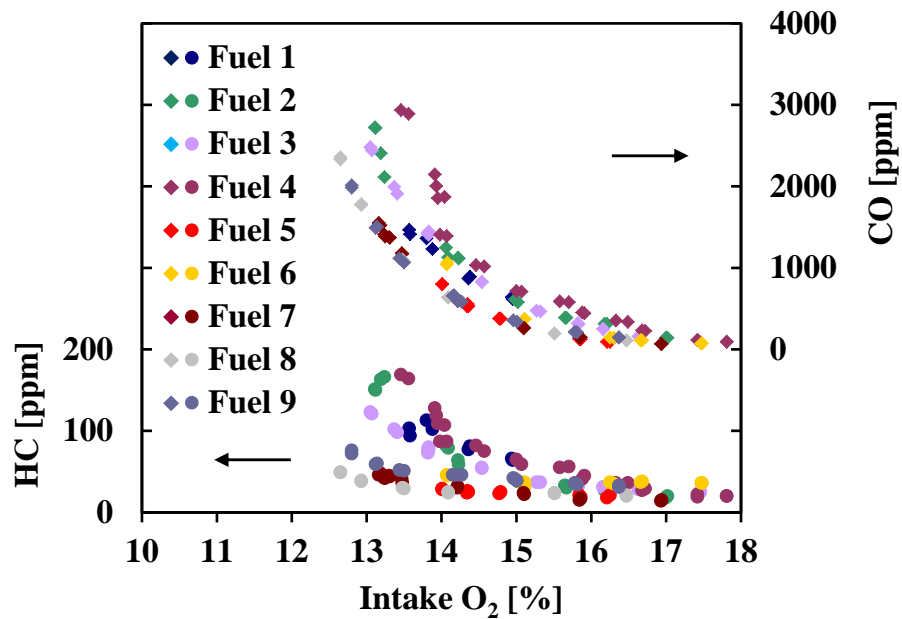


Figure 4.23 FACE EGR Sweep 10.6 bar IMEP – HC, CO

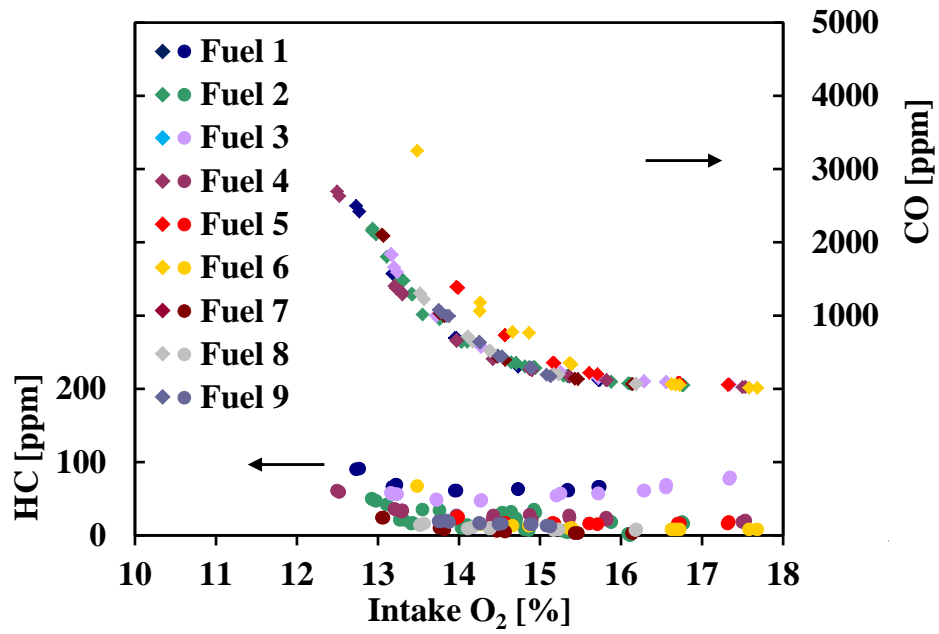


Figure 4.24 FACE EGR Sweep 14.6 bar IMEP – HC, CO

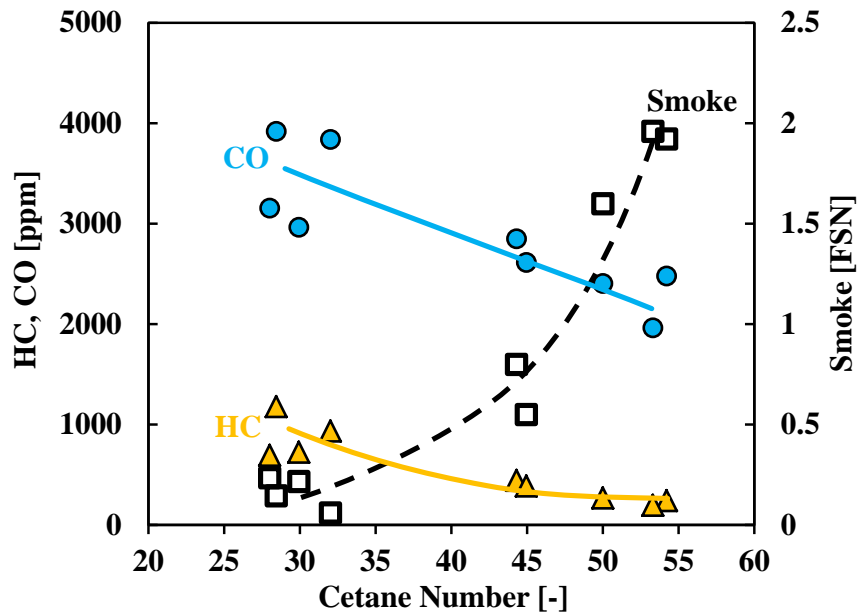


Figure 4.25 Cetane Number Effects 5.5 bar IMEP – Smoke, HC, CO

#### **4.7 Summary of Diesel Fuel Property Effects**

The fuel property change starts to noticeably impact the ignition and combustion processes as the engine approaches the LTC operation where the ignition delay is prolonged and more time is available for the physical changes and chemical reactions of the cylinder charge. In HTC, the variations of the given fuel properties have negligible effects on the combustion events and the resultant exhaust emissions.

The use of a low Cetane fuel improves the trade-off between NO<sub>x</sub> and smoke emissions across the engine operating loads. However, the impact on the emissions weakens as the engine load increases. The higher aromatic contents in the diesel fuels prolong the ignition delay, but the smoke emissions are not necessarily reduced. The fuel volatility, within the examined range, has minor impact on ignition delay. Nonetheless, the higher volatility promotes the evaporation of the injected fuel spray, thereby improving the homogeneity of the cylinder charge. In general, a fuel (diesel or others) that can withhold auto-ignition and can evaporate rapidly is preferred to improve the homogeneity of the cylinder charge and facilitate the enabling of the LTC operation.

## CHAPTER V

### FUELS AND FUELLING STRATEGIES FOR CLEAN COMBUSTION

As demonstrated in Chapter IV, the variations of fuel properties become important influencing factors in the ignition and combustion processes when the engine operation approaches the LTC mode. The study presented in this chapter continues to investigate the desirable fuels for the LTC enabling. In order to improve the mixture homogeneity, three additional fuel types are examined besides the regular diesel, namely the n-butanol, high Octane gasoline, and ethanol, which offer a desired range of improved volatility and reduced fuel reactivity. Adaptive fuelling strategies are also developed to accommodate each fuel's physical and chemical properties. Compared with the regular diesel fuel, the use of n-butanol, gasoline, and ethanol can substantially facilitate the enabling of the LTC operation on the research engines, as demonstrated in the following subsections.

#### 5.1 LTC Enabling with Regular Diesel

The experiments with the regular diesel fuel serve as a baseline; and the subsequent experimental results using other fuels are compared with the baseline results to evaluate the fuel suitability for the LTC enabling.

The single-shot injection strategy is applied for the regular diesel fuel on the high compression ratio (18.2:1) research engine. The engine runs through EGR sweeps at different intake boost and injection pressures. The adjustment of the injection timing compensates for the combustion phasing drift and maintains the combustion phasing (CA50) at 367°CA during the EGR sweeps. In each experiment, the commanded injection duration and injection pressure remain constant and thus the fuelling rate is

considered to be nearly unchanged throughout each EGR sweep. Two levels of nominal engine loads, namely 8 bar and 10 bar IMEP, are studied. It is noted that the engine load reduces at high EGR rates, especially in the LTC operation; no additional fuels are added to top up the load unless explicitly specified.

In Figures 5.1 to 5.4, the results of major exhaust emissions are shown for different EGR sweeps at varied intake boost and fuel injection pressures. These results indicate that the EGR application is a very effective measure to reduce the NO<sub>x</sub> emissions regardless of different levels of fuel injection pressure or intake boost. At intake oxygen concentrations lower than 14%, low NO<sub>x</sub> emissions (*e.g.* below 0.2 g/kW-hr) are achieved in all the investigated cases. As the EGR rate progressively increases, the classical NO<sub>x</sub> and smoke trade-off is observed until the combustion enters the LTC operation where the NO<sub>x</sub> and smoke emissions reduce simultaneously. However, excessively high smoke emissions can be produced before the engine operation enters the LTC mode, especially when the injection pressure or the intake boost is inadequate. Only when the intake and injection pressures are sufficiently elevated for the respective engine load level, the excessively high smoke emissions can be avoided and the necessary amount of EGR for enabling LTC can be applied.

The HC and CO emissions generally increase at higher EGR rates, and they start to rise sharply once the engine operation enters the LTC mode. The CO emissions in certain LTC cases exceed the measureable range (5000 ppm) of the CO analyzer used in this work.

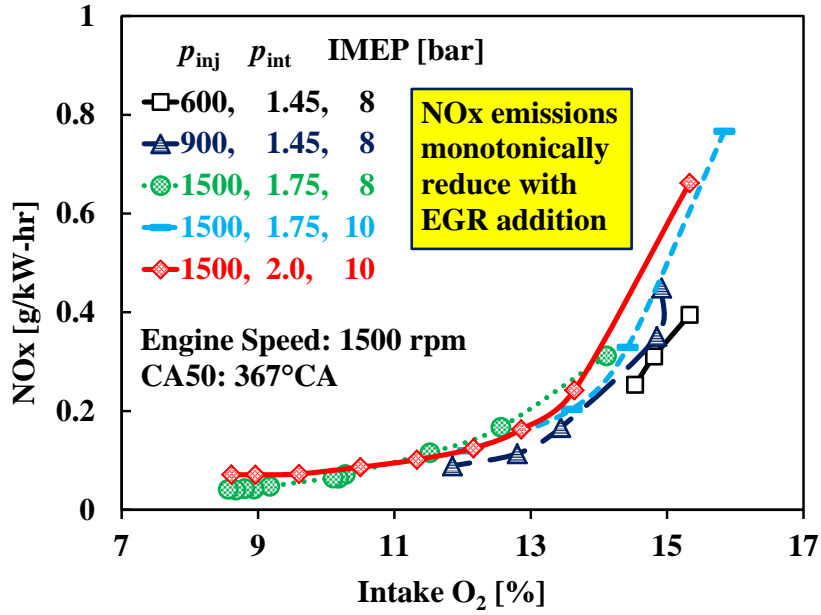


Figure 5.1 Diesel Baseline EGR Sweeps – NOx

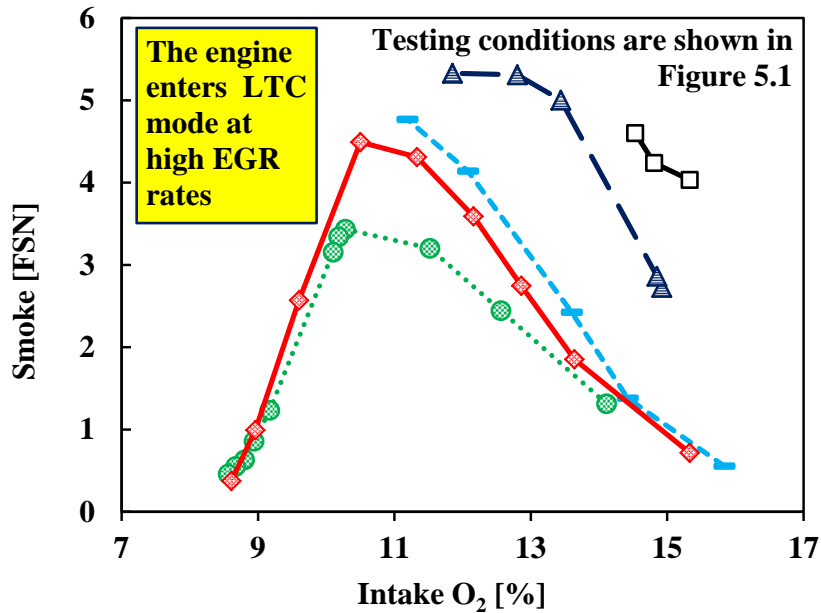


Figure 5.2 Diesel Baseline EGR Sweeps – Smoke

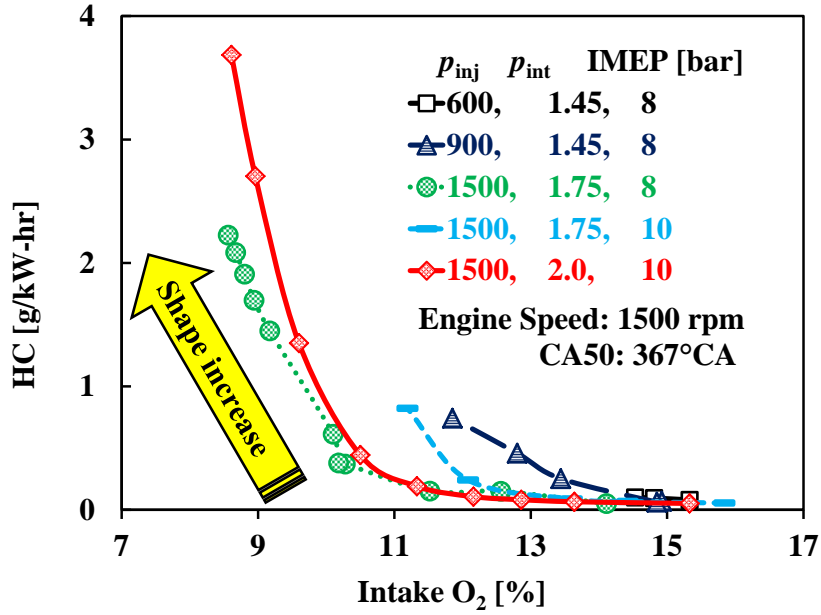


Figure 5.3 Diesel Baseline EGR Sweeps – HC

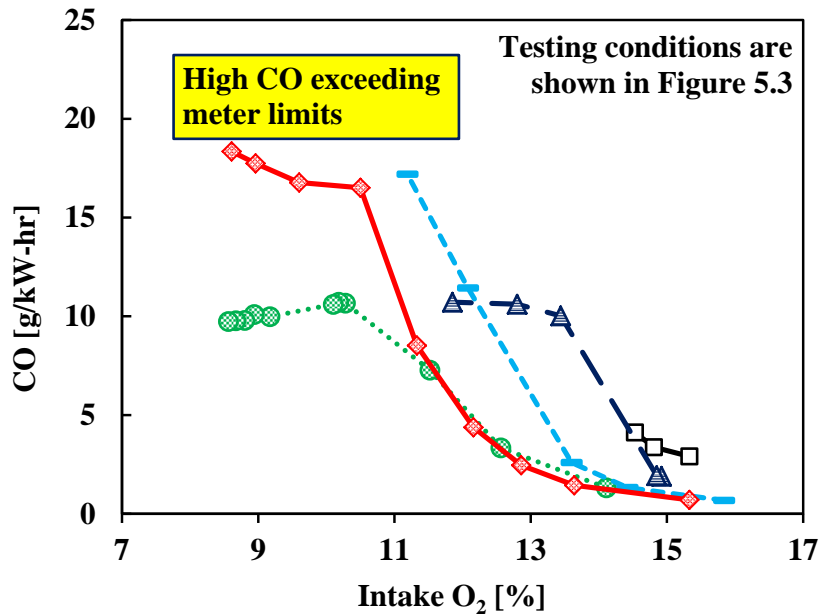


Figure 5.4 Diesel Baseline EGR Sweeps – CO

The experimental results suggest that a high EGR rate is usually required to enable the LTC operation with a regular diesel fuel. However, the necessary EGR rate may be unattainable under certain engine operating conditions. For instance, practically the engine cannot afford further EGR addition, for an extended duration of operation, when the smoke emissions reach 5~6 FSN, otherwise smoke plugging related damage is imminent. As a partial solution, the increase of the injection pressure has been very effective to lower the smoke emissions, thereby allowing heavier EGR application.

Another factor is the oxygen availability. In Figure 5.5, the exhaust oxygen concentration is shown for the investigated cases. At a lower intake boost, the exhaust oxygen concentration approaches 2% at high EGR rates, which indicates that the engine essentially runs in near-stoichiometric combustion. The correlations between the intake oxygen and the equivalence ratio  $\Phi$  (or the air excess ratio  $\lambda$ ) at varying rates of EGR and boost are explained by Usman *et al* in [109]. This also in part explains the sharp increase of the HC and CO emissions as the exhaust oxygen concentration drops below a certain level (3~4% as shown in Figures 5.6 & 5.7).

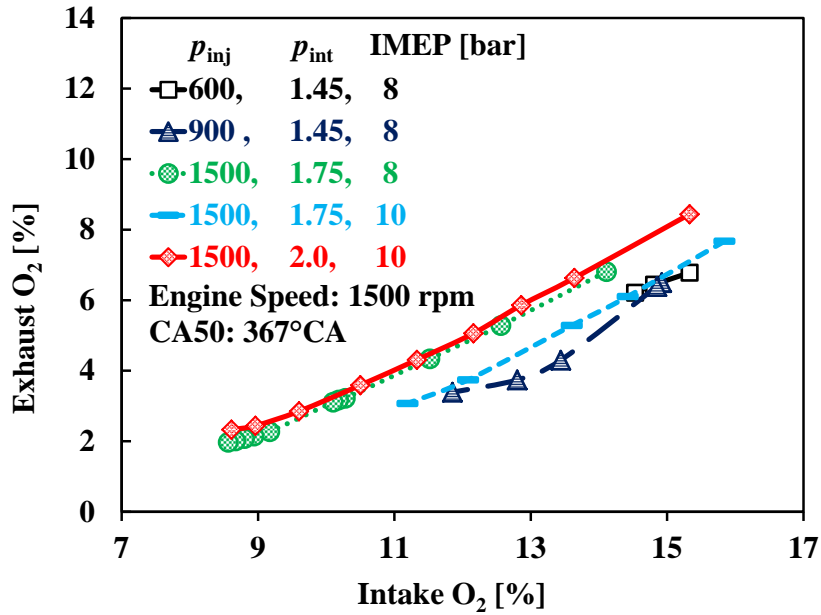


Figure 5.5 Diesel Baseline EGR Sweeps – Exhaust O<sub>2</sub>

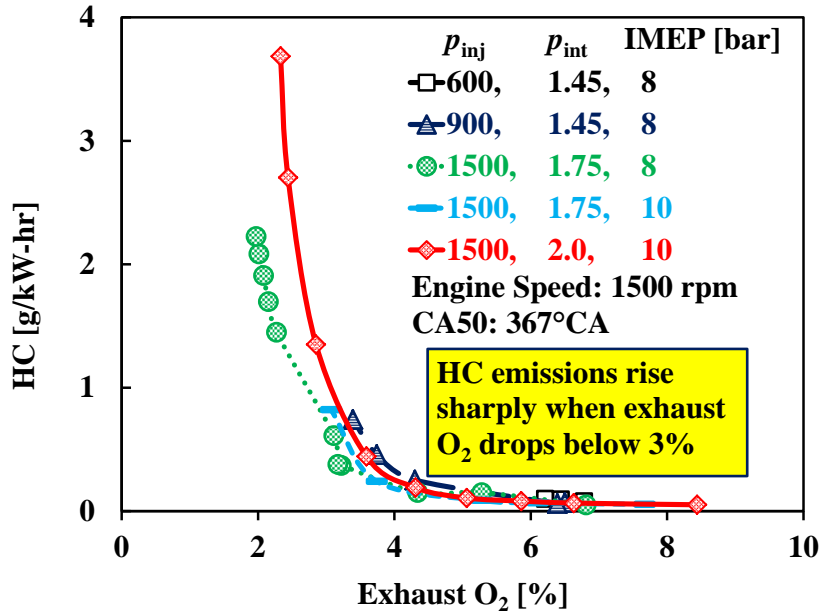


Figure 5.6 Diesel Baseline EGR Sweeps – HC, Exhaust O<sub>2</sub>

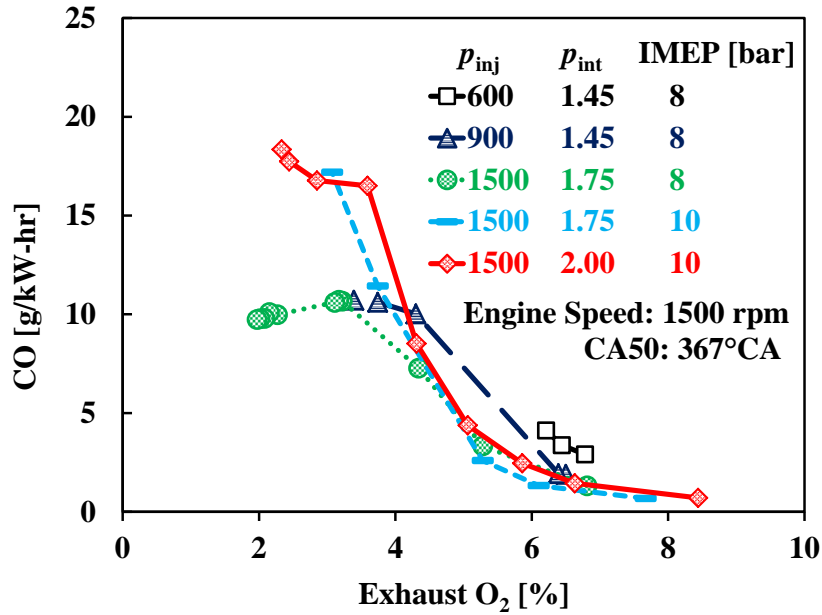


Figure 5.7 Diesel Baseline EGR Sweeps – CO, Exhaust O<sub>2</sub>

In order to accomplish the ultra-low smoke and NO<sub>x</sub> emissions simultaneously, the engine operating conditions need to allow the diesel fuel to have sufficient mixing with air. For the direct-injection applications, the adequate ignition delay is therefore of paramount importance. In Figure 5.8, the results of the ignition delay are shown as a function of the intake oxygen concentration for the same series of diesel baseline experiments, while the start of injection (SOI) is shown in the same figure. For all the cases, as the EGR rate increases, the ignition delay is prolonged and the diesel injection timing is advanced to maintain the combustion phasing. These results also indicate that the elevation of injection pressure and intake boost actually shortens the ignition delay; however, the smoke emissions are generally improved. Therefore, the improved spray atomization at higher injection pressure and the increased oxygen availability from elevated intake boost are considered effective to reduce the smoke emissions.

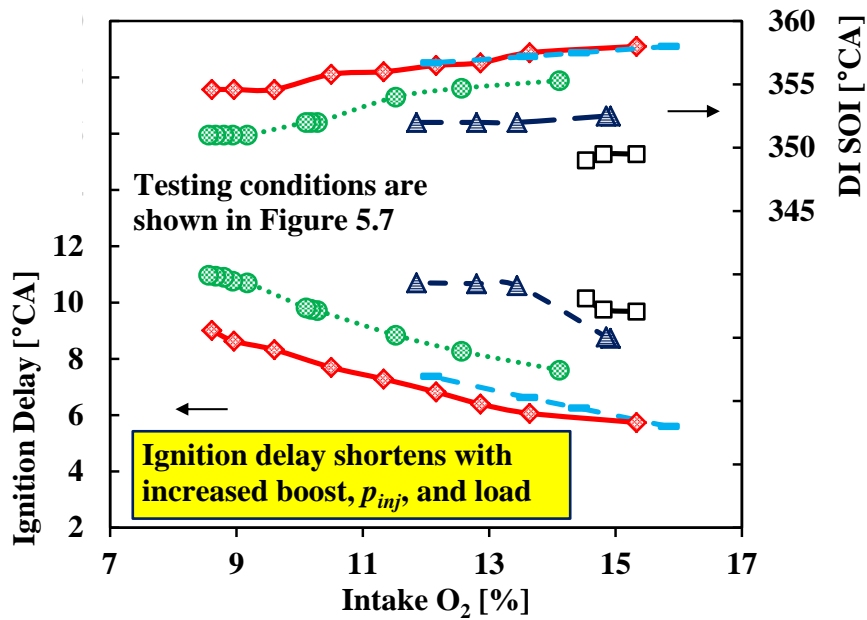


Figure 5.8 Diesel Baseline EGR Sweeps – Ignition Delay, DI SOI

As mentioned earlier, the injection duration remains unchanged and thus the fuelling rate is considered constant in each EGR sweep. The engine operation becomes less efficient as EGR progressively increases, as evidenced by the IMEP drop (as shown in Figures 5.9 & 5.10). Although the IMEP values are 8 bar and 10 bar in the conventional HTC operation, the achievable engine load drops to 7.2 bar and 7.9 bar respectively when the engine operation enters the LTC mode.

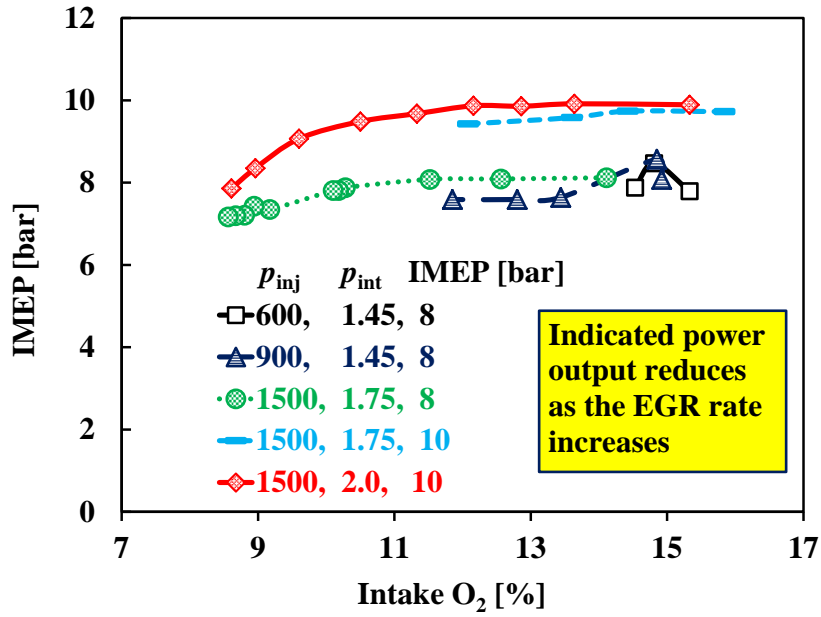


Figure 5.9 Diesel Baseline EGR Sweeps – IMEP

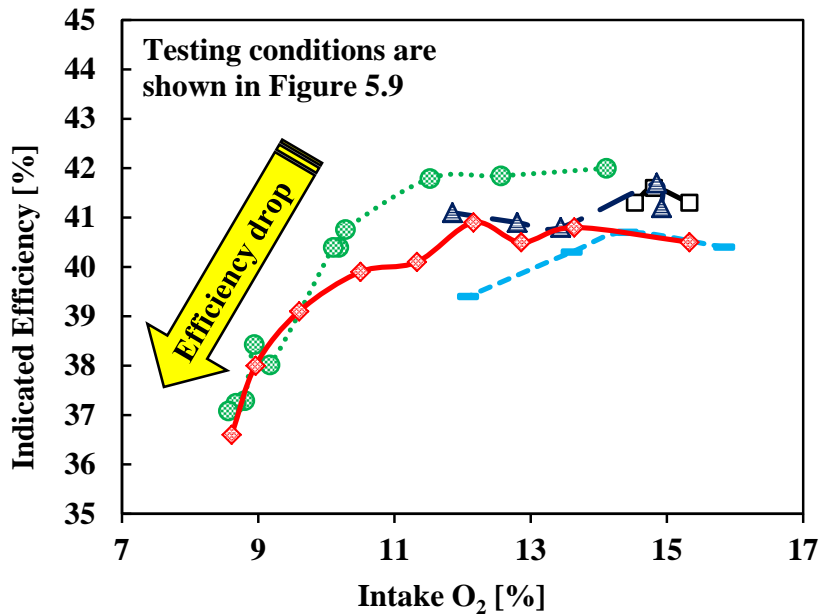


Figure 5.10 Diesel Baseline EGR Sweeps – Indicated Efficiency

In summary, the baseline experiments demonstrate that the LTC enabling heavily relies on the injection pressure, intake boost and EGR when using the regular diesel fuel. Under the studied engine operating conditions, the simultaneously low NO<sub>x</sub> and soot emissions are achievable with extremely high EGR rates (60~70%), which is feasible in the advanced research environment but not yet practical or readily available for the present production engines. Moreover, the engine efficiency deteriorates substantially in the LTC operation.

In the subsequent sections, the engine performances of other fuels are compared with the diesel baseline. Since the change of the engine load can significantly affect the LTC enabling, the subsequent investigations with other fuels are conducted at similar engine load levels as the diesel baseline (8~10 bar IMEP). The LTC load improvements will be presented in Chapter VII.

## **5.2 n-Butanol LTC Enabling**

The n-Butanol fuel has been widely studied in engine applications. Most of previous researchers used n-butanol blends with gasoline or diesel fuels [47, 97, 105]. In this dissertation, n-butanol is employed as a representative fuel of higher volatility (boiling temperature at 117.5 °C) and lower reactivity (Cetane number ~25) to compare with the regular diesel fuel. More importantly, n-butanol can be directly compared with diesel using the high-pressure direct-injection. The injection strategies applied herein include the conventional single-shot injection, multiple early injections, and port fuel injection.

### 5.2.1 n-Butanol Single-shot Direct-injection

The neat n-Butanol has a much lower Cetane number than a typical diesel. With the direct-injection, n-butanol is expected to undergo a prolonged ignition delay period and, as a result, the attainment of the same combustion phasing requires advancing the injection timing. In Figure 5.11, a schematic of the n-butanol direct-injection is illustrated for the single-shot injection strategy in relation to the combustion event. In Figures 5.12 & 5.13, the experimental results are shown for n-butanol and diesel to compare their combustion characteristics and exhaust emissions under the same engine operating conditions, while the SOI is swept.

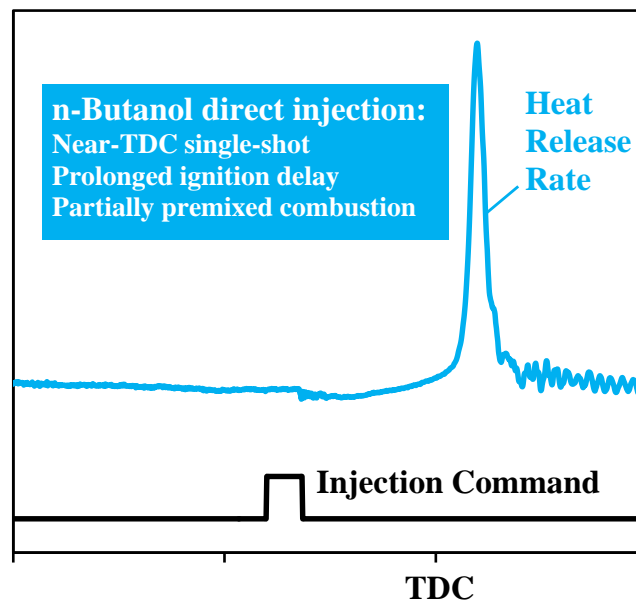


Figure 5.11 Schematic of n-Butanol Single-shot Injection Strategy

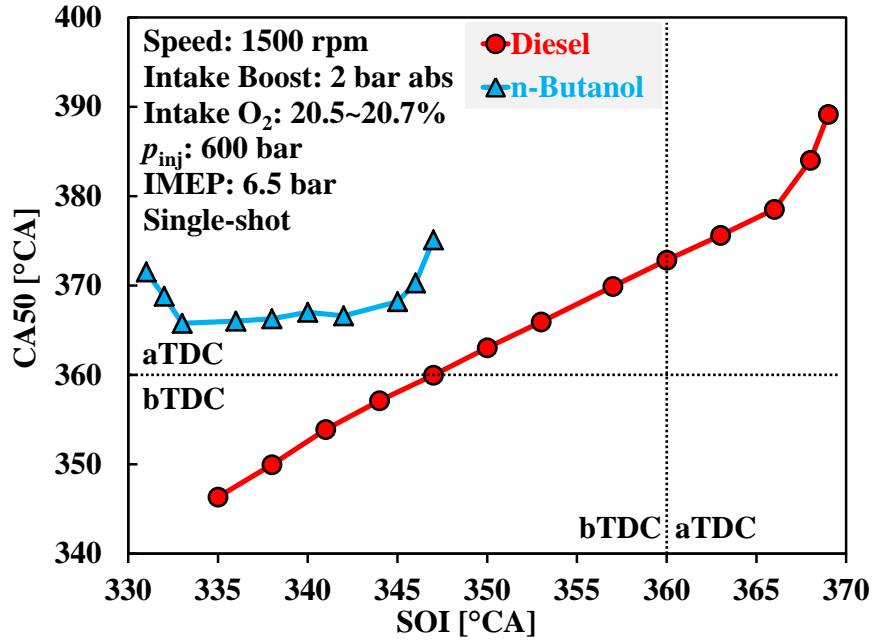


Figure 5.12 n-Butanol versus Diesel Single-shot SOI Sweep – CA50

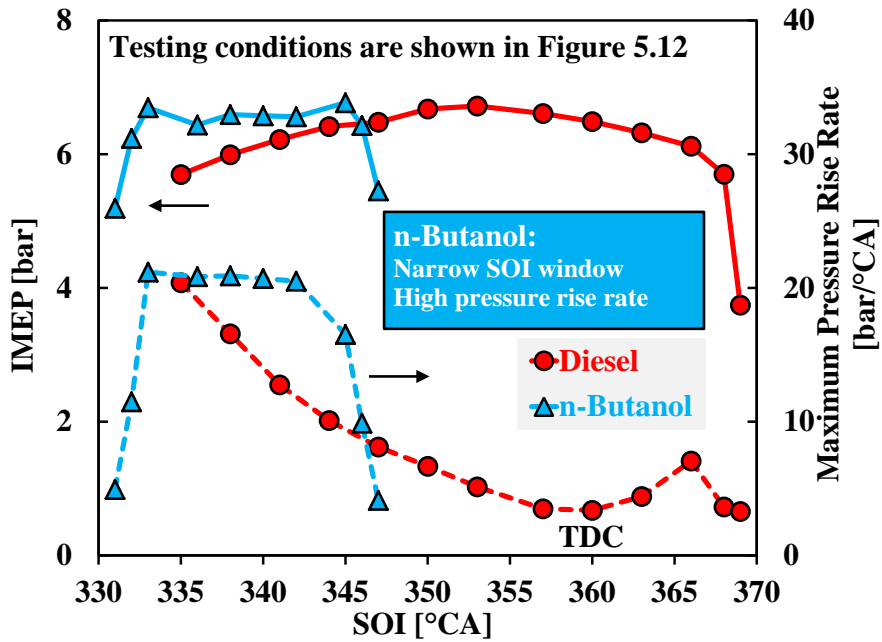


Figure 5.13 n-Butanol versus Diesel Single-shot – IMEP, PRR<sub>max</sub>

The engine runs with near-zero EGR and an intake pressure of 2 bar absolute. The injection pressure is 600 bar for both fuels. Due to the different energy density represented by the lower heat value (LHV), the n-butanol injection has longer commanded injection duration than the diesel case to achieve the same engine load of ~6.5 bar IMEP. It is noted that the combustion phasing has a major impact on the thermal efficiency, and the IMEP reduces as the CA50 moves away from the optimal phasing. The IMEP reduction becomes significant when the engine starts to misfire. Two safety factors are considered to determine the feasible SOI sweeping range, namely the misfire and the combustion roughness represented by the maximum pressure rise rate.

In the diesel case, the engine load substantially decreases when the injection timing is delayed to 368°CA and 369°CA. The cylinder charge expands as the piston moves down, which effectively counteracts the temperature and pressure needed to maintain an efficient combustion process and thus misfire tends to occur. For the early injection timing, the SOI advancement stops at 335°CA when the maximum pressure rise rate reaches 20 bar/°CA. In stark contrast, the n-butanol combustion is only feasible in a considerably narrower SOI window restricted by misfire. However, the cause for misfire at early injection timings is different from that at retarded injection timings. In Figures 5.14 & 5.15, the ignition delay and CA5 are shown for the same SOI sweeps. As the commanded injection timing retards from 335°CA towards TDC, the increased surrounding pressure and temperature during the n-butanol injection shortens the ignition delay, but the combustion initiation (represented by CA5) in fact further postpones into the expansion stroke. The effects of the expansion become so influential in the case of injection timing at 347°CA that the CA5 is delayed as late as 10°CA after TDC.

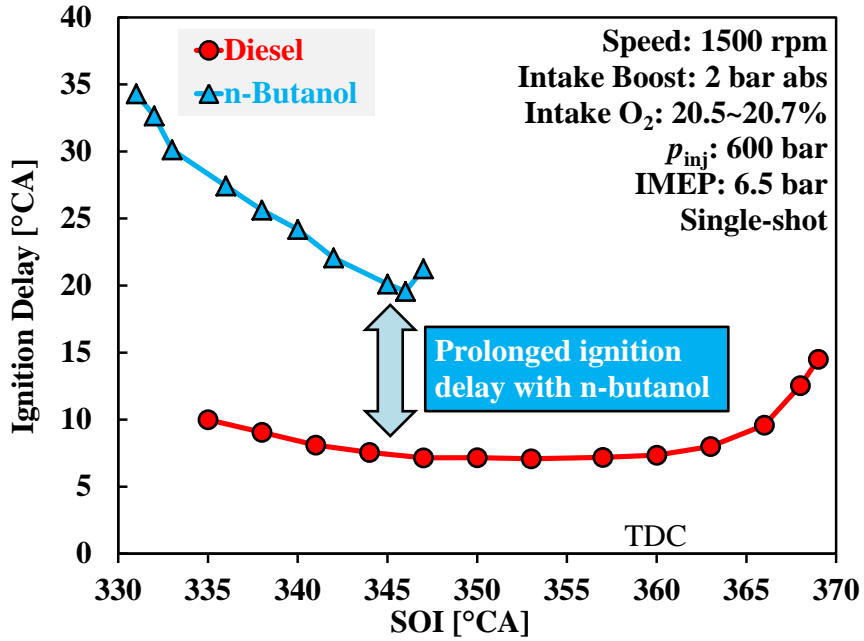


Figure 5.14 n-Butanol versus Diesel Single-shot SOI Sweep – Ignition Delay

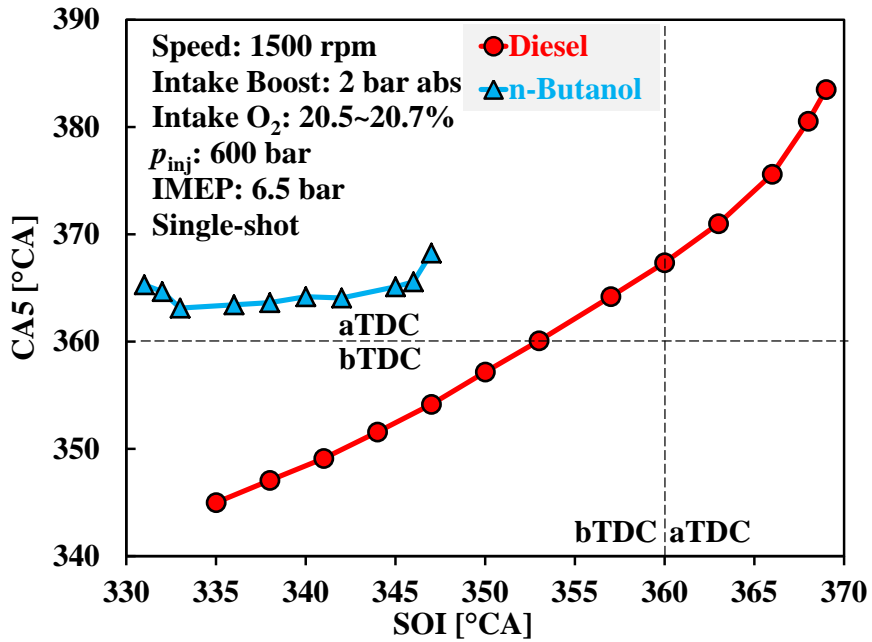


Figure 5.15 n-Butanol versus Diesel Single-shot SOI Sweep – CA5

With the postponed injection timings, the low reactivity of n-butanol and the late combustion during the expansion stroke both oppose the sustainability of the combustion process, ultimately leading to misfire. Such an n-butanol misfire resembles the misfire observed in the diesel case. On the other hand, the n-butanol misfire incidences at early injection timings are attributable to the over-mixing of n-butanol and air. The injected n-butanol undergoes extremely long ignition delay periods (*e.g.*  $30^{\circ}\text{CA}$ ), during which it rapidly vaporizes and thoroughly mixes with the intake air towards forming a lean mixture. Such a mixing process diminishes the availability of locally stoichiometric regions where the ignition tends to initiate and ultimately increases the misfire probability.

With the single-shot injection strategy, the burning processes of n-butanol tend to exhibit high levels of combustion noise. The maximum pressure rise rate can easily reach levels higher than  $20 \text{ bar}/^{\circ}\text{CA}$ . In Figures 5.16 & 5.17, comparisons are made for the cylinder pressure, heat release rate, and burned mass fraction for n-butanol and diesel. The selected two cases have the same combustion phasing ( $\text{CA}_{50}$  at  $\sim 366^{\circ}\text{CA}$ ) while the SOI of n-butanol is  $17^{\circ}\text{CA}$  earlier than that of diesel. By examining the pressure traces, the n-butanol combustion has a sharper pressure rise immediately after the combustion start, while the compression pressure prior to the combustion is approximately 7 bar lower than the diesel case. It appears that, due to the high latent heat of n-butanol, the in-cylinder evaporation of n-butanol absorbs energy from the cylinder charge, resulting in noticeably lowered cylinder pressure.

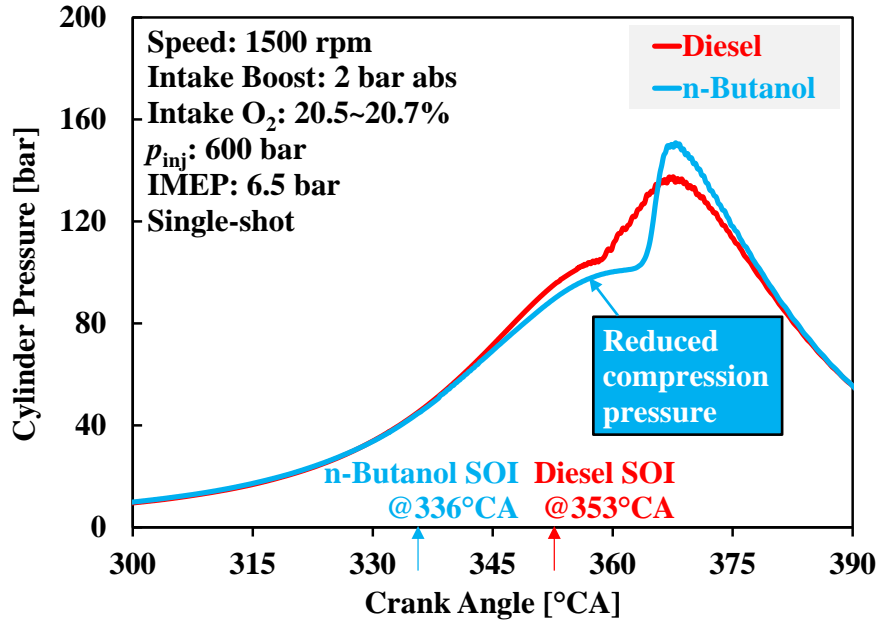


Figure 5.16 n-Butanol versus Diesel Single-shot – Pressure

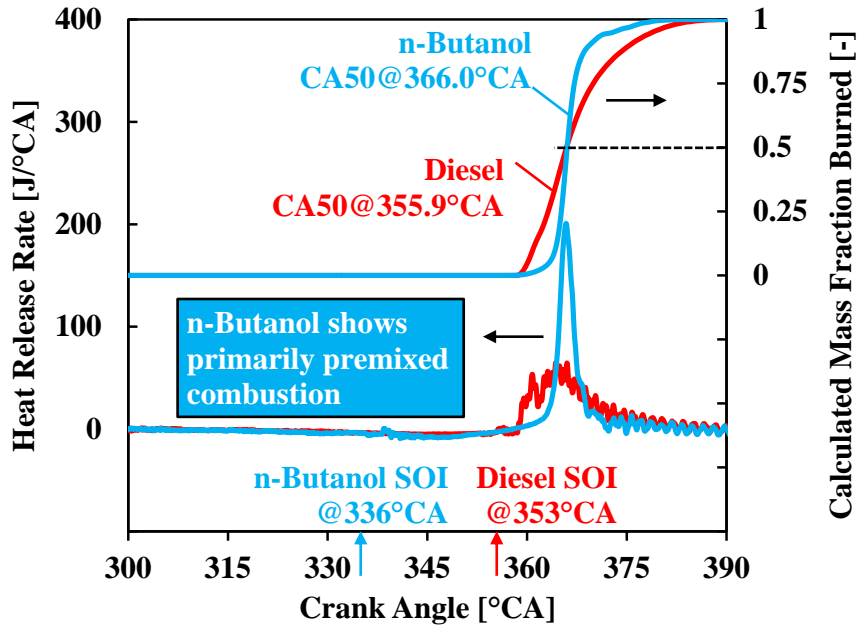


Figure 5.17 n-Butanol versus Diesel Single-shot – Heat Release

The sharp pressure rise of n-butanol combustion is the result of the rapid heat release, as shown by the heat release rate profiles. It is clear that a significant proportion of the partially premixed cylinder charge rapidly burns in a short duration. The peak heat release rate is almost triple of its counterpart in the diesel combustion.

Despite the rough combustion, the compression ignition of the partially premixed n-butanol and air mixture has shown substantial benefits in terms of NO<sub>x</sub> and smoke emissions. In Figures 5.18 to 5.21, the results of major exhaust emissions are shown for the same SOI sweeps. Compared with diesel, the n-butanol combustion produces considerably lower NO<sub>x</sub> emissions and near-zero smoke. When the misfire is absent, the NO<sub>x</sub> emissions of the n-butanol combustion can be as low as 0.3 g/kW-hr at an engine load of 6.5 bar IMEP. Without the use of EGR (as in the presented cases), it is extremely difficult to achieve the same low NO<sub>x</sub> levels using the regular diesel fuel unless the combustion phasing is significantly postponed. The long ignition delay and the consequently enhanced mixing, offered by the use of n-butanol, enable the LTC effectively.

For both fuels, the incomplete combustion products rise sharply when misfire occurs. Comparing the results during stable engine operations, the exhaust from the n-butanol combustion contains higher unburned HC and CO emissions, which may also suggest lower levels of the flame temperature.

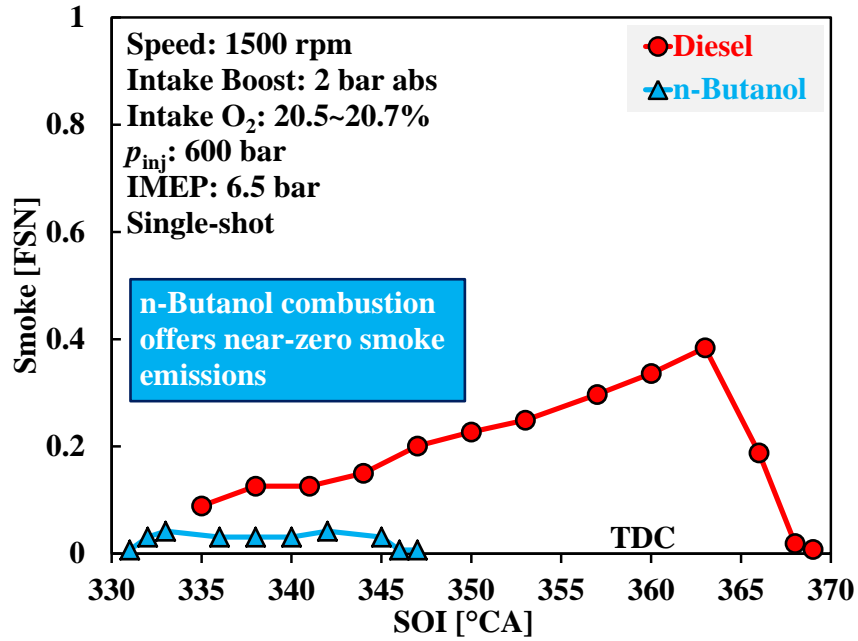


Figure 5.18 n-Butanol versus Diesel Single--shot – Smoke

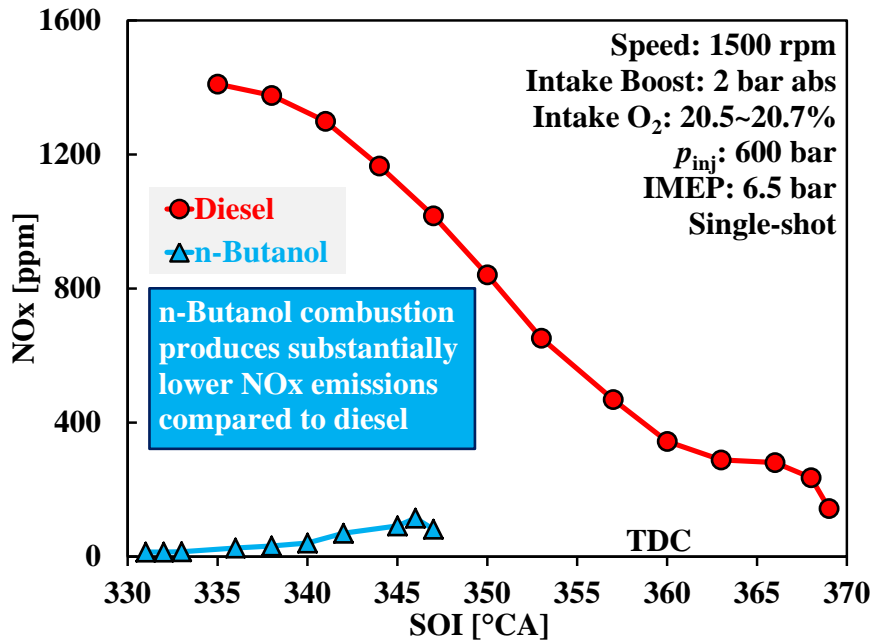


Figure 5.19 n-Butanol versus Diesel Single-shot – NOx

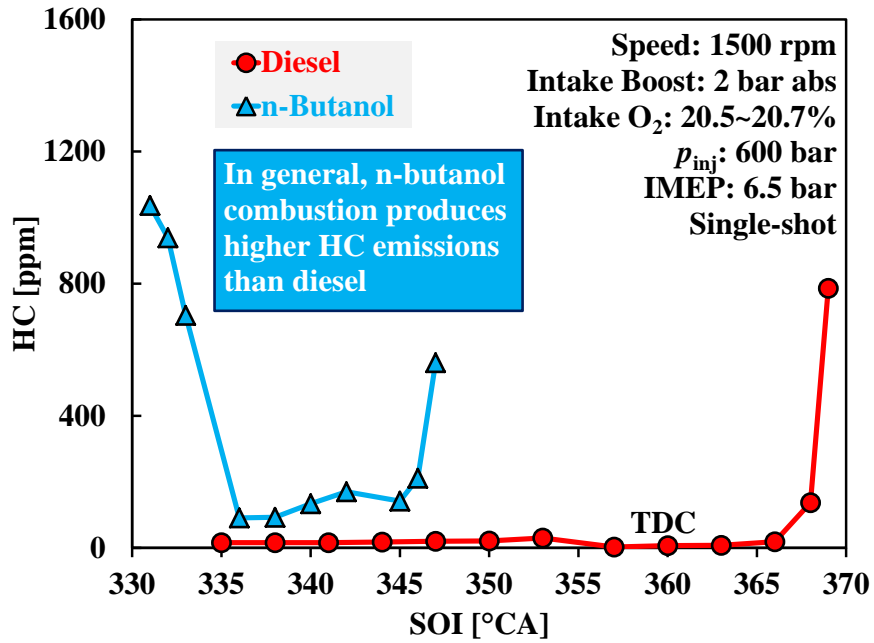


Figure 5.20 n-Butanol versus Diesel Single-shot – HC

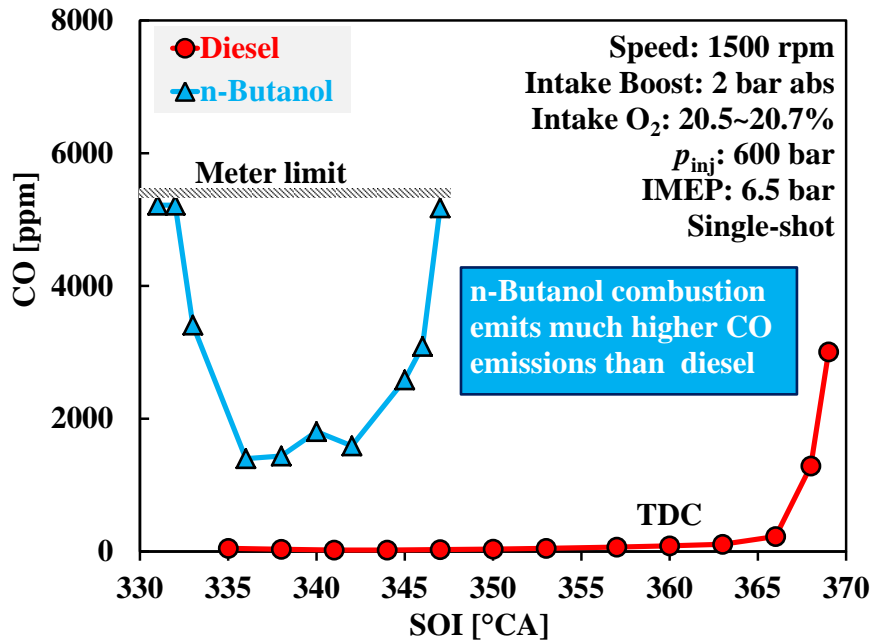


Figure 5.21 n-Butanol versus Diesel Single-shot – CO

The EGR effects on the n-butanol combustion are shown in Figures 5.22 & 5.23 using the cylinder pressure and heat release profiles. The commanded injection timing is fixed at 335°CA with the single-shot injection strategy. The EGR addition postpones the ignition timing and the combustion phasing and, as a result, the cylinder pressure and the pressure rise rate decrease. The resultant prolonged ignition delay (noted as “ID” in Figure 5.23) causes a slight increase in the combustion variability represented by the coefficient of variation of the IMEP ( $COV_{IMEP}$ ), but the  $COV_{IMEP}$  is still within the acceptable range (e.g. below 3%) under the studied engine operating conditions.

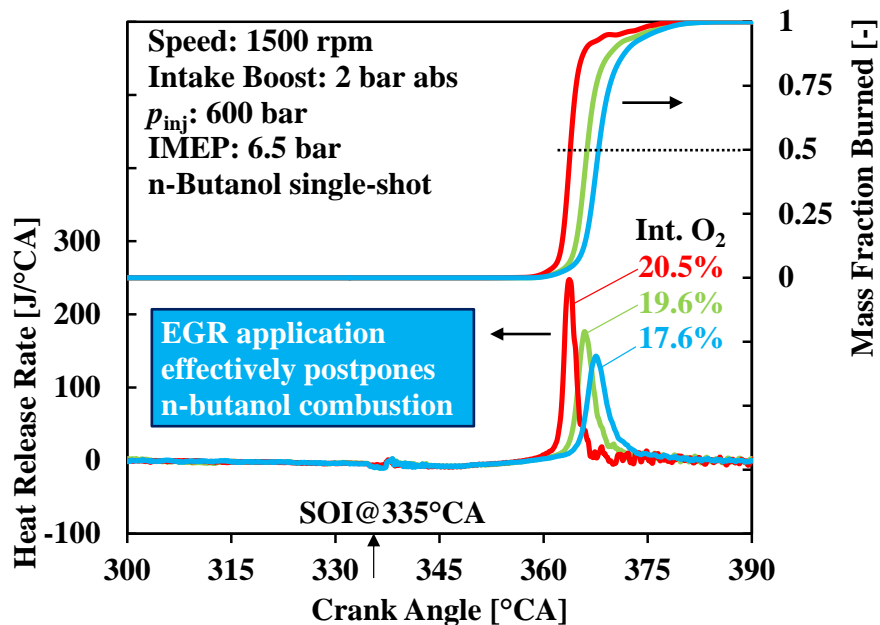


Figure 5.22 n-Butanol Single-shot with EGR – Heat Release

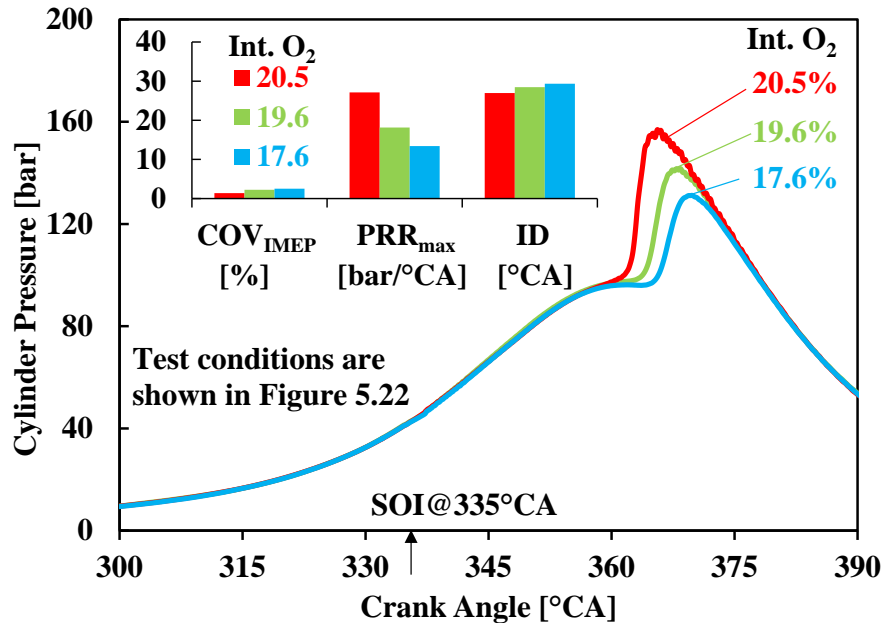


Figure 5.23 n-Butanol DI Single-shot with EGR – Pressure

### 5.2.2 n-Butanol Multiple-shot Direct-injection

The EGR application effectively reduces the combustion noise but further increases the propensity to misfire. In order to practically implement the n-butanol combustion, it requires better control techniques to appropriately organize the ignition and combustion processes, for instance, by creating a stratified cylinder charge via multiple injections.

Although the findings in Section 5.2.1 are based on the single-shot injection strategy, they are actually of significant importance for the development of the multiple injection strategy. In the misfire cases where the early injections are applied, the chemical reactions of the n-butanol and air release a certain amount of heat that however is insufficient to establish a successful ignition or sustain the subsequent combustion events. Nevertheless, such an early injection is useful to form a highly homogeneous cylinder charge that barely auto-ignites, and a main injection near TDC can thereafter be applied to ignite that cylinder charge.

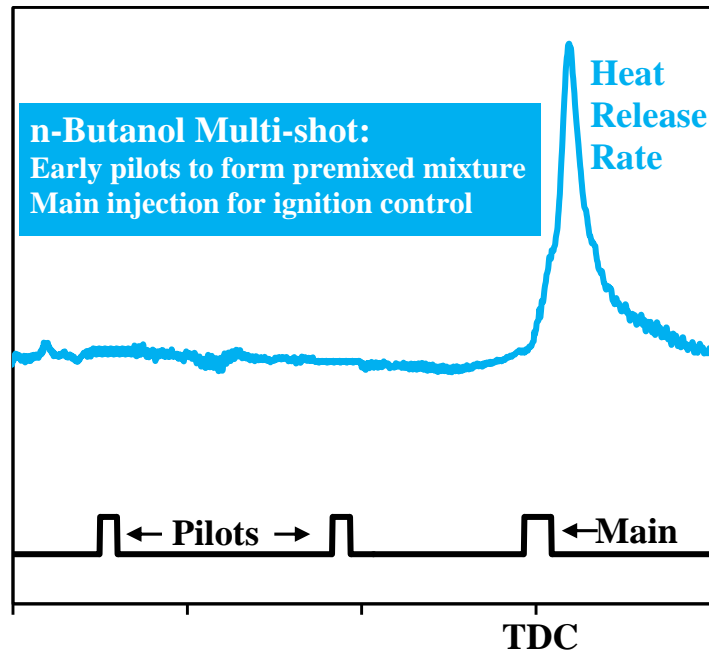


Figure 5.24 Schematic of Butanol Multiple-shot Injection Strategy

A schematic of the multiple-shot injection strategy for n-butanol is shown in Figure 5.24. The experimental results using such a multiple-shot strategy demonstrate that the adjustment of the main injection timing is capable of controlling the combustion phasing, as shown in Figures 5.25 & 5.26. The engine runs at a low EGR rate of 10% and an intake oxygen concentration of 20%. The early pilot injection is commanded at  $325^{\circ}\text{CA}$  with a duration of  $600\ \mu\text{s}$ . A fixed duration of  $900\ \mu\text{s}$  is commanded for the main injection at varied timings in a range of  $354^{\circ}\text{CA}$  to  $362^{\circ}\text{CA}$ . As the combustion phasing retards, the pressure rise rate reduces from  $18.6\ \text{bar}/^{\circ}\text{CA}$  to  $7\ \text{bar}/^{\circ}\text{CA}$ . The combustion stability remains within an acceptable range ( $\text{COV}_{\text{IMEP}}$  between 1.5% and 1.8%). With the roughness of combustion under control, the engine load can be raised to 10 bar IMEP, in comparison to 6.5 bar in the single-shot cases.

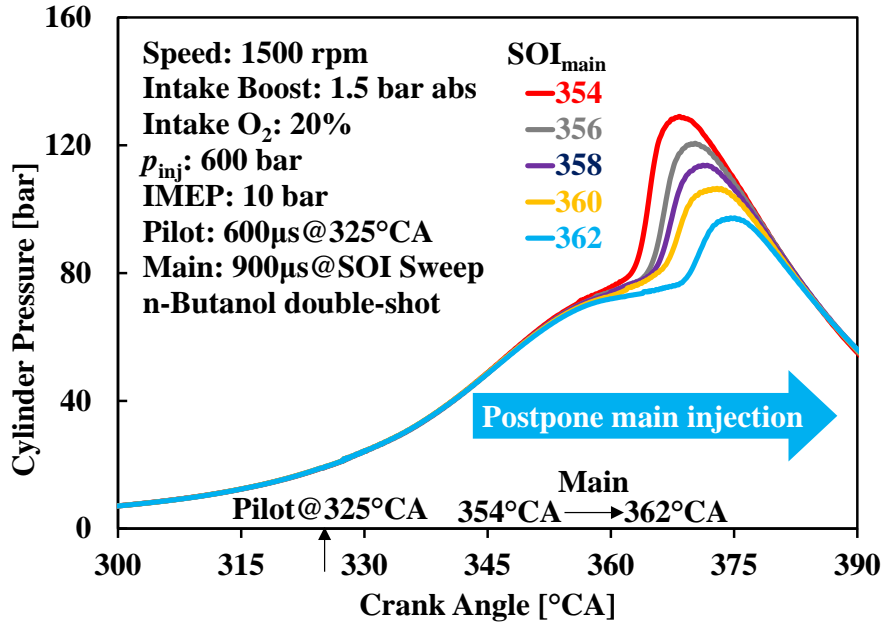


Figure 5.25 n-Butanol DI Pilot Plus Main – Pressure

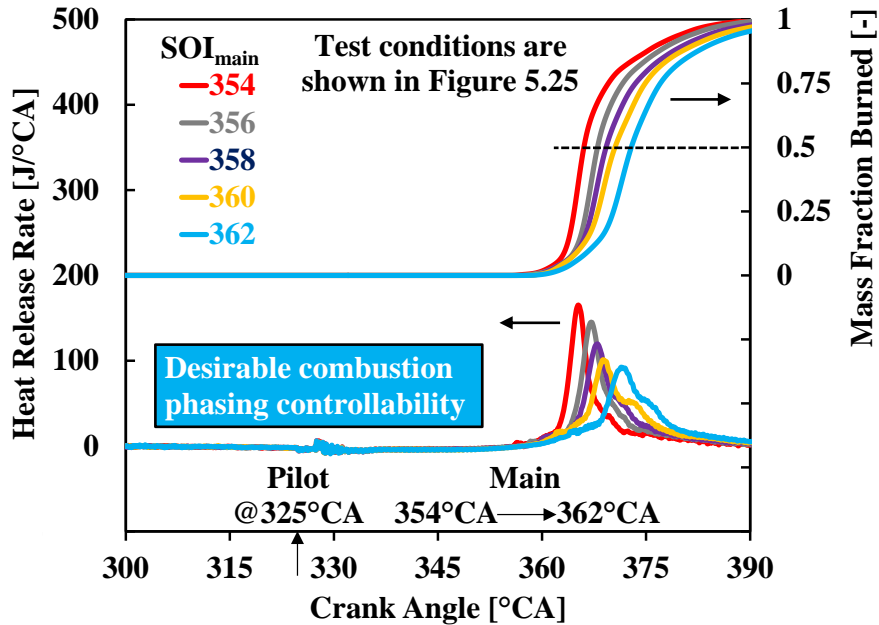


Figure 5.26 n-Butanol DI Pilot Plus Main – Heat Release

The results of NO<sub>x</sub> and smoke emissions are plotted in Figure 5.27 for the same series of experiments, and the CA<sub>5</sub>, CA<sub>50</sub> and ignition delay of the main injection are shown in Figure 5.28. The overall NO<sub>x</sub> and smoke levels increase noticeably compared to the previous single-shot results. The higher engine load in part contributes to the increase of NO<sub>x</sub> and smoke emissions, but such a drastic increase is primarily attributed to the diffusion burning of the n-butanol fuel delivered during the main injection. Minor changes in CA<sub>5</sub> are observed across the SOI<sub>main</sub> sweep, which indicates that the initial heat (the first 5%) is mainly released from the combustion of the early injected n-butanol. The cylinder pressure and temperature are therefore increased by these exothermic reactions, and when the main injection enters the combustion chamber, it ignites almost spontaneously, resulting in the diffusion burning of n-butanol. The ignition delay of the main injection is around 2 to 8°CA, much shorter than that in the single-shot cases.

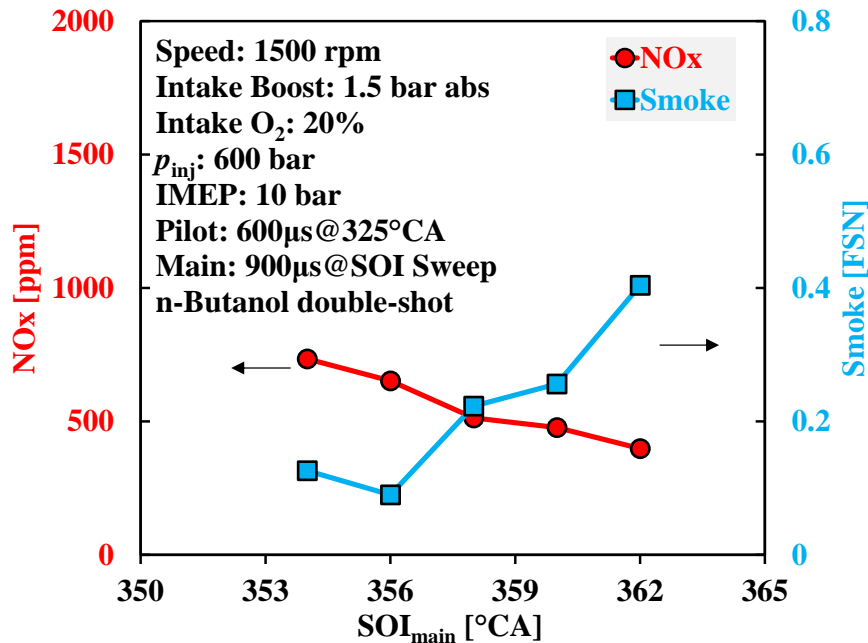


Figure 5.27 n-Butanol DI Pilot Plus Main – NO<sub>x</sub> and Smoke

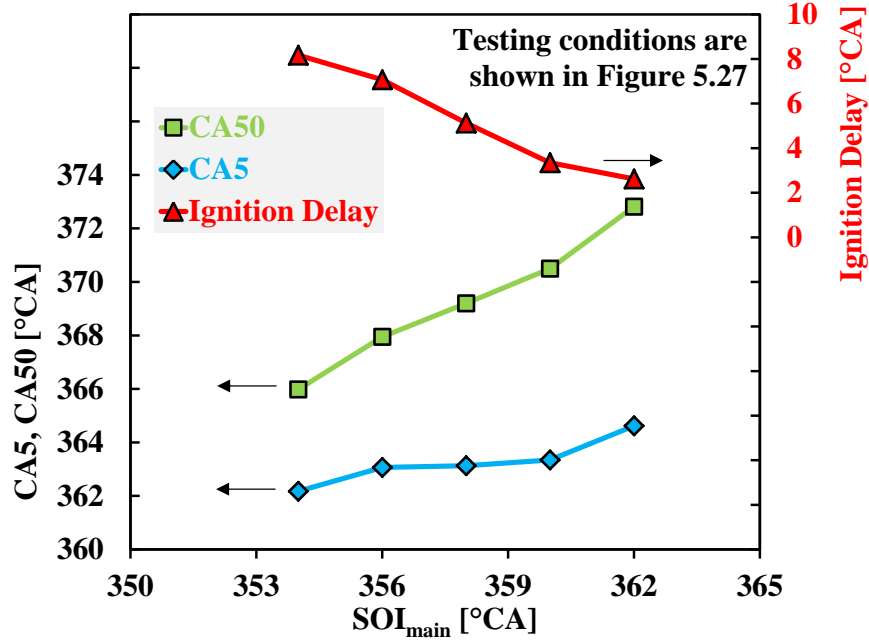


Figure 5.28 n-Butanol Pilot Plus Main – CA5, CA50, and Ignition Delay

In order to reduce the NO<sub>x</sub> emissions, higher EGR rates can be applied. At the same time, it is necessary to lower the extent of the diffusion burning to avoid the smoke penalty. Therefore, the amount of the main injection needs to be reduced by re-distributing the multiple shots. In Figures 5.29 & 5.30, the heat release and pressure profiles are shown for the n-butanol combustion using the triple-shot injection strategy, where the main injection duration is reduced to 550 μs and two early pilots (a duration of 450 μs for each) are applied. The engine load is raised to 11 bar IMEP. As the EGR rate increases to 38% and 42%, the intake oxygen concentration reduces to 16.0% and 14.8% respectively; and accordingly the NO<sub>x</sub> emissions drop to 50 ppm and 34 ppm respectively. The injection pressure is also increased to 900 bar to suppress the smoke production and, as a result, the smoke is controlled below 1 FSN (0.617 FSN and 0.717 FSN respectively).

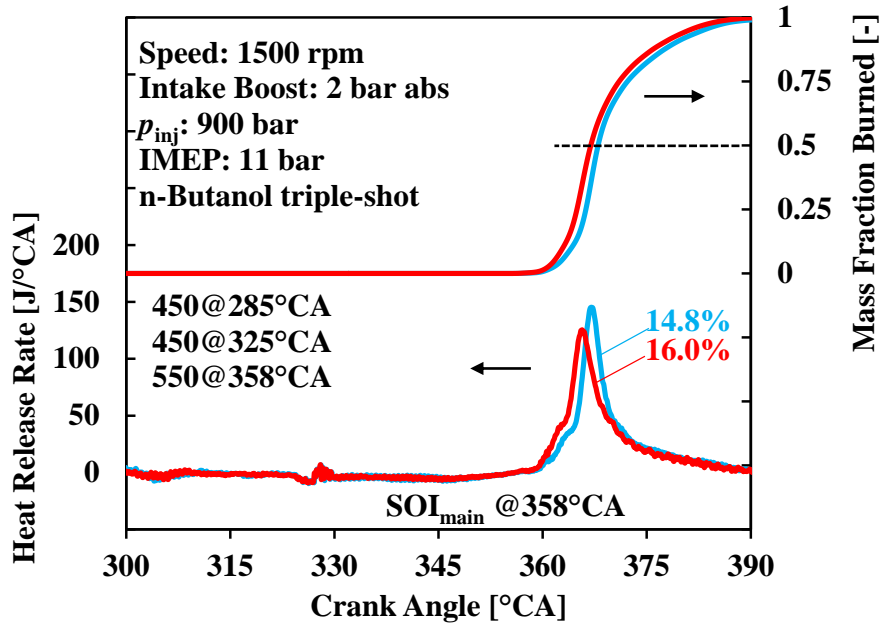


Figure 5.29 n-Butanol DI Triple-shot, Two Pilots Plus Main – Heat Release

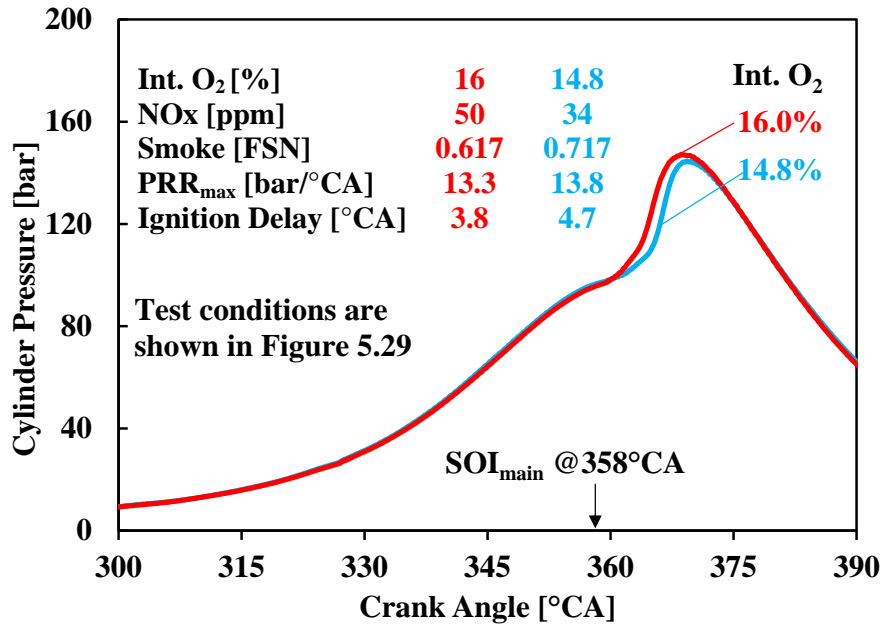


Figure 5.30 n-Butanol Triple-shot, Two Pilots Plus Main – Pressure

With the injection strategy using the early pilots plus main injection, the n-butanol combustion can tolerate higher EGR rates without misfire incidences. Stable LTC operations are achieved with tolerable combustion noise at higher engine load levels. However, the smoke emissions are increased compared to the near-zero smoke in the experiments using the single-shot injection strategy. The main injection with the substantially shortened ignition delay is the main cause for higher smoke emissions. In fact, if the early pilots are appropriately scheduled along with the controlled EGR rates, the near-TDC injection can be removed for smoke reduction while maintaining stable engine operations.

In Figures 5.31 & 5.32, the heat release and pressure profiles are shown for the n-butanol combustion using the early double-shot injection strategy without the main injection. The injection timings are  $305^{\circ}\text{CA}$  and  $325^{\circ}\text{CA}$ . As the EGR rate is increased from 32% to 41%, the ignition delay of the second injection is prolonged from  $34^{\circ}\text{CA}$  to  $40^{\circ}\text{CA}$ . At an EGR rate of 41%, the overall burning slows down and the combustion phasing postpones. The engine load reduces slightly from 10 bar to 9.5 bar IMEP, but simultaneously low NO<sub>x</sub> and smoke emissions are achieved.

Compared with the single-shot injection strategy, the early multiple-shot injections can stratify the cylinder charge and thus provide an improved control over the ignition and combustion processes. Such an injection strategy offers ultra-low NO<sub>x</sub> and smoke emissions at medium engine loads. However, the early multiple-shot strategy primarily relies on the precise EGR control to avoid excessively rough combustion and potential misfire events. On the other hand, the strategy using pilots plus main injection can tolerate a greater extent of the EGR variation.

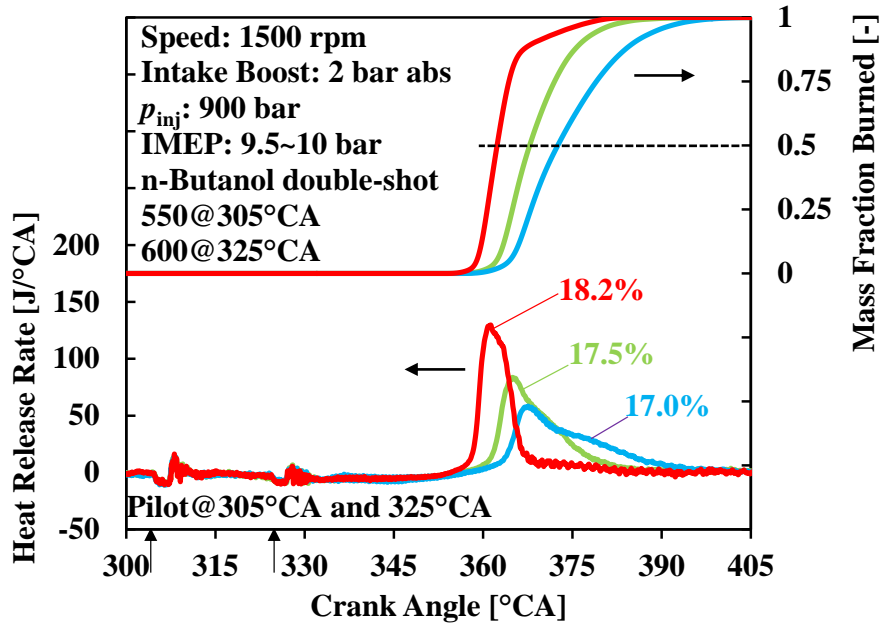


Figure 5.31 n-Butanol DI Double-shot, Two Early Pilots – Heat Release

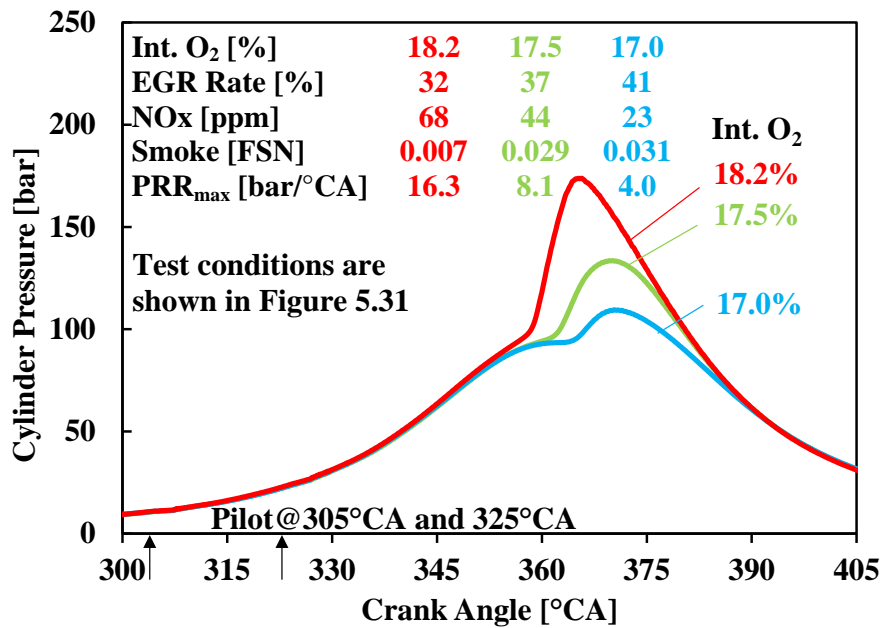


Figure 5.32 n-Butanol DI Double-shot, Two Early Pilots – Pressure

### 5.2.3 n-Butanol HCCI via Port Injection

The neat n-butanol has a boiling temperature (117.5°C) that is on the lower side of the boiling temperature range of gasoline (60~200°C). Thus the intake port injection can be applied to n-butanol. When a homogeneous cylinder charge of n-butanol and air auto-ignites under the compression temperature and pressure, the engine essentially runs in the HCCI operation. The experimental results (heat release rates) of n-butanol HCCI are shown in Figure 5.33. The engine runs in stable operation at low loads between 2.1 and 6.7 bar IMEP. The EGR application is not applied in these experiments, and the intake oxygen concentration is around 20.7%. The engine produces near-zero NO<sub>x</sub> and smoke emissions.

In Figure 5.34, the cylinder pressure and calculated mean cylinder temperature are shown for the n-butanol HCCI operation. The high volatility and the long mixing duration both contribute to the enhanced cylinder charge homogeneity. For the burning of such a thoroughly homogeneous charge, the calculated bulk gas temperature can be used to estimate the flame temperature. As the fuelling rates are increased for higher engine loads, the mean cylinder gas temperatures increase. However, the maximum mean cylinder temperature is still below the NO<sub>x</sub> formation threshold, *e.g.* ~1800K as suggested in the literature [6].

The heat release profiles also indicate that the ignition process becomes earlier and sharper with the increasing fuelling rate and, as a result, the peak cylinder pressure and the maximum pressure rise rate both increase (as shown in Figure 5.35). The high combustion noise represented by the maximum pressure rise rate hinders further increase of the engine load.

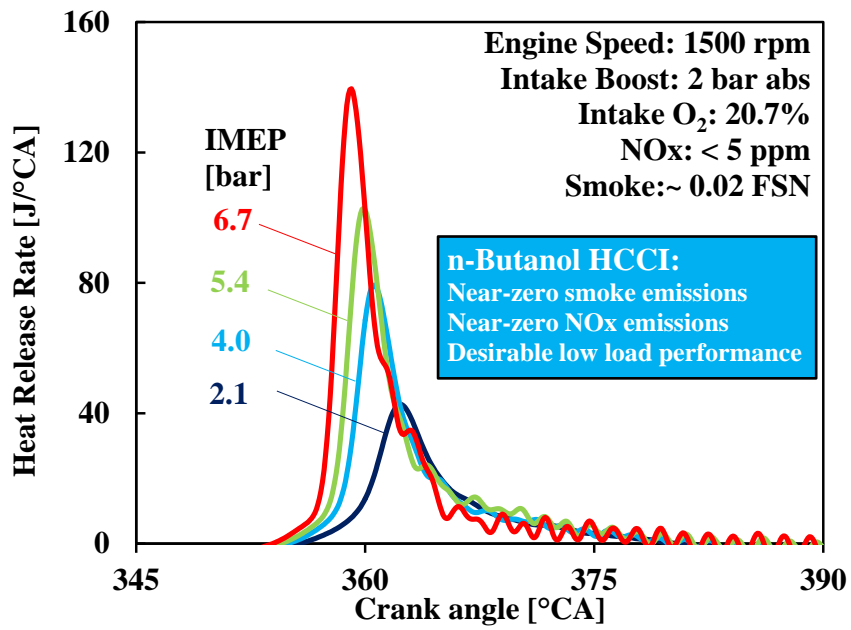


Figure 5.33 n-Butanol HCCI without EGR – Heat Release

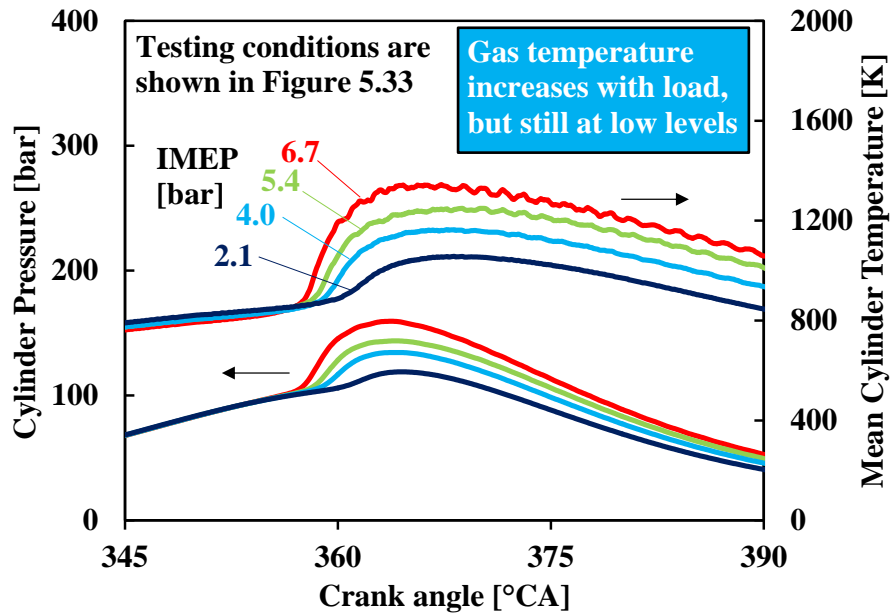


Figure 5.34 n-Butanol HCCI without EGR – Pressure, Temperature

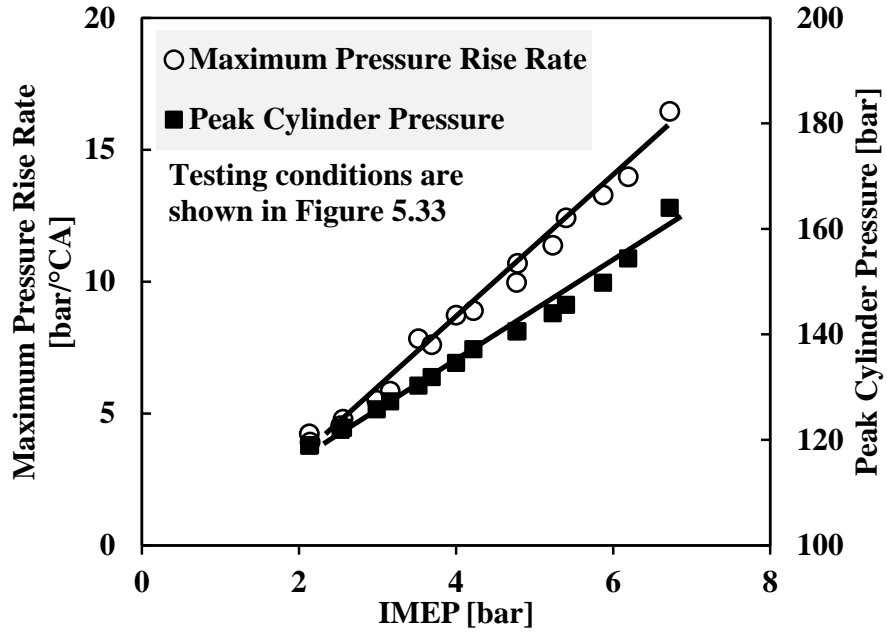


Figure 5.35 n-Butanol HCCI without EGR –  $dp_{max}$ ,  $p_{max}$

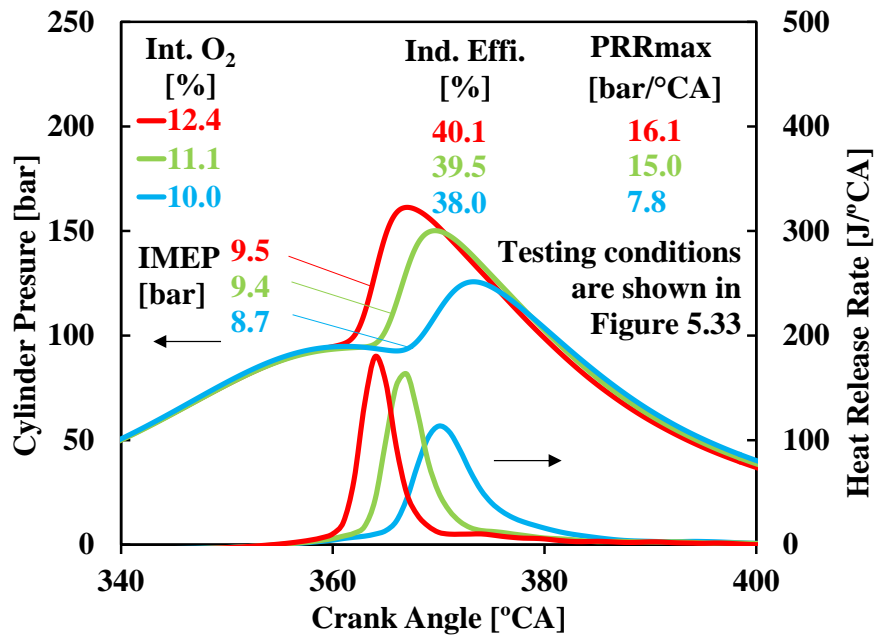


Figure 5.36 n-Butanol HCCI with EGR – Pressure, Heat Release

The EGR application can be used to postpone the combustion phasing and reduce the pressure rise rate. In Figure 5.36, three cases are shown for n-butanol HCCI at higher engine loads with the EGR application. The intake oxygen concentration is reduced to a level as low as 10%. Compared with maximum load achieved without EGR, the engine load is increased from 7 bar to 9 bar IMEP with increased fuel injection. In general, for n-butanol HCCI operation, the use of EGR is able to delay the combustion events, reduce the combustion rate, and lower the combustion noise, thereby allowing safe operations at higher engine loads. However, the EGR addition noticeably deteriorates the engine efficiency, while the NO<sub>x</sub> and smoke emissions remain ultra-low.

#### 5.2.4 Dual-fuel Combustion of n-Butanol and Diesel

When n-butanol is injected at the intake port, diesel pilots via direct-injection can be applied to implement the dual-fuel combustion (DFC). The non-dimensional constituent of port-injected fuel usage ( $\chi$ ) is defined by the percentage of the port fuel energy contribution to the total energy input from both fuels in DFC, following Equation (5-1). In other DFC modes with gasoline ( $\chi_{gas}$ ) and ethanol ( $\chi_{eth}$ ) fuels, the same definition applies.

$$\chi_{nbut} = \dot{m}_{nbut} \times LHV_{nbut} / (\dot{m}_{nbut} \times LHV_{nbut} + \dot{m}_{di} \times LHV_{di}) \times 100\% \quad (5-1)$$

Where,

$\chi_{nbut}$	the non-dimensional constituent of n-butanol in DFC	[%]
$\dot{m}_{nbut}$	the fuel flow rate of n-butanol	[mg/cycle]
$LHV_{nbut}$	the lower heating value of n-butanol	[MJ/g]
$\dot{m}_{di}$	the fuel flow rate of diesel	[mg/cycle]
$LHV_{di}$	the lower heating value of diesel	[MJ/g]

In Figure 5.37, the pressure and heat release rate profiles are shown for DFC with n-butanol and diesel. The experiments are conducted at two  $\chi_{nbut}$  values, 25% and 75%. During the experiments, the diesel injection timing needs to be delayed to maintain the same CA50 when a greater  $\chi_{nbut}$  is used. With a low level of n-butanol usage, the overall ignition timing can be controlled by the diesel injection. As  $\chi_{nbut}$  increases to 75%, however, the port delivered n-butanol auto-ignites prior to the diesel injection, even when a high EGR rate of 40% is applied. Although the n-butanol auto-ignition is expected to produce near-zero NO<sub>x</sub> and smoke emissions (as supported by the previous n-butanol HCCI study), the direct-injection of the diesel fuel during the n-butanol combustion often leads to significant diffusion burning where substantial NO<sub>x</sub> and smoke emissions are generated.

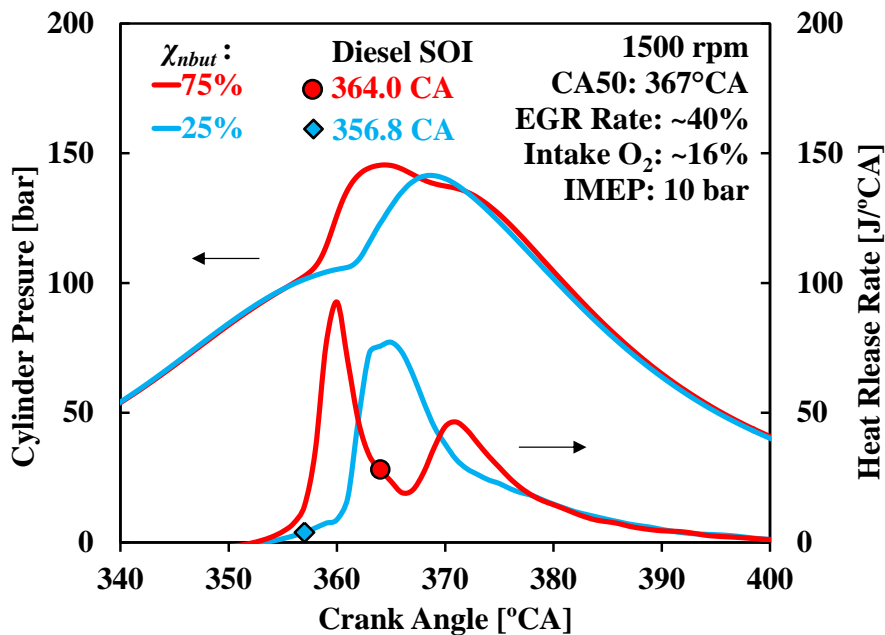


Figure 5.37 DFC of n-Butanol and Diesel – Pressure, Heat Release

The NO<sub>x</sub> and smoke emissions are shown in Figure 5.38 across the EGR sweep for the DFC operation with n-butanol and diesel. The results include three levels of n-butanol usage, namely  $\chi_{nbut}$  of 25%, 50%, and 75%. The emissions present a NO<sub>x</sub> versus smoke trade-off, similar to that of the conventional diesel combustion. Compared with the previous results of the neat n-butanol combustion, the NO<sub>x</sub> and smoke emissions from DFC are significantly higher. In regard to the n-butanol usage, the NO<sub>x</sub> emissions reduce with increased  $\chi_{nbut}$ , while minor difference is observed in smoke emissions under the tested conditions. As discussed earlier, the smoke emissions mainly come from the diffusion burning of the near-TDC injected fuel, and a major cause for the diffusion burning is the n-butanol premature auto-ignition that leaves little time for the mixing of the pilot diesel. Based on these test results, the DFC strategy is deemed unsuitable for the combination of n-butanol and diesel fuels, especially with the high compression ratio (18.2:1) used in the study.

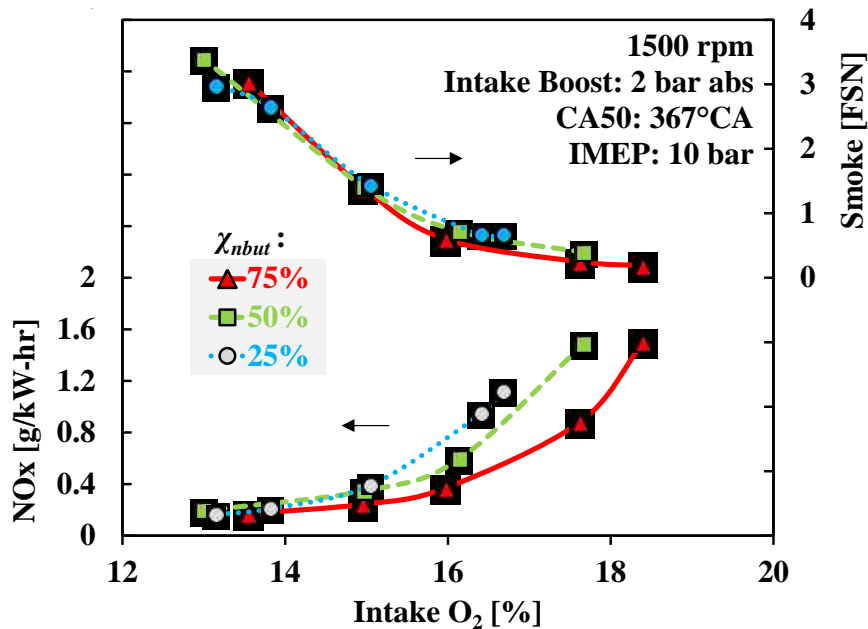


Figure 5.38 DFC of n-Butanol and Diesel – NO<sub>x</sub>, Smoke

To summarize the investigation on n-butanol, the use of n-butanol, via either the high-pressure direct-injection or the intake port fuel delivery, has shown significant advantages over the regular diesel fuel for the LTC enabling on the compression ignition research engine. Compared to the diesel baseline results, the EGR application is typically unnecessary for the port delivered n-butanol to achieve LTC, so long as the fuel strength in the mixture is not excessive, because the high volatility and prolonged ignition delay substantially enhance the cylinder charge homogeneity. In fact, EGR is usually applied as a control measure for the combustion phasing correction. Moreover, due to the premature auto-ignition, the intake port delivery of n-butanol is deemed unsuitable for the DFC operation under the tested conditions. A lower compression ratio may help to withhold the premature auto-ignition.

### **5.3 Gasoline LTC Enabling**

Compared with n-butanol, the high Octane gasoline (Octane number 91) has a further reduced fuel reactivity. However, the poor lubricity of the gasoline fuel makes it incompatible with the high-pressure direct-injection system unless a substantial amount of the lubricity improver is added to the fuel [31]. In this dissertation, the port fuel injection is applied in the investigation

#### **5.3.1 Gasoline HCCI**

Similar to the previous n-butanol HCCI experiments, the gasoline HCCI operation can also be enabled with the port fuel injection strategy, although to a limited load range only. Under the same engine operating conditions as in the n-butanol cases, the high Octane gasoline misfires at low fuelling rates. Stable combustion can only be established at an engine load of ~10 bar IMEP without EGR, if the intake temperature and the

compression ratio are left intact from the conventional diesel setup. It is noted that the intake heating is effective to enable low load gasoline HCCI [58, 60-61].

As suggested by the previous investigation, the engine load plays a critical role to achieve successful compression ignition of gasoline for a baseline diesel engine and operating under diesel-like conditions [106]. In Figure 5.39, the heat release rate profiles of the gasoline compression ignition are compared at different engine load levels. The excess air ratio ( $\lambda$ ) for gasoline is kept constant at 3.2. A late diesel injection is applied in each case to achieve the intended engine load, and the diesel injection timings are marked by the markers on the heat release profiles.

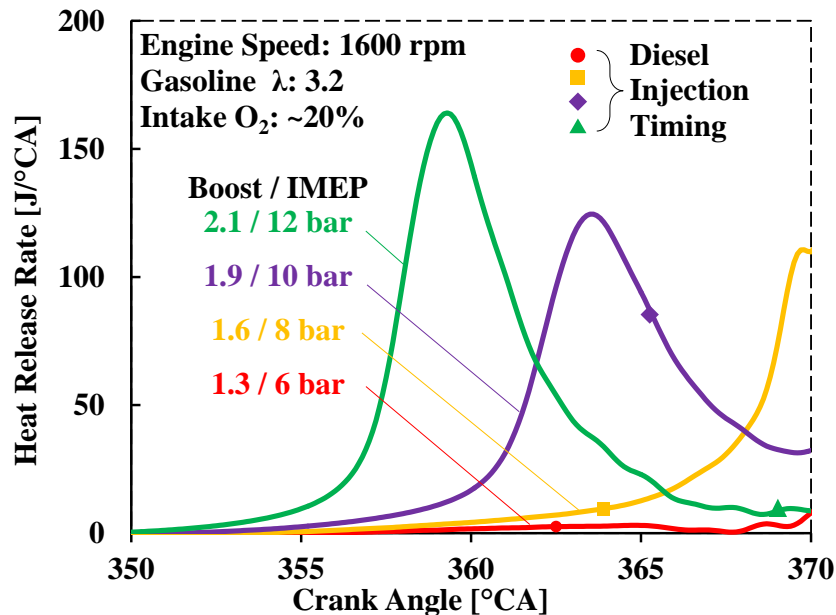


Figure 5.39 Gasoline Compression Ignition – Heat Release, Load

At engine loads of 6 and 8 bar IMEP, minor heat release is observed from the gasoline-air reactions prior to the diesel injection. When the engine load is raised to 10 bar IMEP, an obvious gasoline auto-ignition event is observed. The reaction rate becomes much more

rapid as the engine load is further increased to 12 bar IMEP, and the majority of the gasoline heat release occurs before or near TDC.

Compared with n-butanol, the low reactivity of the high Octane gasoline results in unacceptable low load performance, while the gasoline HCCI can be safely enabled at medium engine loads. In comparison, engine knocking may occur to n-butanol HCCI at the same engine loads. As shown in Figures 5.40 & 5.41, for instance, the gasoline HCCI is enabled at an engine load around 10 bar IMEP, a load proven to be unsafe for n-butanol HCCI. The heat release profiles in Figure 5.40 demonstrate that the low temperature reactions, although barely visible, start earlier than 10°CA before TDC and transition to accelerated reactions at around 7°CA after TDC. A slight fuel addition leads to a significant advancement of the combustion phasing and a steeper slope of the heat release rate trace. The presented gasoline HCCI operation produces ultra-low NOx and smoke emissions at a high indicated thermal efficiency of 46%.

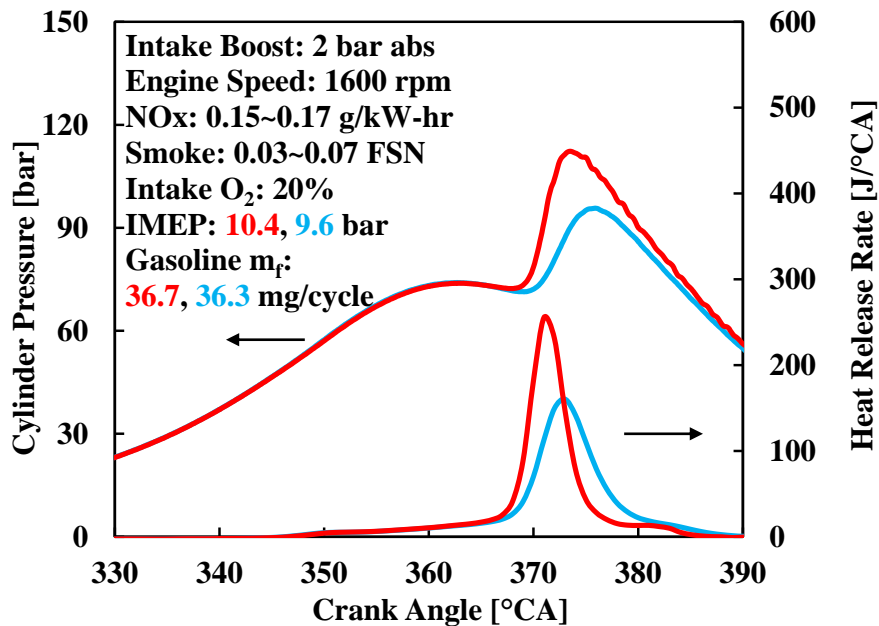


Figure 5.40 Gasoline HCCI – Pressure, Heat Release

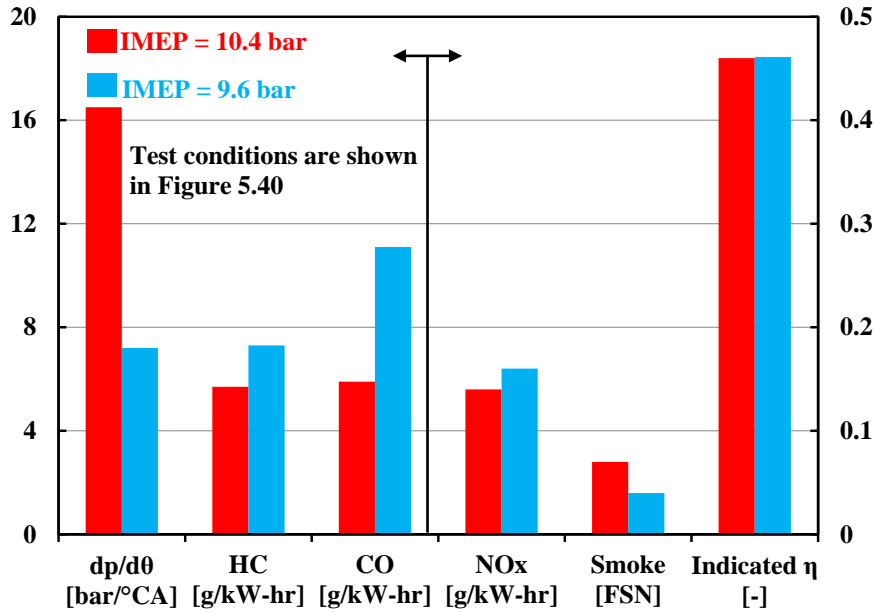


Figure 5.41 Gasoline HCCI – Emissions,  $PRR_{max}$ , Efficiency

With the port-injection, the compression ignition of a premixed gasoline-air charge surrenders the ignition control almost entirely to the kinetics of chemical reactions, since no effective control measures can be practically applied to the cylinder charge once the gasoline-air mixture is trapped in the cylinder. Consequently, the ignition control for HCCI combustion typically relies on the modulation of the intake boost and EGR. In Figure 5.42, the cylinder pressure and heat release traces are shown for the gasoline HCCI operation at different levels of intake boost and EGR, and the corresponding NO<sub>x</sub> and smoke emissions are shown in Figure 5.43. The engine load is raised up to 11.6 bar IMEP. An EGR rate of 56% is required to delay the combustion to an appropriate phasing. With an elevated intake boost of 2.5 bar abs, a high cylinder peak pressure of 170 bar is observed.

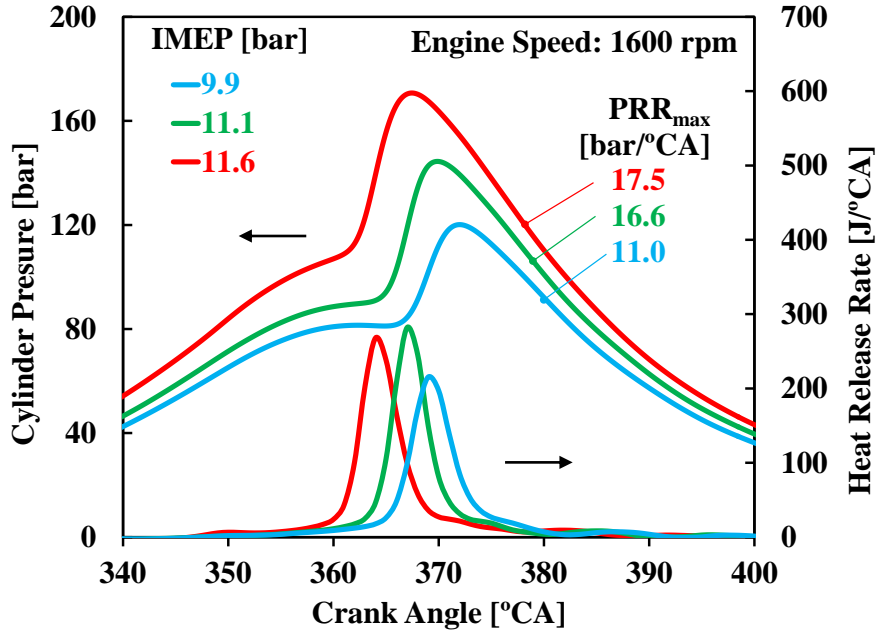


Figure 5.42 Gasoline HCCI with EGR – Pressure, Heat Release

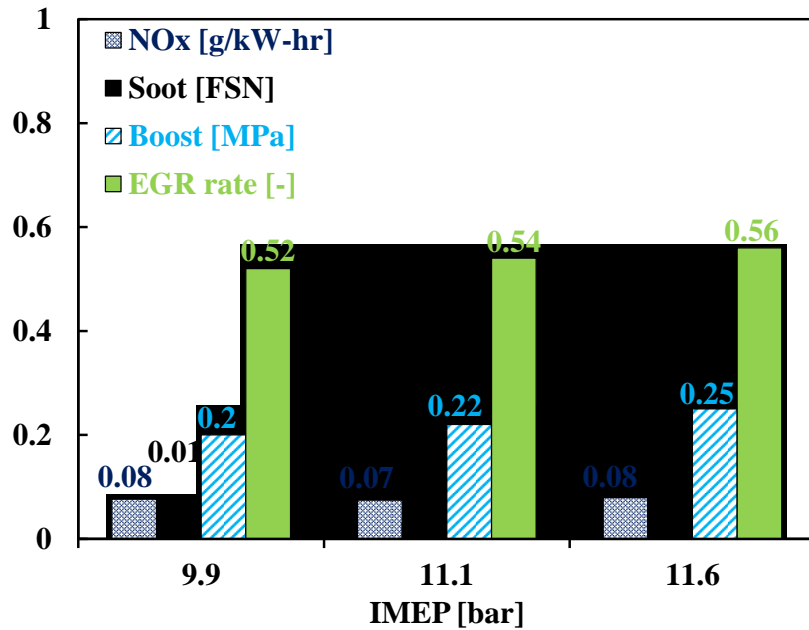


Figure 5.43 Gasoline HCCI with EGR – Emissions, Intake Boost, EGR

### 5.3.2 Dual-fuel Combustion of Gasoline and Diesel

A major problem for DFC with n-butanol and diesel has been the premature auto-ignition of the port delivered n-butanol. On the other hand, the gasoline HCCI investigation indicates that the gasoline fuel tends to misfire until the engine load increases to around 10 bar IMEP. Therefore, compared with n-butanol, the high Octane gasoline fuel can be a better choice to avoid the premature auto-ignition in the DFC operation.

Two heat release rate traces are shown in Figure 5.44 for the DFC operation with gasoline and diesel. The engine runs at 8 bar IMEP with near-zero EGR. The intake oxygen concentration is 20.5%. The  $\chi_{gas}$  values (non-dimensional constituent of gasoline in DFC, similarly defined in Section 5.2.4) are 38% and 76%. The diesel injection timing is fixed at 364 °CA.

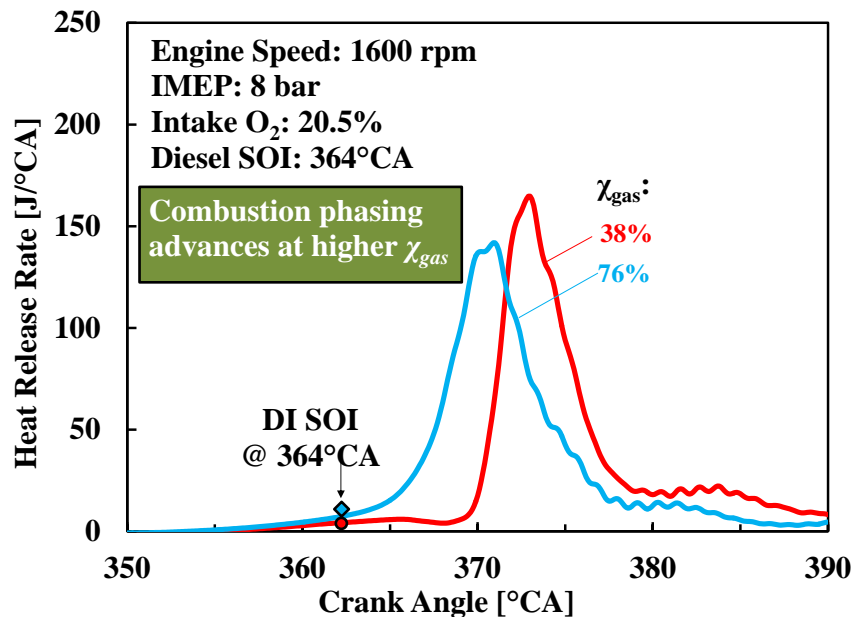


Figure 5.44 DFC with Gasoline and Diesel – Heat Release

As the gasoline usage is increased, the overall combustion event advances for the same diesel injection timing. The premature auto-ignition of gasoline does not occur even without EGR. However, comparing the heat release rate prior to the start of the diesel injection (at 364°CA), the pre-ignition reactions of gasoline noticeably release more energy with the increase of gasoline usage (higher  $\chi_{gas}$  values).

The results of exhaust emissions are shown in Figures 5.45 & 5.46 for a sweep of the  $\chi_{gas}$ . Due to the near-TDC diesel injection, the engine produces relatively high levels of NOx emissions without EGR. However, the increasing use of gasoline reduces NOx and smoke simultaneously. It is an indication that the use of gasoline facilitates the LTC enabling. The increase of the unburned HC emissions also suggests lowered flame temperatures.

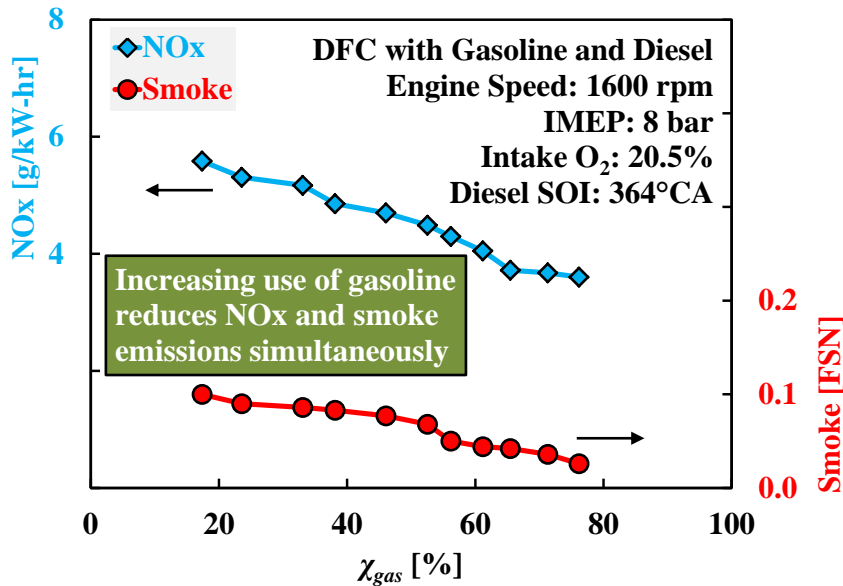


Figure 5.45 DFC with Gasoline and Diesel –  $\chi_{gas}$ , NOx, Smoke

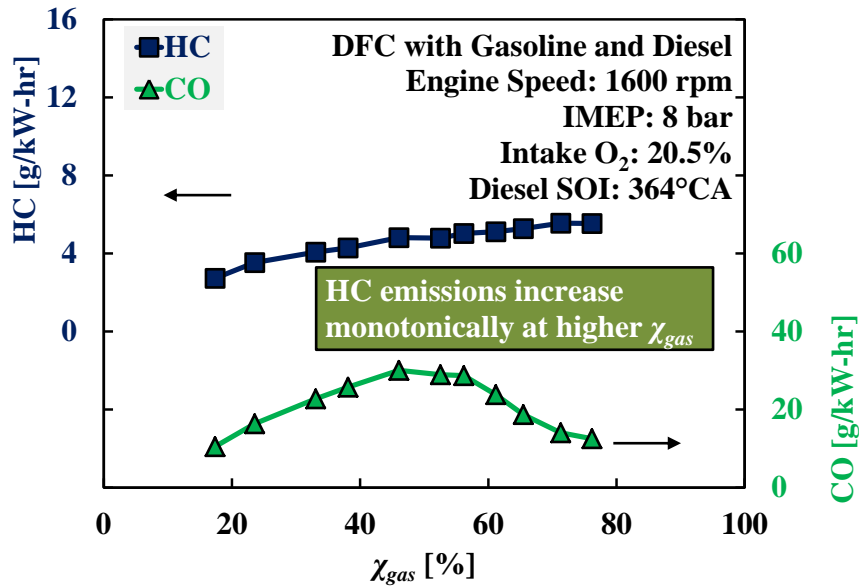


Figure 5.46 DFC with Gasoline and Diesel –  $\chi_{gas}$ , HC, CO

In the diesel baseline study, the EGR application is the most effective measure to reduce the NO<sub>x</sub> emissions associated with the near-TDC injected diesel fuel. The same methodology is therefore applied to reduce NO<sub>x</sub> emissions of the DFC operation. The efficacy of EGR on the NO<sub>x</sub> reduction is demonstrated in Figure 5.47. The engine runs at a high  $\chi_{gas}$  of 90%. As the EGR rate increases from 10% to 45%, the NO<sub>x</sub> emissions reduce substantially and eventually reach the desirable low level (*e.g.* <0.2 g/kW-hr).

Compared with the diesel combustion in the baseline experiments, the DFC with gasoline and diesel presents a few distinctive characteristics in terms of the NO<sub>x</sub> and smoke emissions. In order to achieve the desired low NO<sub>x</sub> emissions, the DFC operation only requires the intake oxygen concentration to be lowered to a level around 16% rather than 13~14% in the diesel baseline case, for similar or higher loads. Moreover, the smoke emissions from DFC remain at an ultra-low level (<0.2 FSN) despite the increased EGR rate from 10% to 45%, given that a high  $\chi_{gas}$  is applied. As a result, the simultaneously

low NO<sub>x</sub> and smoke emissions are achieved at an intake oxygen concentration of 15%~16%, which is substantially less demanding for the engine air system to achieve, compared to the 8~9% intake oxygen concentration required for diesel LTC in the baseline experiments.

The incomplete combustion products increase at higher EGR rates (Figure 5.48). It is however noted that the levels of the HC and CO emissions are comparable to those observed in the baseline diesel LTC. As the combustion phasing is controllable via the diesel injection, the maximum pressure rise rates of gasoline diesel DFC are in a relevantly acceptable range of 8~14 bar/°CA (as shown in Figure 5.49). Such a desirable controllability over the combustion phasing offers a great potential for the LTC load expansion.

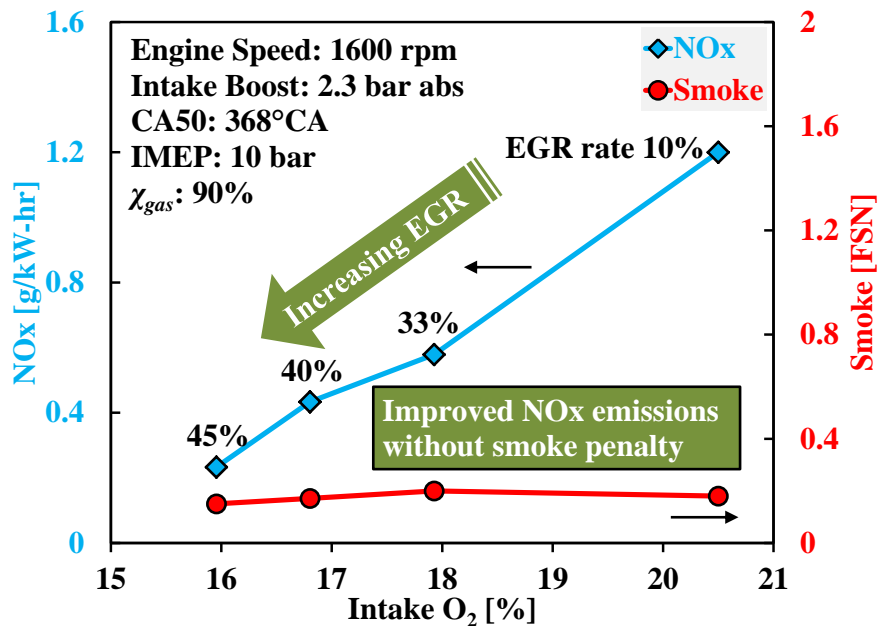


Figure 5.47 DFC with Gasoline and Diesel – EGR, NO<sub>x</sub>, Smoke

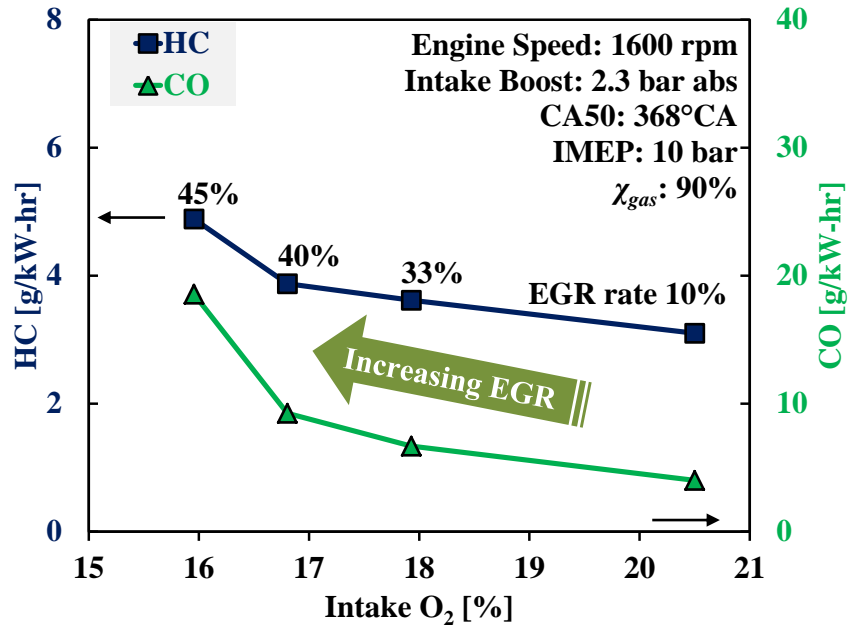


Figure 5.48 DFC with Gasoline and Diesel – EGR, HC, CO

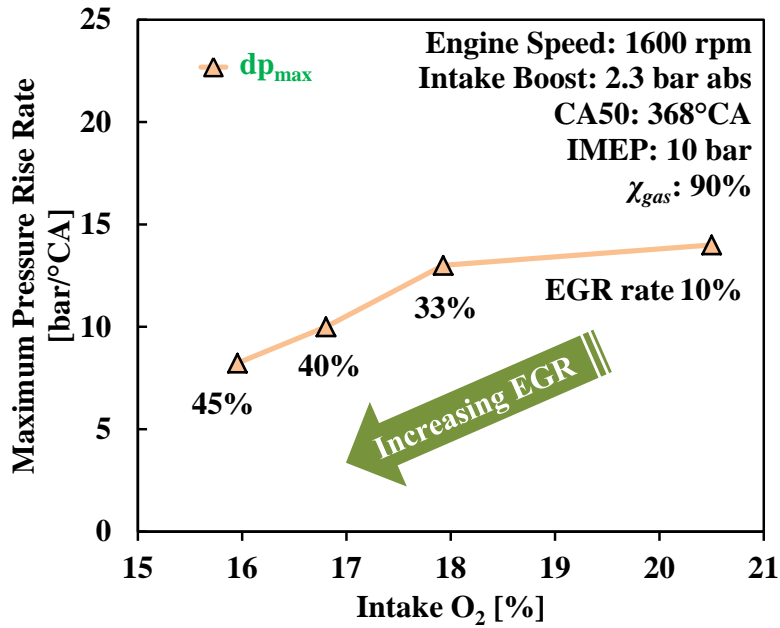


Figure 5.49 DFC with Gasoline and Diesel – EGR,  $dp_{max}$

In general, the port-injection of gasoline can significantly improve the overall homogeneity of the cylinder charge. Under the studied engine operating conditions (*e.g.* the compression ratio and fuel reactivity), the gasoline is suitable for the HCCI operation at medium engine loads, while the engine operation can encounter misfire at lower loads and rough combustion at higher loads. The DFC strategy using gasoline and diesel substantially improves the NO<sub>x</sub> and smoke emissions and, at the same time, offers desirable combustion controllability.

#### **5.4 Ethanol LTC Enabling**

For engine applications, ethanol is typically delivered via the intake port injection. In fact, the implementation of ethanol high-pressure direct-injection is challenging because of its poor lubricity and high volatility.

While gasoline misfires at low engine loads, ethanol does not auto-ignite even with the high compression ratio under the same engine operating conditions. A successful ignition might be achieved with high ethanol fuelling rates, which however can result in excessively high pressure rise rates and peak cylinder pressures. As suggested in the literature [99], additional intake heating is generally necessary for enabling ethanol HCCI.

In this dissertation, the DFC strategy solely is applied for ethanol, along with the regular diesel fuel as pilots. Compared with gasoline diesel DFC where the diesel injection essentially assists the gasoline auto-ignition and combustion, the DFC with ethanol and diesel however requires the diesel pilots to serve as a reliable ignition source in order to ensure the ignition and combustion events. The injection strategy for DFC with ethanol

and diesel is illustrated in Figure 5.50. The near-TDC diesel pilot is applied because it offers desirable control over the ignition timing and combustion phasing.

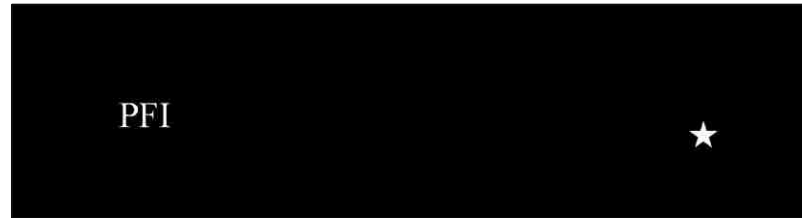


Figure 5.50 Injection Strategy for DFC with Ethanol and Diesel

The cylinder pressure and heat release rate traces are shown in Figure 5.51 for the DFC operation with ethanol and diesel. Three levels of ethanol usage are applied at an engine load of 10 bar IMEP. The  $\chi_{eth}$  values (following similar definition as described in Section 5.2.4) are 22%, 48%, and 79%. The diesel injection timing is fixed at 358°CA and the intake oxygen concentration is 18% at an EGR rate of 25%.

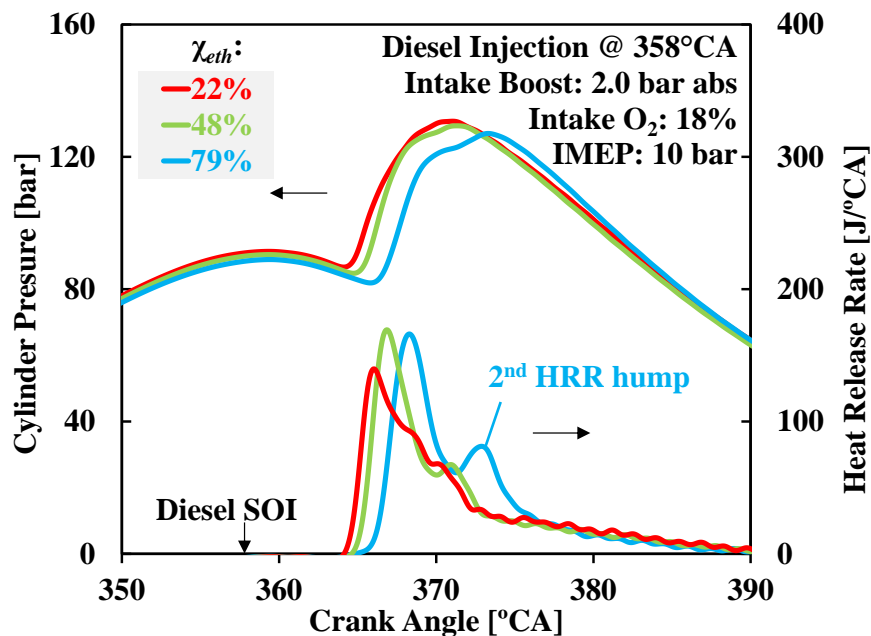


Figure 5.51 DFC with Ethanol and Diesel – Pressure, Heat Release

The heat release profiles indicate that a greater  $\chi_{eth}$  retards the ignition timing and combustion phasing. When the engine runs with a  $\chi_{eth}$  of 79%, the heat release presents a double-hump pattern. The appearance of the second heat release peak is similar to that of the diffusion burning phase in a conventional diesel combustion event. However, such a second peak is not attributed to diffusion burning but more likely to the limited rate of flame propagation of ethanol that is ignited by the diesel flame. Compared with the DFC cases of gasoline and diesel (as shown in Figure 5.44), the premature auto-ignition does not occur owing to the low reactivity of ethanol. The stability of the ethanol diesel DFC heavily depends on the ignition quality of the near-TDC injected diesel pilot.

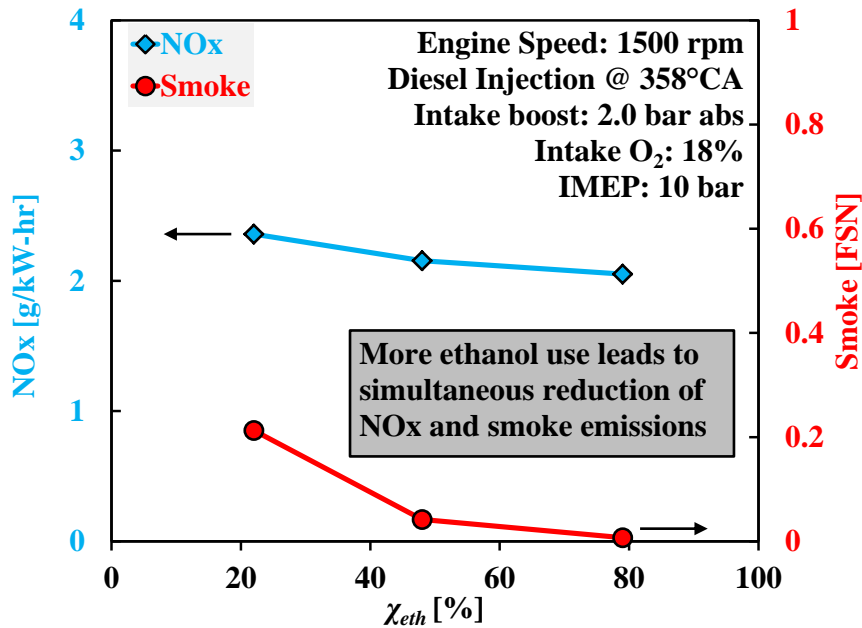


Figure 5.52 DFC with Ethanol and Diesel –  $\chi_{eth}$ , NOx, Smoke

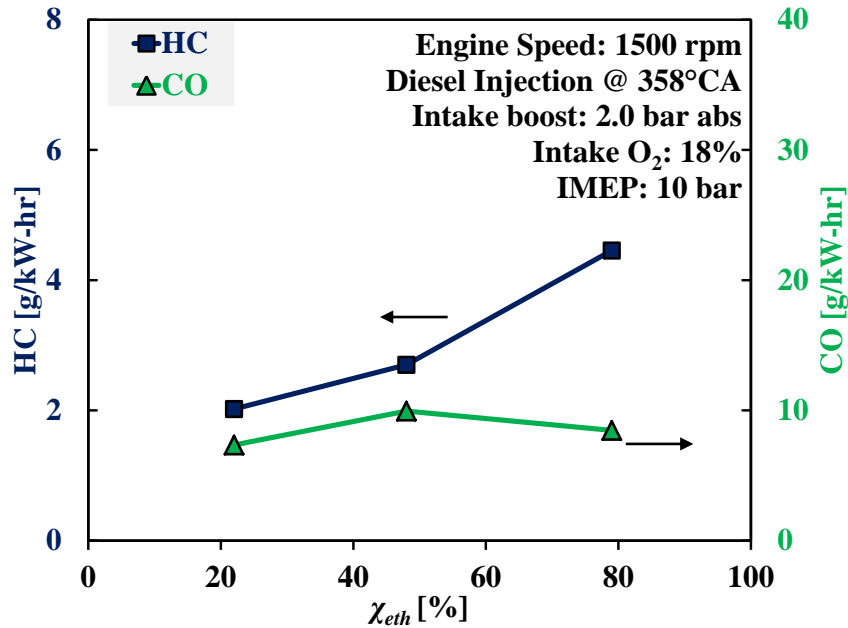


Figure 5.53 DFC with Ethanol and Diesel –  $\chi_{eth}$ , HC, CO

The corresponding emission results for the  $\chi_{eth}$  sweep are shown in Figures 5.52 & 5.53. The overall trend of the exhaust emissions agrees with the results from gasoline diesel DFC experiments presented earlier in this work. The increasing use of a volatile fuel (*i.e.* gasoline or ethanol) reduces the smoke and NO<sub>x</sub> emissions simultaneously but results in higher unburned HC emissions.

As discussed earlier, the diesel injection is necessary to avoid complete misfires in the DFC operation, but the near-TDC diesel injection incurs a certain extent of the cylinder charge heterogeneity that leads to substantial smoke and NO<sub>x</sub> emissions. In order to reduce these undesirable emissions, an elevated diesel injection pressure can be applied for smoke reduction, and an increased EGR rate can be used to lower the NO<sub>x</sub> emissions.

The results of the smoke and NO<sub>x</sub> emissions are shown in Figures 5.54 & 5.55 for the EGR sweeps at different diesel injection pressures. The ethanol usage is fixed ( $\chi_{eth}$  of 60%). An increase of the diesel injection pressure clearly lowers the smoke emissions of the ethanol diesel DFC. The NO<sub>x</sub> emissions, however, are insensitive to the change of the diesel injection pressure, while the EGR application is again very effective for the NO<sub>x</sub> reduction. The improved NO<sub>x</sub> versus smoke trade-off is shown in Figure 5.56.

The advantages of the DFC with ethanol and diesel are demonstrated in Figure 5.57. The DFC results are compared with the diesel LTC baseline under the same engine operating conditions. The use of ethanol substantially improves the overall cylinder charge homogeneity, thereby offering significant benefits in the smoke emissions. The decreased quantity of the near-TDC diesel injection effectively alleviates the dependence on EGR for NO<sub>x</sub> reduction.

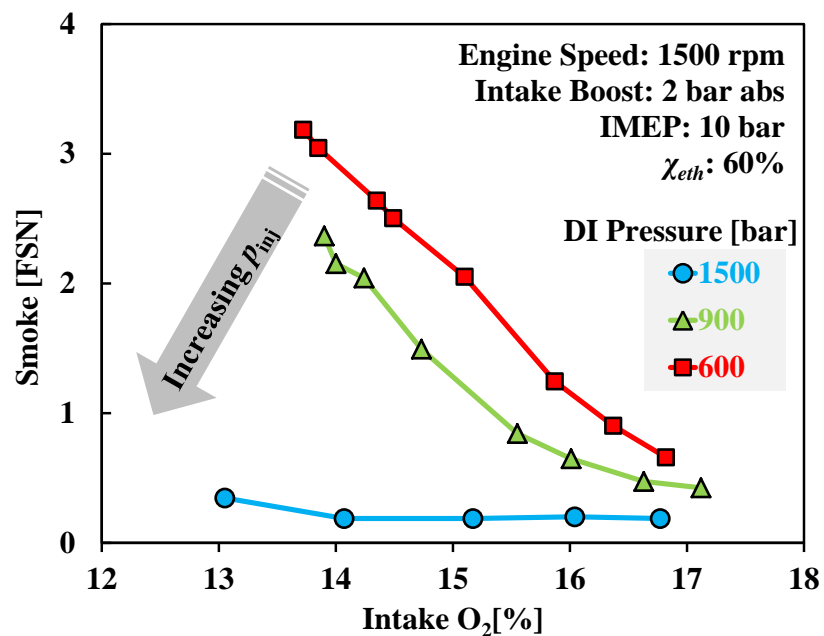


Figure 5.54 DFC with Ethanol and Diesel – DI  $p_{inj}$ , Smoke

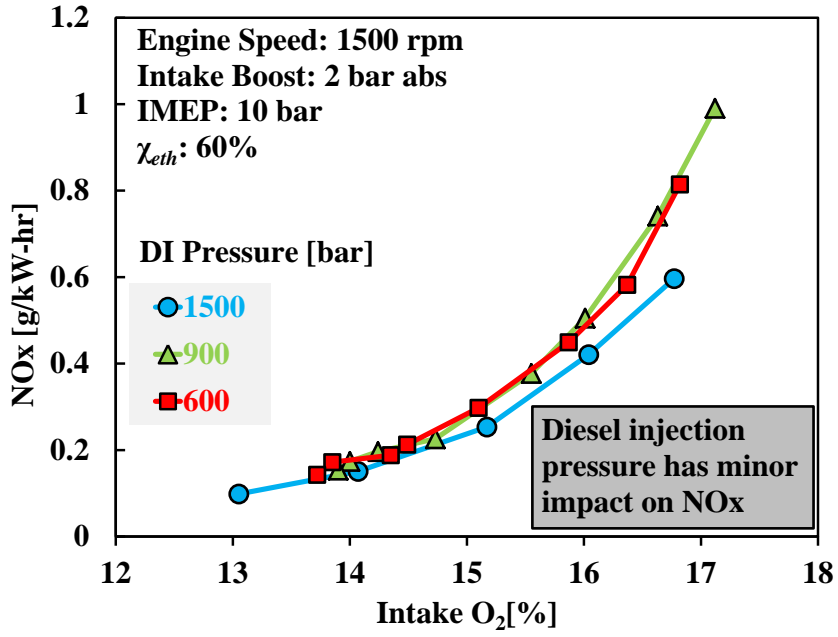


Figure 5.55 DFC with Ethanol and Diesel – DI  $p_{inj}$ , NOx

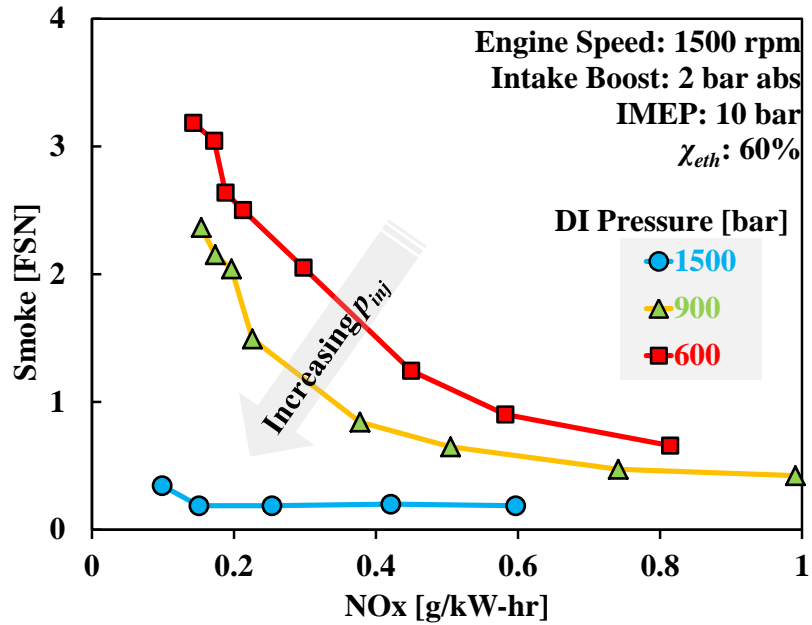


Figure 5.56 DFC with Ethanol and Diesel – DI  $p_{inj}$ , NOx, Smoke

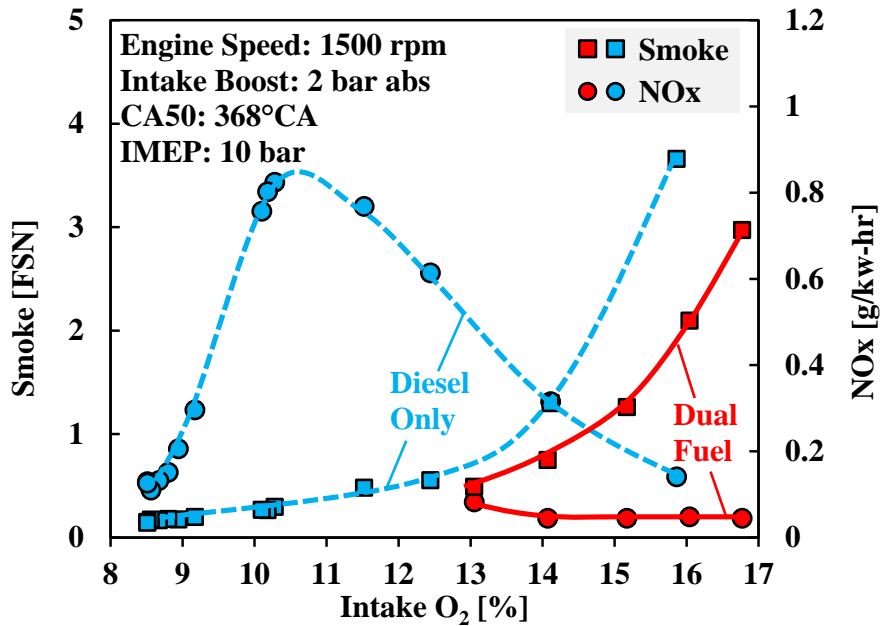


Figure 5.57 DFC with Ethanol and Diesel versus Diesel LTC

In Figures 5.58 & 5.59, the results of NO<sub>x</sub> and smoke emissions are shown for the  $\chi_{eth}$  sweep to study the ethanol effect at an increased engine load of 10 bar IMEP. With a moderate EGR rate (e.g. 40%) applied, the NO<sub>x</sub> emissions are reduced to desired low levels of 0.2~0.3 g/kW-hr. These results agree with the earlier findings at the engine load of 8 bar IMEP (as shown in Figure 5.52) in that the increasing use of ethanol leads to simultaneous reduction of NO<sub>x</sub> and smoke emissions. At this increased engine load of 10 bar IMEP, ultra-low NO<sub>x</sub> and smoke emissions are achieved simultaneously at a  $\chi_{eth}$  value of 76%.

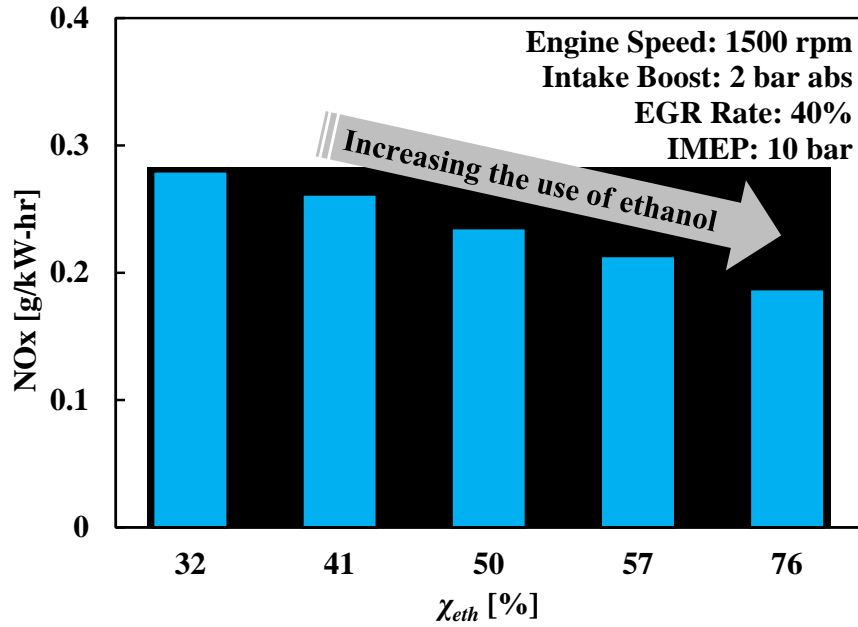


Figure 5.58 DFC with Ethanol and Diesel with EGR –  $\chi_{eth}$ , NOx

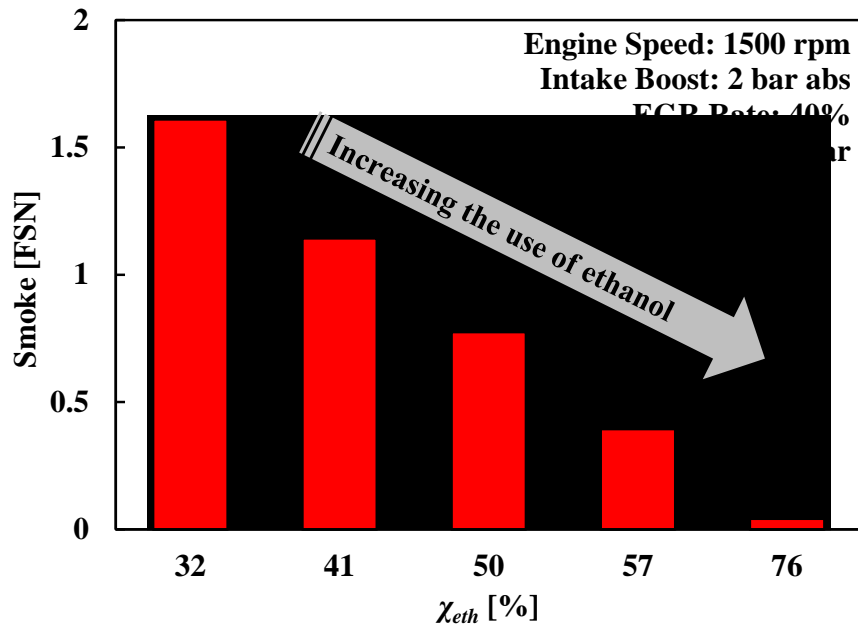


Figure 5.59 DFC with Ethanol and Diesel with EGR –  $\chi_{eth}$ , Smoke

When more ethanol is used, the diesel injection needs to advance to compensate for the loss of the overall fuel reactivity and maintain the same combustion phasing, as shown in Figure 5.60. The prolonged ignition delay of diesel is also observed as the ethanol use is progressively increased, as shown in Figure 5.61, which is likely attributed to the background suppression of the pre-ignition chemical activities. As a result, the earlier diesel injection timing and longer ignition delay help to achieve a greater separation between the injection and combustion events, which contributes to the simultaneous reductions of NO<sub>x</sub> and smoke emissions. However, the engine efficiency reduces by increasing the ethanol use (as shown in Figure 5.62). The optimal use of ethanol (represented by  $\chi_{eth}$ ) requires balancing between the emissions and engine efficiency. A control methodology is developed in this dissertation to determine the optimal  $\chi_{eth}$  in real time, which will be presented in the Chapter VI.

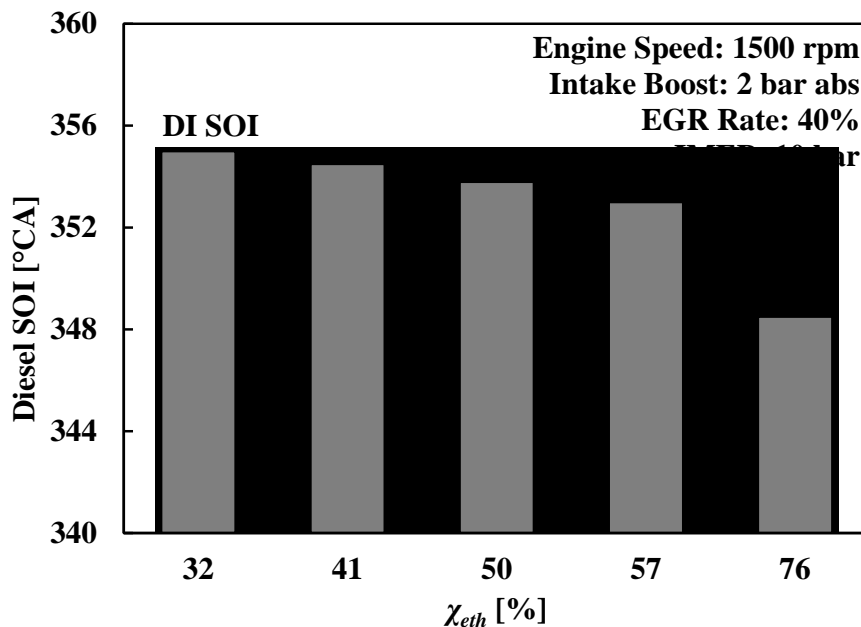


Figure 5.60 DFC with Ethanol and Diesel with EGR –  $\chi_{eth}$ , DI SOI

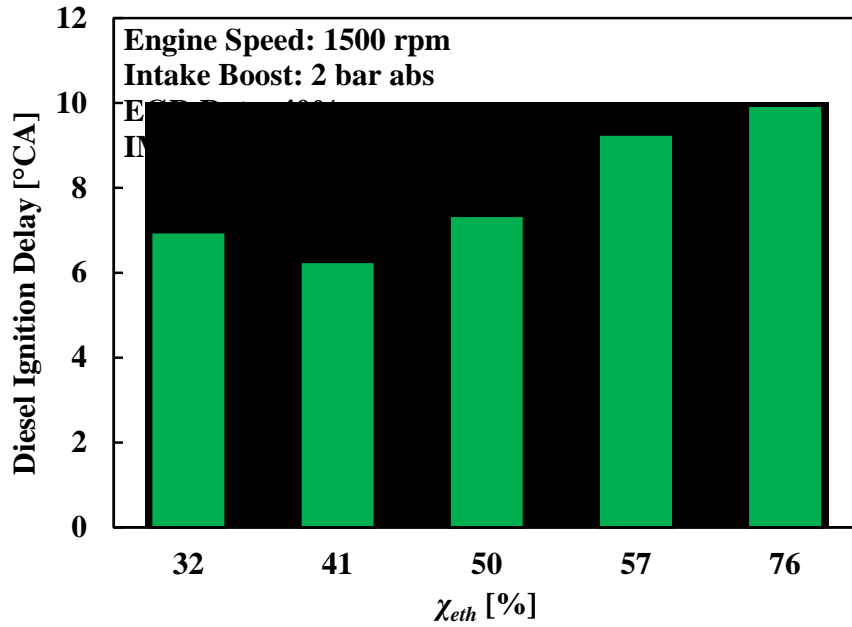


Figure 5.61 DFC with Ethanol and Diesel with EGR –  $\chi_{eth}$ , Ignition Delay

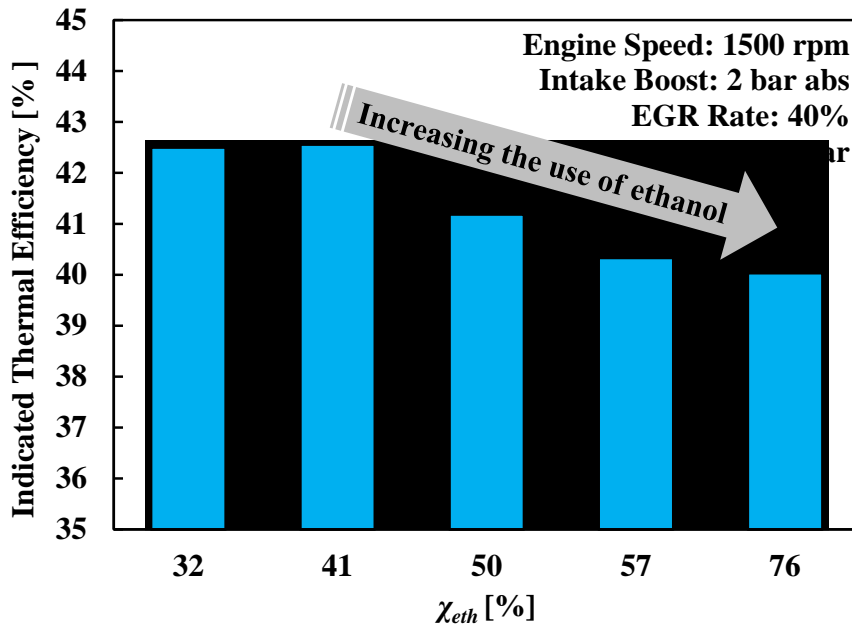


Figure 5.62 DFC with Ethanol and Diesel with EGR –  $\chi_{eth}$ , Efficiency

## 5.5 Comparison of Different Fuels

In this chapter, fuels including the diesel, n-butanol, high Octane gasoline, and ethanol, along with the advanced fuelling strategies are extensively studied for the LTC enabling. In Figure 5.63, the fuelling strategies and combustion modes are summarized for each investigated fuel. In general, compared with a regular diesel fuel, the use of a more volatile and less reactive fuel significantly facilitates the LTC enabling on the high compression ratio research engines.

When applied with the high-pressure direct-injection, the n-butanol combustion does not necessarily require EGR to enable the LTC operation, although limited to a moderate engine load level. With the assistance of EGR and multiple-shot injections to avoid rough combustion, the LTC operation of n-butanol can achieve up to an engine load of 12 bar IMEP that is extremely difficult for diesel LTC enabling under the same conditions (*e.g.* with a high compression ratio of 18.2:1).

As to the HCCI operation, the difference in the fuel reactivity results in different engine load performance. The neat n-butanol offers desired low to medium load performance, but the high pressure rise rate limits further load extension. The high Octane gasoline, on the other hand, cannot be used for HCCI combustion at low engine loads (without intake heating) due to misfire, while improved engine operations (compared with n-butanol) at medium loads have been established. The HCCI type of combustion is not applicable to ethanol without intake heating because of misfire under the investigated conditions. In the DFC mode, n-butanol is deemed unsuitable as the port delivered fuel owing to the demanding control over the premature auto-ignition. The gasoline and ethanol fuels have lower tendency towards early auto-ignition and thus outperform n-butanol in this regard.

	<u>Diesel</u>	<u>Butanol</u>	<u>Gasoline</u>	<u>Ethanol</u>
<b>Direct Injection</b>	Applicable		Not readily available	Not readily available
	<ul style="list-style-type: none"> <li>LTC enabling relies on EGR, boost, and injection pressure</li> <li>Low to medium load; 8 bar IMEP</li> </ul>	<ul style="list-style-type: none"> <li>Much easier than diesel for LTC; EGR is not always necessary</li> <li>Low to medium load; 11 bar IMEP</li> </ul>		
<b>Port Injection</b>	Requires additional control, e.g. intake heating	Suitable		
<b>HCCI</b>		<ul style="list-style-type: none"> <li>Good low load performance</li> <li>2~9 bar IMEP</li> <li>Phasing control via EGR</li> </ul>	<ul style="list-style-type: none"> <li>Only applicable in medium load range</li> <li>10~12 bar IMEP</li> </ul>	<ul style="list-style-type: none"> <li>Not applicable without intake heating</li> </ul>
<b>DFC</b>	<ul style="list-style-type: none"> <li>Serve as the direct injection pilot fuel</li> <li>Near TDC injection produces NO<sub>x</sub> and smoke emissions</li> </ul>	<ul style="list-style-type: none"> <li>Unsuitable as the port injected fuel</li> <li>Difficult to avoid premature auto-ignition</li> </ul>	<ul style="list-style-type: none"> <li>Suitable as the port injected fuel</li> <li>Premature auto-ignition may occur at extended loads</li> </ul>	<ul style="list-style-type: none"> <li>Suitable as the port injected fuel</li> <li>Premature auto-ignition not observed</li> <li>Potential for high load LTC</li> </ul>

Figure 5.63 Comparison of Fuel Types and Fuelling Strategies

It is therefore conclusive that different fuel types, with suitable fuelling and combustion strategies, can substantially facilitate the LTC enabling on compression ignition engines. In addition, the requirements for a desired fuel can change as the engine operating conditions vary (*e.g.* an engine load change). Even with the advanced control of the engine air system, it is still difficult to accommodate different engine load conditions with a single fuel that is available presently. The real-time fuel design and active fuelling control are therefore deemed beneficial for LTC engine operations, which is presented in the next chapter.

## CHAPTER VI

### DYNAMIC COMBUSTION CONTROL

The advantages of using n-butanol, gasoline, and ethanol fuels under optimized engine operating conditions have been identified in Chapter V. Therein, the need for suitable fuelling strategies has also been highlighted for the LTC enabling using those fuels. This chapter presents a detailed discussion on the dynamic combustion control for the dual-fuel combustion, with an emphasis on the active injection control in relation to the ignition, combustion, and exhaust emissions.

#### 6.1 Injection Pressure Control

The research engines used in this dissertation are equipped with common-rail injection systems. In order to regulate the common-rail pressure, these common-rail systems often utilize two electronic-controlled valves, namely the volume control valve (VCV) and pressure control valve (PCV). The VCV is responsible for the total fuel supply to the high-pressure generation components of a common-rail pump. A wider opening of the VCV results in more fuel delivered at the plungers for compression, and thus it is possible to achieve a higher injection pressure; but this generally consumes more power. The control of the PCV determines the final high-pressure output of the pump by regulating the high-pressure fuel leakage back to the fuel return of the pump. These two valves are usually controlled via pulse width modulation (PWM) signals at certain frequencies (*e.g.* 250 Hz). For laboratory tests, a simplified control can be achieved by only regulating the PCV duty cycle for a desired pressure while keeping the VCV at a constant and sufficient opening to ensure an adequate fuel supply.

## 6.2 Injection Timing and Duration Control

The control flexibility over the injection timing and duration is essential for investigating different fuelling strategies. The implementation of the active injection control requires advanced hardware to meet the demands for fast computation and prompt execution, in addition to adequate power of activation. The specifications of the hardware used for the injection control are listed in Table 6.1.

Table 6.1 Specifications of Hardware for Injection Control

Hardware	Model	Specifications
Embedded controller	NI PXI 8110	2.26 GHz quad-core processor
Controller chassis	NI PXI 1031	Real-time OS <sup>1</sup>
Vertex 5 LX85 FPGA	NI PXI 7853R	40 MHz 96 DIO <sup>2</sup> 8 AI <sup>3</sup> , 8 AO <sup>4</sup> , and 3 DMA <sup>5</sup>
Vertex II 3M gate FPGA	NI PXI 7813R	40 MHz 160 DIO 25 ns resolution
Injector drivers	EFS IPOD 8232 Solenoid EFS IPOD 8370 Piezo	Programmable voltage and current for injector
Pressure transducer	AVL GU13P (Ford engine) Kistler 6052B (SCRE)	Range: 0~250 bar
Charge amplifier	Kistler 5010B	Range: 10~999000 pC Sensitivity: 0.01~9990 pC/MU <sup>6</sup>
Encoder	Gurley Precision	0.1 °CA resolution

<sup>1</sup> Operating System

<sup>2</sup> Digital Input and Output

<sup>3</sup> Analogue Input

<sup>4</sup> Analogue Output

<sup>5</sup> Direct Memory Access

<sup>6</sup> Mechanical Unit

The primary control unit for the real-time computation is the embedded controller. The controller hosts a chassis that provides a high-speed bus for the data communication between the embedded controller and other control hardware such as the FPGA (field programmable gate array) devices. The FPGA devices have sufficient input and output channels (analogue and digital) to interface with the measuring system for the cylinder pressure and the power driver units for the port and direct injectors.

An optical encoder mounted on the engine crankshaft provides information of the engine rotation positioning. The encoder outputs consist of two signals, namely the index consisting of one transistor-transistor logic pulse (TTL) per revolution and the ticks consisting of 3600 TTL pulses per revolution. The index is physically aligned with the engine TDC, and thus the piston position can be determined by counting the ticks after each index. In this particular setup, a crank angle resolution of  $0.1^\circ\text{CA}$  can be achieved. In addition, a camshaft rotation signal is used to distinguish a compression TDC from a gas exchange TDC.

The control over the injection timing is implemented on a crank angle basis, which is different from the common control algorithms that work in the time domain. The injection control algorithm iterates every engine cycle and the injection needs to occur at a specific crank angle. However, the injection duration, which primarily governs the injection quantity at a given injection pressure, requires control in the time domain (*e.g.*  $500\ \mu\text{s}$ ). In order to achieve simultaneous control deterministically in two different domains, the FPGA code includes two separate execution loops that run in parallel. The first loop receives signals from the encoder and the cam sensor to determine the piston position and, at the same time, compares the current piston position (crank angle) with

the commanded injection timing. At the instant that the engine crank angle matches the injection timing, the execution loop for the injection duration control is triggered.

At the start of the commanded injection, the designated digital output turns from “0” to “1” and holds for a time period equal to the commanded injection duration. The controller therefore generates a TTL signal with a rising edge at the crank angle of the commanded injection and a pulse width equal to the commanded injection duration. The dynamic control of the injection can therefore be established by controlling the injection timing and duration according to the desired set points.

### **6.3 Real-time Feedback Control**

The cylinder pressure is used as the feedback for the real-time injection control. A cylinder pressure transducer, a charge amplifier, and designated high-speed DAQ systems are used to acquire the cylinder pressure. By convention, the cylinder pressure is acquired in the crank angle domain, and thus the encoder signals are used to trigger and sample the cylinder pressure.

The flow chart of the injection feedback control is shown in Figure 6.1. The feedback control algorithm takes advantages of the high sampling rates of the FPGA devices and the high computational performance of the embedded controller. As the cylinder pressure is sampled by the FPGA 7853R over one engine cycle, the pressure data is stored in the FPGA memory.

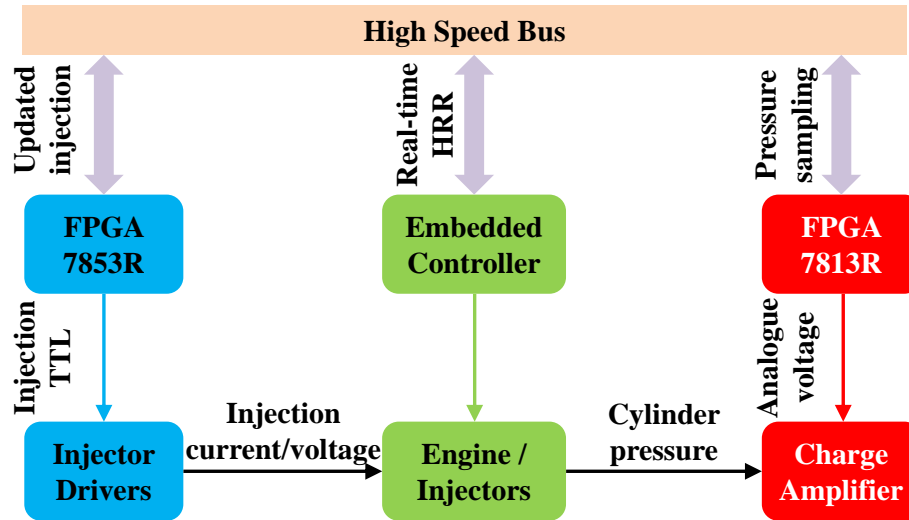


Figure 6.1 Feedback Injection Control – Flow Chart

At the end of the engine cycle, 7200 data points of cylinder pressure (the first data point corresponds to the cylinder pressure of the gas exchange TDC) are collected and immediately transferred to the embedded controller via the pre-set direct memory access (DMA) channels. Using the sampled cylinder pressure, the real-time heat release analysis is performed on the embedded controller to calculate important combustion parameters (*e.g.* IMEP and CA50). After comparing the set points and the feedbacks, the control algorithm updates the injection command (timing and duration) and sends the signal to the FPGA for execution in the next cycle. The entire process, which consists of the data transfer (between the controller and FPGA devices), real-time combustion analysis, and the injection command update, typically finishes in a fraction of one millisecond (less than 9 degrees CA at 1500 rpm). Therefore, within the first millisecond of the current engine cycle, an updated injection command is ready for execution. The validation of the real-time injection control will be presented in Section 6.5.

It is important to understand the correlation between the control parameters (*e.g.* injection timing and duration) and the combustion characteristics (*e.g.* combustion phasing and

load). In general, a longer injection duration results in more fuel delivered into the cylinder and most likely an increased engine power output. However, the change of the injection timing, under different engine operating conditions, may lead to wide variations in the response of combustion phasing. In Figure 6.2, for instance, the combustion phasing (CA50) response to the change of the diesel injection timing is shown for the DFC operation (using ethanol and diesel) at three different engine loads.

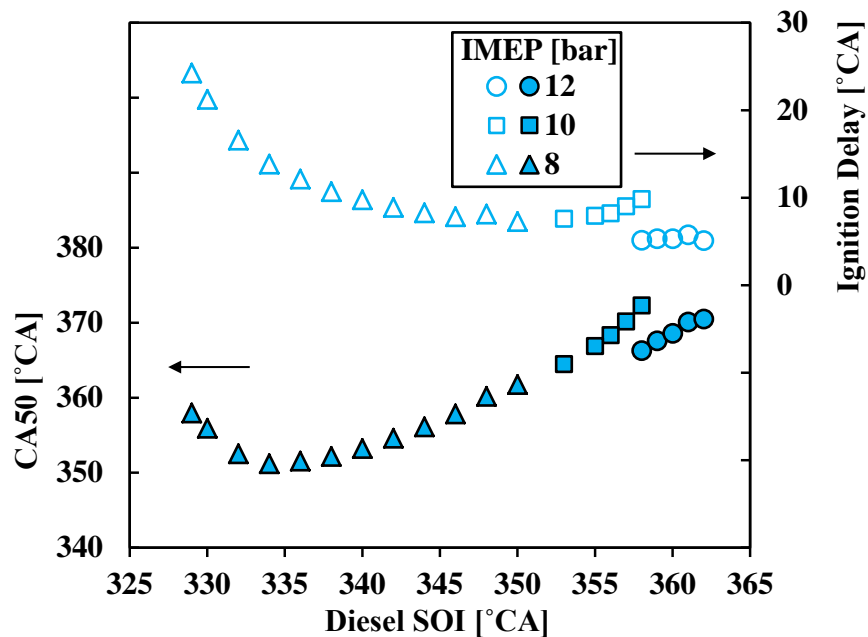


Figure 6.2 DFC with Ethanol and Diesel – CA50, Diesel Ignition Delay

A linear correlation exists between the diesel injection timing and the combustion phasing for a quite wide range; however, when the diesel ignition delay is significantly prolonged with earlier injection timings (*e.g.* earlier than 335°CA), an advancement of the diesel injection can lead to a postponed combustion phasing. The near-TDC diesel pilot is therefore preferred to utilize the quasi-linear relationship between the combustion phasing and injection timing.

## 6.4 Correlation of Injection, Combustion, and Smoke Emissions

The control over the combustion phasing and engine load primarily improves the stability of the engine operation. More importantly, the fuel injection has significant impacts on the combustion processes and the resultant exhaust emissions. Therefore, efforts should be made to incorporate the emission related strategies in the real-time injection control.

Different injection strategies for the LTC enabling share a common feature, *i.e.* the separation of the injection from the combustion events (as previously shown in Figure 2.1). Conventionally, the ignition delay is the primary parameter to evaluate this separation. As indicated by the previous work, an ignition delay longer than one millisecond is considered merely sufficient for the diesel LTC enabling using the single-shot injection strategy [107]. The ignition delay is conventionally defined as the duration between the start of the injection command and the onset of the combustion (represented by CA5 in this dissertation). With the injector needle lift measured, the needle lift profile can be used instead of the injection command (a TTL signal) to more precisely represent the injection process.

However, neither of these two methods can characterize the injection process sufficiently. For a piezo injector, for instance, it can take hundreds of microseconds (*e.g.* 200~300  $\mu\text{s}$ ) for the diesel fuel to actually exit the injector nozzle after the start of the injection command. This time period is typically defined as the injector opening delay. Similarly, the injector closing delay can be as long as 500~900  $\mu\text{s}$  for the same type of injectors. Since the injection duration for a light-duty diesel engine commonly ranges from 200  $\mu\text{s}$  to 1000  $\mu\text{s}$ , therefore, the timing of the injection command can deviate extensively from that of the actual injection process. To date, the rate of injection (ROI), which is generally

measured on offline designated equipment (*e.g.* the long tube method) rather than on engines, is deemed as the best way to characterize the injection process for a particular injector.

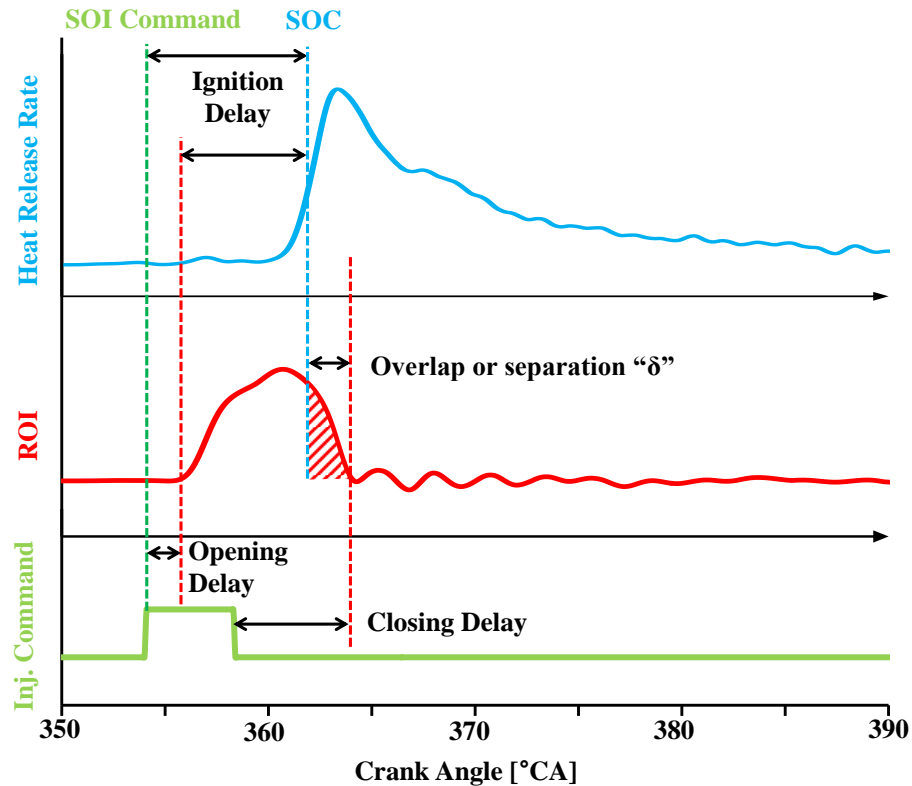


Figure 6.3 Schematic of Injection Command, ROI, and Heat Release

Moreover, relative to the aforementioned “separation”, the end of injection is of more importance than the start of injection and, in most cases, an “*overlap*” instead of a “*separation*” typically exists between the injection and the combustion events, as shown in Figure 6.3. In this work, the notation of this temporal overlap or separation is “ $\delta$ ”; a negative value of  $\delta$  indicates a separation while a positive value of  $\delta$  indicates an overlap.

In order to determine the actual timing of the injection process, an offline injection testing bench is employed in this dissertation. The injection bench (EFS 8405) is capable

of measuring the ROI curves under simulated engine operating conditions. A preliminary empirical model is therefore proposed for describing the opening and closing delays for the injectors used in this work, the detail of which is shown in Appendix C. This ROI model is integrated into the real-time injection control.

An example of the correlation between the smoke emissions and the separation  $\delta$  is shown in Figure 6.4. EGR sweeps are carried out with diesel at two levels of injection pressure. The engine runs at a load of 8 bar IMEP and a fixed CA50 of 368°C.

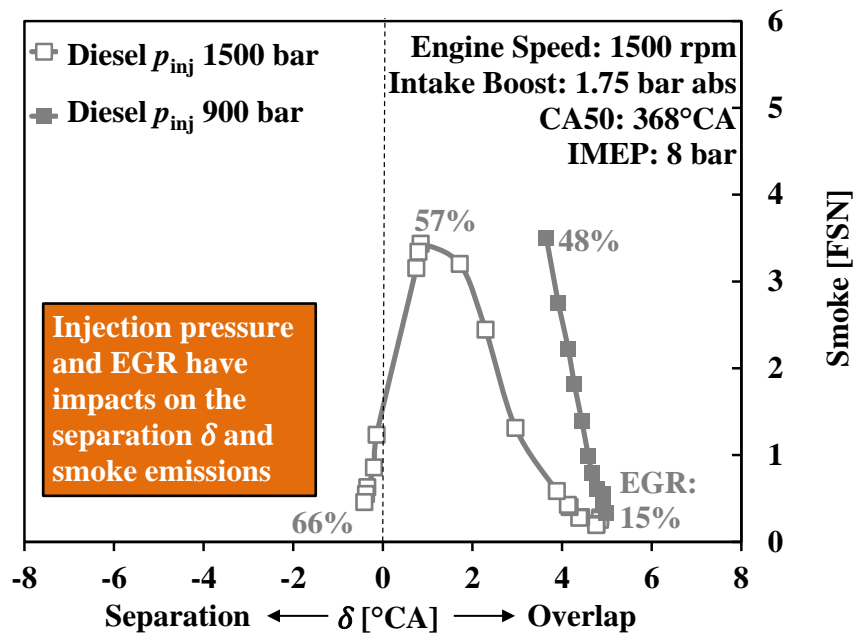


Figure 6.4 Correlation between Separation  $\delta$  and Smoke

As the EGR rate increases, the  $\delta$  changes towards the “separation” direction. However, the reduced oxygen causes increased smoke emissions before the injection and combustion are entirely separated. With the injection pressure of 900 bar, the EGR rate is limited to 48% because of the high smoke, and the desired “separation” is not achieved. In the case of 1500 bar injection pressure, further EGR addition eventually leads to the

“separation”, and the smoke emissions start to drop sharply and the engine operation enters the LTC mode.

Due to the high reactivity of most diesel fuels, extremely high EGR rates are usually required to delay the ignition and create a separation. For diesel combustion, the EGR and injection pressure are the primary measures to modulate the separation  $\delta$ . The DFC with ethanol and diesel, on the other hand, offers additional control leverage, *i.e.* the ethanol usage  $\chi_{eth}$  that is capable of dynamically adjusting the separation  $\delta$  for the near-TDC diesel pilot. As demonstrated in Section 5.4 of Chapter V, the increasing use of ethanol prolongs the ignition delay of the diesel pilots and reduces the pilot injection duration (Figure 5.60 and Figure 5.61). As a result, the use of a higher  $\chi_{eth}$  typically helps to separate the near-TDC diesel injection from the combustion events.

The effectiveness of the  $\chi_{eth}$  control is shown in Figure 6.5, compared with the diesel cases shown in Figure 6.4. Experiments are performed in the DFC operation with ethanol and diesel at three constant EGR rates. All other engine operating conditions are the same as those in the diesel case of 900 bar injection pressure. At each EGR rate, a  $\chi_{eth}$  sweep is carried out for the DFC operation varying  $\chi_{eth}$  from 20% to 80% with an interval of 10%. For each DFC curve, the smoke emissions reduce with increased  $\chi_{eth}$ . Despite the EGR rate applied for the DFC operation, the value of  $\delta$  ultimately reduces below zero (a separation is created) when  $\chi_{eth}$  is greater than 70% in all the three DFC cases. Compared with the corresponding diesel case, in which the LTC cannot be enabled due to the high smoke emissions, the  $\chi_{eth}$  control in the DFC strategy apparently facilitates the LTC enabling. It is also noted that the moderate EGR levels applied here (*e.g.* 40~48%) are

needed for NO<sub>x</sub> reduction in the DFC operation, as demonstrated in Section 5.4 of Chapter V (Figure 5.57).

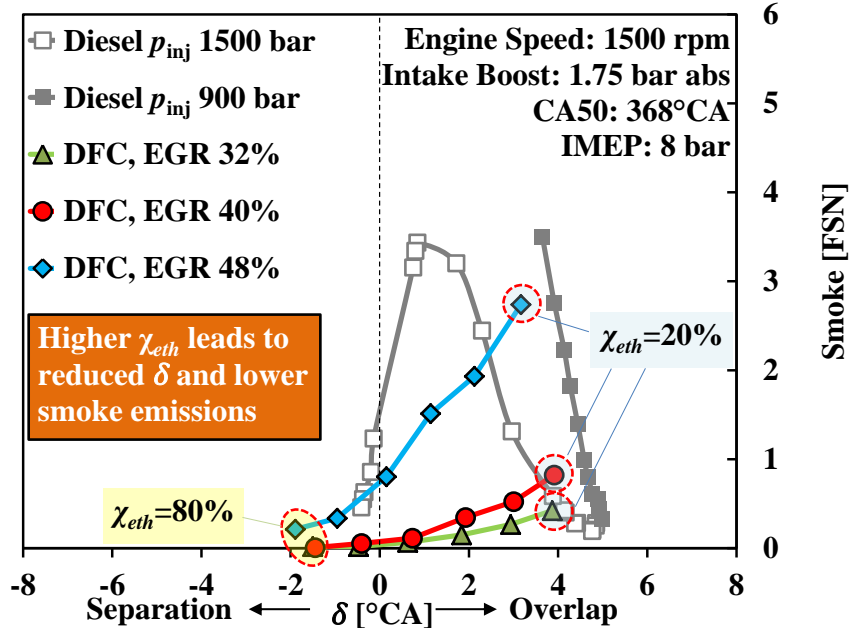


Figure 6.5 Effectiveness of  $\chi_{eth}$  Control on Separation  $\delta$  and Smoke

The  $\chi_{eth}$  control has its great significance for the dynamic combustion control. On modern diesel engines, a NO<sub>x</sub> sensor can provide a prompt validation for the feedback control. However, the transient smoke measurement is commonly unavailable. This new control parameter, *i.e.* the separation  $\delta$ , can therefore be an important benchmark to determine a threshold for the smoke emissions in real-time. Moreover, for the DFC of ethanol and diesel fuels, the  $\chi_{eth}$  control over  $\delta$  can also help to determine the minimum but necessary ethanol usage for optimized engine efficiency and emissions. When running in the DFC mode, the engine air system can apply EGR to lower the NO<sub>x</sub> emissions, while the dynamic  $\chi_{eth}$  control can assist to achieve low smoke emissions.

## 6.5 Control Validation

For the dynamic combustion control developed in this dissertation, the control parameters comprise the diesel injection duration, diesel injection timing, and ethanol injection duration, which respectively control the engine load (IMEP), combustion phasing (CA50), and the fuel to heat release separation ( $\delta$ ). The control algorithms are validated through extensive engine experiments, and an example is presented here:

At the initial state, the engine runs with a lower level of ethanol usage ( $\chi_{eth}$  of 18.5%) and the  $\delta$  value is around 5.3°CA. At an intake oxygen concentration of 14.5% (EGR rate of 40%), the smoke and NOx emissions are 1.42 FSN and 35 ppm respectively at this initial state. In order to lower these emissions by reducing the diffusion burning, the set point of  $\delta$  is commanded to zero to initiate the  $\delta$  control. During the execution of the  $\delta$  control, there are multiple targets to meet, *e.g.* the modulated  $\delta$  as target 1, the maintained IMEP as target 2, and the maintained CA50 as target 3.

The responses of the  $\delta$  control are shown by the experimental results plotted in Figures 6.6 to 6.11. In Figure 6.6, a continuous recording of 200 consecutive engine cycles is shown for the separation  $\delta$ . The dynamic combustion control adjusts the injection durations of ethanol and diesel to achieve the  $\delta$  set point while maintaining the IMEP (target 2) and CA50 (target 3). The ethanol injection duration, equivalently the fuelling rate, is increased for a greater  $\chi_{eth}$  and a reduced  $\delta$ . The diesel injection duration is shortened to maintain a constant engine load and, at the same time, the diesel injection timing is adjusted to keep the CA50 at 368°CA (as shown in Figures 6.7 to 6.11).

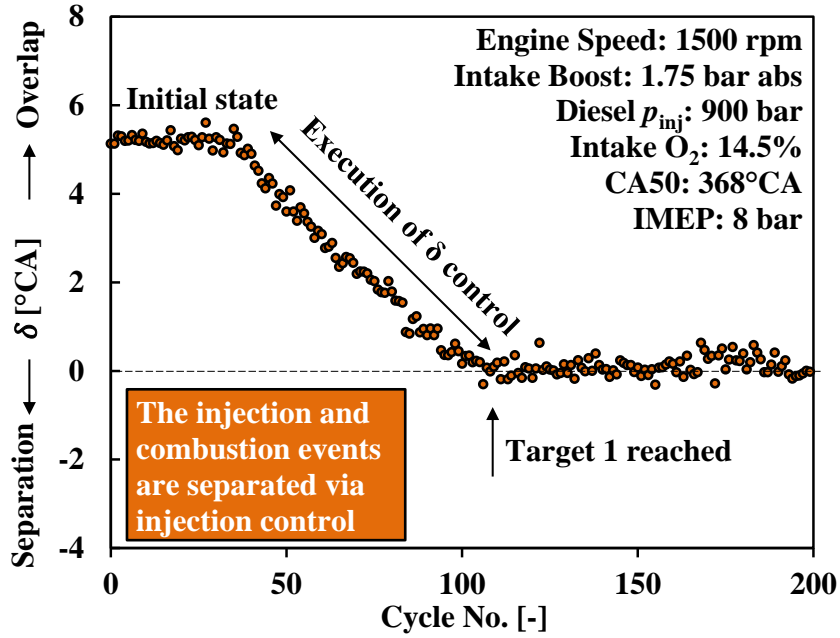


Figure 6.6 Dynamic Control Validation – Separation

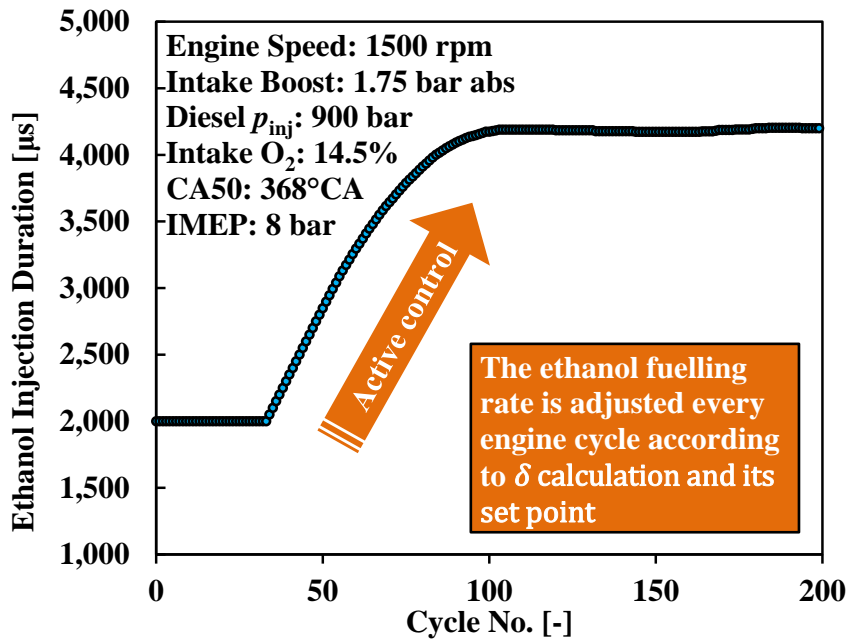


Figure 6.7 Dynamic Control Validation – Ethanol Injection Duration

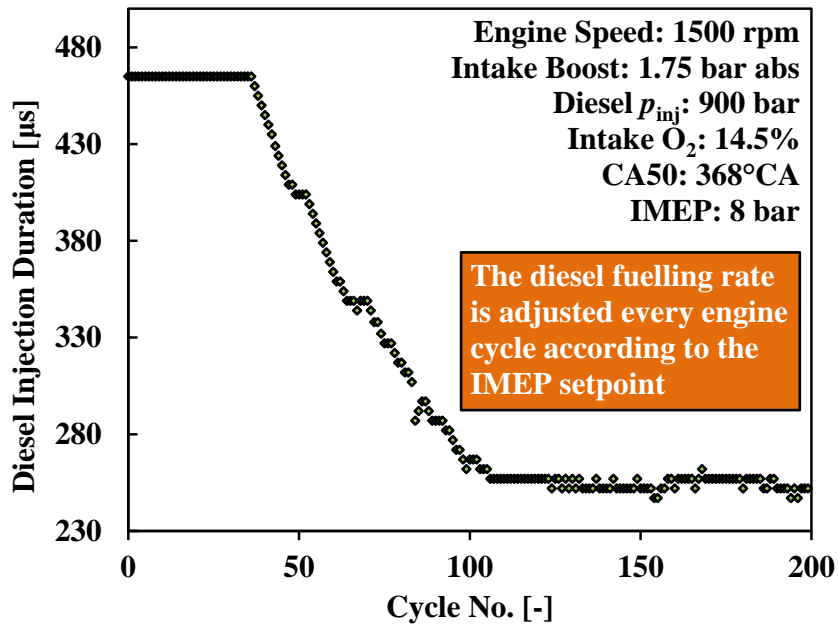


Figure 6.8 Dynamic Control Validation – Diesel Injection Duration

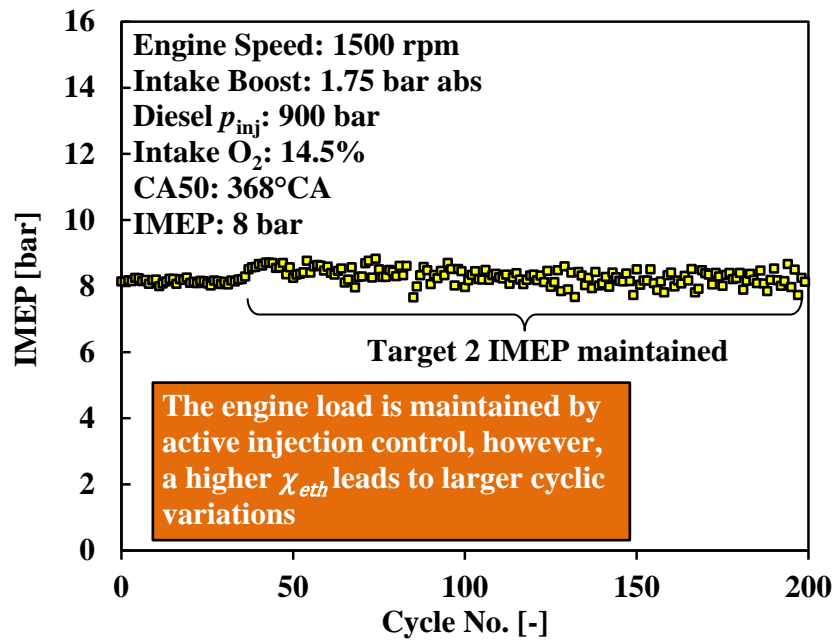


Figure 6.9 Dynamic Control Validation – IMEP

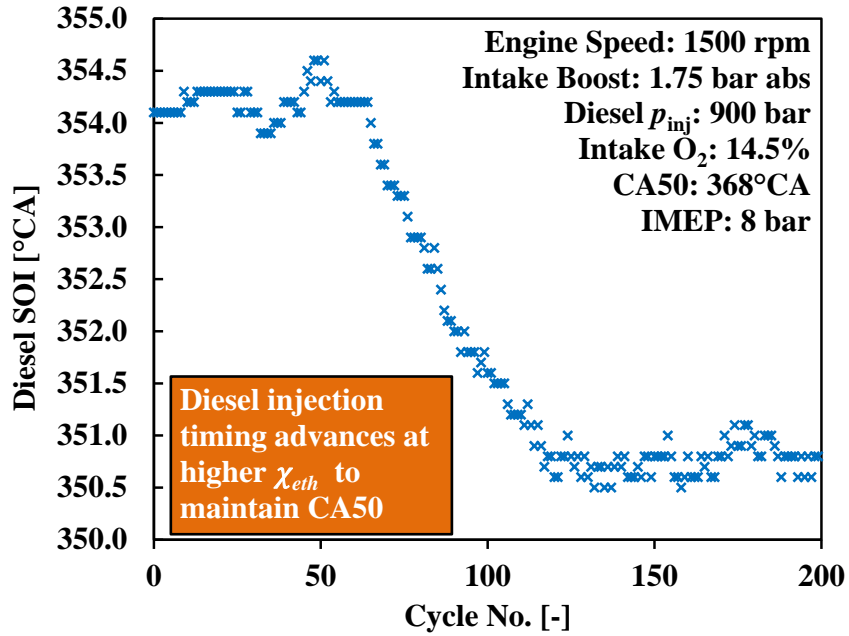


Figure 6.10 Dynamic Control Validation – Diesel SOI

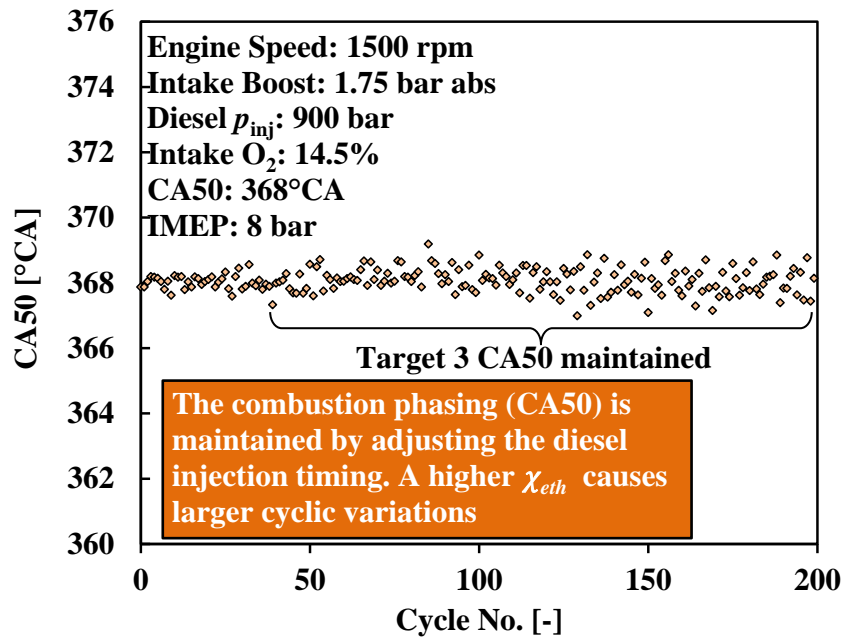


Figure 6.11 Dynamic Control Validation – CA50

At higher  $\chi_{eth}$ , slightly larger variations are observed on the IMEP and CA50, which is another drawback of the heavy ethanol usage. However, the cyclic variations are still in the acceptable range (below 3%). Within 70 engine cycles, the  $\delta$  set point is achieved. It is noted that the control can be programmed much faster with increased control gains and feed-forward tables. Small gains are used intentionally to slow down the control process for the demonstration purpose.

The heat release rate profiles shown in Figures 6.12 to 6.14 corresponding to the combustion before, during, and after the dynamic control transient. As  $\chi_{eth}$  increases, the smoke emissions reduce from 1.42 FSN to 0.03 FSN within 70 engine cycles.

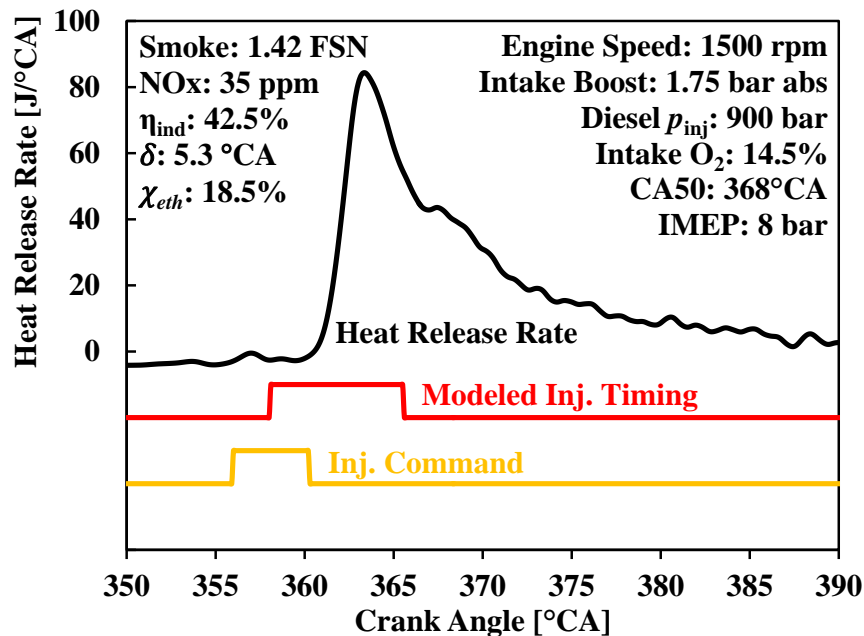


Figure 6.12 Dynamic Control Validation – Initial Heat Release

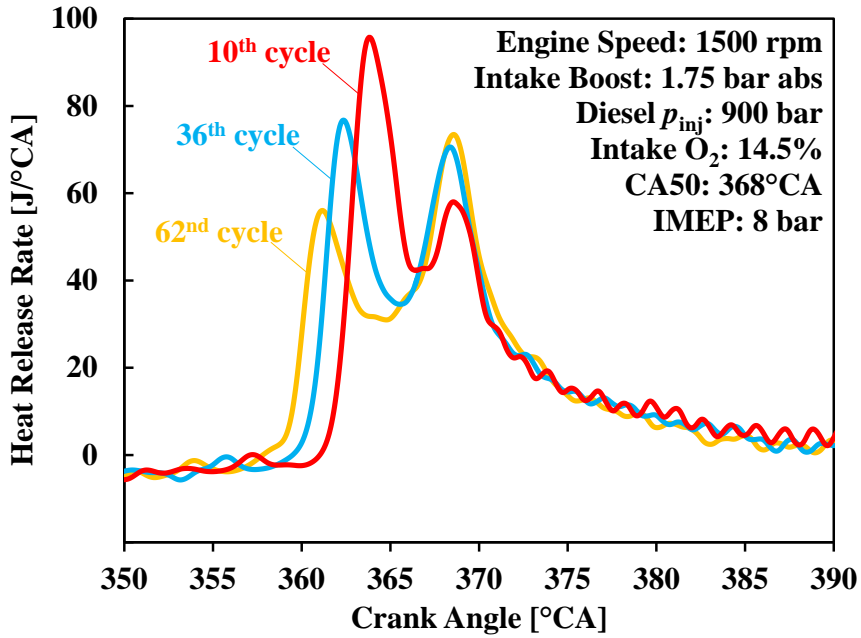


Figure 6.13 Dynamic Control Validation – Heat Release during Transient

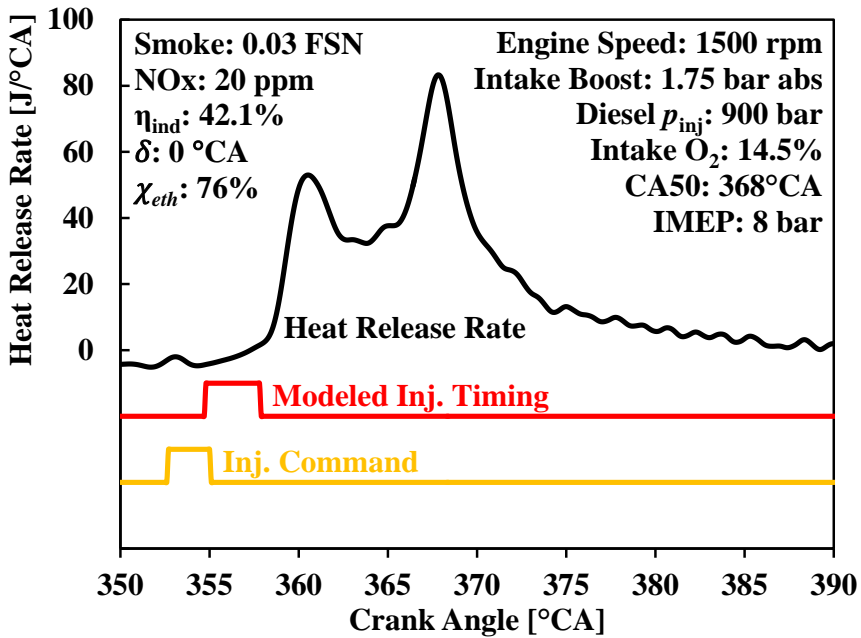


Figure 6.14 Dynamic Control Validation – Final Heat Release

## CHAPTER VII

### HIGH LOAD IMPROVEMENTS WITH CLEAN COMBUSTION

The previous investigations reported in Chapters IV to VI have assisted the development of in-depth understanding on the preferred fuel properties, fuel types, fuelling strategies, and dynamic LTC control. In this chapter, these findings are applied to improve the high load performance of the engine in the LTC operation. The dual-fuel combustion strategy is adopted to take advantage of its desirable combustion controllability. The gasoline and ethanol are used as the port injected fuels, along with the direct-injection of diesel as pilots or the main fuel. At each engine load level, the engine performance is optimized through extensive experiments. The LTC operation (of ultra-low NO<sub>x</sub> emissions) at the full engine load (up to 18.5 bar IMEP) is enabled with the DFC strategy using ethanol and diesel fuels.

#### 7.1 Load Sweep with Gasoline Diesel DFC

The emission targets are set to NO<sub>x</sub> < 0.2 g/kW-hr and smoke < 2 FSN across the examined engine loads. The control parameters include the  $\chi_{gas}$ , EGR rate, and diesel injection timing. As a comparison, experiments are also performed with the regular diesel fuel only under the same conditions. The intake pressure and diesel injection pressure are listed in Table 7.1. However, the emission targets for the diesel experiments are less stringent (NO<sub>x</sub> < 0.5 g/kW-hr and smoke < 2 FSN).

Table 7.1 Optimized Fuel &amp; Air Management for Engine Load Sweeps

IMEP [bar]	Intake Boost [bar abs]	Diesel Injection Pressure [bar]
4	1.21	1030
6	1.35	1160
8	1.57	1360
10	1.87	1480
12	2.06	1530
14	2.3	1580
16	2.52	1610
18	2.83	1650
20	3.10	1730

In Figures 7.1 to 7.4, the experimental results of major exhaust emissions are shown to compare the DFC operation with the conventional diesel combustion. The DFC with gasoline and diesel apparently offers the benefits of low NO<sub>x</sub> and smoke emissions but with higher levels of the incomplete combustion products. It is important to understand that, for the engine operation with the regular diesel fuel only, the simultaneously low NO<sub>x</sub> (0.2 g/kW-hr) and smoke (< 2 FSN) emissions are not achievable at higher engine loads (*e.g.* at IMEP higher than 10 bar), unless the engine compression ratio is substantially reduced [25].

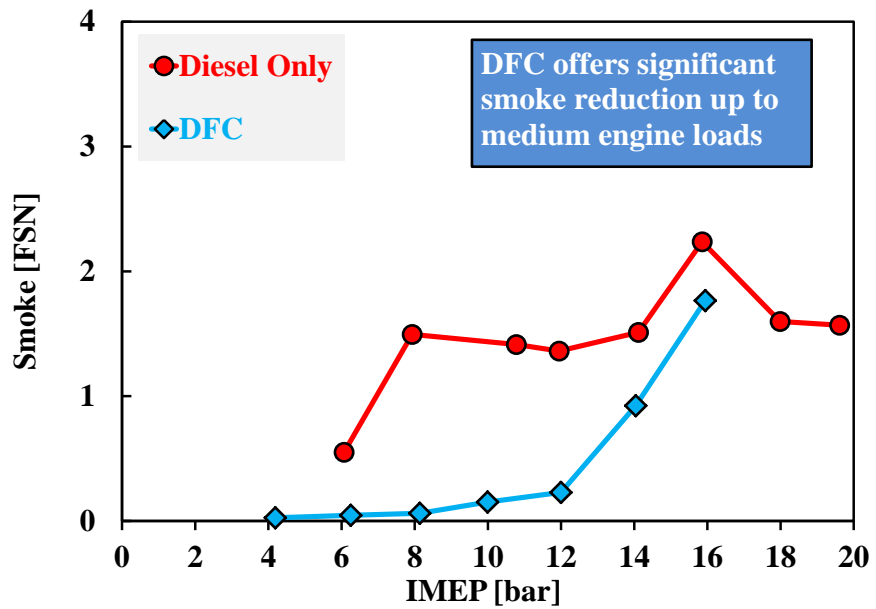


Figure 7.1 DFC versus Diesel Baseline – Load Sweep, Smoke

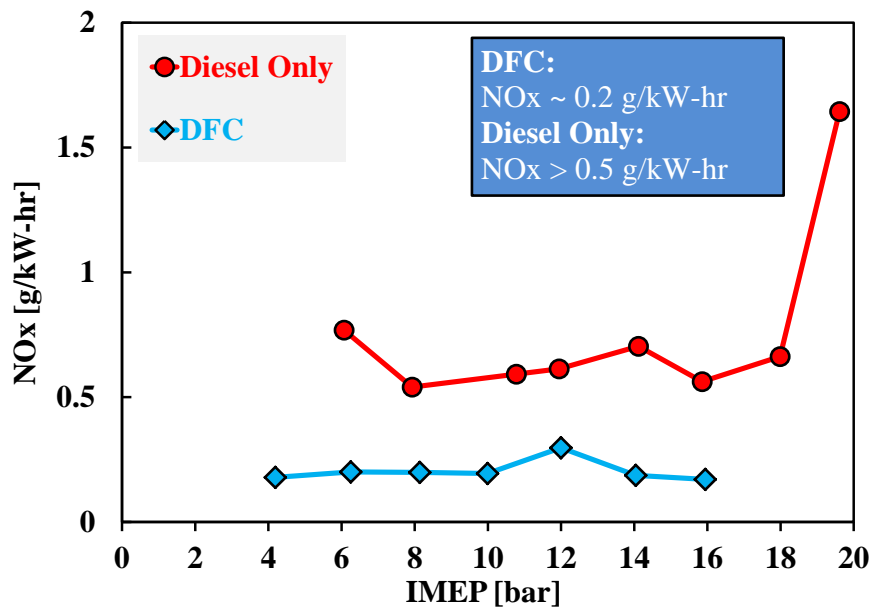


Figure 7.2 DFC versus Diesel Baseline – Load Sweep, NOx

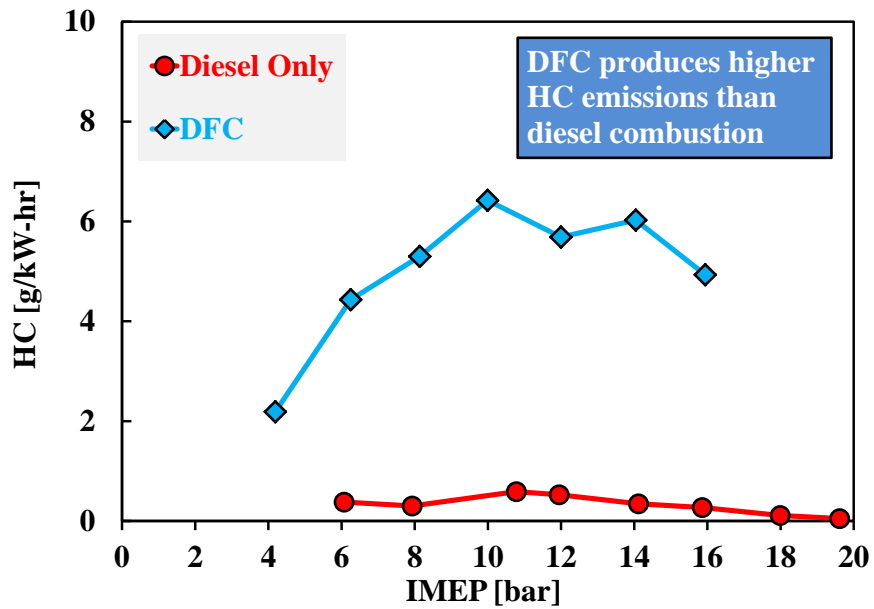


Figure 7.3 DFC versus Diesel Baseline – Load Sweep, HC

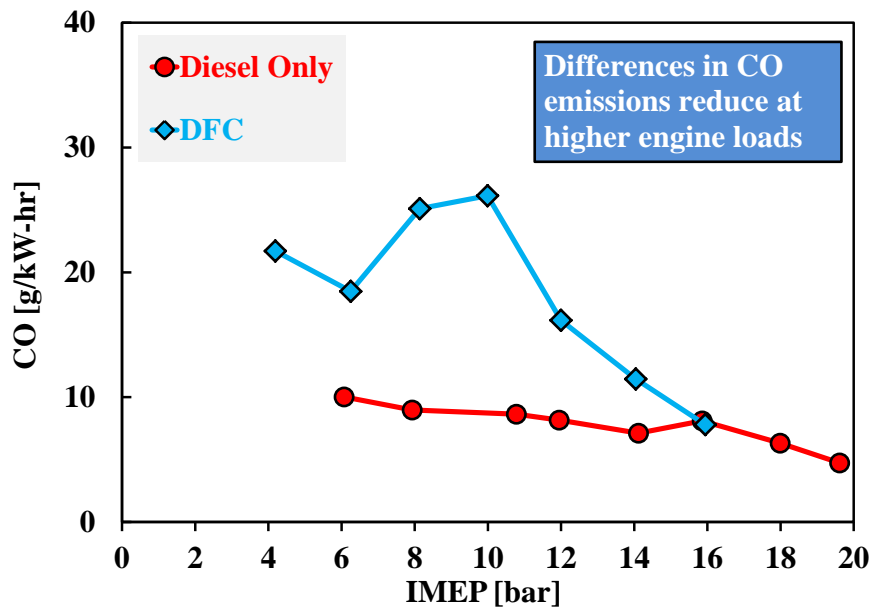


Figure 7.4 DFC versus Diesel Baseline – Load Sweep, CO

As shown in Figure 7.5, the gasoline usage ( $\chi_{gas}$ ) is increased at higher engine loads to improve the cylinder charge homogeneity. At engine loads below 12 bar IMEP, the increasing gasoline usage helps to reduce NO<sub>x</sub> emissions and only moderate levels of EGR are required to achieve the targeted NO<sub>x</sub> emissions (0.2 g/kW-hr). However, it is necessary to apply more EGR at 14~16 bar IMEP to withhold the premature auto-ignition of the port-injected gasoline (as shown in Figure 7.6). The increased EGR usage deteriorates the smoke emissions, and the smoke emissions of the DFC operation start to rise substantially at higher engine loads of 14~16 bar IMEP.

The experimental results of the maximum pressure rise rate and combustion phasing (CA50) are shown in Figures 7.7 & 7.8 for the same engine load sweep. The DFC with gasoline and diesel generally exhibits higher levels of the maximum pressure rise rate than the diesel combustion. It is important to note that the combustion phasing (CA50) is significantly postponed for the diesel combustion to reduce NO<sub>x</sub> emissions at higher engine loads, which effectively contributes to the reduction of the pressure rise rate at the same time. In the DFC operation, the combustion phasing is controlled in the optimal timing window for the engine efficiency; as a result, the DFC offers substantial efficiency improvements (as shown in Figure 7.9) despite higher incomplete combustion products (HC and CO emissions shown in Figures 7.3 & 7.4 respectively).

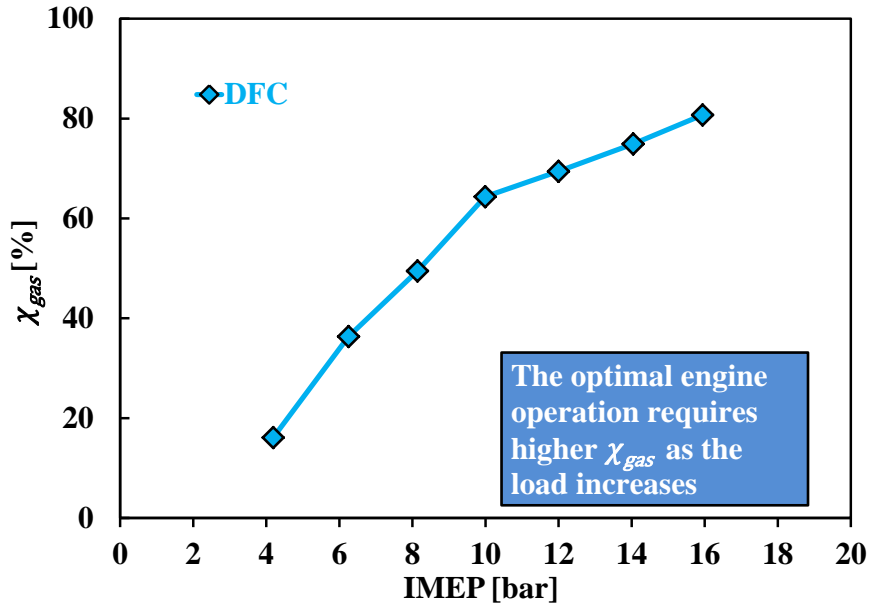


Figure 7.5 DFC – Load Sweep,  $\chi_{gas}$

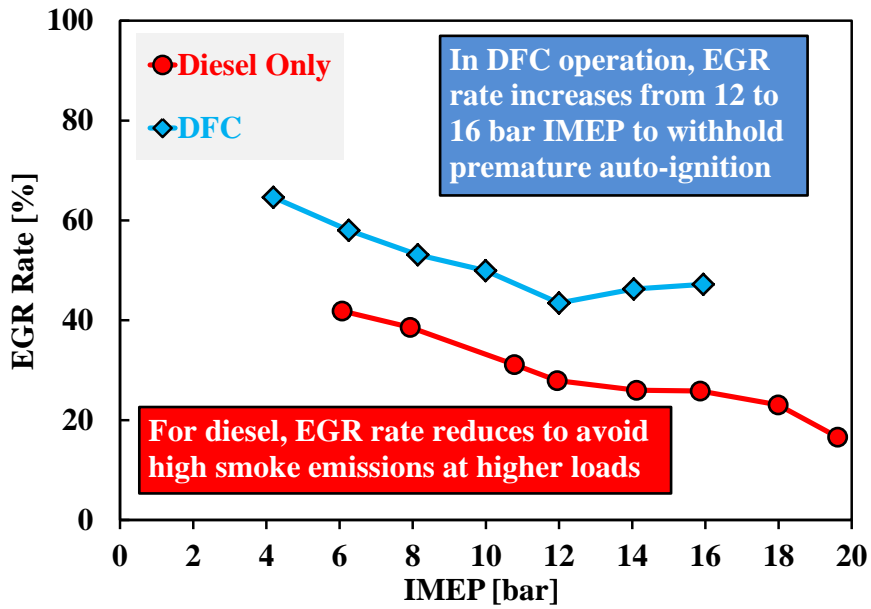


Figure 7.6 DFC versus Diesel Baseline – Load Sweep, EGR Rate

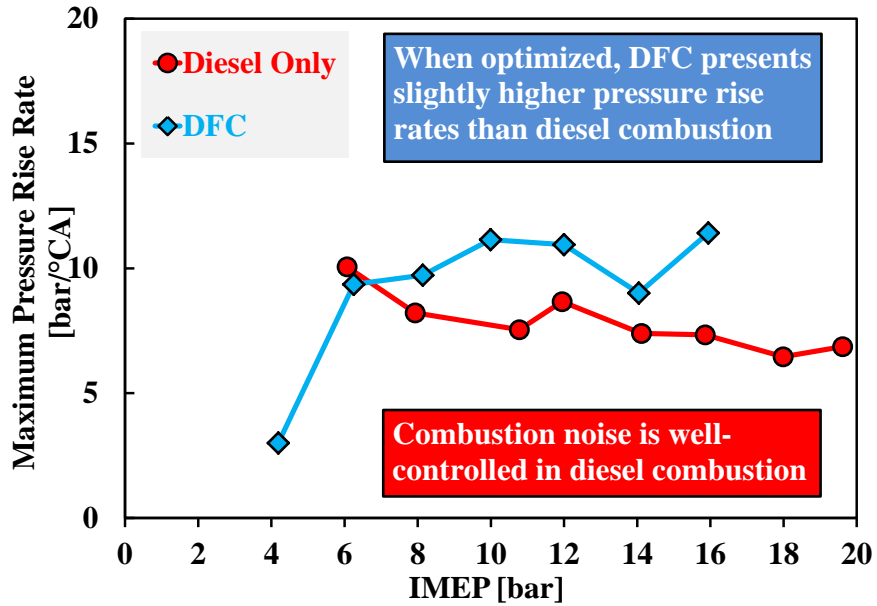


Figure 7.7 DFC versus Diesel Baseline – Load Sweep,  $dp_{max}$

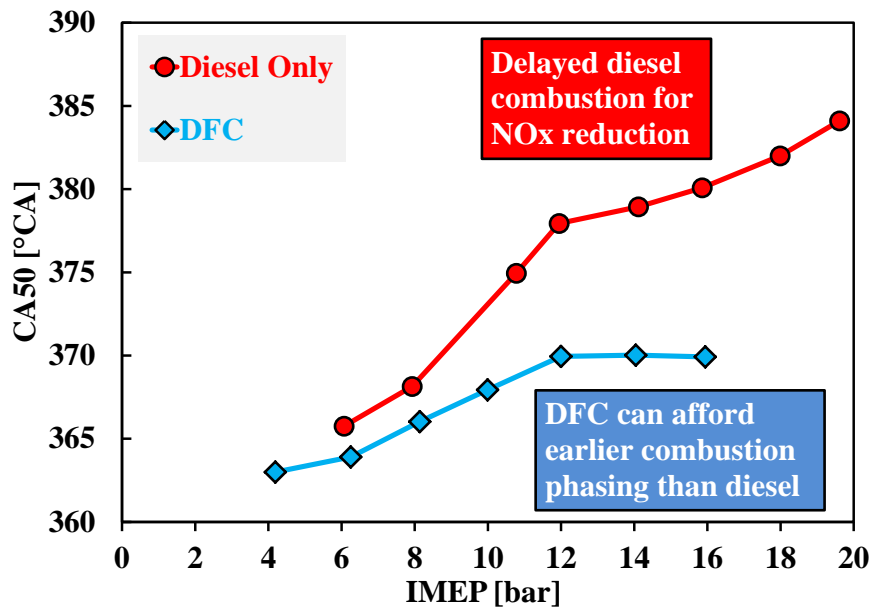


Figure 7.8 DFC versus Diesel Baseline – Load Sweep, CA50

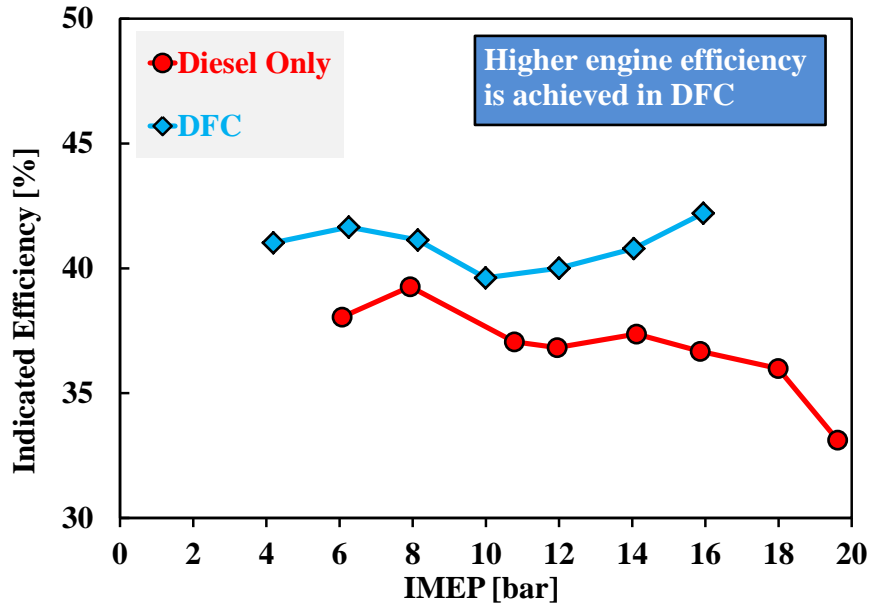


Figure 7.9 DFC versus Diesel Baseline – Load Sweep, Efficiency

## 7.2 High Load LTC Enabling

It is critical to overcome the premature auto-ignition in the DFC mode for further engine load extension. The gasoline fuel is therefore replaced by ethanol as the port delivered fuel. Engine experiments are performed to study the LTC operation at engine loads from 16 bar IMEP to the full engine load. The NO<sub>x</sub> emissions are targeted at < 0.2 g/kW-hr and smoke emissions < 2 FSN.

At high engine loads, the DFC operation with ethanol and diesel relies on increased intake boost and EGR to achieve the emission targets. In Figures 7.10 & 7.11, the NO<sub>x</sub> and smoke emissions are shown for engine operations under different intake boost and EGR rates at an engine load range of 15.2~16.5 bar IMEP. Ultra-low NO<sub>x</sub> and smoke emissions are eventually achieved with 40% EGR and 2.5 bar abs intake boost.

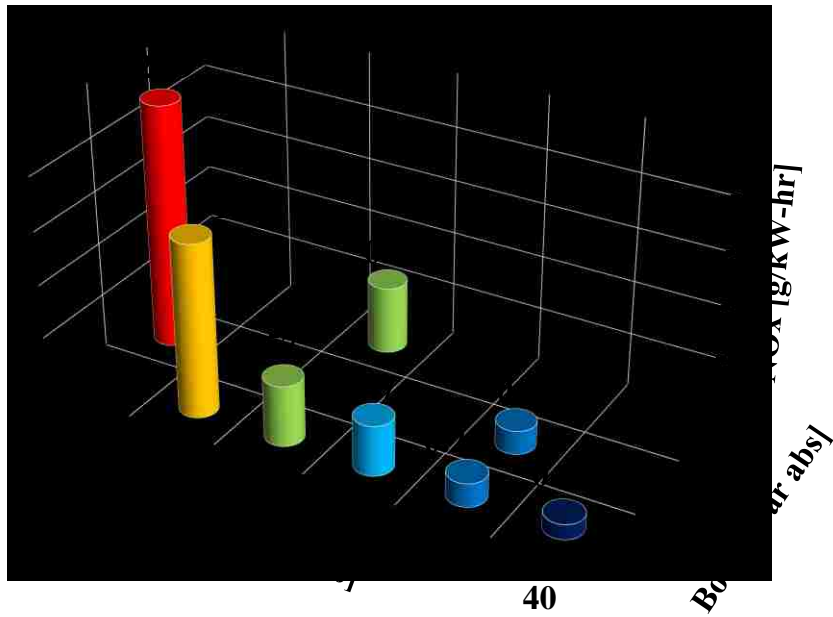


Figure 7.10 DFC with Ethanol and Diesel – High Load, NOx

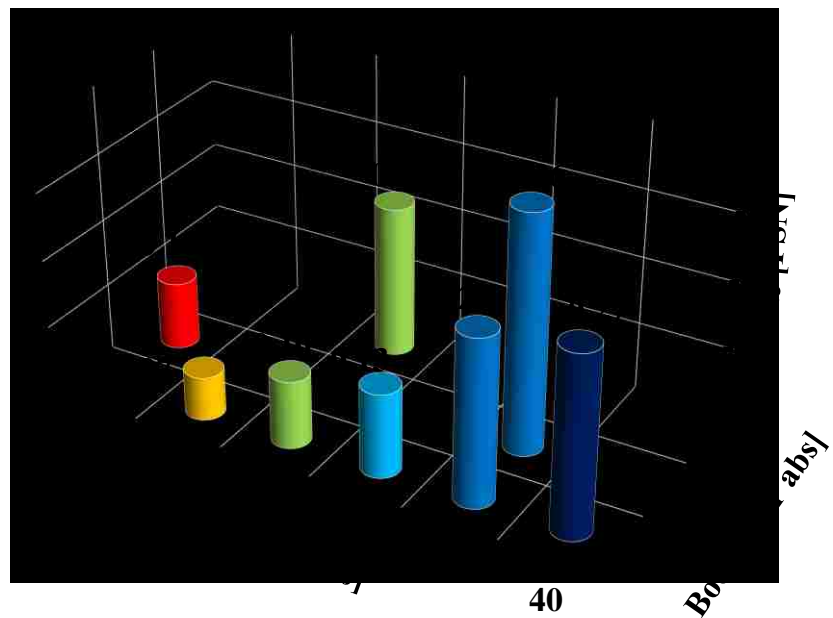


Figure 7.11 DFC with Ethanol and Diesel – High Load, Smoke

The cylinder pressure and heat release rate traces are shown in Figure 7.12 for the engine operation at 16.4 bar IMEP. The plot includes the pressure traces of 200 consecutive engine cycles, and the thick black lines represent the averaged pressure and heat release profiles. At such a high engine load that is deemed extremely challenging for diesel LTC, the engine running in the DFC mode produces NO<sub>x</sub> emissions of 24 ppm or 0.14 g/kW-hr and smoke emissions of 0.27 FSN or 0.01 g/kW-hr, which meet the current US EPA standards without any after-treatment.

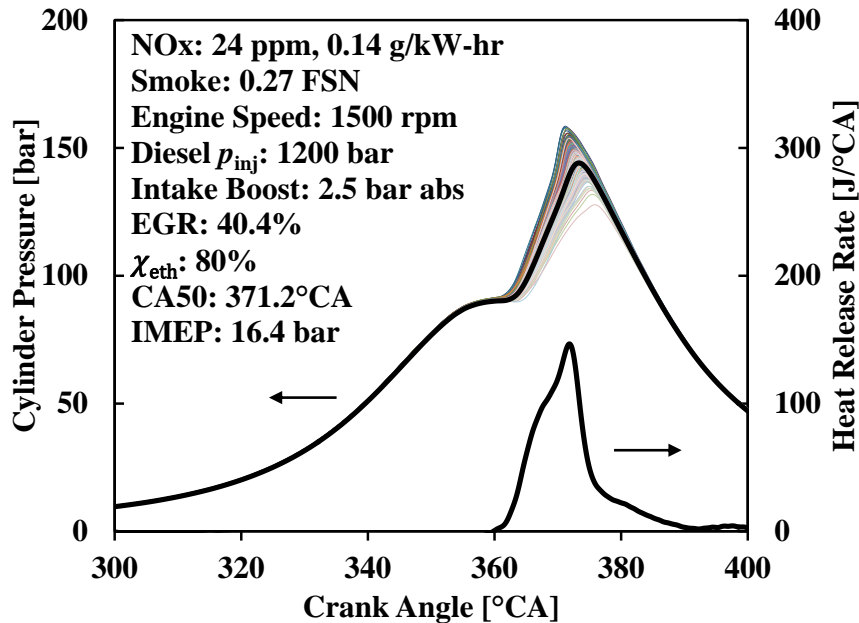


Figure 7.12 DFC with Ethanol and Diesel at 16.4 bar IMEP

At 18.1 bar IMEP (nearly the full engine load), the LTC operation is enabled with the DFC strategy as shown in Figure 7.13. The pressure traces are plotted for 200 consecutive engine cycles. The combustion phasing (CA50) is delayed to 375.4°CA, and the ethanol usage increases to a  $\chi_{eth}$  value of 90%. The engine runs with an intake boost of 2.5 bar absolute and a moderate EGR rate of 37.7%.

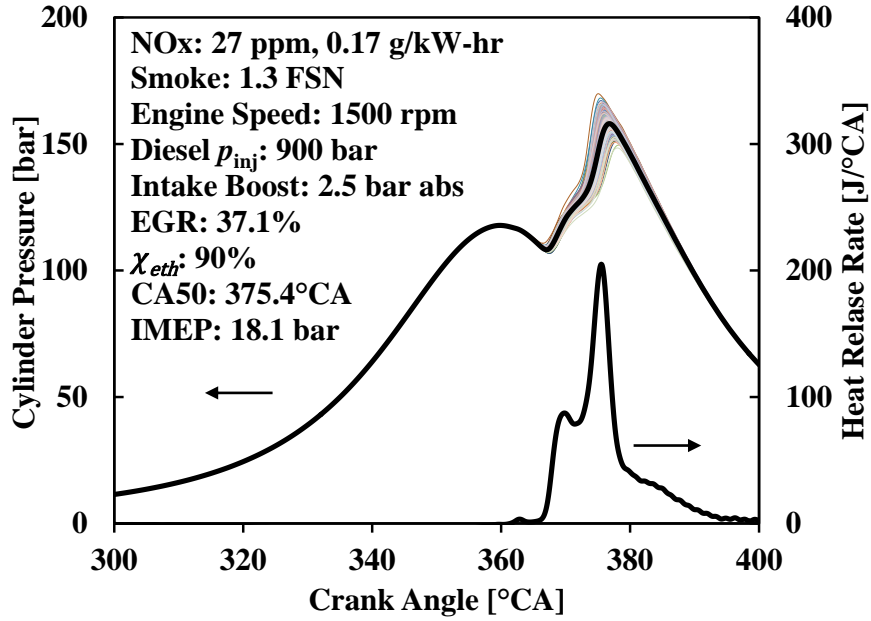


Figure 7.13 DFC with Ethanol and Diesel at 18.1 bar IMEP

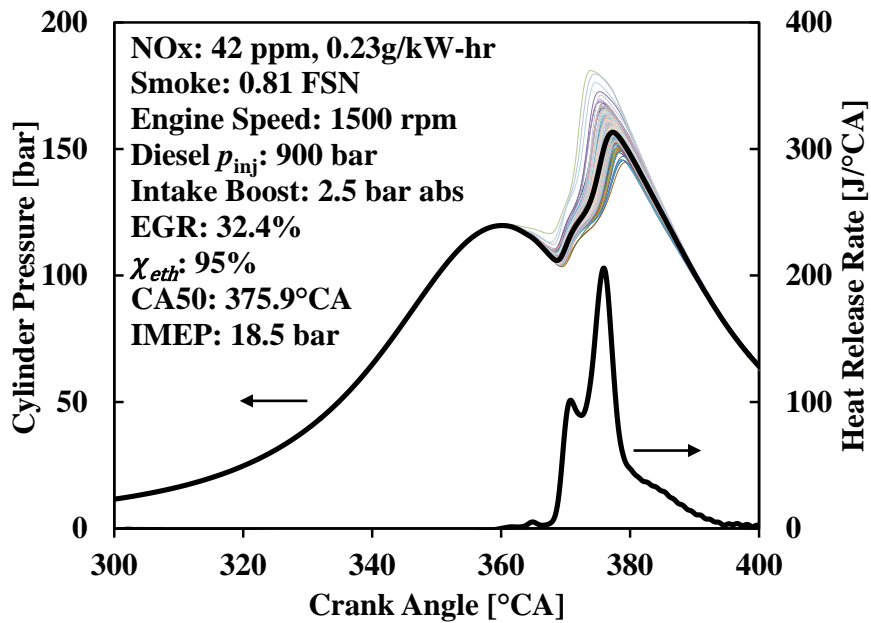


Figure 7.14 DFC with Ethanol and Diesel at 18.5 bar IMEP

The engine produces 0.17 g/kW-hr of NO<sub>x</sub> and 1.3 FSN of smoke emissions, along with moderate HC (4.6 g/kW-hr) and CO (6.8 g/kW-hr) emissions. A high indicated thermal efficiency of 47.7% is achieved, which is a substantial improvement compared to the indicated thermal efficiency of 37% in the diesel only case (Figure 7.9). The maximum pressure rise rate of the DFC operation is 12.8 bar/°CA that is higher than a typical production engine but acceptable for research purposes.

Another example of the DFC operation at the high engine load is shown in Figure 7.14. The engine load is further raised to 18.5 bar IMEP (engine full load). The ethanol usage increases to a high  $\chi_{eth}$  value of 95%. The engine produces 0.23 g/kW-hr of NO<sub>x</sub> and 0.81 FSN of smoke. The indicated thermal efficiency is 46.9%. The DFC operation using ethanol as a main energy supply therefore demonstrates superior performance of optimized engine efficiency and emissions over the conventional diesel combustion and diesel LTC.

## CHAPTER VIII

### CONCLUSIONS

The primary objective of this research is to improve the emissions and efficiency of compression ignition engines under LTC by investigating different fuels and fuelling strategies. The emission targets are set as 0.2 g/kW-hr for NO<sub>x</sub> and 2 FSN for smoke, based on the current US EPA emission regulations. The research methodology includes the detailed testing of ten types of diesel fuels (nine FACE fuels and one regular diesel) and three additional fuels (n-butanol, gasoline, and ethanol), and systematic data analyses to assess the impact of diesel fuel properties (Cetane numbers, aromatic contents, and boiling temperatures) on the LTC enabling. These findings are applied to

- develop and implement appropriate fuelling strategies and new control algorithms to improve the LTC emissions and efficiency;
- examine the operating range of the different fuelling schemes;
- extend the engine load range under LTC operation with advanced fuelling approach and fuel combination.

The conclusions and the recommendations from the research are presented below.

#### **8.1 Impact of Diesel Fuel Properties**

In the conventional diesel high temperature combustion, the examined diesel fuel properties (Cetane numbers, aromatic contents, and boiling temperatures) have an insignificant effect on the combustion characteristics and exhaust emissions. However, when the engine operation enters the LTC regime, changes in the fuel properties start to

have a greater impact on the ignition characteristics and the subsequent combustion processes.

- A lower Cetane number (less reactive fuel) significantly increases the ignition delay, allowing for the preparation of an air-fuel mixture with a high degree of homogeneity that assists the LTC enabling.
- The increase of aromatic contents also prolongs the ignition delay. However, the aromatic structure itself can contribute to smoke formation which counteracts the effects of the prolonged mixing time. As a result, smoke reduction is not clearly observed with the high aromatic fuels.
- The lower boiling temperature accelerates the fuel evaporation inside the combustion chamber that benefits the early injections during the compression stroke by minimizing potential wall-wetting and enhancing the mixing process time. At medium engine loads, the more volatile fuels produce less smoke emissions.
- Within the investigated range, these fuel properties do not exhibit a noticeable effect on the NO<sub>x</sub> emissions that are much more sensitive to EGR.

Among the examined fuel properties, the Cetane number shows the strongest impact on the ignition delay and the smoke emissions. In general, the preferred fuel for LTC should have a low Cetane number, low aromatics and high volatility so that the combustion tends to produce less smoke emissions, thereby offering improved NO<sub>x</sub> versus smoke trade-off as observed empirically.

## 8.2 Fuel Types and Fuelling Strategies for Clean CI Combustion

The implementation of LTC in high compression ratio diesel engines is substantially facilitated with the use of a less reactive and more volatile fuel. Such fuels also make it possible for high load operations in the LTC modes. The LTC characteristics of the three alternate fuels are summarized as follows:

- The combustion of n-butanol with the high-pressure direct-injection system can produce ultra-low NO<sub>x</sub> and smoke emissions without EGR, although limited to a moderate engine load range. The rapid rate of heat release, however, generally leads to increased combustion noise, which can be moderately mitigated with the multi-shot injection strategy.
- These volatile fuels are more suited for intake port injection to enable either HCCI or the dual-fuel combustion strategies. In the HCCI mode, however, the engine operation is restricted by the combustion characteristic of each particular fuel.
  - a. n-Butanol HCCI offers superior performance at low engine loads (*e.g.* below 7 bar IMEP) but the medium load operation is unachievable due to high pressure rise rates;
  - b. Gasoline HCCI, without intake heating, requires a minimum engine load level (~10 bar IMEP) to avoid misfire but with precise control over the intake boost and the EGR rate, offers desirable medium load performance;
  - c. As the fuel reactivity further reduces, ethanol HCCI combustion becomes unattainable even under the high compression ratio of 18.2:1.

- With the less reactive and highly volatile fuels (gasoline and ethanol), the dual-fuel combustion with the diesel pilot as the ignition source offers both the requisite emission reductions and combustion controllability in LTC. The port-injection of the volatile fuel forms a highly homogeneous air-fuel mixture during the compression stroke while the direct-injection of diesel initiates the combustion in the desired ignition timing window.
- The port fuel injection not only requires a fuel with high volatility but also a low reactivity. The reactivity of the mixture plays a critical role in the control of the combustion and exhaust emissions. When the homogeneous mixture possesses a high reactivity, for example, in the case of dual-fuel combustion with gasoline and diesel, the premature auto-ignition can occur, resulting in the loss of control over the ignition and combustion phasing.
- The high-pressure direct-injection of the diesel pilot delivers fuel directly into the cylinder and combustion chamber. It thus, to a great extent, has direct control over the fuel penetration, in-cylinder distribution, ignition, and the combustion rate. In terms of combustion control, the direct-injection should be the preferred approach to precisely initiate the combustion.
- The direct-injection of the diesel pilot generally results in a certain degree of heterogeneity which may adversely affect the NO<sub>x</sub> or smoke emissions; therefore, the minimum amount of the pilot injection quantity that provides a reliable ignition source with sufficient ignition energy should be used.
- In addition, different engine loads place different requirements on the design of ideal fuel properties. The use of the in-cylinder blending of two fuels can

dynamically adjust the fuel ratio and thus modulate the mixture reactivity as needed.

### **8.3 Dynamic Combustion Control and High Load LTC**

The combustion phasing and the engine load can be dynamically modulated through the injection timing and duration control with the cylinder pressure feedback. It is important to understand the correlation between the control parameters (injection timing and duration) and the combustion characteristics (phasing and load). In general, a longer injection duration delivers more fuel and is likely to produce higher torque. However, the change of the injection timing under different engine operating conditions may result in wide variations in the combustion phasing.

The standard definition of ignition delay does not provide a consistent relationship between the injection control and the LTC emissions. To allow the emission reduction strategies to be incorporated in the real-time injection control, a new definition of ignition delay in terms of the injector opening and closing delays is formulated that correlates the “separation” or “overlap” between the injection and combustion events to the smoke emissions. This dynamic feedback and control system allows the optimization of the combustion process by ensuring the minimization of the overlap period, thereby reducing the smoke emissions.

The engine load under LTC is extended to nearly the rated engine specification (up to 18.5 bar IMEP) with the ethanol diesel dual-fuel combustion while achieving ultra-low NO<sub>x</sub> (0.17 g/kW-hr; target: 0.2 g/kW-hr) and 1.3 FSN smoke (target: less than 2 FSN). The use of the dynamic control system ensures an optimal combustion phasing and the

minimization of the combustion inefficiency so that a high indicated thermal efficiency of ~47% has been achieved.

#### **8.4 Additional Remarks and Future Work**

The experiments so far have left the injection and combustion hardware (*e.g.* the injector nozzle and the combustion chamber) intact, which could be better designed in accordance to the fuel types and the innovative combustion processes other than diesel. Moreover, the research heavily emphasizes on the NO<sub>x</sub> and smoke over the HC and CO emissions. Although the low temperature combustion in nature tends to produce incomplete combustion products, better fuel and air admission and engine design improvements (*e.g.* the piston bowl pattern) can improve the combustion efficiency and reduce the energy loss in the exhaust, thereby increasing the engine efficiencies. In fact, the novel LTC operations that drastically differ from the conventional diesel combustion necessitate new piston designs, such as lowering the piston surface area, to accommodate the low flame temperature and the resultant higher tendency of producing HC and CO emissions.

The study of the FACE fuels clearly proves that the changes of diesel fuel properties affect the combustion processes and exhaust emissions. However, the design of the FACE fuels only covers limited ranges of the three fuel properties. Especially for the fuel Cetane number, further research should be conducted to study a wider range with a focus on the low Cetane numbers. Comparing the lowest Cetane FACE fuel (Cetane number 28) with n-butanol (Cetane number ~25), the Cetane numbers are close; however, the ignition delay of the two fuels differs substantially. Detailed investigation of their respective ignition mechanism should be performed.

---

**REFERENCES**

1. T. Johnson, "Diesel Particulate Filter Technology," Illustrated Edition, SAE International, ISBN 0-13: 978-0-7680-1707-6, 2007.
2. H. Houben, A. Marto, F. Pechhold, M. Haußner, and M. Borgers, "Pressure Sensor Glow Plug for Diesel Engines," MTZ Worldwide, Volume 65, Issue 11, pp. 8-10, 2004.
3. Robert Bosch GmbH, "Diesel-Engine Management," 3<sup>rd</sup> Edition, SAE International, ISBN 0-13: 0-7680-1343-7, 2004.
4. J. Heywood, "Internal Combustion Engine Fundamentals," 1<sup>st</sup> Edition, McGraw-Hill Science/Engineering/Math, ISBN 0-13: 978-0-0702-8637-5, 1988.
5. <http://www.sandia.gov/ecn/cvdata/expDiag/hsmovie.php>, accessed 2014.
6. A. M. Mellor, J. P. Mello, K. P. Duffy, W.L. Easley, J. C. Faulkner, "Skeletal Mechanism for NO<sub>x</sub> Chemistry in Diesel Engines," SAE Technical Paper 981450, 1998.
7. C. Idicheria and L. Pickett, "Soot Formation in Diesel Combustion under High-EGR Conditions," SAE Technical Paper 2005-01-3834, 2005.
8. K. Omae, Y. Watanabe, S. Matsushita and I. Sakata, "Reduction of HC Emission for Passenger Car Diesel Engine," SAE Technical Paper 2007-01-0663, 2007.
9. <http://www.epa.gov/otaq/standards/heavy-duty/hdci-exhaust.htm>, accessed 2014.
10. <http://www.dieselnet.com/standards/fuels.php>, accessed 2014.
11. T. Johnson, "Vehicular Emissions in Review," SAE International Journal of Engines, Volume 6, Issue 2, pp. 699-715, 2013.

12. M. Zheng, Y. Tan, M. Mulenga, and M. Wang, "Thermal Efficiency Analyses of Diesel Low Temperature Combustion Cycles," SAE Technical Paper 2007-01-4019, 2007.
13. R. Kumar and M. Zheng, "Fuel Efficiency Improvements of Low Temperature Combustion Diesel Engines," SAE Technical Paper 2008-01-0841, 2008.
14. J. Bittle, B. Knight, and T. Jacobs, "Heat Release Parameters to Assess Low Temperature Combustion Attainment," SAE Technical Paper 2011-01-1350, 2011.
15. Y. Tan, M. Zheng, G. Reader, X. Han, "An Enabling Study of Diesel Low Temperature Combustion via Adaptive Control," SAE International Journal of Engines, Volume 2, Issue 1, pp. 750-763, 2009.
16. C. Koci, Y. Ra, R. Krieger, M. Andrie, "Multiple-Event Fuel Injection Investigations in a Highly-Dilute Diesel Low Temperature Combustion Regime," SAE International Journal of Engines, Volume 2, Issue 1, pp. 837-857, 2009.
17. T. Kitamura, T. Ito, J. Senda, H. Fujimoto, "Mechanism of Smokeless Diesel Combustion with Oxygenated Fuels Based on the Dependence of the Equivalence Ratio and Temperature on Soot Particle Formation," International Journal of Engine Research, Volume 3, Issue 4, pp. 223-248, 2002.
18. L. Starck, B. Lecointe, L. Forti and N. Jeuland, "Impact of Fuel Characteristics on HCCI Combustion: Performances and Emissions," Fuel, Volume 89, Issue 10, pp. 3069-3077, 2010.
19. E. Silke, W. Pitz, C. Westbrook, and M. Sjöberg, "Understanding the Chemical Effects of Increased Boost Pressure under HCCI Conditions," SAE International Journal of Fuels and Lubricants, Volume 1, Issue 1, pp. 12-25, 2009.

20. R. Buchwald, G. Lautrich, O. Maiwald, and A. Sommer, "Boost and EGR System for the Highly Premixed Diesel Combustion," SAE Technical Paper 2006-01-0204, 2006.
21. W. De Ojeda, T. Bulicz, X. Han, M. Zheng, "Impact of Fuel Properties on Diesel Low Temperature Combustion," SAE International Journal of Engines, Volume 4, Issue 1, pp. 188-201, 2011.
22. A. M. Ickes, S. V. Bohac, D. N. Assanis, "Effect of Fuel Cetane Number on a Premixed Diesel Combustion Mode," International Journal of Engine Research, Volume 10, pp. 251-263, 2009.
23. A. Warey, J. P. Hardy, M. Hennequin, M. Tatur, D. Tomazic, W. Cannella, "Fuel Effects on Low Temperature Combustion in a Light-duty Diesel Engine," SAE Technical Paper 2010-01-1122, 2010.
24. P. W. Bessonette, C. H. Schleyer, K. P. Duffy, W. L. Hardy, M. P. Liechty, "Effects of Fuel Property Changes on Heavy-duty HCCI Combustion," SAE Technical Paper 2007-01-0191, 2007.
25. U. Asad, X. Han, and M. Zheng, "An Empirical Study to Extend Engine Load in Diesel Low Temperature Combustion," SAE International Journal of Engines, Volume 5, Issue 3, pp. 709-717, 2012.
26. G. T. Kalghatgi, P. Risberg, H. E. Ångström, "A Method of Defining Ignition Quality of Fuels in HCCI Engines," SAE Technical Paper 2003-01-1816, 2003.
27. P. Risberg, G. T. Kalghatgi, H. E. Ångström, "Auto-ignition Quality of Gasoline-like Fuels in HCCI Engines," SAE Technical Paper 2003-01-3215, 2003.

28. G. T. Kalghatgi, R. A. Head, "The Available and Required Auto-ignition Quality of Gasoline-like Fuels in HCCI Engines at High Temperatures," SAE Technical Paper 2004-01-1969, 2004.
29. P. Risberg, G. T. Kalghatgi, H. E. Ångström, "The Influence of EGR on Auto-Ignition Quality of Gasoline-like Fuels in HCCI Engines," SAE Technical Paper 2004-01-2952, 2004.
30. G. Shibata, K. Oyama, T. Urushihara, T. Nakano, "The Effect of Fuel properties on Low and High Temperature Heat Release and Resulting Performance of an HCCI Engine," SAE Technical Paper 2004-01-0553, 2004.
31. C. Lewander, B. Johansson, and P. Tunestal, "Extending the Operating Region of Multi-Cylinder Partially Premixed Combustion using High Octane Number Fuel," SAE Technical Paper 2011-01-1394, 2011.
32. Y. Wada, K. Okimoto, N. Kitamura, K. Ueda, "Effect of Octane Rating and Charge Stratification on Combustion and Operating Range with DI PCCI Operation," SAE Technical Paper 2007-01-0053, 2007.
33. H. Machrafi, S. Cavadias, P. Gilbert, "An Experimental and Numerical Analysis of the HCCI Auto-ignition Process of Primary Reference Fuels, Toluene Reference Fuels and Diesel Fuel in an Engine, Varying the Engine Parameters," Fuel Process Technology, Volume 89, pp.1007-1016, 2008.
34. L. Koopmans, E. Stromberg, I. Denbratt, "The influence of PRF and Commercial Fuels with High Octane Number on the Auto-ignition Timing of an Engine Operated in HCCI Combustion Mode with Negative Valve Overlap," SAE Technical Paper 2004-01-1967, 2004.

35. A. S. Cheng, B. T. Fisher, G. C. Martin, C. J. Mueller, "Effects of Fuel Volatility on Early Direct-injection, Low-temperature Combustion in an Optical Diesel Engine," *Energy and Fuel*, Volume 24, pp. 538-551, 2010.
36. G. T. Kalghatgi, "Auto-ignition Quality of Practical Fuels and Implication for Fuel Requirements of Future SI and HCCI Engines," SAE Technical Paper 2005-01-0239, 2005.
37. T. Gao, P. Divekar, U. Asad, X. Han, G. T. Reader, M. Wang, M. Zheng and J. Tjong, "An Enabling Study of Low Temperature Combustion with Ethanol in a Diesel Engine," *Journal of Energy Resources Technology*, Volume 135, Issue 4, 8 pages, 2013.
38. J. Andrae, D. Johansson, P. Björnbom, P. Risberg, G. Kalghatgi, "Co-oxidation in the Auto-ignition of Primary Reference Fuels and n-Heptane/toluene Blends," *Combustion and Flame*, Volume 140, pp. 267-286, 2005.
39. J. P. Szybist, B. G. Bunting, "The Effects of Fuel Composition and Compression Ratio on Thermal Efficiency in an HCCI Engine," SAE Technical Paper 2007-01-4076, 2007
40. J. Hiltner, R. Agama, F. Mauss, B. Johansson, M. Christensen, "Homogeneous Charge Compression Ignition Operation with Natural Gas: Fuel Composition Implications," *Journal of Engineering for Gas Turbines and Power*, Volume 125, pp. 837-844, 2003.
41. G. Shibata, K. Oyama, T. Urushihara, T. Nakano, "Correlation of Low Temperature Heat Release with Fuel Composition and HCCI Engine Combustion," SAE Technical Paper 2005-01-0138, 2005.

42. W. de Ojeda, Y. Zhang, K. Xie, X. Han, M. Wang, M. Zheng, "Exhaust Hydrocarbon Speciation from a Single-Cylinder Compression Ignition Engine Operating with In-Cylinder Blending of Gasoline and Diesel Fuels," SAE Technical Paper 2012-01-0683, 2012.
43. K. Hashimoto, "Effect of Ethanol on the HCCI Combustion," SAE Technical Paper 2007-01-2038, 2007.
44. H. Yamada, M. Yoshii, A. Tezaki, "Chemical mechanistic Analysis of Additive Effects in Homogeneous Charge Compression Ignition of Dimethyl Ether," Proceedings of Combustion Institute, Volume 30, pp. 2773-2780, 2005.
45. P. Saisirirat, F. Foucher, S. Chanchaona, C. Mounaïm-Rousselle, "Effects of Ethanol, n-Butanol, n-Heptane Blended on Low Temperature Heat Release and HRR Phasing in Diesel-HCCI," SAE Technical Paper 2009-24-0094, 2009.
46. X. C. Lu, L. B. Ji, L. L. Zu, Y. C. Hou, C. Huang, Z. Huang, "Experimental Study and Chemical Analysis of n-Heptane Homogeneous Charge Compression Ignition Combustion with Port Injection of Reaction Inhibitors," Combustion and Flame, Volume 149, pp. 261-270, 2007.
47. X. C. Lu, Y. C. Hou, L. B. J, L. L. Zu, Z. Huang, "Heat Release Analysis on Combustion and Parametric Study on Emissions of HCCI Engines Fueled with Propanol/n-heptane Blend Fuels," Energy and Fuel, Volume 20, pp. 1870-1878, 2006.
48. X. C. Lu, Y. C. Hou, L. L. Zu, Z. Huang, "Experimental Study on the Auto-ignition and Combustion Characteristics in the Homogeneous Charge Compression Ignition (HCCI) Combustion Operation with Ethanol/n-heptane Blend Fuels by Port Injection," Fuel, Volume 85, pp. 2622-2631, 2006.

49. H. Ogawa, N. Miyamoto, N. Kaneko, H. Ando, "Combustion Control and Operating Range Expansion with Direct Injection of Reaction Suppressors in a Premixed DME HCCI Engine," SAE Technical Paper 2003-01-0746, 2003.
50. M. Zheng, X. Han, Y. Tan, M. Kobler, S. Ko, M. Wang, "Low Temperature Combustion of Neat Biodiesel Fuel on a Common-rail Diesel Engine," SAE Technical Paper 2008-01-1396, 2008.
51. M. K. Veltman, P. Karra, S. C. Kong, "Effects of Biodiesel Blends on Emissions in Low Temperature Diesel Combustion," SAE Technical Paper 2009-01-0485, 2009.
52. W. F. Northrop, S. V. Bohac, D. N. Assanis, "Premixed Low Temperature Combustion of Biodiesel and Blends in a High Speed Compression Ignition Engine," SAE Technical Paper 2009-01-0133, 2009.
53. T. G. Fang, C. F. Lee, "Bio-diesel Effects on Combustion Processes in an HSDI Diesel Engine Using Advanced Injection Strategies," Proceedings of Combustion Institute, Volume 32, pp. 2785-2792, 2009.
54. T. G. Fang, Y. C. Lin, T. M. Fong, C. F. Lee, "Biodiesel Combustion in an Optical HSDI Diesel Engine under Low Load Premixed Combustion Conditions," Fuel, Volume 88, pp. 2154-2162, 2009.
55. P. Wolters, W. Salber, J. Geiger, M. Duesmann, J. Dilthey, "Controlled Auto Ignition Combustion Process with an Electromechanical Valve Train," SAE Technical Paper 2003-01-0032, 2003.
56. O. Lang, W. Salber, J. Hahn, S. Pischinger, K. Hortmann, C. Bucker, "Thermodynamical and Mechanical Approach towards a Variable Valve Train for

- 
- the Controlled Auto Ignition Combustion Process,” SAE Technical Paper 2005-01-0762, 2005.
57. L. Koopmans, I. Denbratt, “A Four-stroke Camless Engine, Operated in Homogeneous Charge Compression Ignition Mode with Commercial Gasoline,” SAE Technical Paper 2001-01-3610, 2001.
58. A. Fuerhapter, E. Unger, W. Piock, G. Fraidl, “The New AVL CSI Engine HCCI Operation on a Multi-cylinder Gasoline Engine,” SAE Technical Paper 2004-01-0551, 2004.
59. S. Mori, O. Lang, W. Salber, S. Pischinger, C. Bucker, “Type Analysis of EGR Strategies for Controlled Auto Ignition (CAI) by Using Numerical Simulations and Optical Measurements,” SAE Technical Paper 2006-01-0630, 2006.
60. J. E. Dec, Y. Yang, “Boosted HCCI for High Power without Engine Knock and with Ultra-low NO<sub>x</sub> Emissions Using Conventional Gasoline,” SAE Technical Paper 2010-01-1086, 2010.
61. J. Dec, Y. Yang, and N. Dronniou, “Boosted HCCI - Controlling Pressure-Rise Rates for Performance Improvements Using Partial Fuel Stratification with Conventional Gasoline,” SAE International Journal of Engines, Volume 4, Issue 1, pp. 1169-1189, 2011.
62. D. Yap, A. Megaritis, M. L. Wyszynski, H. Xu, “Effect of Inlet Valve Timing on Boosted Gasoline HCCI with Residual Gas Trapping,” SAE Technical Paper 2005-01-2136, 2005.
63. A. Cairns, H. Blaxill, “The Effects of Combined Internal and External Exhaust Gas Recirculation on Gasoline Controlled Auto-ignition,” SAE Technical Paper 2005-01-0133, 2005.

64. J. A. Gaynor, R. Fleck, R. J. Kee, R. G. Kenny, G. Cathcart, "A Study of Efficiency and Emissions for a 4-stroke SI and a CAI Engine with EGR and Light Boost," SAE Technical Paper 2006-32-0042, 2006.
65. H. Yun, N. Wermuth, P. Najt, "Extending the High Load Operating Limit of a Naturally-aspirated Gasoline HCCI Combustion Engine," SAE Technical Paper 2010-01-0847, 2010.
66. M. Alriksson, T. Rente and I. Denbratt, "Low Soot, Low NO<sub>x</sub> in a Heavy Duty Diesel Engine Using High Levels of EGR," SAE Technical Paper 2005-01-3836, 2005.
67. U. Asad, and M. Zheng, "Efficacy of EGR and Boost in Single-Injection Enabled Low Temperature Combustion," SAE International Journal of Engines, Volume 2, Issue 1, pp. 1085-1097, 2009.
68. W. F. Colban, D. Kim, P. C. Miles, S. Oh, R. Opt, R. Krieger, "A Detailed Comparison of Emissions and Combustion Performance between Optical and Metal Single-cylinder Diesel Engines at Low Temperature Combustion Conditions," SAE Technical Paper 2008-01-1066, 2008.
69. H. Ogawa, T. Li, N. Miyamoto, "Characteristics of Low Temperature and Low Oxygen Diesel Combustion with Ultra-high Exhaust Gas Recirculation," International Journal of Engine Research, Volume 8, pp. 365-378, 2009.
70. W. F. Colban, P. C. Miles, S. Oh, "Effect of Intake Pressure on Performance and Emissions in an Automotive Diesel Engine Operating in Low Temperature Combustion Regimes," SAE Technical Paper 2007-01- 4063, 2007.
71. J. Dec, "A Conceptual Model of DI Diesel Combustion Based on Laser-sheet Imaging," SAE Technical Paper 970873, 1997.

- 
72. M. Zheng, G. T. Reader, J. G. Hawley, "Diesel Engine Exhaust Gas Recirculation: A Review on Advanced and Novel concepts," *Energy Conversion and Management*, Volume 45, Issue 6, pp. 883-900, 2004.
  73. S. Kimura, H. Ogawa, M. Matusi and Y. Enomoto, "An Experimental Analysis of Low Temperature and Premixed Combustion for Simultaneous Reduction of NO<sub>x</sub> and Particulate Emissions in Direct Injection Diesel Engines," *International Journal of Engine Research*, Volume 3, Issue 4, pp. 249-259, 2002.
  74. C. A. Idicheria and L. M. Pickett, "Soot Formation in Diesel Combustion under High-EGR Conditions," SAE Technical Paper 2005-01-3834, 2005.
  75. J. O. Olsson, P. Tunestal and B. Johansson, "Boosting for High Load HCCI," SAE Technical Paper 2004-01-0940, 2004.
  76. H. Ogawa, N. Miyamoto, H. Shimizu, S. Kido, "Characteristics of Diesel Combustion in Low Oxygen Mixtures with Ultra-high EGR," SAE Technical Paper 2006-01-1147, 2006.
  77. S. Kook, C. Bae, P. C. Miles, D. Choi and L. M. Pickett, "The Influence of Charge Dilution and Injection Timing on Low-temperature Diesel Combustion and Emissions," SAE Technical Paper 2005-01-3837, 2005.
  78. U. Asad, M. Zheng, X. Han, G. T. Reader, M. Wang, "Fuel Injection Strategies to Improve Emissions and Efficiency of High Compression Ratio Diesel Engines," *SAE International Journal of Engines*, Volume 117, Issue 3, pp. 1220-1233, 2008.
  79. A. Helmantel and I. Denbratt, "HCCI Operation of a Passenger Car Common-rail DI Diesel Engine with Early Injection of Conventional Diesel Fuel," SAE Technical Paper 2004-01-0935, 2004.

- 
80. M. Zheng, G. T. Reader, R. Kumar, C. Mulenga, U. Asad, Y. Tan and M. Wang, "Adaptive Control to Improve Low Temperature Diesel Engine Combustion," 12<sup>th</sup> Diesel Engine-Efficiency and Emission Reduction Conference (DEER), 2006.
  81. Y. Takeda, K. Nakagome, K. Niimura, "Emission Characteristics of Premixed Lean Diesel Combustion with Extremely Early Staged Fuel Injection," SAE Technical Paper 961163, 1996.
  82. L. Shi, K. Deng, Y. Cui, "Study of Diesel-fuelled Homogeneous Charge Compression Ignition Combustion by In-cylinder Early Fuel Injection and Negative Valve Overlap," Proceedings of the Institution of Mechanical Engineers, Volume 219, pp. 1193-1201, 2005.
  83. M. Christensen, P. Einewall, B. Johansson, "Homogeneous Charge Compression Ignition (HCCI) Using Isooctane, Ethanol and Natural Gas: A Comparison with Spark-ignition Operation," SAE Technical Paper 972874, 1997.
  84. M. Christensen, B. Johansson, "Homogeneous Charge Compression Ignition with Water Injection," SAE Technical Paper 1999-01-0182, 1999.
  85. H. Ohtsubo, T. Nakazono, T. Shirouzu, K. Yamane, K. Kawasaki, "Application of a Multi-cylinder Natural Gas PCCI Engine with Spark Ignition to Generator," SAE Technical Paper 2008-01-0015, 2008.
  86. K. Kawasaki, A. Takegoshi, K. Yamane, H. Ohtsubo, T. Nakazono, K. Yamauchi, "Combustion Improvement and Control for a Natural Gas HCCI Engine by the Internal EGR by Means of Intake-valve Pilot-opening," SAE Technical Paper 2006-01-0208, 2006.

87. C. Arcoumanis, C. S. Bae, R. Crookes, E. Kinoshita, "The Potential of Dimethyl Ether (DME) as an Alternative Fuel for Compression-ignition Engines: A Review," *Fuel*, Volume 87, pp. 1014-1030, 2008.
88. J. J. Zhang, X. Q. Qiao, Z. Wang, B. Guan, Z. Huang, "Experimental Investigation of Low-temperature Combustion (LTC) in an Engine Fueled with Dimethyl Ether (DME)," *Energy and Fuel*, Volume 23, pp. 170-174, 2009.
89. Y. Wang, L. B. Zhou, "Performance and Emissions of a Compression-ignition Engine Fueled with Dimethyl Ether and Rapeseed Oil Blends," *Energy and Fuel*, Volume 21, pp. 1454-1458, 2007.
90. S. H. Park, H. J. Kim, C. S. Lee, "Effects of Dimethyl-ether (DME) Spray Behavior in the Cylinder on the Combustion and Exhaust Emissions Characteristics of a High Speed Diesel Engine," *Fuel Process Technology*, Volume 91, pp. 504-513, 2010.
91. T. Ohmura, M. Ikemoto, N. Iida, "A Study on Combustion Control by Using Internal and External EGR for HCCI Engines Fuelled with DME," *SAE Technical Paper 2006-32-0045*, 2006.
92. J. Y. Jang, C. S. Bae, "Effects of Valve Events on the Engine Efficiency in a Homogeneous Charge Compression Ignition Engine Fueled by Dimethyl Ether," *Fuel*, Volume 88, pp. 1228-1234, 2009.
93. J. Y. Jang, K. Yang, K. Yeom, C. S. Bae, S. Oh, K. Kang, "Improvement of DME HCCI Engine Performance by Fuel Injection Strategies and EGR," *SAE Technical Paper 2008-01-1659*, 2008.
94. H. Joseph, "Fuel Economy Program in Brazil," *Presentation at Fuel Economy Symposium, Brazilian Vehicle Manufacturers Association*, 2011.

- 
95. Y. F. Li, H. Zhao, N. Brouzos, "CAI Combustion with Methanol and Ethanol in an Air Assisted Direct Injection Gasoline Engine," SAE Technical Paper 2008-01-1673, 2008.
  96. H. Xie, Z. P. Wei, B. Q. He, H. Zhao, "Comparison of HCCI Combustion Respectively Fueled with Gasoline, Ethanol and Methanol through the Trapped Residual gas Strategy," SAE Technical Paper 2006-01-0635, 2006.
  97. S. Yamamoto, Y. Agui, N. Kawaharada, H. Ueki, "Comparison of Diesel Combustion between Ethanol and Butanol Blended with Gas Oil," SAE Technical Paper 2012-32-0020, 2012.
  98. S. Chockalingam and S. Ganapathy, "Performance and Emission Analysis of a Single Cylinder Constant Speed Diesel Engine Fuelled with Diesel-Methanol-Isopropyl Alcohol Blends," SAE Technical Paper 2012-01-1683, 2012.
  99. M. Shen, M. Tuner, B. Johansson and W. Cannella, "Effects of EGR and Intake Pressure on PPC of Conventional Diesel, Gasoline and Ethanol in a Heavy Duty Diesel Engine," SAE Technical Paper 2013-01-2702, 2013.
  100. N. Shimazaki, A. Minato and T. Nishimura, "Premixed Diesel Combustion using Direct Injection near Top Dead Centre," International Journal of Engine Research, Volume 8, pp. 259-270, 2007.
  101. S. Kokjohn, R. Hanson, D. Splitter and R. Reitz, "Experiments and Modelling of Dual-Fuel HCCI and PCCI Combustion Using In-Cylinder Fuel Blending," SAE International Journal of Engines, Volume 2, Issue 2, pp. 24-39, 2010.
  102. X. Han, K. Xie, J. Tjong and M. Zheng, "Empirical Study of Simultaneously Low NOx and Soot Combustion with Diesel and Ethanol Fuels in Diesel Engine,"

- 
- Journal of Engineering for Gas Turbines and Power, Volume 134, pp. 251-259, 2012.
103. Y. Zhang, I. Sagalovich, W. De Ojeda, A. Ickes, "Development of Dual-Fuel Low Temperature Combustion Strategy in a Multi-Cylinder Heavy-Duty Compression Ignition Engine Using Conventional and Alternative Fuels," SAE International Journal of Engines, Volume 6, Issue 3, pp.1481-1489, 2013.
104. [http://www.afdc.energy.gov/fuels/fuel\\_properties.php](http://www.afdc.energy.gov/fuels/fuel_properties.php), accessed 2014.
105. Zoldy, M., Hollo, A., and Thernesz, A., "Butanol as a Diesel Extender Option for Internal Combustion Engines," SAE Technical Paper 2010-01-0481, 2010.
106. X. Han, K. Xie, M. Zheng, and W. De Ojeda, "Ignition Control of Gasoline-Diesel Dual Fuel Combustion," SAE Technical Paper 2012-01-1972, 2012.
107. R. Kumar, M. Zheng, U. Asad and G. T. Reader, "Heat Release Based Adaptive Control to Improve Low Temperature Diesel Engine Combustion," SAE Technical Paper 2007-01-0771, 2007.
108. U.S. Superintendent of Documents, "Code of Federal Regulations," Title 40, Protection of Environment, Revised as of July 1<sup>st</sup>, pp. 483, 2010.
109. U. Asad and M. Zheng, "Exhaust Gas Recirculation for Advanced Diesel Combustion Cycles," Applied Energy, Volume 123, pp. 242-252, 2014.

**APPENDICES****APPENDIX A****A. Zero-dimensional Simulation**

The engine combustion involves multiple parameters. The zero-dimensional simulations are capable of providing useful guidance to the empirical investigations. This dissertation uses the simulation code developed by the Clean Diesel Engine Group at the University of Windsor. In this analysis, the Woschni heat transfer model and the Weibe heat release model are applied to simulate the engine combustion processes, and it is compared with experimental results. The primary investigated engine parameters include the indicated thermal efficiency, peak cylinder pressure, and the maximum pressure rise rate. The simulation inputs are the combustion duration and phasing that characterize the combustion events (Figure A.1).

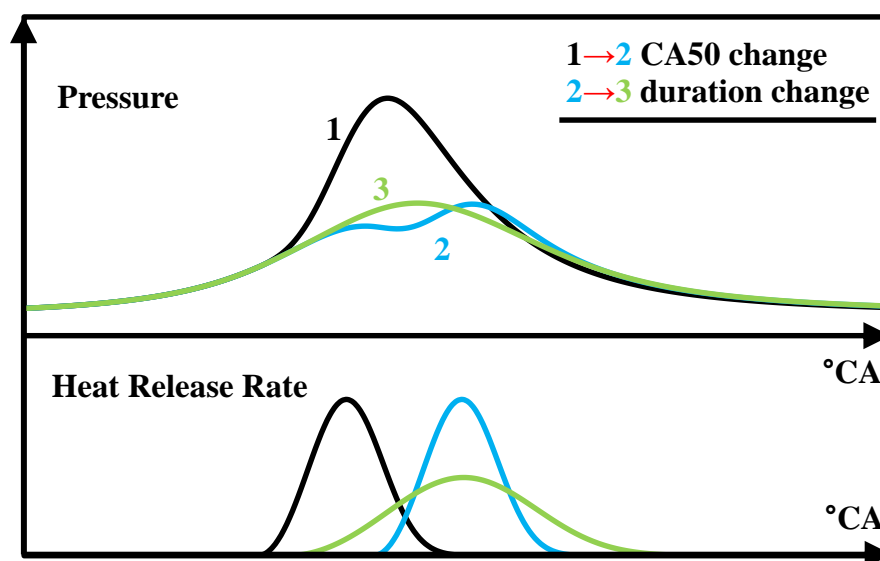


Figure A.1 Simulation Inputs – Heat Release Phasing and Duration

The simulation conditions are summarized in Table A.1. Three fuelling rates that represent the low, medium, and high engine loads are studied. The intake oxygen concentration is fixed at 20.9%, and thus the simulation does not account for the EGR effects. The engine speed is 1500 rpm, and the intake temperature is 30°C. The engine geometry is the same as the Ford research engine used in this dissertation.

Table A.1 Simulation Conditions

Fuelling Rate [mg/cycle]	Intake Boost [bar abs]	IMEP <sub>max</sub> [bar]	Figures [-]
15	1.3	6.3	A.2, A.5, A.8
30	1.5	12.7	A.3, A.6, A.9
50	2.5	21.6	A.4, A.7, A.10

### A.1 Indicated Thermal Efficiency

The simulation results of the indicated thermal efficiency are shown in Figures A.2 to A.4 for the three investigated engine loads. In general, longer combustion durations result in a reduced thermal efficiency. The combustion phasing has much stronger impacts on the engine efficiency than the combustion duration. As the engine load increases, the optimal combustion phasing postpones slightly. By large, the combustion phasing window for the highest engine efficiency is in a range of 7~12 °CA after TDC, regardless of the engine load levels. Therefore, the engine control should do the best endeavor to attain such an optimal combustion phasing for engine efficiency improvements.

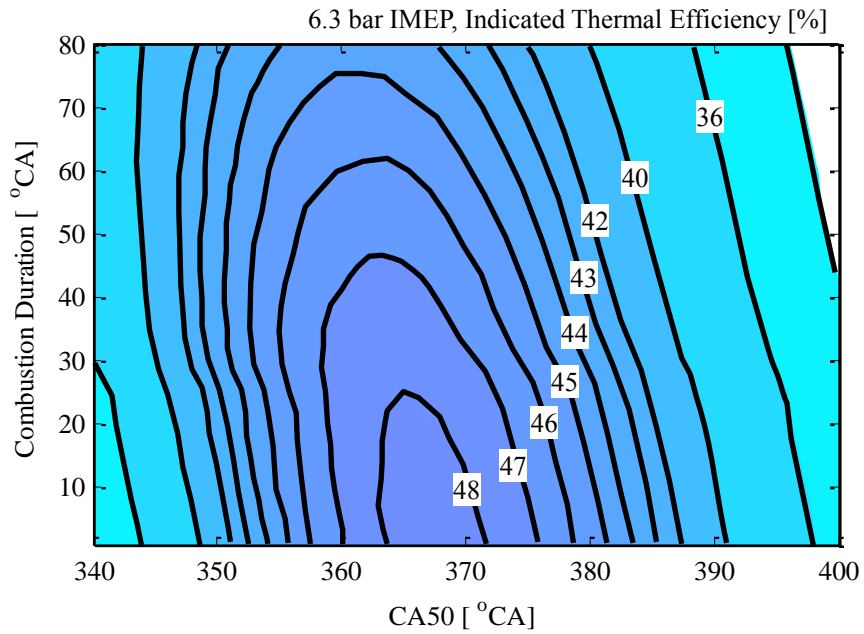


Figure A.2 Simulated Low Load – Indicated Thermal Efficiency

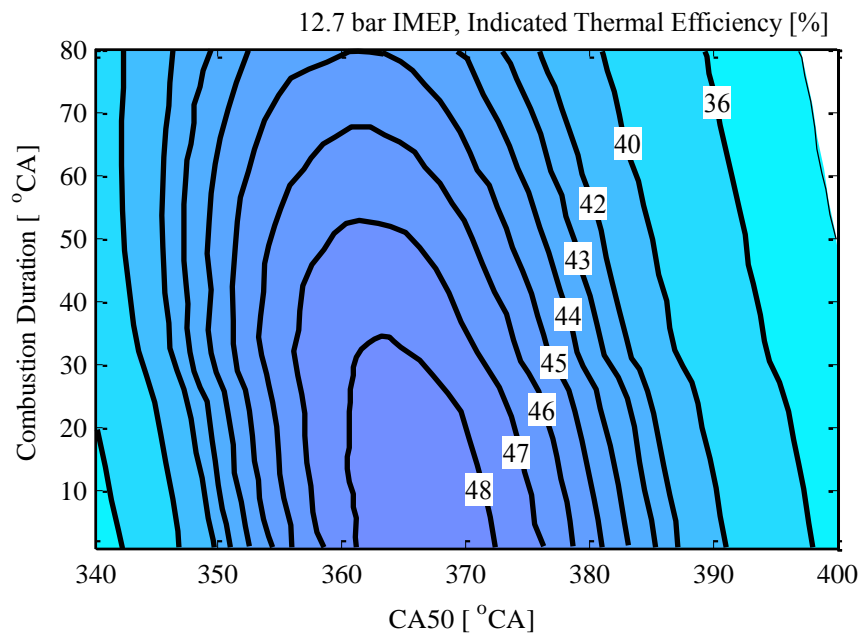


Figure A.3 Simulated Medium Load – Indicated Thermal Efficiency

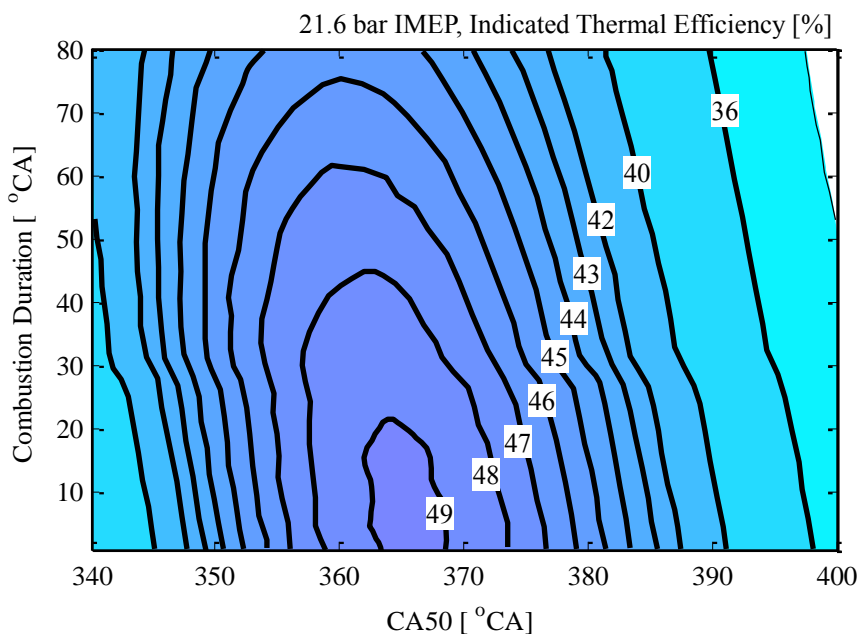


Figure A.4 Simulated High Load – Indicated Thermal Efficiency

## A.2 Maximum Pressure Rise Rate

The operation in LTC modes commonly encounters engine knocking at higher engine loads. Moreover, the pressure rise rate also correlates to the combustion noise. The calibration of an automotive diesel engine normally limits the maximum pressure rise rate to 6~8 bar/°CA; in a research environment, however, this upper limit can be increased to 20 bar/°CA for the engine safety.

The simulation results for the maximum pressure rise rates are shown in Figures A.5 to A.7. When the maximum pressure rise rate exceeds 20 bar/°CA, the dashed lines are used to indicate the values.

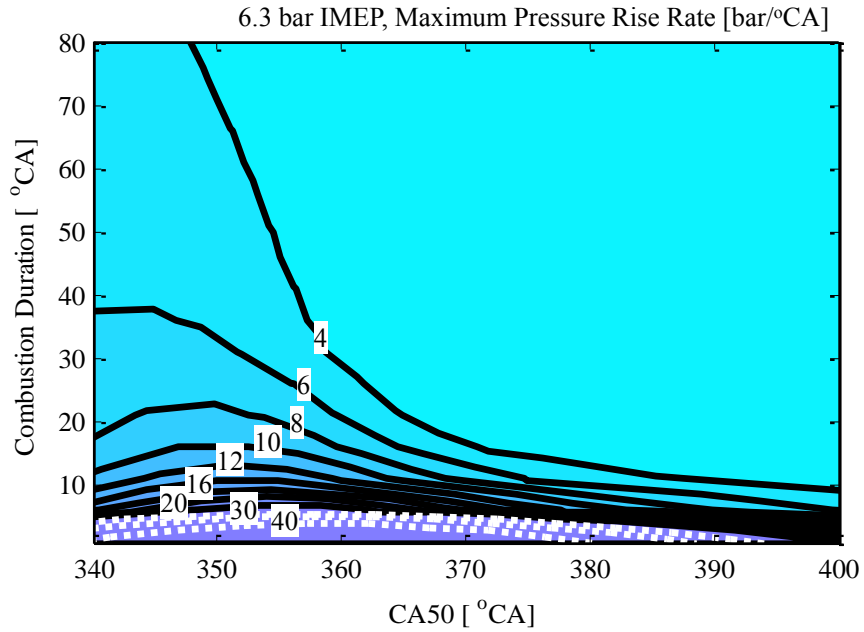


Figure A.5 Simulated Low Load – Maximum Pressure Rise Rate

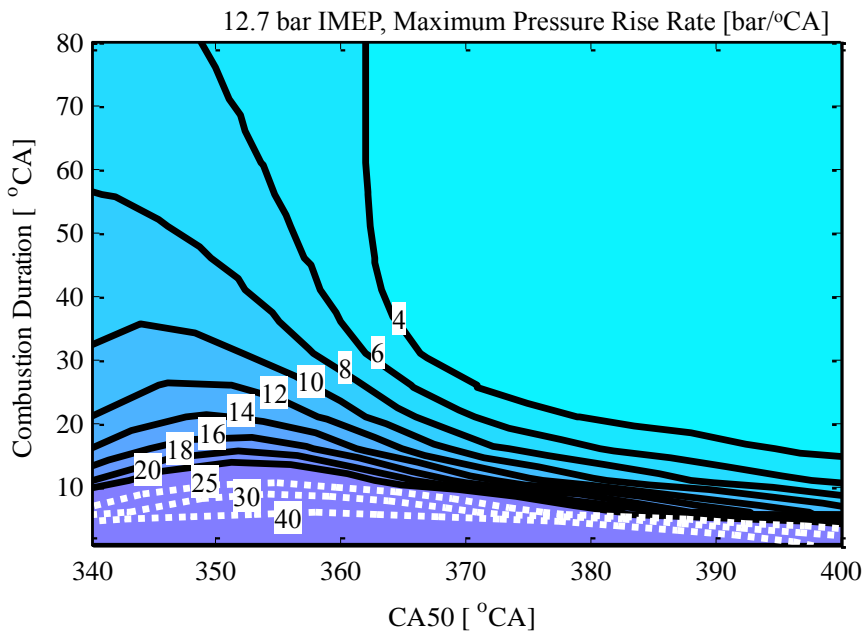


Figure A.6 Simulated Medium Load – Maximum Pressure Rise Rate

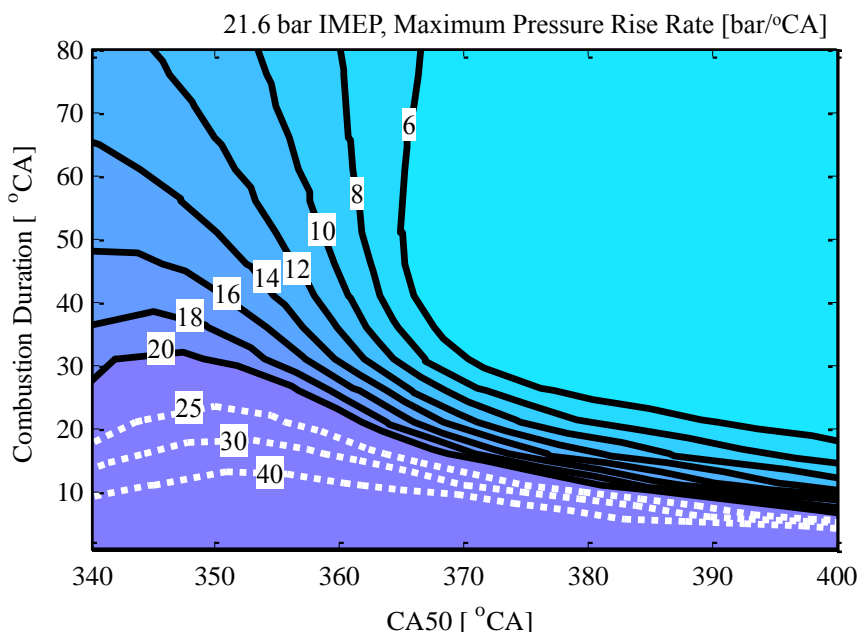


Figure A.7 Simulated High Load – Maximum Pressure Rise Rate

As indicated by the simulation results, high pressure rise rates tend to occur at earlier combustion phasings and with shorter combustion durations. At higher engine loads, the maximum pressure rise rate can easily exceed the prescribed limit (20 bar/°CA).

The clean combustion modes prefer the compression ignition of a highly homogeneous cylinder charge, which is usually accompanied by rapid heat release within short durations. When the combustion duration is sufficiently short (*e.g.* less than 6~10 °CA), the combustion event essentially becomes (almost) constant volume combustion, and the maximum pressure rise rate always exceeds the prescribed limit, regardless of the combustion phasing and/or engine loads. Therefore, the control of the combustion rate is critical to avoid excessive combustion noise and potential engine knocking. In fact, the efficient engine operation can afford reasonably prolonged durations of combustion, since the combustion duration has minor impacts on the engine efficiency.

The simulation results also suggest that a late combustion event can lower the pressure rise rate. When the major or entire combustion event occurs after TDC, the cylinder charge starts to expand as the piston moves downwards. The effect of the expansion counteracts the combustion pressure increase, thereby helping to reduce the pressure rise rate. However, the postponement of the combustion can substantially deteriorate the engine efficiency. At high engine loads, the reasonable combustion phasing is a compromise between the efficiency and the maximum pressure rise rate.

### A.3 Peak Cylinder Pressure

The prescribed limit of the peak cylinder pressure is 200 bar in accordance with the specifications of the research engines. In the simulation results, the peak cylinder pressure exceeding 200 bar are presented by dashed lines. The contours of the peak cylinder pressure are shown in Figures A.8 to A.10.

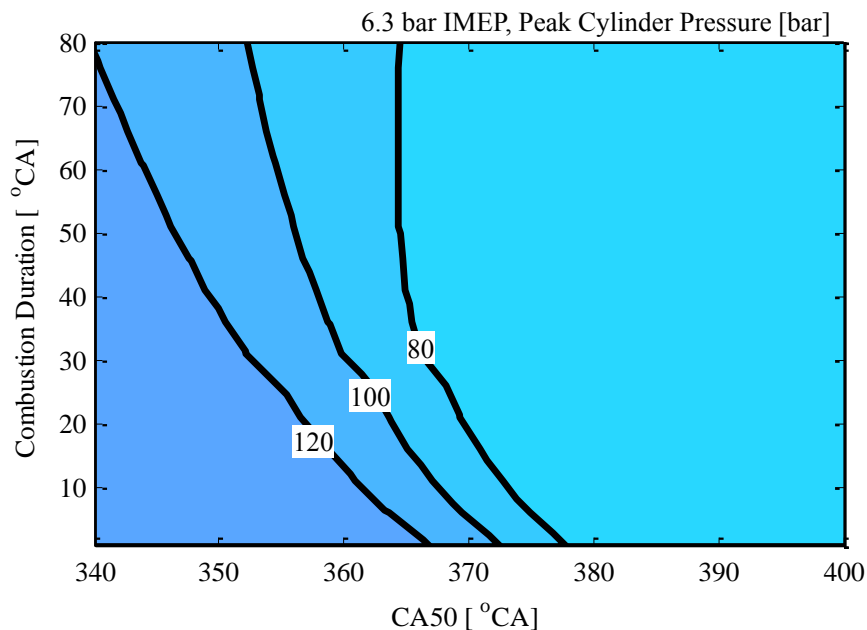


Figure A.8 Simulated Low Load – Peak Cylinder Pressure

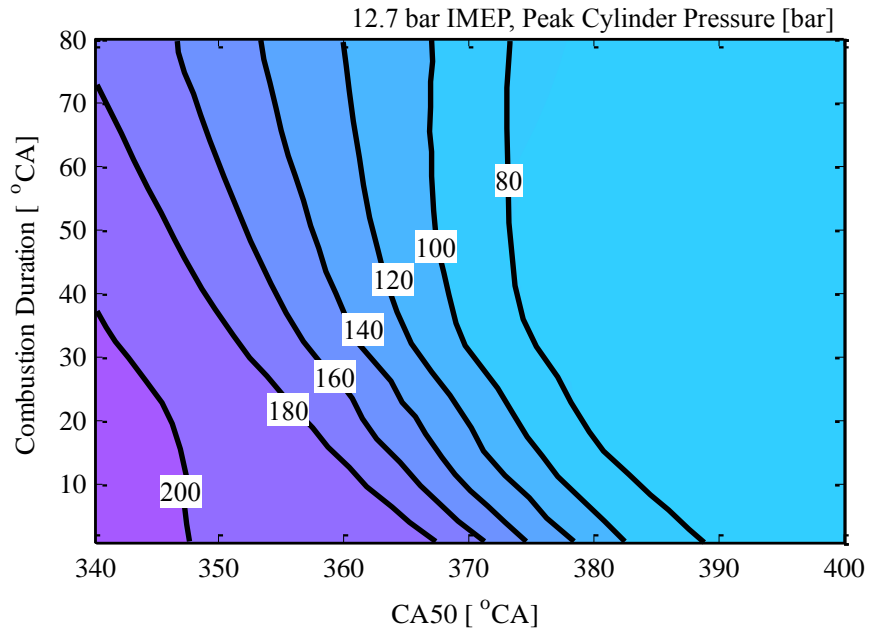


Figure A.9 Simulated Medium Load – Peak Cylinder Pressure

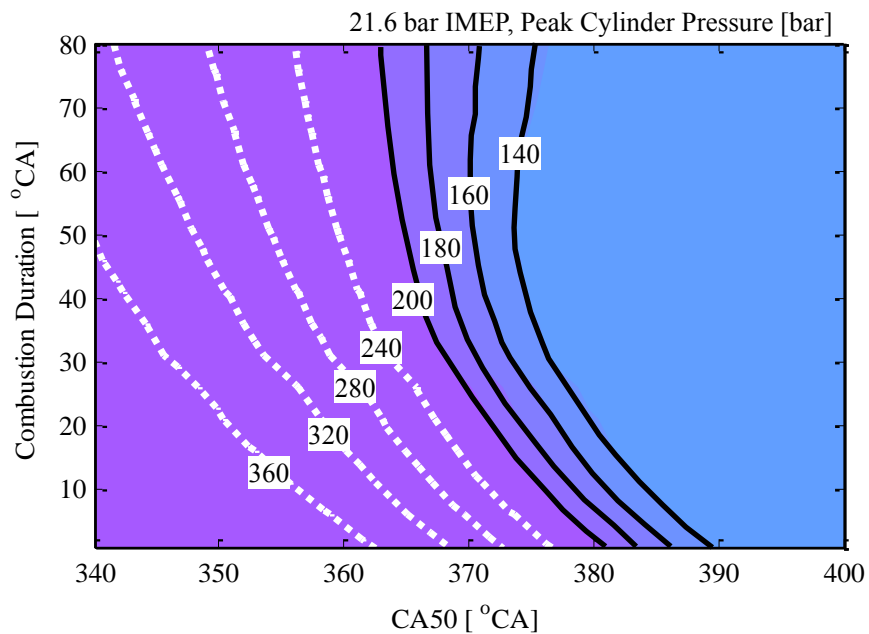


Figure A.10 Simulated High Load – Peak Cylinder Pressure

Similar to the maximum pressure rise rate, the peak cylinder pressure is sensitive to the combustion phasing, combustion duration, and the engine load. In general, excessively high cylinder pressures tend to occur at an earlier combustion phasing, with short combustion duration, and at higher engine loads. The postponement of the combustion events into the expansion stroke can effectively reduce the peak cylinder pressure. When the combustion occurs at an extremely late timing, the combustion pressure can even be lower than the compression pressure.

In summary, the simulation results provide a guideline to safely operate the engine towards the optimal engine efficiency. When safely deployable, the combustion phasing should be maintained at 7~12 °CA after TDC for efficient combustion. As the engine load increases, the postponement of the combustion becomes necessary to avoid excessively high pressure rise rates and cylinder pressures. A wider margin becomes available for the maximum pressure rise rate once the combustion duration is longer than 10~20 °CA with minor efficiency penalties.

## APPENDIX B

### B. Evaluation of Engine Performance

#### B.1 Engine Power Performance Characteristics

The engine fuel efficiency is commonly represented in the brake specific fuel consumption (BSFC) [g/kW-hr], which is the net fuel consumption rate,  $\dot{m}_f$  [g/s] divided by the brake power,  $\dot{W}_{brake}$  [kW]:

$$BSFC = 3600 \times \dot{m}_f / \dot{W}_{brake} \quad (\text{B-1})$$

The brake thermal efficiency of the engine is the brake power divided by the rate of fuel energy supplied into the cylinders:

$$\eta_{brake} = \dot{W}_{brake} / (\dot{m}_f \times LHV) \times 100\% \quad (\text{B-2})$$

The engine load is normally evaluated by the BMEP [bar] which represents the engine shaft torque [Nm] on per engine displacement,  $V_d$  [m<sup>3</sup>], per cycle:

$$BMEP = 4\pi \times Torque / (V_d \times 100000) \quad (\text{B-3})$$

In order to evaluate a single-cylinder engine, however, the indicated performance is more commonly used to exclude the power loss discrepancies of the auxiliary equipment such as the high-pressure injection pump. The IMEP [bar] of the single cylinder is calculated from the net area enclosed by the  $p$ - $V$  diagram:

$$IMEP = \int_0^{720} p(\theta) dV / V_d \quad (\text{B-4})$$

The indicated power  $\dot{W}_{ind}$  [kW] is calculated from the IMEP [bar],  $V_d$  [m<sup>3</sup>], and engine speed  $n$  [rpm]:

$$\dot{W}_{ind} = IMEP \times V_d \times n/1.2 \quad (\text{B-5})$$

The indicated specific fuel consumption (ISFC) [g/kW-hr] is determined by the fuel consumption rate,  $\dot{m}_f$  [g/s] and the indicated power  $\dot{W}_{ind}$  [kW]:

$$ISFC = 3600 \times \dot{m}_f / \dot{W}_{ind} \quad (\text{B-6})$$

The indicated thermal efficiency is therefore calculated from:

$$\eta_{brake} = \dot{W}_{ind} / (\dot{m}_f \times LHV) \times 100\% \quad (\text{B-7})$$

## B.2 Apparent Heat Release Analysis

By assuming that the cylinder contents are fully mixed, the first law of Thermodynamics can be applied to the cylinder charge for the time period between the intake valve closing and the exhaust valve opening (*i.e.* the closed system), in which there is no mass transfer.

The heat released by combustion  $dQ$  is given by Equation (B-8):

$$dQ = dU + dW + dQ_{ht} \quad (\text{B-8})$$

Where  $dU$  is the internal energy change,  $dW$  is the work done, and  $dQ_{ht}$  is the heat transfer during this process. By evaluating each term in Equation (B-8) using the following equations:

$$dU = mc_v dT \quad (\text{B-9})$$

$$pv = mRT \quad (\text{B-10})$$

$$dW = pdv \quad (\text{B-11})$$

The net (apparent) heat release rate on a crank angle ( $\theta$ ) basis is given by Equation (B-12):

$$\frac{dQ_{net}}{d\theta} = \frac{1}{(\gamma - 1)} \times \left[ \gamma P \frac{dV}{d\theta} + V \frac{dp}{d\theta} \right] \quad (\text{B-12})$$

This apparent heat release analysis is applied in the investigation of the dissertation work.

### B.3 Exhaust Emission Calculation

The gaseous emissions (NO<sub>x</sub>, CO, HC, and CO<sub>2</sub>) are normally measured in parts per million (ppm). However, the EPA regulation requires reporting on a brake-specific basis in g/bhp-hr (or g/kW-hr). Equation (B-13) shows the formula to convert the emissions from ppm to g/kW-hr where  $Y_i$  is the volumetric concentration of exhaust emission  $i$  in ppm,  $M_i$  is the molecular weight of emission  $i$  in kg/kmol,  $MAF$  is the mass air flow rate in g/s,  $\dot{m}_f$  is the fuel flow rate in g/s, and  $\dot{W}_{brake}$  is the brake power output in kW.

$$X_i = (Y_i/1000000) \times (M_i/29) \times (MAF + \dot{m}_f) \times 36000/\dot{W}_{brake} \quad (\text{B-13})$$

The smoke emissions are measured using an AVL smoke meter, and the smoke reading is given in filter smoke number (FSN). The smoke readings in FSN are first converted into the soot concentration in mg/m<sup>3</sup> using Equation (B-14) provided by the manufacturer:

$$Soot [mg/m^3] = 4.95 \times FSN \times \exp(0.38 \times FSN)/0.405 \quad (\text{B-14})$$

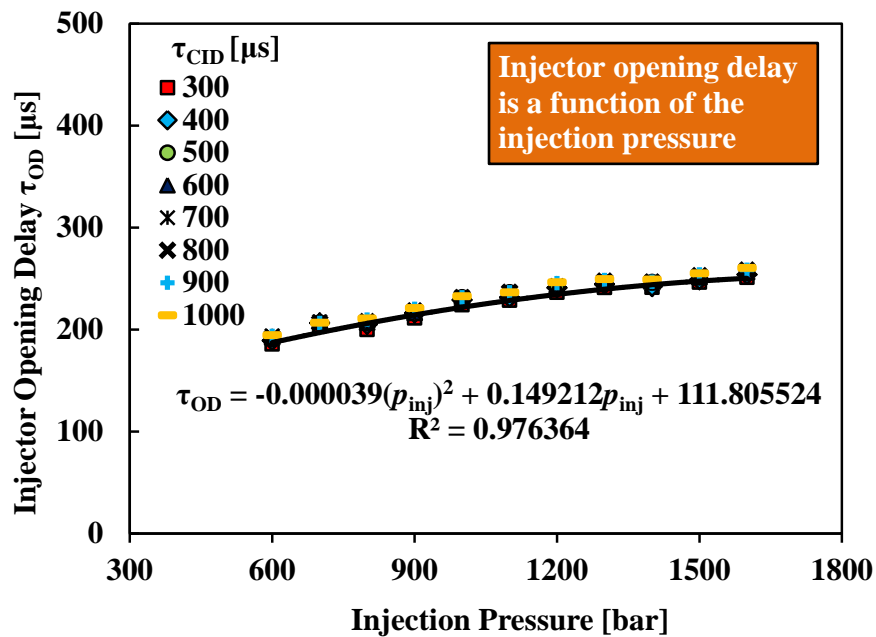
With the soot concentration known, Equation (B-15) can be used to calculate the brake specific soot emissions in g/kW-hr where  $Y_{soot}$  is the soot concentration in mg/m<sup>3</sup>,  $MAF$  is the mass flow rate of the fresh air into the engine in g/s,  $\rho_{exh}$  is the density of the exhaust gas in kg/m<sup>3</sup>, and  $\dot{W}_{brake}$  is the brake power output.

$$X_{soot} = (Y_{soot}/1000) \times (MAF \times 3.6)/\rho_{exh}/\dot{W}_{brake} \quad (\text{B-15})$$

## APPENDIX C

## C. Modelling of Injector Delays

The rate of injection is measured on an offline injection bench (EFS 8405). The measurement results of the opening delay ( $\tau_{OD}$ ) and closing delay ( $\tau_{CD}$ ) are shown in Figures C.1 & C.2 for the same type of injector used on the single cylinder research engine. The control parameters that affect these injector delays include the commanded injection duration ( $\tau_{CID}$ ) and the fuel injection pressure ( $p_{inj}$ ). As indicated by the measurement results, the injector opening delay does not show a strong correlation with the injection duration but it increases at higher injection pressures. However, the injector closing delay is affected by both the injection pressure and injection duration.

Figure C.1 Injector Opening Delay  $\tau_{OD} - \tau_{CID}$ ,  $p_{inj}$

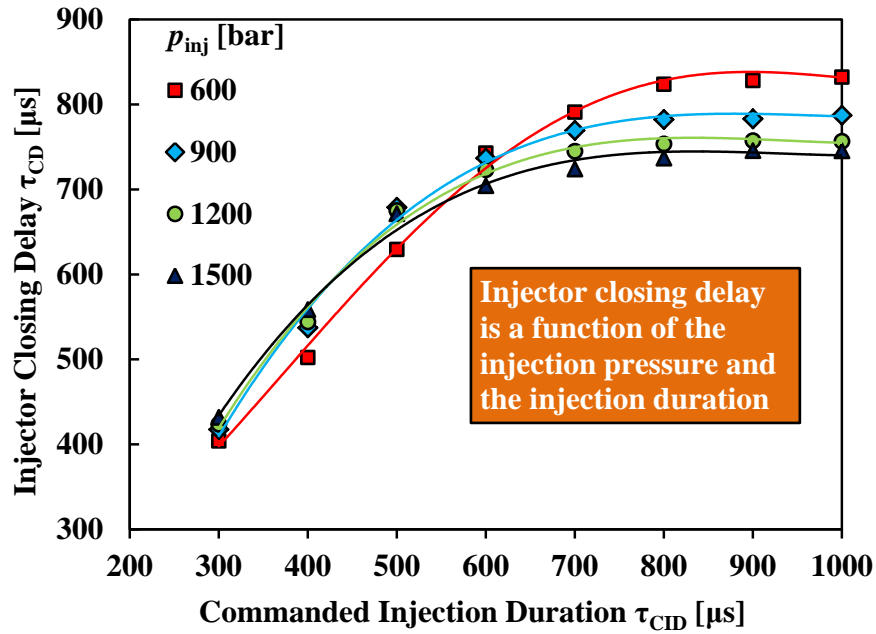


Figure C.2 Injector Closing Delay  $\tau_{CD} - \tau_{CID}$ ,  $p_{inj}$

Based on the experimental data, the injector closing delay is modelled by the following equation:

$$\tau_{CD} = a_4(\tau_{CID})^4 + a_3(\tau_{CID})^3 + a_2(\tau_{CID})^2 + a_1\tau_{CID} + a_0 \quad (C-1)$$

Where,

$\tau_{CD}$	the injector closing delay	[ $\mu s$ ]
$\tau_{CID}$	the commanded injection duration	[ $\mu s$ ]
$a_i$	the polynomial coefficient values listed in Table C.1	[-]

Table C.1 Polynomial Coefficients for Closing Delay Equation

$p_{inj}$ [bar]	$a_4$	$a_3$	$a_2$	$a_1$	$a_0$
600	7.609E-9	-2.014E-5	1.779E-2	-5.299	873.896
900	0	1.356E-6	-3.931E-3	3.762	-402.354
1200	0	1.641E-6	-4.428E-3	3.959	-416.465
1500	0	1.883E-6	-4.756E-3	4.021	-399.456

The equations below are therefore used to evaluate the overlap or separation “ $\delta$ ” between the injection and combustion events:

$$EOI_{cmd} = SOI_{cmd} + 6 \times 10^{-6} n \tau_{CID} \quad (C-2)$$

$$EOI_{mdl} = EOI_{cmd} + 6 \times 10^{-6} n \tau_{CD} \quad (C-3)$$

$$\delta = EOI_{mdl} - SOC \quad (C-4)$$

Where,

$EOI_{cmd}$	the commanded end of injection	[°CA]
$SOI_{cmd}$	the commanded start of injection	[°CA]
$n$	the engine speed	[rpm]
$\tau_{CID}$	the commanded injection duration	[ $\mu$ s]
$EOI_{mdl}$	the modeled end of injection	[°CA]
$\tau_{CD}$	the injector closing delay	[ $\mu$ s]
$\delta$	the separation of injection and combustion events	[°CA]
$SOC$	the start of combustion, represented by CA5	[°CA]

When  $\delta > 0$ ,  $\delta$  is the temporal overlap between the injection and combustion events; when  $\delta \leq 0$ ,  $\delta$  is the temporal separation between the injection and combustion events.

This zero-dimensional model is integrated into the program for the real-time injection control, which calculates the  $\delta$  value for every engine cycle and adjusts the injection accordingly in the next engine cycle.

## APPENDIX D

## D. Equipment List

Table D.1 List of Equipment for Engine Tests

Equipment	Model	Remarks
Engine	Ford, Duratorq	Reconfigured for single cylinder research
Pressure transducer	AVL GU13P	Adaptor: AVL AG03.42
Air flow meter	Roots, 2M175, SN 1055122	1 pulse = 0.005 ft <sup>3</sup>
Fuel flow meter	Ono Sokki, FP-2140H, SN 44300252	Reading unit: Ono Sokki, DF-210A
Fuel filter	SMC FH150-03-012-P005X27	Element: EP910-005V
Intake pressure regulator	SMC ITV 3051-314S5	Pressure range: 5~900 kPa
Backpressure valve	Sinclair Collins, K31-42122000	Pneumatic controlled valve
Intake surge tank	Manchester Tank, CAT# 302404	Volume: 75 Liters
Exhaust surge tank	Prentex Tanks, SN D550	Pressure rating : 300 psig @ 100°F
Blow-off valve	Precision, SN 0100020	Pressure setting: 5 bar
Dynamometer	Schenck, WS230, SN: LWH0747	Eddy current dynamometer
Dynamometer controller	DyneSystemsCo. DYN-LOC IV	Digital dynamometer controller
Injector	Delphi R01001D	Common-rail injector
Encoder	Gurley Precision, 9125S03600H5L01E18SQ06EN	0.1°CA resolution optical encoder
Lubricant conditioning unit	FEV, LUC11001110	Up to 10 bar, up to 150°C
Coolant conditioning unit	FEV, COC11001100	Up to 10 bar, up to 130°C

## APPENDIX E

## E. Specifications of Diesel Fuel

Table E.1 Specifications of Studied Diesel Fuel

Test	Method	Units	Specifications			Results		
			min	target	max			
Distillation-IBP <sup>1</sup>	ASTM D86	°F	340		400	373		
5%		°F						
10%		°F	400		460	428		
20%		°F						450
30%		°F						473
40%		°F	470		540	497		
50%		°F						520
60%		°F						541
70%		°F	560		630	562		
80%		°F						585
90%		°F						611
95%		°F	610		690	634		
Distillation-EP <sup>2</sup>		°F						653
Recovery		vol %		Report		98.4		
Residue		vol %		Report		0.8		
Loss		vol %		Report		0.8		
Gravity	ASTM D4052	°API	32.0		37.0	33.4		
Specific Gravity	ASTM D4052		0.840		0.865	0.858		
Flash Point	ASTM D93	°F	130			164		
Cloud Point	ASTM D2500	°F		Report		-9		
Pour Point	ASTM D97	°F		Report		-31		
Viscosity, 40°C	ASTM D445	cSt	2.0		3.2	2.7		
Sulfur	ASTM D5453	ppm	7		15	9		
Carbon	ASTM D5291	wt %		Report		86.80		
Hydrogen	ASTM D5291	wt %		Report		12.90		
Composition, aromatics	ASTM D5186	wt %		Report		32.8		
Composition, aromatics	ASTM D1319	vol %	27			30		
Composition, olefins	ASTM D1319	vol %		Report		5		
Composition, saturates	ASTM D1319	vol %		Report		65		
Cetane Number	ASTM D613		40		50	46.5		
Cetane Index	ASTM D4737		40		50	44.8		
Net heat content	ASTM D240	btu/lb		Report		18119		
HFRR @60°C	ASTM D6079	mm		Report		0.300		

<sup>1</sup>IBP: initial boiling point<sup>2</sup>EP: end point

**LIST OF PUBLICATIONS*****Refereed Journals:***

1. **Xiaoye Han**, Jimi Tjong, Graham T. Reader, Ming Zheng, “Ethanol Diesel Dual Fuel Clean Combustion with FPGA Enabled Control” International Journal of Powertrains, Volume 3, No.2, pp. 242-257, 2014.
2. Tadanori Yanai, **Xiaoye Han**, and Ming Zheng, “Extension of Diesel Engine Load Range with Simultaneous Reduction of NOx and Soot by using Ethanol Port Injection, High Intake Boost and EGR,” Transactions of Society of Automotive Engineers of Japan, Volume 44, No. 5, pp. 1169-1174, 2013
3. **Xiaoye Han**, Ming Zheng, Jianxin Wang, “Fuel Suitability for Low Temperature Combustion in Compression Ignition Engines,” Fuel, Volume 109, pp. 336-349, 2013.
4. Tongyang Gao, Prasad Divekar, Usman Asad, **Xiaoye Han**, Graham T. Reader, Meiping Wang, Ming Zheng and Jimi Tjong, “An Enabling Study of Low Temperature Combustion With Ethanol in A Diesel Engine,” Journal of Energy Resources Technology, Volume 135, Issue 4, 8 pages, 2013.
5. **Xiaoye Han**, Jimi Tjong, Ming Zheng and Kelvin Xie, “Empirical Study of Simultaneously Low NOx and Soot Combustion With Diesel and Ethanol Fuels in Diesel Engine,” Journal of Engineering for Gas Turbines and Power, Volume 134, No.11, pp. 251-259, 2012.
6. Usman Asad, **Xiaoye Han**, and Ming Zheng, “An Empirical Study to Extend Engine Load in Diesel Low Temperature Combustion,” SAE International Journal of Engines, Volume 5, Issue 3, pp.709-717, 2012.

7. Usman Asad, Raj Kumar, **Xiaoye Han**, Ming Zheng, “Precise Instrumentation of A Diesel Single-cylinder Research Engine,” *Measurement*, Volume 44, pp. 1267-1278, 2011.
8. William de Ojeda, Tytus Bulicz, **Xiaoye Han**, Ming Zheng, Frederick Cornforth, “Impact of Fuel Properties on Diesel Low Temperature Combustion,” *SAE International Journal of Engines*, Volume 4, Issue 1, pp. 188-201, 2011.
9. Marko Jeftić, Shui Yu, **Xiaoye Han**, Graham T. Reader, Meiping Wang, and Ming Zheng, “Effects of Post injection Application with Late Partially Premixed Combustion on Power Production and Diesel Exhaust Gas Conditioning,” *Journal of Combustion*, Volume 2011, 9 pages, 2011.
10. Ming Zheng, **Xiaoye Han**, Graham T. Reader, “Empirical Studies of EGR Enabled Diesel Low Temperature Combustion,” *Journal of Automotive Safety and Energy*, Volume 1, No. 3, pp. 219-228, 2010.
11. Ming Zheng, Usman Asad, **Xiaoye Han**, Meiping Wang, Graham T. Reader, “Hydrocarbon Impact and NO<sub>x</sub> Survivability during Diesel Low Temperature Combustion Cycles,” *Proceedings of the Institution of Mechanical Engineers, Part D: Journal of Automobile Engineering*, Volume 24, No. D2, pp. 271-284, 2010.
12. Ming Zheng, Yuyu Tan, **Xiaoye Han**, Graham T. Reader, Meiping Wang, “An Enabling Study of Diesel Low Temperature Combustion via Adaptive Control,” *SAE International Journal of Engines*, Volume 2, Issue 1, pp.750-763, 2009.

13. Usman Asad, Ming Zheng, **Xiaoye Han**, Graham T. Reader, and Meiping Wang, "Fuel Injection Strategies to Improve Emissions and Efficiency of High Compression Ratio Diesel Engines," SAE International Journal of Engines, Volume 1, Issue 1, pp.1220-1233, 2008.

***Refereed Conference Proceedings***

14. Prasad Divekar, Usman Asad, **Xiaoye Han**, Xiang Chen, and Ming Zheng, "Study of Cylinder Charge Control for Enabling Low Temperature Combustion in Diesel Engines," Proceedings of the ASME 2013 Internal Combustion Engine Division's Fall Technical Conference, ICEF2013, Dearborn, Michigan, USA, October, 2013.
15. Tadanori Yanai, **Xiaoye Han**, Graham T. Reader, Ming Zheng and Jimi Tjong, "Preliminary Investigation of Direct Injection Neat n-Butanol in a Diesel Engine," Proceedings of the ASME 2013 Internal Combustion Engine Division Fall Technical Conference, ICEF2013-19219, 2013.
16. **Xiaoye Han**, Jimi Tjong, Meiping Wang, Graham T. Reader, and Ming Zheng, "Renewable Ethanol Use for Enabling High Load Clean Combustion in a Diesel Engine," SAE Technical Paper 2013-01-0904, SAE World Congress, Detroit, MI, USA, April, 2013.
17. Shui Yu, **Xiaoye Han**, Kelvin Xie, Meiping Wang, Liguang Li, Jimi Tjong, and Ming Zheng, "Multi-Coil High Frequency Spark Ignition to Extend Diluted Combustion Limits," Proceedings of the 2012 FISITA, Beijing, China, November, 2012.

18. **Xiaoye Han**, Kelvin Xie, Ming Zheng, and William De Ojeda, "Ignition Control of Gasoline-Diesel Dual Fuel Combustion," Proceedings of SAE 2012 Commercial Vehicle Engineering Congress, SAE Technical Paper 2012-01-1972, Chicago, USA, October, 2012.
19. **Xiaoye Han**, Jimi Tjong, Graham T. Reader and Ming Zheng, "Ethanol Diesel Dual Fuel Clean Combustion with FPGA Enabled Control," Powertrain Modelling and Control Conference, Bradford, UK, September, 2012.
20. Prasad Divekar, **Xiaoye Han**, Tadanori Yanai, Shui Yu, Xiang Chen, and Ming Zheng, "Control Techniques of Low NO<sub>x</sub> Combustion in a High Compression Diesel Engine," Powertrain Modelling and Control Conference, Bradford, UK, September, 2012.
21. Tongyang Gao, Prasad Divekar, Usman Asad, **Xiaoye Han**, Graham T. Reader, Meiping Wang, Ming Zheng and Jimi Tjong, "An Enabling Study of Low Temperature Combustion With Ethanol in a Diesel Engine," Proceedings of the ASME 2012 Internal Combustion Engine Division's Fall Technical Conference ICEF2012, Paper number: ICEF2012-92176, Vancouver, British Columbia, Canada, September, 2012.
22. **Xiaoye Han**, Kelvin Xie, Graham T. Reader, Xiang Chen, Jimi Tjong, Meiping Wang, and Ming Zheng, "The Impact of Fuels and Fuelling Strategy on Enabling of Clean Combustion in a Diesel Engine," The International Conference on Modelling and Diagnostics for Advanced Engine Systems (COMODIA), paper FL2-1, Fukuoka, Japan, July, 2012.
23. **Xiaoye Han**, Tongyang Gao, Usman Asad, Kelvin Xie, and Ming Zheng, "Empirical Study Of Simultaneously Low NO<sub>x</sub> and Soot Combustion with

- Diesel and Ethanol Fuels in Diesel Engine,” Proceedings of the ASME 2012 Internal Combustion Engine Division Spring Technical Conference ICES2012, Torino, Piemonte, Italy, May, 2012.
24. William De Ojeda, Yu Zhang, Kelvin Xie, **Xiaoye Han**, Meiping Wang, and Ming Zheng, “Exhaust Hydrocarbon Speciation from a Single-Cylinder Compression Ignition Engine Operating with In-Cylinder Blending of Gasoline and Diesel Fuels,” SAE Technical Paper 2012-01-0683, SAE World Congress, Detroit, MI, USA, April, 2012.
  25. Shui Yu, **Xiaoye Han**, Kelvin Xie, Ming Zheng, and Liguang Li, “Spark Ignition Strategies for Extending Combustion Limits of Diluted Charge for Modern Engines,” ICACMVE, Shanghai, China, November, 2011.
  26. Marko Jeftić, Usman Asad, **Xiaoye Han**, Kelvin Xie, Shui Yu, Meiping Wang, and Ming Zheng, “An Analysis of the Production of Hydrogen and Hydrocarbon Species by Diesel Post Injection Combustion,” ICEF2011-60135, Proceedings of the ASME 2011 Internal Combustion Engine Division Fall Technical Conference , Morgantown, West Virginia, October, 2011.
  27. Shui Yu, Kelvin Xie, **Xiaoye Han**, Marko Jeftic, Tongyang Gao, and Ming Zheng, “A Preliminary Study of the Spark Characteristics for Unconventional Cylinder Charge with Strong Air Movement,” ASME 2011 Internal Combustion Engine Division Fall Technical Conference, Morgantown, West Virginia, October, 2011.
  28. Kelvin Xie, **Xiaoye Han**, Usman Asad, Graham T. Reader, and Ming Zheng, “Empirical Study of Energy in Diesel Combustion Emissions with EGR

- Application,” SAE Technical Paper 2011-01-1817, Kyoto, Japan, September, 2011.
29. Nazila Rajaei, **Xiaoye Han**, Xiang Chen, and Ming Zheng, “Model Predictive Control of Exhaust Gas Recirculation Valve,” SAE Technical Paper 2010-01-0240, SAE World Congress, Detroit, MI, USA, April, 2010.
30. **Xiaoye Han**, Graham T. Reader, Kelvin Xie, Meiping Wang, and Ming Zheng, “The Impact of Cetane Number on Diesel Low Temperature,” Proceedings of the ASME 2010 International Mechanical Engineering Congress & Exposition, IMECE2010, Paper IMECE2010-39076, Vancouver, British Columbia, Canada, November, 2010.
31. **Xiaoye Han**, Tongyang Gao, Ming Zheng and Jimi Tjong, “Fuel Injection Strategies to Enable Low Temperature Combustion in a Light-Duty Diesel Engine,” Global Powertrain Congress, Troy, Michigan, November, 2010.
32. Ming Zheng, Usman Asad, **Xiaoye Han**, Meiping Wang, and Graham T. Reader, “Hydrocarbon Impacts on Diesel HCCI Engine Cycles,” Proceedings of the ASME Internal Combustion Engine Division 2009 Fall Technical Conference, ICEF2009-14012, Lucerne, Switzerland, September 27-30, 2009.
33. Ming Zheng, Usman Asad, Graham T. Reader, Yuyu Tan, **Xiaoye Han**, and Meiping Wang, “Prompt Heat Release Analysis to Improve Diesel Low Temperature Combustion,” Powertrains, Fuels and Lubricants Meeting, SAE paper 2009-01-1883, Florence, Italy, June, 2009.
34. Ming Zheng, **Xiaoye Han**, Graham T. Reader, Usman Asad, Yuyu Tan, Kelvin Xie, and Meiping Wang, “An Enabling Study of Diesel Low-

- Temperature Combustion via Adaptive Control,” Diesel Engine Efficiency and Emission Research Conference (DEER), Detroit, MI, USA, August, 2008.
35. Ming Zheng, Usman Asad, Graham T. Reader, **Xiaoye Han**, Mohammad Pournazeri, David S-K Ting and Meiping Wang, “Diesel EGR Fuel Reformer Improvement with Flow Reversal and Central Fuelling,” 2008 SAE International Powertrains, Fuels and Lubricants Congress, 2008-01-1607, Shanghai, China, June 22-25, 2008.
36. Ming Zheng, Mwila Clarence Mulenga, **Xiaoye Han**, Yuyu Tan, Martin S. Kobler, Suek-Jin Ko, Meiping Wang, and Jimi Tjong, “Low Temperature Combustion of Neat Biodiesel Fuel on a Common-rail Diesel Engine,” SAE 2008 World Congress, SP-2176, paper 2008-01-1396, Detroit, MI, USA, April, 2008.
37. Ming Zheng, Siddhartha Banerjee, Xiaohong Xu, Usman Asad, **Xiaoye Han**, Meiping Wang, and Graham T. Reader, “Energy Efficiency Improvement of Diesel Aftertreatment with Flow Reversal and Central Fuelling,” Proceedings of the 2007 Fall Technical Conference of the ASME Internal Combustion Engine Division, paper ICEF2007-1631, pp. 435-446, Charleston, South Carolina, USA, October, 2007.

**VITA AUCTORIS**

NAME: Xiaoye Han

PLACE OF BIRTH: Benxi, Liaoning, China

YEAR OF BIRTH: 1983

EDUCATION: Tsinghua University, B.Sc., Beijing, China, 2006  
University of Windsor, M.Sc., Windsor, ON, Canada, 2008  
University of Windsor, Ph.D., Windsor, ON, Canada, 2014